NASA CR-172152

A Study of Interior Noise Levels, Noise Sources and Transmission Paths in Light Aircraft

by

R.E. Hayden
B.S. Murray
M.A. Theobald

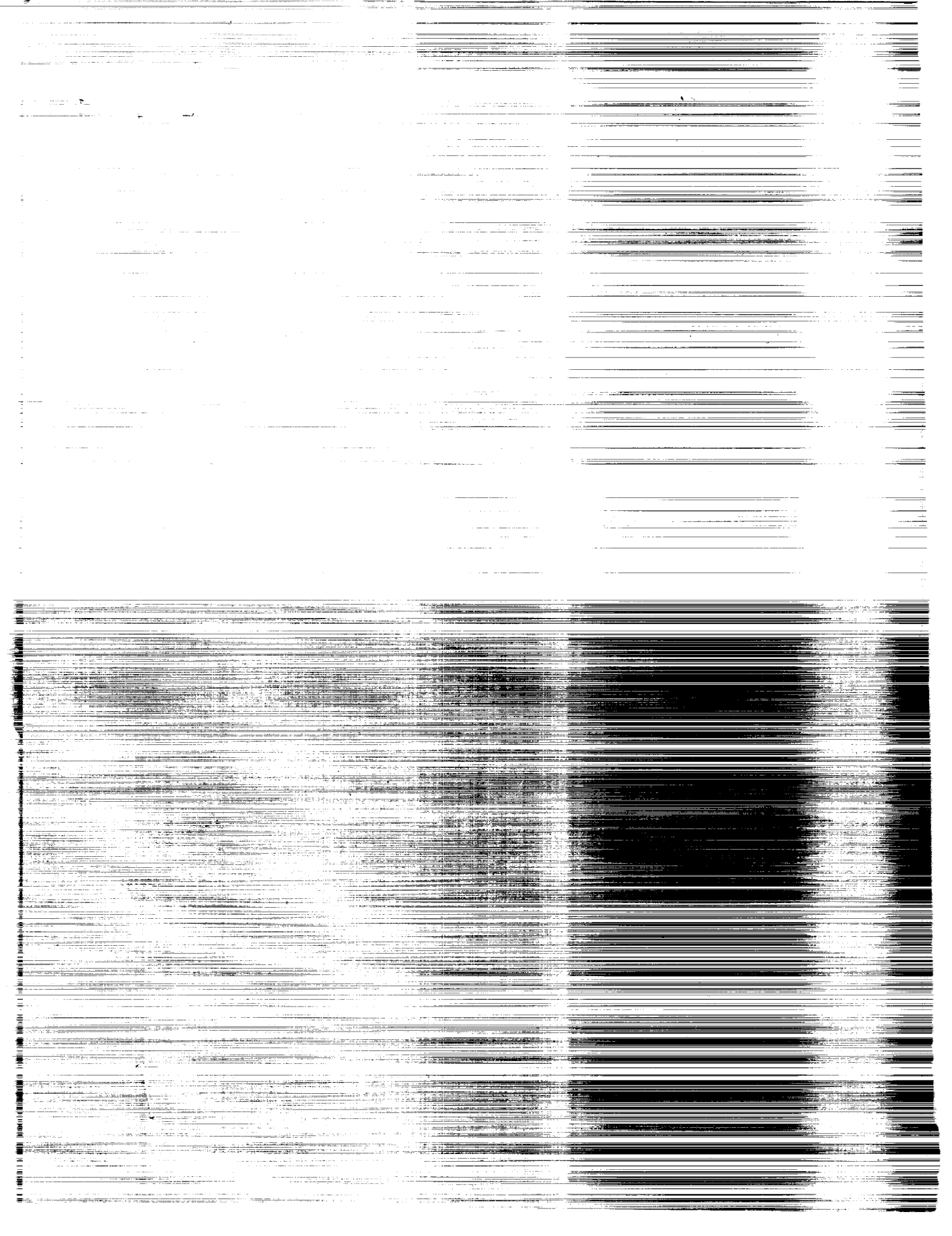Prepared Under Contract No. NAS1-16138

by

Bolt Beranek and Newman Inc.
Cambridge, MA 02238

for

NASA

National Aeronautics and
Space Administration

Langley Research Center
Hampton, Virginia 23665
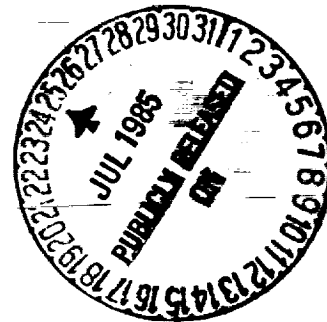
A STUDY OF INTERIOR NOISE LEVELS, NOISE SOURCES AND

TRANSMISSION PATHS IN LIGHT AIRCRAFT

R.E. Hayden
B.S. Murray
M.A. Theobald

July 1983

Review for general release____July 1985_____

TABLE OF CONTENTS

LIST OF FIGURES

LIST OF FIGURES

LIST OF FIGURES

iv

page

page

LIST OF TABLES

x

I. INTRODUCTION

Bolt Beranek and Newman Inc (BBN) is under contract to NASA Langley Research Center (NAS1-16138) to carry out the first phase of a program to demonstrate to the US manufacturers of propeller-driven light aircraft, methods for designing treatments for effective reduction of interior noise of their aircraft. The program consists of several phases, leading to a technology transfer from the program directly into the hands of the US manufacturers.

The motivations for this study were several: (1) the recognition that a satisfactory acoustic environment for crews and passengers is desirable from the point of view of comfort and safety, and necessary for reliable voice communications on board and through radio links; (2) evidence that many general aviation propeller aircraft types have cabin acoustic environments which are unsatisfactory to a large percentage of the prospective user population; (3) weight constraints on light aircraft which present a substantial challenge in applying noise control treatment without excessive penalties; (4) the belief that considerable technology is available for the modeling, diagnosis, and control of sound transmission into aircraft; and (5) recognition that it was important and timely to evaluate such available technology in an operational context on representative light aircraft.

The technical efforts began with a survey of all propeller-driven general aviation aircraft of US manufacture to determine their relative performance ranges, their impact on the total fleet (both present and future), and their internal noise characteristics. From these aircraft, 18 were selected for flight surveys. The purpose of the flight surveys was to measure internal noise levels and identify principal noise sources and paths under a carefully-controlled and standardized set of flight procedures. Once the survey had been completed and the results analyzed, one aircraft model was chosen for more detailed application of advanced noise source and path diagnosis. This aircraft was subjected to a second round of flight tests in which more detailed measurements of sources and paths were made and additional diagnostic ground tests were performed.

The results of the flight survey phase of the work confirmed that the present-day designs of both single-and twin-engine aircraft produce cabin noise levels which, when compared with results of careful psychoacoustic tests, would be considered

1

highly annoying to a large percentage of the population. The flight surveys also produced consistent evidence of propeller noise as a primary contributor to cabin noise in all types of aircraft, as well as revealing some evidence of engine and airflow noise being of considerable importance in most aircraft. The flight surveys are described in Sec. 2 and App. A of this report.

The diagnosis of one single-engine aircraft illustrated that to successfully separate the contributions of all sources and paths, extensive ground and flight measurements are required, and that further component-by-component testing is desirable in order to isolate the contributions of various paths by which the energy from a given source reaches the cabin. However, within the context of the tests and analyses carried out, a source-path model was constructed which, in composite form, produced predicted noise levels which agreed quite well with measurements. The diagnostic efforts are described in Sec. 3 and App. A of this report.

2. SURVEY OF IN-FLIGHT NOISE LEVELS OF REPRESENTATIVE LIGHT AIRCRAFT

2.1 Objectives

The ability to design noise control treatments applicable to a class of aircraft depends upon clear evidence that all the aircraft for which control measures are desired share common noise generation and transmission characteristics. Many measurements of interior noise have been made on general aviation aircraft and studies of sources [4,5,8,9, 21,27,28] and paths on particular aircraft have been conducted [1,2,3,6,7,10-20,22, 23, 24,29-38] . However, the published interior noise data for different aircraft was often taken under different flight conditions, thus making it difficult to use such data for a survey and comparison of a large segment of the fleet, or to derive consistent trends from the data regarding sources and paths on aircraft of contemporary design. Therefore, a controlled survey was indicated on a sample of aircraft of modern design. In an effort to characterize the interior noise environments of a representative segment of the fleet under nominally identical conditions, a flight test program was devised with the following objectives:

- Survey a representative sample of the general aviation fleet under similar and controlled operating conditions to document the interior noise levels of current generation production aircraft;

- Identify principal noise sources and paths in the aircraft under a standardized set of flight procedures; and

- Conduct as many diagnostic tests as possible to quantify noise source "strengths" and paths in terms of their importance to cabin noise.

From this series of tests, an aircraft which was representative of a large portion of the fleet could be selected for detailed diagnosis and later use as a study vehicle for design of noise control treatment.

3

Aircraft Selection

The aircraft considered for inclusion in the flight test survey were selected from a master matrix which included model designation, first year of airframe production, total number in service, sales trends, passenger capacity, weight, range, engine type and power. The characteristics of those chosen are listed in Appendix A, Tables A.1 and A.2. In selecting the actual models to be tested, the major criteria applied were:

* vintage of the airframe design, with contemporary designs being strongly preferred;

* current and projected sales volume;

* status of prior noise control efforts on the particular airframe;

* availability of aircraft for test purposes, and of support services of manufacturer.

The majority of the aircraft tested were new airframes with factory-installed interiors. Additional flights on several aircraft without interiors allowed diagnostic measurements on structural members which would normally be covered by trim material, as well as measurements of the noise in the untreated cabins. Other diagnostic tests conducted on the ground provided additional data on transmission paths. The range of aircraft available allowed testing of combinations of turbocharged and normally-aspirated engines with two- or three- bladed propellers. Also, several large turbine-powered twins were available for the survey portion of the study.

2.2 Flight Test Conditions and Instrumentation

Figure 1 illustrates schematically the standardized flight program devised to acquire survey and diagnostic data. The aim of the flight tests was to measure noise and vibration levels under representative yet controlled conditions. In attempting to choose a "standardized" operating condition for a large number of aircraft types, one is confronted with a number of issues. These include normal aircraft performance and operating ranges and the variability in atmospheric parameters which affect sound generation and transmission (such as density and sound speed). Flight manuals for the various aircraft tested describe cruise

4

Economy a)

Maximum Speed b)

③ LEVEL FLIGHT AT 5000 ft

② FULL POWER TAKEOFF

④ POWER-OFF DIVE

① TIE DOWN RUNUP TESTS
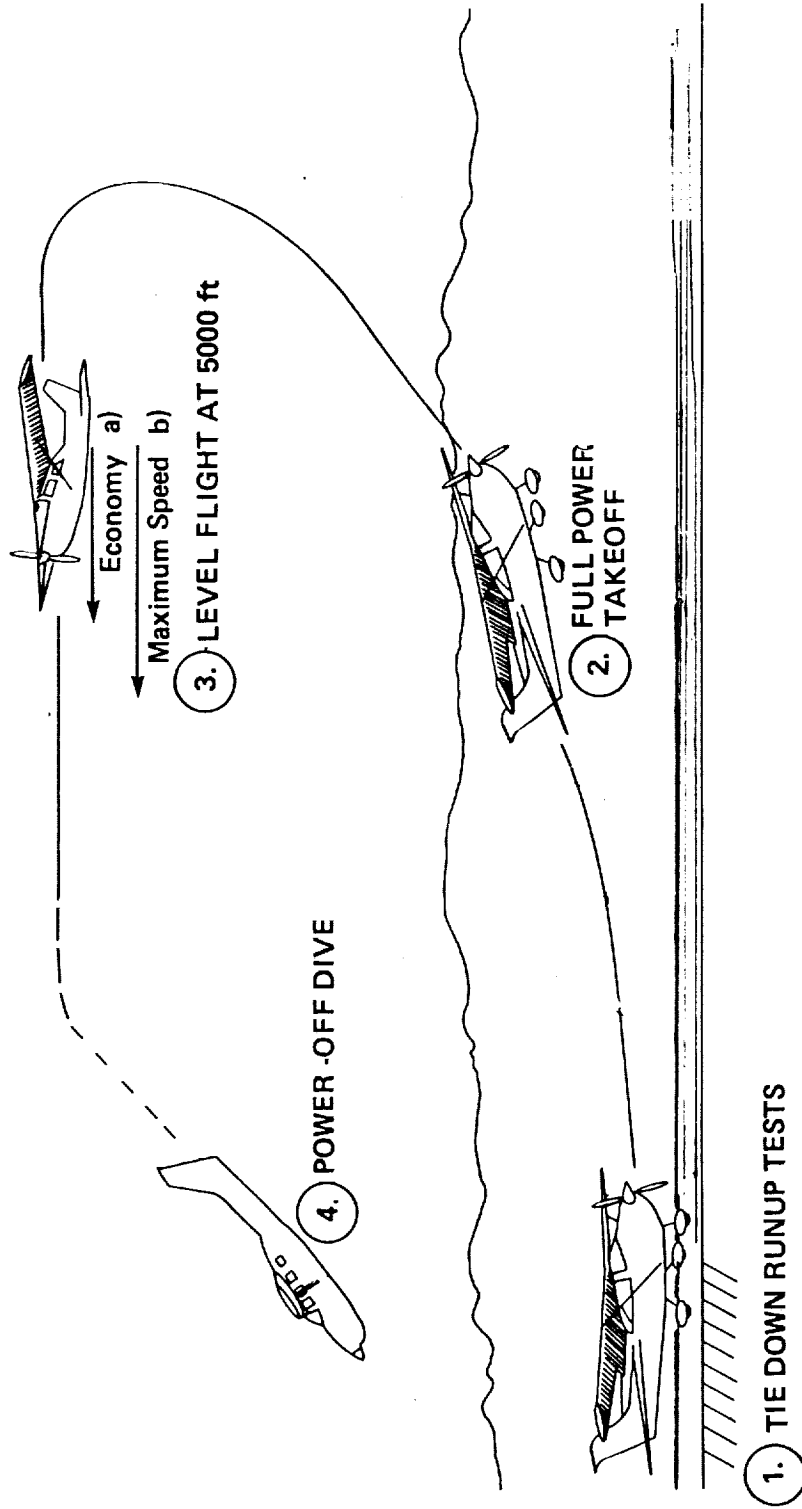
FIG. 1. SCHEMATIC OF STANDARD FLIGHT TEST

5

operations at altitudes varying from 610 m (2000 ft) to over
10,000 m (>35,000 ft). Figure 2a shows "typical" variation in
pertinent atmospheric parameters over that range of altitudes;
note that the exact values vary with geographic location and
weather condition, but the trends shown are typical. Thus,
conducting "standardized" tests at a different altitude for each
aircraft would require accounting for the effects of density and
acoustic impedance variations on source and path character-
istics. Furthermore, the performance of aircraft varies with
altitude for a nominal engine setting (which, in the case of
piston aircraft, consists of fixing the manifold pressure and
engine speed). Figure 2b illustrates the range of performance
variables which would be expected from a typical piston engine
aircraft (with turbocharger). Since most of the aircraft tested
were piston engine types, it was desired to choose a "standard"
altitude where the power produced by a normally-aspirated engine
was comparable to that produced by a turbocharged version of the
same engine. A nominal altitude of 1500 m (5000 ft) was deter-
mined to satisfy that criterion. However, that altitude was
unrealistically low for some of the larger twins which normally
are pressurized to allow comfort at higher altitudes. Therefore,
for the large twin and one pressurized single engine aircraft,
tests were conducted at their "normal" cruise altitudes, which
were usually in the range of 3100 - 3800 m (10,000 - 12,000
ft). In the analysis of test data, considerable variability in
levels was found at one altitude on particular aircraft; there-
fore, it was not possible to systematically isolate the effects
of altitude on interior noise levels. Most tests were performed
during straight and level cruise operation. Some data were also
taken during takeoff and climb, and a number of "tiedown" tests
on the runway and power-off dive tests were conducted.

The engines of piston-engined aircraft were operated at
"maximum continuous cruise speed" and at "most economical cruise
speed". This translates into engine speeds of 2400 RPM and 2100
RPM for most of the aircraft tested. Figure 2b shows typical
engine power output at these settings, as a function of alti-
tude. The actual conditions for each test are summarized in
Appendix A, Tables A.1 and A.2.

The passenger load on most single engine piston-powered
aircraft consisted of a pilot, an engineer in the copilot seat,
and an engineer in a rear passenger seat; the passenger and crew
weight was thus around 230 kg (510 lb). Passenger and crew loads
on the large piston-and turbine-powered twin engine aircraft
consisted of a pilot and copilot with two engineers in the

(a) Typical Atmospheric Properties

(b) Aircraft Performance
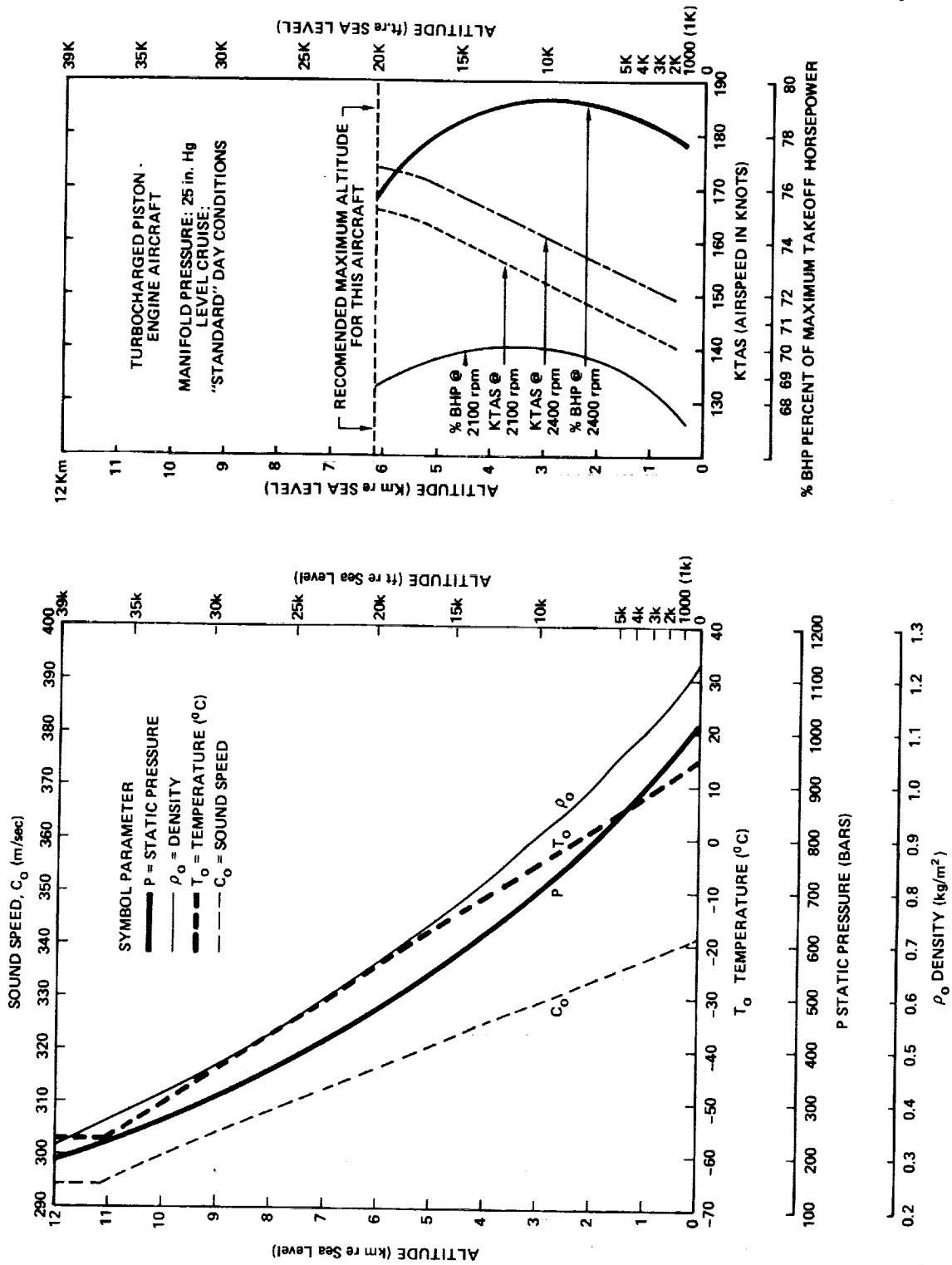
FIG. 2. TYPICAL VARIATIONS IN ATMOSPHERIC PARAMETERS AND AIRCRAFT PERFORMANCE
WITH ALTITUDE.

7

passenger cabin, a typical weight being about 310 kg (680 lb). No extra weight was placed aboard the aircraft beyond that of the recording instruments. This weight was approximately 14 kg (≈30 lbs) for survey flights, and 70 kg (≈150 lbs) for diagnostic flights, respectively.

During these tests, all air conditioning, heating, and ventilating systems were shut down for cabin noise measurements. Although these systems may be important noise sources in a quiet cabin, noise control treatments for them are well understood as compared to treatments for reducing propeller noise, engine-induced structureborne noise, and flow-induced noise.

Weather conditions for the flight tests varied widely from 43°C (110°F) ground level temperatures in Wichita, Ks, in July 1980, to 4.4°C (40°F) in Boston, Ma, the following October. No precipitation was encountered and winds aloft were usually strong. In all cases, attempts were made to find non-turbulent air near the desired flight altitudes for the actual data recording.

Two main sets of instrumentation were used for the flight tests:

(1) Recording instrumentation for survey flights of fully furnished aircraft consisted of:

   a) one-half in. (1.27 cm) condenser microphone with foam windscreen with battery-powered microphone preamplifier;

   b) 2 gm piezoelectric accelerometer, with internal preamplifier; and

   c) 2-channel instrumentation-type tape recorder.

The microphone and accelerometer were moved about the cabin during flights to record noise and vibration near important panels such as the windshield, side windows, etc. The mass of the accelerometer chosen for use was very small (2 grams) to avoid loading the light-weight panels used in aircraft construction. All transducers, preamplifiers, and recording equipment had a frequency response flat to at least 10 kHz.

(2)   Recording instruments for the detailed diagnostic
        flights (discussed in Sec. 3) consisted of:

        a)   Seven channel FM recorder (10 kHz bandwidth)

        b)   Six low noise amplifiers.

    The survey tests collected noise and vibration data for
important areas within the furnished cockpit/cabin. The minimum
data collected were:

    a)   Noise spectra at:

           - center of cabin between pilot and copilot (for all but
             turbine-powerd aircraft);

           - windshield

           - copilot side window

           - second side window (aft of doors)

           - rear window (if existing on the particular model)

    b)   Point, single-axis*, vibration spectra at:

           - windshield

           - seat rail and/or wing spar

           - copilot side window

           - second side window (aft of doors)

           - rear window.

2.3 Summary of Results of Survey

    A large quantity of data was obtained during the survey of
18 aircraft. Appendix A presents an expanded discussion of the
data itself. In this section of the report, a summary of overall
trends is presented.

---

*acceleration normal to local surface

A-weighted sound pressure levels (SPL) and speech inter-
ference levels (SIL (0.5, 1, 2, 4))** were calculated from data
gathered during the survey flights. Figure 3(a) presents a
summary of the range of cabin sound pressure levels which were
measured in single-engine aircraft, twin piston engine aircraft,
and twin turboprop aircraft, as a function of their maximum gross
weight. Only those with production interiors are included in
Fig. 3, although data for aircraft with partial or no interior
trim is included elsewhere in this report. Figure 3(b) provides
several curves which may serve as a guide to judging the accept-
ability of various A-levels or SIL's. These curves [from Ref.21]
illustrate the percentage of test subjects who were highly
annoyed when exposed to typical aircraft interior noise spectra,
while sitting (attempting no speech-listening), and while
attempting speech listening and speech communication. Such
curves can serve as guidelines for cabin noise goals or to
evaluate the acceptability of existing acoustic environments. It
is clear from these curves that the acoustic environments in the
18 aircraft surveyed would be unacceptable to well over 50% of a
typical passenger population.

The data presented in Fig. 3(a) consist of ranges of A-
weighted levels and SIL (0.5, 1,2,4) for each aircraft on typical
straight and level cruise flights within the previously-described
standard flight test regimen. On each aircraft sampled, the
sources of the variations in levels include variations in power
settings, engine and flight speeds, in-cabin spatial variations
and flight-to-flight variations. In most cases, only one sample
of each aircraft was tested; thus no aircraft-to-aircraft sample
variability is included, although it would be expected that this
factor could further increase the spread in the data for a given
aircraft. The variability issue is discussed further in this
report in Sec. 2., Sec. 3, and Appendix A.

The data follow reasonably systematic trends with the single
piston engine aircraft producing the highest speech interference
levels and nearly the highest A-weighted levels measured. A
general consistency in the A-level of piston engine aircraft is
observed, with lower levels being seen on turboprop Aircraft E,
the only pressurized single-engine aircraft in the sample, and on
turboprop machines. The reasons for Aircraft E's lower noise
levels may include its pressurization and the attendant heavier
wall construction and airtight seals required, and/or its bed-
mounted engine. The reasons for lower turboprop noise levels
probably include the lower noise and vibration of turboshaft
versus piston engines, the heavier fuselage structures used on

---

**ANSI standard ANSI S3.14-1977 defines the speech interference
level SIL (0.5, 1, 2, 4) as the arithmetic average of the sound
pressure levels (in dB re 2×10^{-5} N/m^2) in the 500 Hz, 1 kHz, 2
kHz, and 4 kHz octave bands.
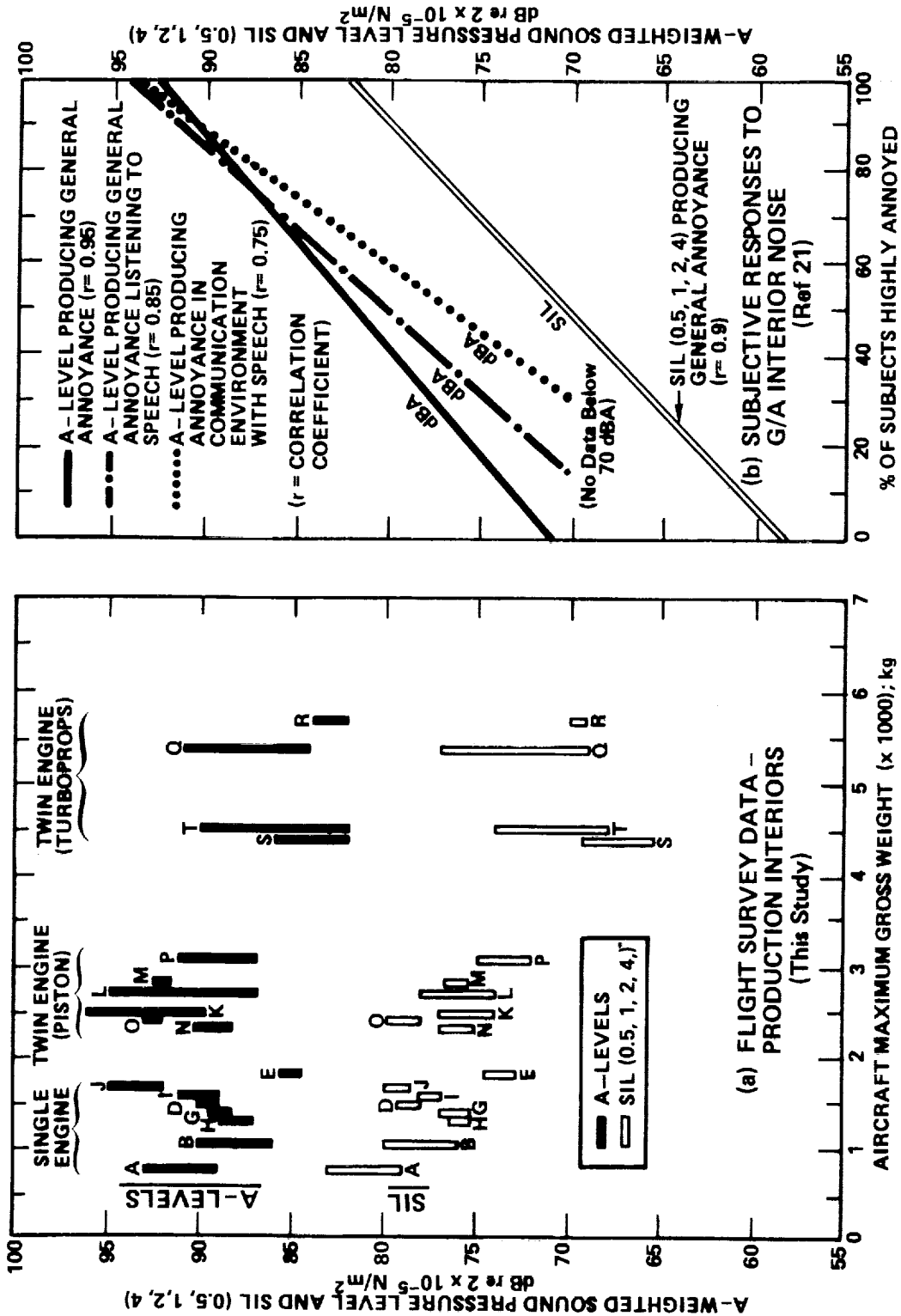
(a) Flight Survey Data

(b) Subjective Judged Acceptability

FIG. 3. SUMMARY OF A-LEVELS AND SIL'S MEASURED IN FLIGHT SURVEY AND JUDGED ACCEPTABILITY.

11

the larger aircraft, flight conditions, (e.g., operating with a smaller fraction of maximum payload thus enabling reduced power and creating slightly different flow field details over the airframe). Furthermore, the steady reduction in SIL with increase in aircraft weight is probably due to the trend toward more cabin noise treatment which is possible in the larger machines due to their relatively larger payload weight margins as compared to the weight margins of the smaller aircraft.

It is interesting to compare these results with noise levels measured in other familiar vehicles. Figure 4 summarizes A-levels for autos, busses, rail cars, CTOL jet transports, helicopters and general aviation aircraft [Ref's 4, 33]. The range of A-levels measured in this survey is toward the lower end of the range reported by Wilby and Smullin [Ref 33]. This may be due to the fact that the present data includes only level cruise conditions, whereas the data in Fig. 4 presumably includes takeoff conditions (for CTOL also). The levels observed in the largest aircraft tested (5700 kg) overlap the upper part of the range of levels in commercial transports.

The range of noise levels observed in most of the aircraft surveyed is sufficiently large that extreme care must be taken in setting reduction goals, and measuring noise reduction. The causes of variability are addressed further in the next section of this report.

Cabin noise and vibration spectra from each aircraft tested are presented in Appendix A. Representative spectra will be discussed in this part of the report to point out trends observed as well as significant factors which may influence noise control design. Figure 5 shows A-weighted third octave spectra for three aircraft covering the full range of those tested. It is convenient to present the analysis after A-weighting has been applied so that the relative acoustic importance of sources in each frequency band to the overall dBA level can be easily assessed. (In Figs. 5(b) and 5(c), the data are abbreviated at the higher frequencies due to the limits of the tape recorder noise floor having been reached; the recordings were made with flat frequency response, with A-weighting being applied on replay.)

Several observations can be made from examination of the three plots in Fig. 5.
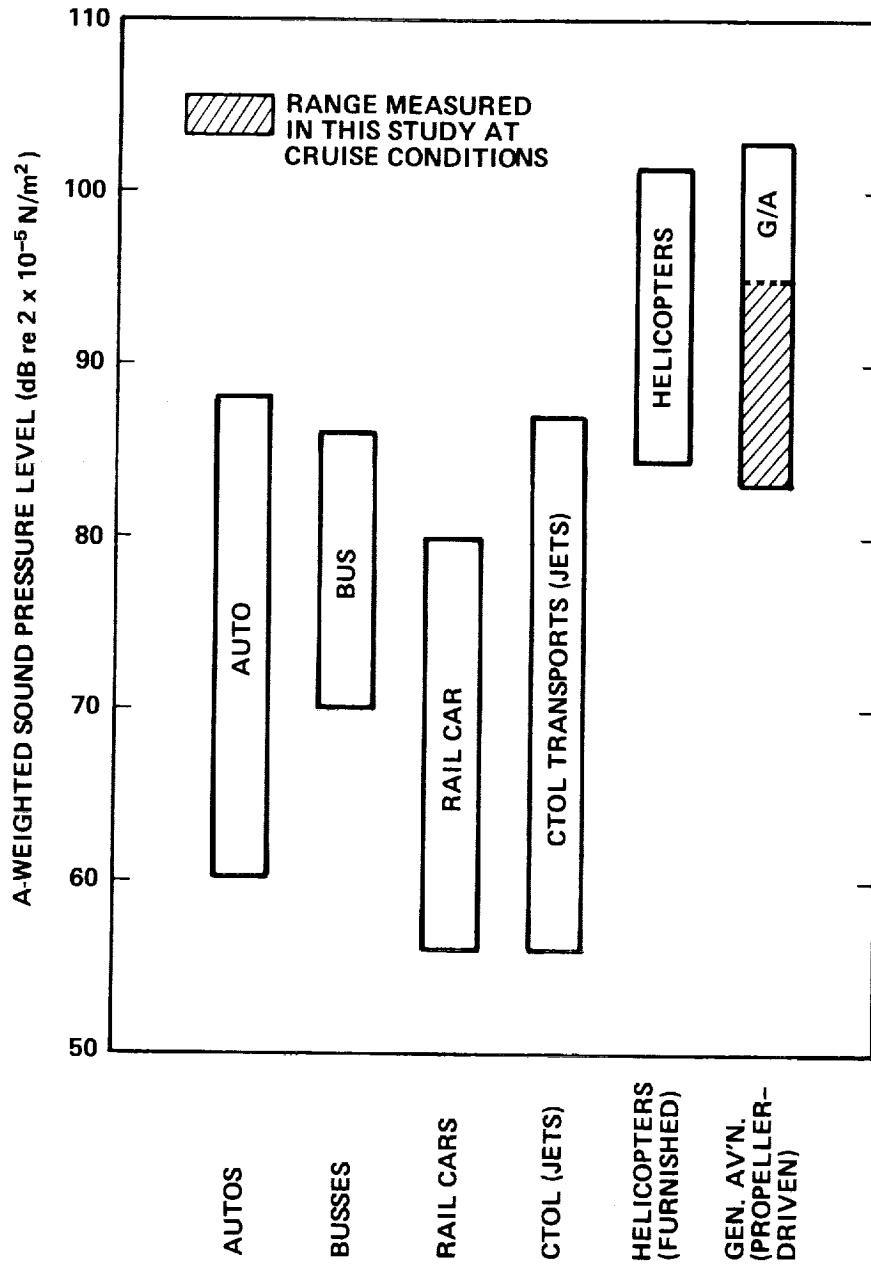
FIG. 4. COMPARISON OF MEASURED NOISE LEVELS WITH THOSE FROM OTHER VEHICLES.
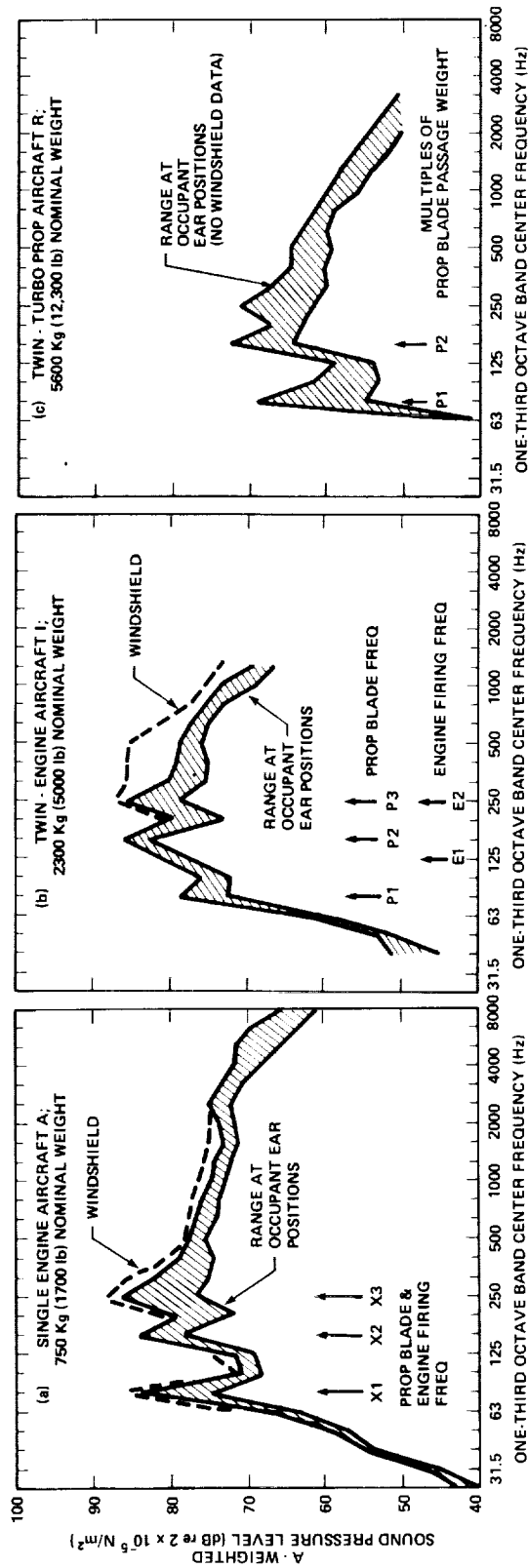
FIG. 5. CABIN NOISE SPECTRA FROM 3 AIRCRAFT COVERING WEIGHT RANGE
OF ALL TESTED.

14

- All three spectra show strong tonal behavior at the propeller blade passage rate and the first few harmonics; typically the energy at the second and third harmonics of the blade rate contribute more to the A-level than that at the fundamental frequency; on Fig. 5(a), the prop blade and engine firing frequencies and their harmonics coincide, so an unambiguous distinction between their relative contributions cannot be made from a simple spectral analysis.

- Considerable variability in the levels around the cabin exists, with the levels near the windshield usually being the highest at most frequencies.

- The energy above the third propeller harmonic makes a significant contribution to the A-level.

- In Fig. 5(b), the cabin noise at the engine firing (E1) frequency can be separated from noise at the propeller fundamental (P1) and first harmonic (P2). In some narrowband analyses, radiated noise is also as evident at 1/2 the firing frequency (E 1/2); however, in some cases, the E 1/2 frequency also does not coincide with a prop rate harmonic, so a reasonably clear separation of contributions can be made.

Such information is helpful in understanding the character of interior noise in general aviation cabins, but does not provide sufficient guidance toward conceiving noise control treatments, since all sources are not explicitly quantified, and the paths by which the energy from each source reaches the cabin are not identified. The discussion that follows describes further analysis of the data which provides additional clarification regarding sources and paths.

15

2.4 Preliminary Observations Relating to Diagnosis of Predominant Sources and Paths

In addition to obtaining surveys of A-weighted and speech interference levels, and 1/3 octave band spectra on 18 aircraft, one objective of the study was ranking of predominant source/path combinations in the various aircraft. This work was aimed at guiding future work on detailed source/path diagnostics and in judging the generality of the applicability of noise control treatments designed for one aircraft.

The ideal way to conduct source and path diagnosis is to eliminate all but one source, and study its characteristics and transmission paths systematically, then repeat the process for each other source. Such a process would probably require a large low noise wind tunnel where the correct aerodynamic loading on the propeller and airframe could be achieved. Since the preliminary survey allowed for only brief time to study each aircraft, other methods had to be relied upon for the diagnosis. The methods included:

- pragmatic experiments, such as: (a) engine-off dive tests, where propulsion sources could be suppressed relative to flow-related sources, and (b) changing number of blades on a propeller from 3 to 2 in order to separate the frequencies of the sound and vibration emanating from the propeller and engine at fundamental blade and firing rates;

- narrowband spectral analysis to assist in deducing spectral contributions associated with periodic phenomena;

- surveys of structural vibration at accessible surfaces in the cabin to help locate the most significant radiating part of the transmission paths.

The amount of experimental diagnostic work possible varied from one test aircraft to another due to aircraft availability, access to structural members for mounting transducers, and extent of interior furnishing. However, even in those aircraft for which only minimum diagnosis was possible, inspection of the interior noise spectra allows for some ranking of predominant sources, although propagation path ranking for a given source is more ambiguous in such cases.

Narrowband Analysis to Identify Constituents of Spectra

In general, the predominant sources of energy which create cabin noise are the propeller, powerplant, and turbulent flow over the airframe. The frequency spectra previously shown in Figs. 5(a) – (c) were examined to attempt to assess the relative contributions of the propeller and the engine. Although the distinctive frequencies produced by the first two sources may be identified in narrowband analysis, the broadband contributions are more difficult to attach to a particular source. The narrowband sources are discussed first.

In engines designed for power ranges below 157 kw (210 hp), the combination of propeller and powerplant in reciprocating engine aircraft usually consists of a two-bladed propeller directly coupled to a 4 cylinder engine. Higher power installations comprise 6 cylinder engines which are usually directly coupled to three-bladed propellers. Since all current aircraft reciprocating engines are four cycle designs, the fundamental firing rate and propeller blade passage rate are the same for the installations described above. (Cylinders are arranged such that opposed pairs of pistons work together, thus producing one firing per revolution per cylinder pair; therefore, a four cylinder engine has a firing rate of 2x RPM, and a 6-cylinder engine has a firing rate of 3x RPM.) It is thus impossible to separate the two sources by simple frequency analysis at a single point in the field or in the cabin for the situations described above.

However, certain single and twin engine aircraft are fitted with 6-cylinder engines and 2-bladed propellers, which leads to frequency separation between the prop and firing fundamental frequencies and many of the harmonics. For example, consider a 6-cylinder engine running at 2400 RPM connected to a two bladed propeller. The engine firing harmonic frequencies will be 120, 240, 360, and 480 Hz etc., and the propeller frequencies will be 80, 160, 240, 320, 400,, and 480 Hz etc. (Note that in some engines, there is also observable acoustic energy radiating from the exhaust at 1/2 firing frequency, or 60 Hz in this case.) Thus the fundamental and third harmonic of the engine firing are separated from the fundamental, 2nd, 4th, 5th of the propeller, and thus allow the contributions of the two sources to be readily identified. Figure 5(b) showed example of this technique applied to a piston-engine twin, while Fig. 5(a) illustrated the ambiguous situation where prop and firing rates were identical.

To clarify the contributions of these two sources for selected aircraft, narrowband analysis was conducted on certain transducer signals. Figure 6 illustrates a narrowband analysis of the noise in the cabin of an aircraft with a single 6-cylinder engine, and a two-bladed propeller (Aircraft D from Appendix A). This analysis is A-weighted to aid in assessment of the relative contribution of the various spectrum features to the A-weighted level. The 400-line analysis extends to 2 kHz to cover the most significant part of the frequency spectrum (Note that Fig. A.3 in Appendix A provides the companion 1/3 octave band survey.) The unambiguous frequencies associated with propeller and engine rates have been indicated as P1, P2, etc., and E1, E3, etc. It is apparent that the majority of the significant peaks up to 600 Hz are due to propeller blade rate harmonics, although the peak at the engine firing frequency (120 Hz) is quite large. The relative contributions at frequencies where both propeller and engine harmonics occur depends, of course, on the harmonic content of each source's spectrum. The relative levels of propeller harmonics are influenced by blade loading details and by the amount of inflow distortion to the prop, which in turn is related in part to the upwash velocities ahead of the wing. The upwash velocity disturbance is a function of aircraft weight and forward speed. The relative levels of engine firing rate harmonics are influenced by the type of exhaust system used, the presence of turbocharger on the inlet, and power output of the engine.

From this narrowband analysis of one aircraft, it is obvious that the propeller is the dominant source of low-frequency tonal noise. The role of airborne vs. structureborne paths is not clarified by simple spectrum analysis. The engine is also clearly contributing at firing rate, and possibly at the first 6 harmonics of firing rate. As was the case with the propeller contribution, this data by itself is insufficient to point out the predominant paths. It can also be observed that broadband contributions are significant - less than 10 dB down from most discrete frequency components, and occuring over more frequency bands. Thus, all that can be concluded from a narrowband analysis is that many sources of cabin noise can be identified, and as with any complex noise control problem, all sources contributing equally or nearly equally will need to be reduced to achieve a significant overall reduction.
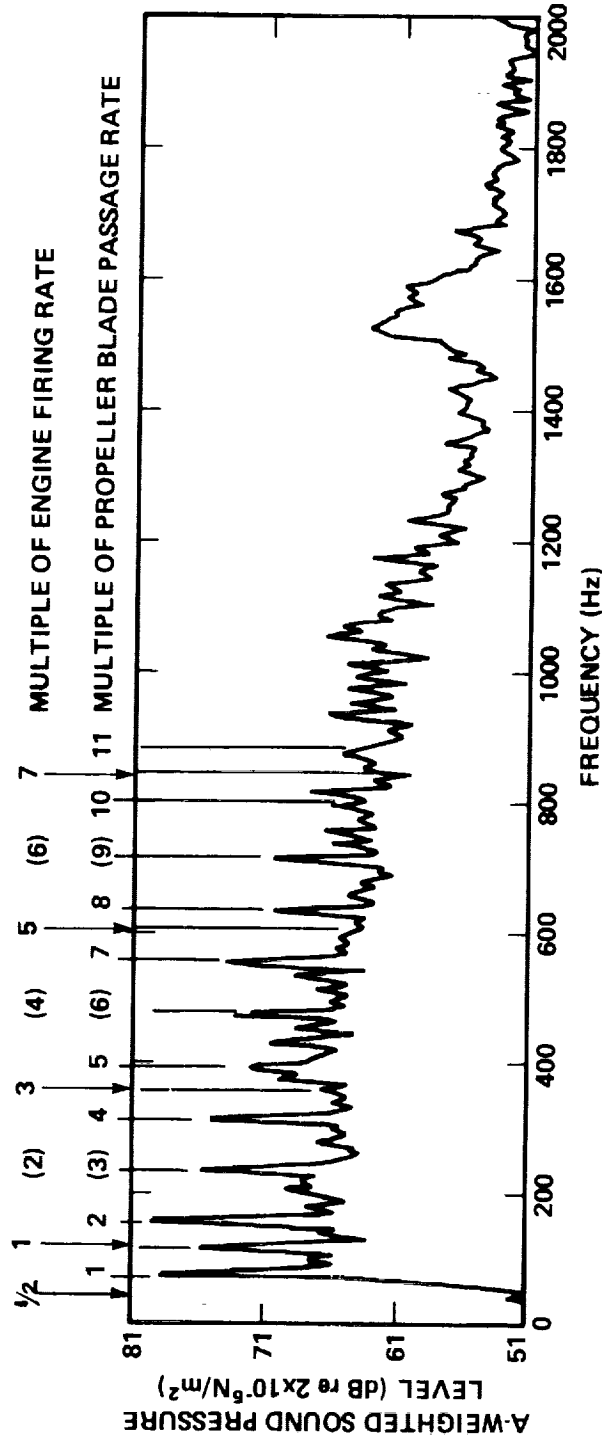
FIG. 6. NARROWBAND ANALYSIS OF CABIN NOISE OF SINGLE-ENGINE AIRCRAFT
(2400 RPM CRUISE).

19

Role of Noise Not Originating in the Propulsion System

It is well-known that current generation commercial passenger-carrying jet transports experience interior noise caused by flow over the airframe (i.e., non-propulsion sources). This flow consists of a turbulent boundary layer over the fuselage which excites vibration of the skin, both hydro-dynamically and acoustically (the distinction being the convection velocity of the disturbances); another form of non-propulsion noise arises when the boundary layer on the wings and control surfaces encounter a surface discontinuity such as the trailing edge, at which point substantial sound may be generated and subsequently radiated onto the exterior of the fuselage. The precise separation of these two classes of sources has not been accomplished convincingly for jet-powered CTOL aircraft, or for propeller-driven light aircraft.

In order to assess the possible role of non-propulsion sources on the aircraft being surveyed, pragmatic experiments were devised and conducted on several aircraft. In several cases, it was possible to conduct a power-off dive test of the aircraft to achieve a steady speed approximately equal to the speed achieved in level flight.

In the case of the twin-engined aircraft, it was possible to fully feather the propeller blades and stop the propellers and engines completely. However, in the case of the single-engine aircraft, it was not possible to feather the propeller completely, and thus the engine continued to turn even though the engine was shut off. In such cases, the propeller noise is expected to be minimal, but its wakes will excite the fuselage; also, the engine vibration continues, and backfiring may occur producing occasional exhaust noise.

Figure 7 shows the result of a test on a single engine airplane, which was fitted with a production interior. The landing gear were retracted for this test as they had been for cruise measurements. It can be seen that the noise during the dive is similar to the magnitude of the noise in normal cruise operation. Figure 8 shows a narrowband analysis of the same test, from which it can be seen that the "power-off" levels are nearly identical to the cruise levels except in about 25 of the 400 bands in the analysis, where engine and propeller harmonics are evident. Since the engine continued to turn during the dive, one could not rule out propulsion-related sources in Fig. 8 without a more thorough monitoring of exhaust pressures, mount vibration, engine compartment noise, and propeller wake charac-

20
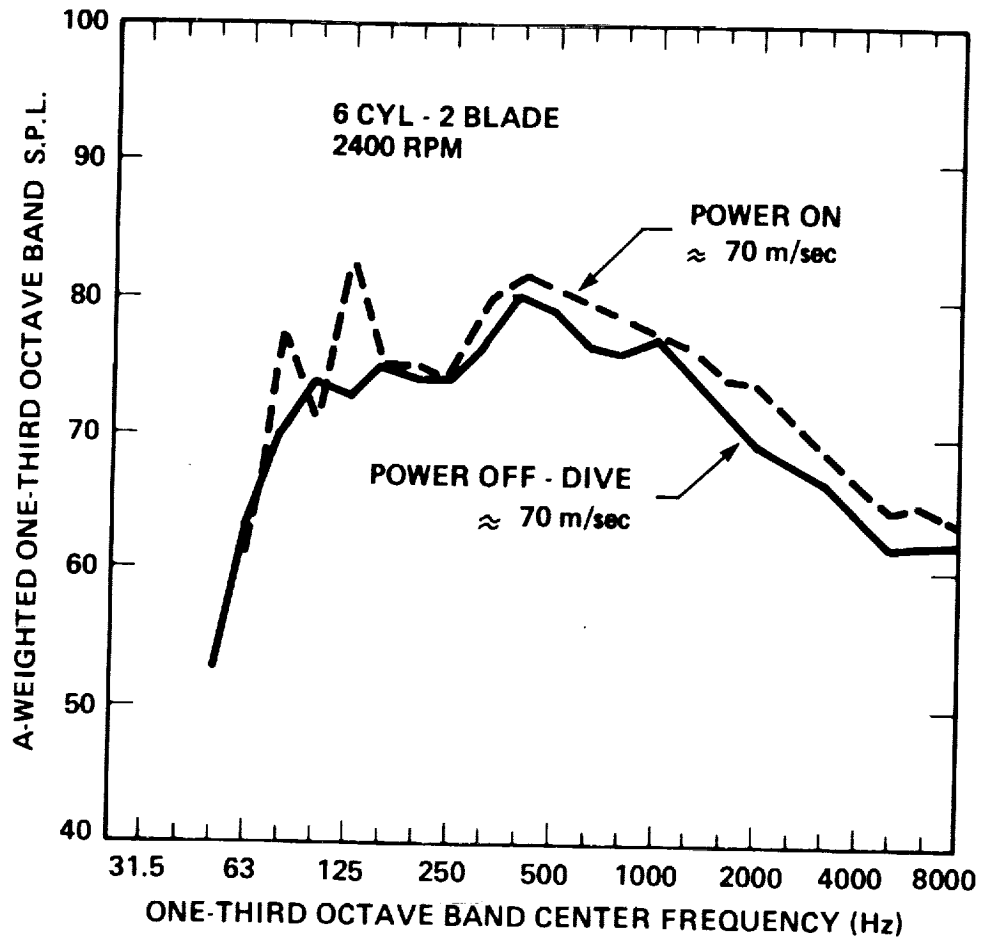
FIG. 7. COMPARISON OF CABIN NOISE ON SINGLE ENGINE DURING CRUISE AND DIVE.
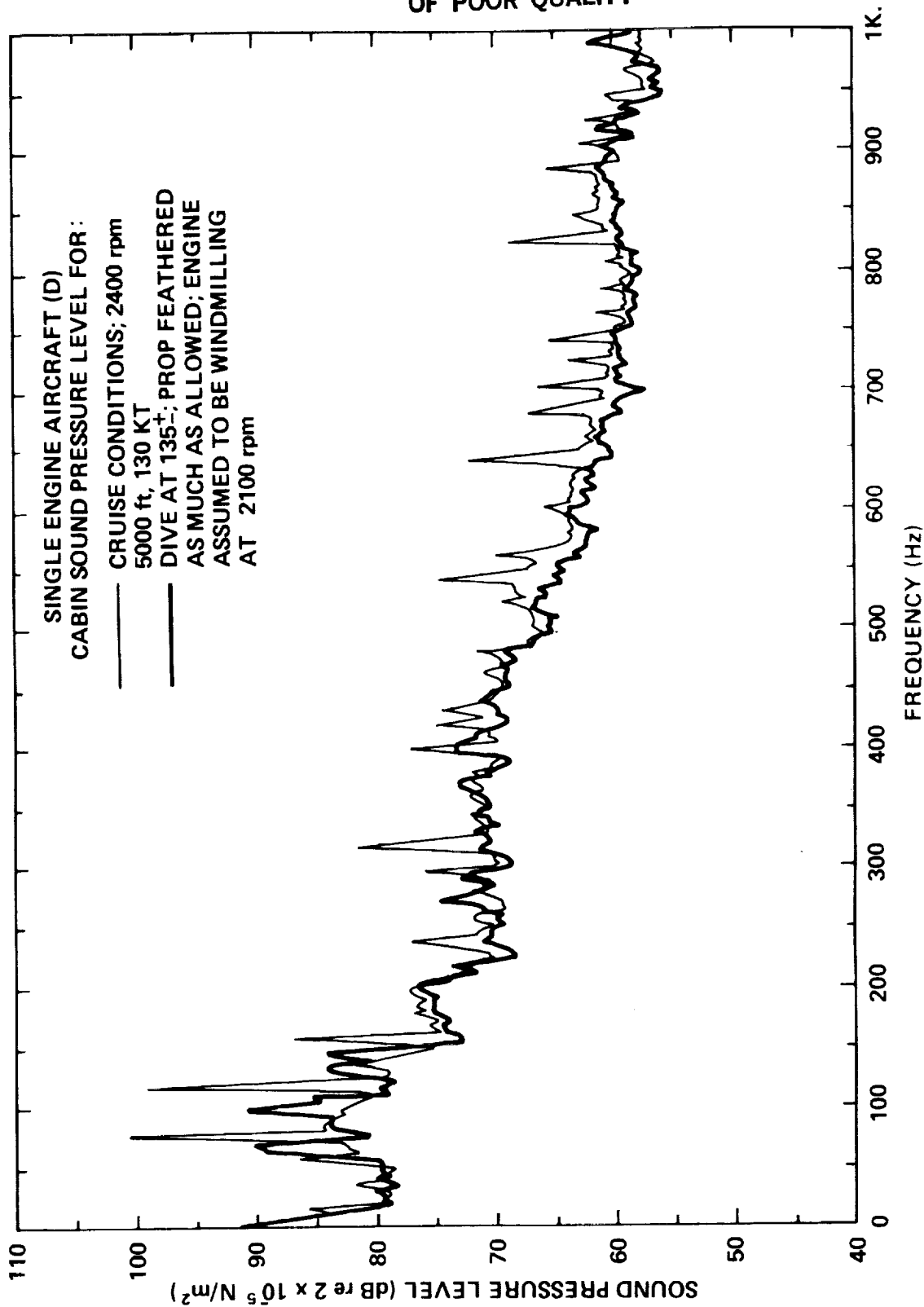
FIG. 8. NARROWBAND ANALYSIS OF CABIN NOISE IN SINGLE ENGINE AIRCRAFT DURING CRUISE AND DIVE.

22

teristics. However, these tests showed that nonpropulsion sources may play a significant role in determining the cabin A-level at cruise for single engine aircraft, and thus treatments may be needed over a large area of the fuselage.

Similar dive tests were carried out with several twin-engine aircraft, on which propellers and engines could be brought completely to a stop without creating unusual propeller wakes which would excite the fuselage in an uncharacteristic manner. In most cases, the dive speed did not reach the cruise velocity. Therefore, a scaling relationship was needed to extrapolate non-propulsion noise measured at a low speed to the cruise velocity for comparison with "all sources". Figure 9 shows the results of one such scaling test, where data taken at 110 kt is scaled to closely match the 150 kt data using a V^4 relationship, which is normally associated with the scaling of mean-square pressures in a turbulent boundary layer, wake, or jet when the turbulence structure remains basically unchanged over the speed (and Reynolds number) range of interest. No frequency shift is applied since it is assumed that:

(1) the spectrum of boundary layer pressure fluctuations is quite flat in the frequency range of interest;

(2) the aircraft structure is responding as a resonant spatial filter; and

(3) the damping and radiation efficiency of the structure do not change over the speed range of interest (i.e., there is insignificant fluid/structural coupling).

These 150 kt data are then scaled to the 178 kt cruise condition by a V^4 relationship; the comparison with "engine on" noise levels is shown in Fig. 10. Again, the non-propulsion contribution to the broadband spectral levels is found to be substantial. In this case, the only major uncertainty is whether or not the flow field over the aircraft was identical between the dive and cruise conditions. Of particular interest is the relatively large contribution to the low frequency levels; this suggests the existence of large scale turbulent structures either along the fuselage (such as at the wing root junction), the generation of low frequency trailing edge noise at the same locations, or possibly, the excitation of low frequency vibration of the tail section by the wing wake or separated flow behind the cabin.

During the same tests, a side window was instrumented with an accelerometer at its geometric center. The vibration levels measured at the 110 kt dive were scaled to 178 kt using the V^4 relationship. Figure 11 shows the comparison of the power on and scaled dive curves, indicating that the window vibration may be largely flow-induced, except at propeller harmonics.

23
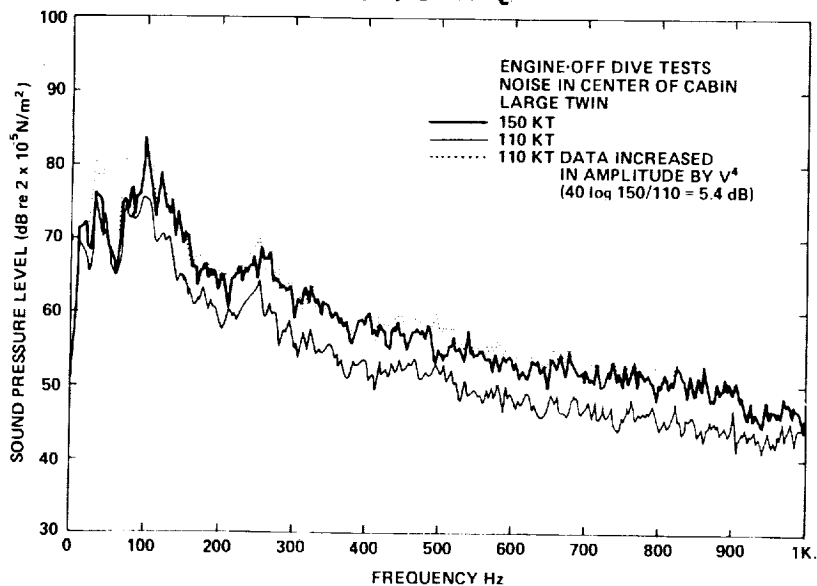
FIG. 9. CABIN NOISE DURING ENGINE-OFF DIVE TESTS OF LARGE TWIN.
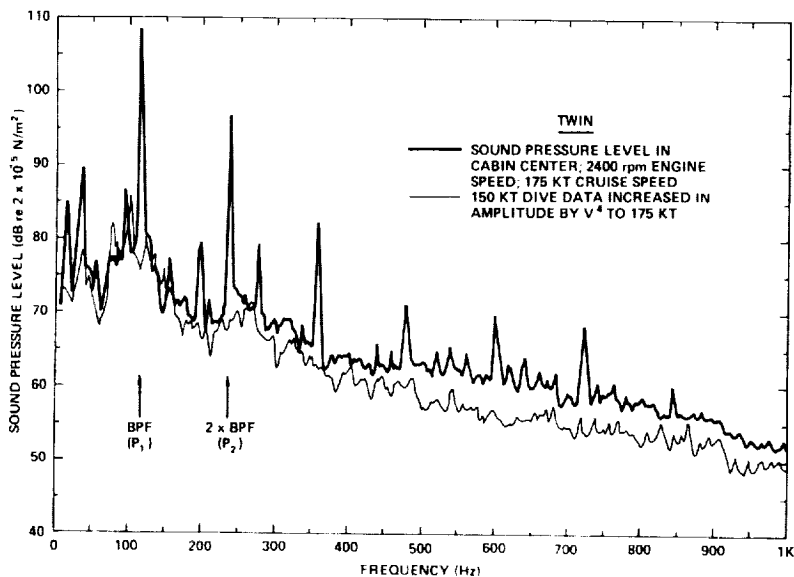
FIG. 10. COMPARISON OF CRUISE CABIN NOISE IN LARGE TWIN WITH
EXTRAPOLATED NONPROPULSION NOISE.

POINT ACCELERATION ON TWIN ENGINE AIRCRAFT
2nd RIGHT HAND SIDE WINDOW

—— MEASURED VIBRATION ON WINDOW
AT 178 KT CRUISE;2400 rpm
—— MEASURED VIBRATION FROM 110 KT DIVE
SCALED TO 178 KT BY V^4 IN AMPLITUDE
(NO FREQUENCY SHIFT)

FREQUENCY (Hz)

ACCELERATION LEVEL (dB re 1g rms)
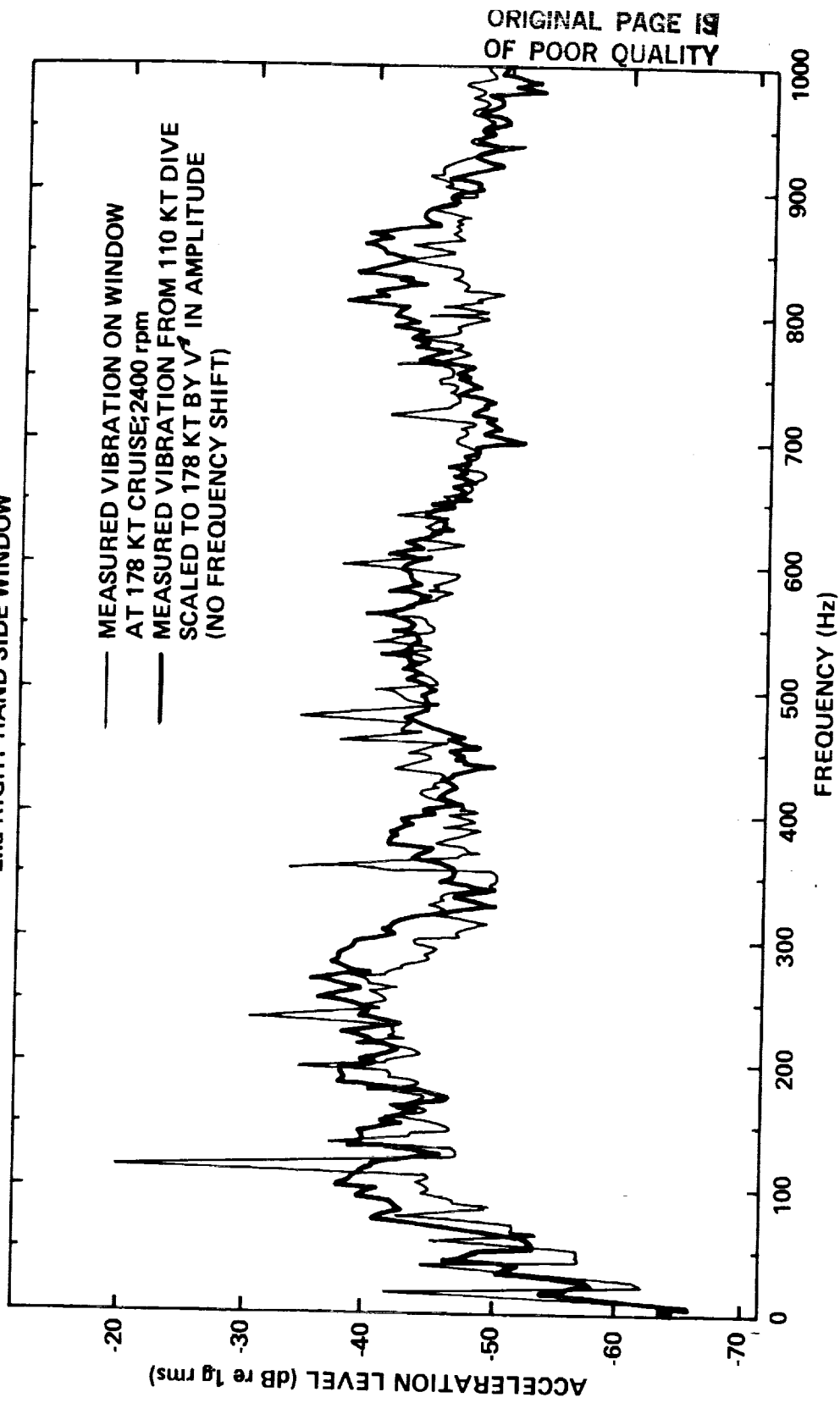
FIG. 11.   COMPARISON OF MEASURED WINDOW VIBRATION IN CRUISE AND
ENGINE OFF DIVE ON A LARGE TWIN.

25

The inference we draw from these limited tests is that, for single engine aircraft, the non-propulsion sources are approximately equal to those of the propulsion system in terms of their contribution to the A-weighted level and SIL when aircraft are operated at their normal cruise speed and altitude (relative contributions may vary at other speeds, altitudes, and power settings). However, the tonal sources related to the propulsion system are probably more annoying. For twin-engine aircraft, the propeller tones dominate the cabin levels, although the non-propulsion-system noise seems to control most of the broadband noise. It is likely (but not necessarily assured) that sidewall treatments which would reduce propeller airborne noise on twins would also reduce the broadband noise from the nonpropulsion sources.

Accelerometer Surveys

During the flight tests, single-point vibration measurements were made on cabin interior surfaces which were considered to be relevant to the radiation of noise into the cabin. Typically, measurements were made on the windshield, cabin windows, and roof panels as these are large areas for potential radiation. Measurements were also made in structural parts of the fuselage such as seat frame rails, door frames and the wing spar (all are summarized in App. A).

No effort was expended on this survey to interpret the vibration measurements unless resolution of a particular issue could be made. One example of such a use is presented for the case of a single 6-cylinder engine aircraft with two-bladed propeller which showed a dominant engine firing rate in the cabin noise spectrum. (As has been discussed, the unambiguous identification of an engine firing rate in the cabin noise spectrum was a somewhat unusual phenomenon and provided impetus for further investigation.) Figure 12 shows a restricted range A-weighted 1/3 octave band noise spectrum in the cabin at three locations, all of which show a high level at engine firing rate (E1). Also shown in Fig. 12 are the vibration readings taken at three locations. Note that none of the locations show evidence of a dominant peak at firing frequency (E1). This suggests that the engine firing frequency is entering the cabin in a localized area, possibly due to firewall radiation or an acoustic leak. The vibration measurements suggest that this noise does not enter through the vibration of the primary airframe structure or the radiating surfaces close to the occupant's ear positions.

While the presence or absence of a dominant frequency may be relatively easy to identify, the comparison between vibration and noise levels can lead to ambiguous conclusions. The vibration levels are significantly higher on the side window than on the

26
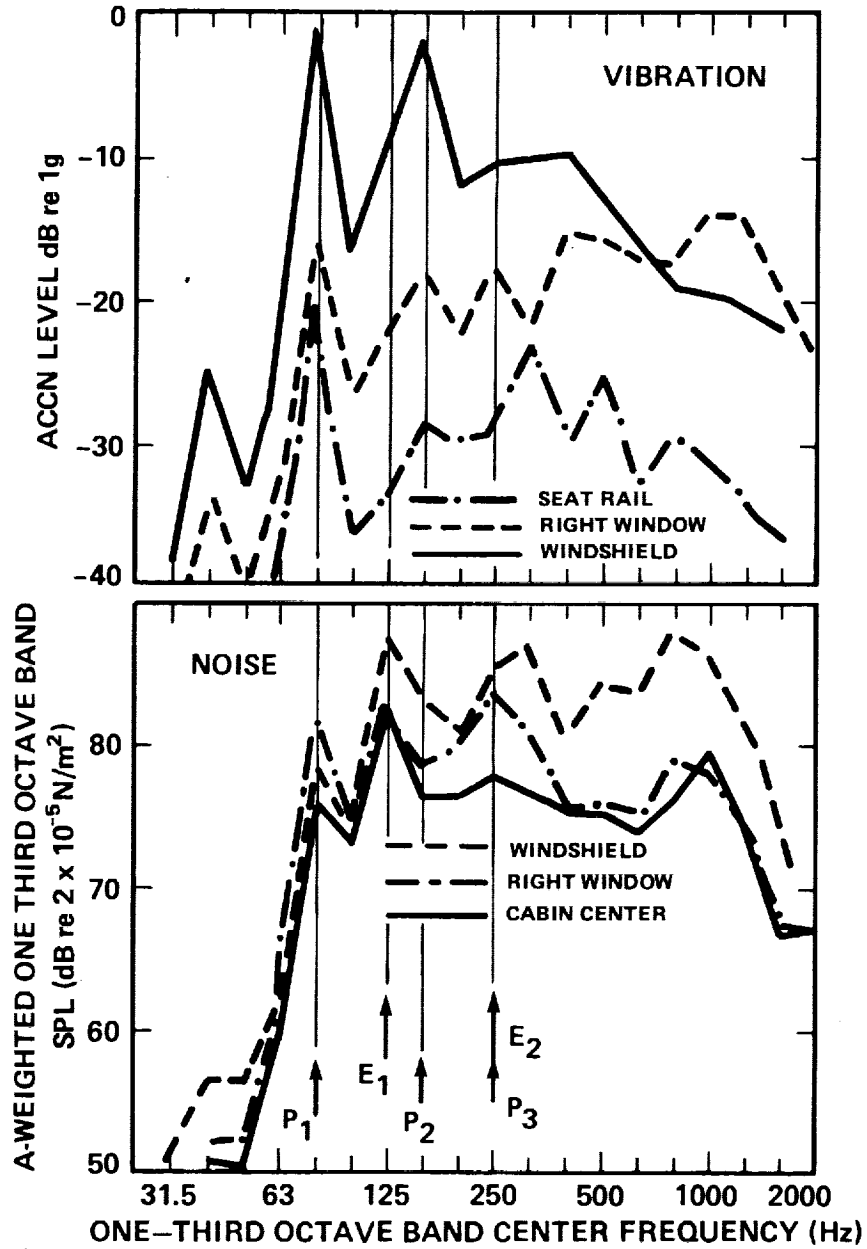
FIG. 12. NOISE AND VIBRATION COMPARISON SHOWING ABSENCE OF
FIRING RATE IN VIBRATION SIGNATURE (AIRCRAFT D).

windshield and yet the noise levels near the windshield are
generally higher than those adjacent to the side window. Never-
theless, the data suggest for the aircraft in question that the
engine firing tone emanates from a local point in the cabin
whereas the propeller noise is transmitted to the cabin by
vibration of a number of surfaces.

Repeatability of Data

Analysis of the flight tests on those aircraft without
interior trim revealed a substantial variation from flight-to-
flight of interior noise for the same nominal flight condi-
tions. Figure 13 shows such variations for the test aircraft at
two engine speeds. The extent of the variability was less in the
aircraft with the production interiors. This effect was not
noted until after the data had been analyzed. All the tests were
conducted with tape applied over the door joints to minimize the
obvious candidate air leaks. The cabin air vents, which are
connected to the wing leading edge, were also closed for these
tests. Although variability due to air leaks may be expected at
higher frequencies, it appears improbable that these are the
cause of variations at the lower orders of propeller blade
tone. This aspect was investigated further as far as the blade
tone variability was concerned and the results are presented
below.

Cabin Noise Amplitude Variation

In many instances the major interior noise level occurs at
the propeller blade frequency. The sources of this noise are
acoustic from the blades' airfoils due to the usual mechanisms of
rotational noise, which is coupled through the air to the cabin
walls, and the vibration of the aircraft at propeller blade rate
which is due to the aerodynamic and structural imbalance forces
acting at the propeller shaft. The aerodynamic imbalance may
fluctuate with the inflow of turbulence or in response to
aircraft control movements.

In-depth analyses of the data taken on one aircraft (having
stripped interior) to gain a greater understanding of the under-
lying causes for variations in amplitude. The time-varying
response of transducers located at key points in the aircraft was
plotted. Figure 14 shows the results of this test at two engine
operating speeds. Each sample consists of time synchronized
recordings made over a three minute period during which the
engineering test pilot maintained the steadiest possible flight
conditions. The time histories represent the RMS amplitudes in
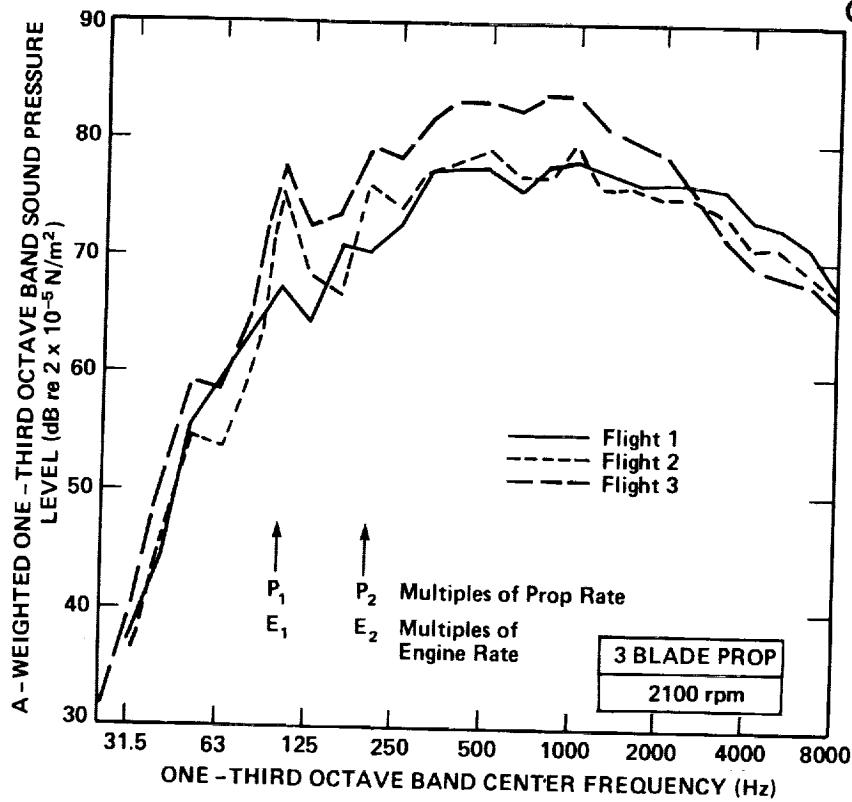
(a) 2100 RPM
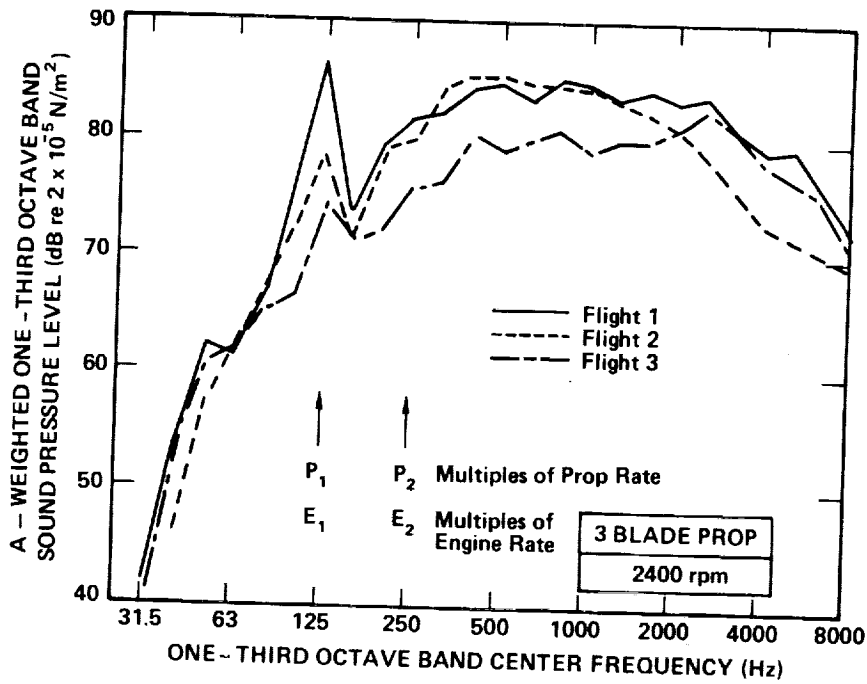
(b) 2400 RPM

FIG. 13. FLIGHT-TO-FLIGHT VARIATION OF CABIN NOISE LEVELS
(SINGLE-ENGINE AIRCRAFT D – STRIPPED INTERIOR)

29
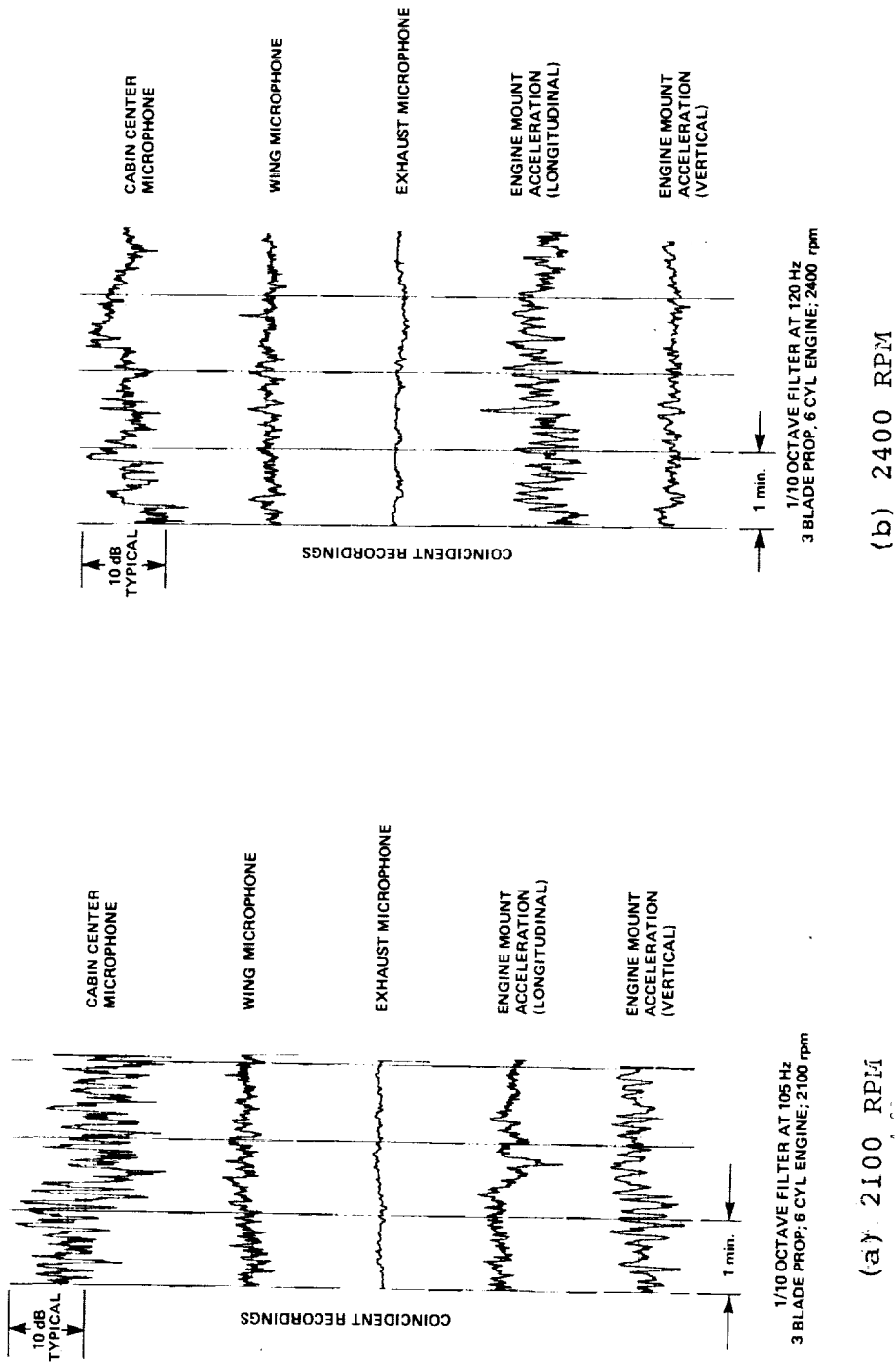
FIG. 14. VARIATION IN AMPLITUDE OF KEY TRANSDUCERS AT PROPELLER BLADE AND
FIRING FREQUENCY. (SINGLE-ENGINE AIRCRAFT D)

(a) 2100 RPM

(b) 2400 RPM

the 1/10 octave band centered on the propeller blade fundamental frequency. Cabin noise amplitude variations greater than 10 dB are observed for both tests. The wing microphone which provides a measure of the acoustic power produced by the propeller is relatively steady compared to the cabin noise. The engine exhaust noise, which is at the same frequency as the propeller blade rate, is extremely stable in its amplitude. The major variations are seen to occur at the engine mounts on the aircraft structure side of the isolator. The flight observers noted that the variations in cabin noise is more pronounced on "rougher" flights which occur during turbulent conditions. Since structural vibration is suspected to be the major variable it is likely that either the aerodynamic unbalance forces on the propeller are changing or that the coupling between engine and structure is varying. If the aerodynamic forces on the propeller vary during turbulent conditions, both the radiated noise and the magnitude of the structureborne unbalance would also change. However, since relatively small changes occur in the propeller acoustic signal from the wing microphone it is unlikely that the propeller loading is changing over a wide range. Thus the data on Fig. 14 indicate tht the variations in interior noise of this aircraft are associated with variations of accelerations of the engine mounts, and thus presumably with the associated variations of the structureborne noise transmitted from one propeller and engine into the cabin. It should be noted that the engine is supported on four mounts and that all of them are potential contributors to the coupling of structural energy. The use of four engine mount isolators that are necessary in the redundant structure makes it likely that the loads carried by each are unequal. The stackup of mechanical tolerances coupled with the stiffness of the mounts indicate high probabilities of non-uniform loading. Loads generated by aircraft pitching during gusty flying conditions will further disturb the mean loading of the mounts. Since the isolators use rubber and are of a non-linear design, then transmissability is a function of the mean loads they support. The mean loads which vary during gusty conditions will lead to variation in the transmission of energy through the mounts and thus varying cabin noise.

From these findings, we conclude that when performing diagnostic studies, one must monitor both the source or path transducer and the cabin (receiver) microphone if precise interpretation is to be expected.

31

2.5 Conclusions from Flight Surveys

The objectives of the flight survey were fulfilled. Surveys of 18 production aircraft produced consistent trends of cabin noise levels, which fall in the range of previously-reported results. Standardizing the flight test procedures allowed meaningful direct comparisons to be made. The survey also identified some potential pitfalls of flight testing, namely variability in levels among nominally-similar operations. Previously-observed variations in sound and vibration levels among different cabin locations were consistently found in all aircraft. Pressurization effects generally provided reduced levels of broadband noise and reduced levels of propeller harmonics.

Energy at propeller blade rate and its harmonics was dominant in all 18 aircraft tested, while the apparent contribution of engine-related noise varied widely; therefore propeller sources and paths must be controlled in all aircraft, but the engine related sources may not control cabin levels in all aircraft, especially large twins. One finding that is perhaps new to the light aircraft community is the apparently strong role of non-propulsion noise in determining the cabin A-weighted noise levels of single-engine aircraft. Inasmuch as treatments for turbulence-excited panel vibration may be different from those which are best-suited for controlling sound-induced vibration (and re-radiation), a more detailed under-standing of this source is needed.

Therefore, the flight survey did not serve to eliminate any sources or paths from possible consideration in the single engine aircraft, although propeller noise is clearly dominant in twins. Thus, future diagnostic efforts on a single aircraft necessarily included a full scope of source and path combinations.

3.   EXPANDED DIAGNOSTIC WORK ON A PARTICULAR AIRCRAFT

3.1   Introduction

The objective of this portion of the study was to build upon the results of the flight survey of 18 aircraft by conducting an in-depth study of an aircraft which would be representative of a significant segment of the fleet in terms of the similarity of its design, operational and acoustic properties. The primary elements of this diagnostic work were (1) to perform controlled studies on one aircraft type to develop a sufficiently refined model of the primary sources and paths that treatment concepts could be developed with minimal additional testing, and (2) to evaluate diagnostic tests and methods themselves to determine whether more sophisticated techniques would be required to optimize the definition of primary source and path combinations, and thereby optimize noise control treatment application. Although the specific details of the work will pertain to the aircraft tested, the methods to be used, trends observed, and treatment concepts studied should have general applicability to other aircraft.

The aircraft to be used for the diagnostic work was selected from those tested, based upon review of the fleet survey data and discussions with manufacturers, of the following factors:

- Contemporary design (of airframe, propeller, and engine)

- Popularity of type (past sales, and sales trends, as a percent of the total fleet)

- Typicality of noise levels, as deduced from flight test program

- Availability of test aircraft for substantial ground and flight testing

- Possibility of configuration changes on test aircraft.

The aircraft selected is a high-wing, single engine design with a retractable undercarriage. It is powered by a 6-cylinder horizontally-opposed engine and could be tested with a two-or three-blade propeller. The model was also available with and without a turbocharger. The maximum takeoff weight was 1400 kg (3100 lb) for both versions. The aircraft was also available with three different levels of interior treatment, ranging from none to a standard production interior. Thus, in this one

33

aircraft type, the following component changes could be evaluated in terms of their effect on noise: propeller blade number, turbocharger, and nominal treatment. The availability of the aircraft at the manufacturer's facility allowed the effect of some engineering changes evaluated. Since approximately 700 aircraft of this model family were sold in 1978, and 1200 in 1979, this aircraft was not only significant in its market share but was increasing its share, thus reflecting its popularity.

The test aircraft in its turbocharged version was one of the aircraft included in the fleet survey and is identified in Fig. 3 as Aircraft D, from which it is seen to be typical of the fleet in terms of cabin noise level. (The aircraft in its partially-fitted or stripped version is identified as Aircraft C in Appendix A.) Data taken during the flight survey (e.g., Figs. 6, 8 and 12) showed that this aircraft had significant and approximately equal contributions to its cabin noise from propeller, engine, and nonpropulsion sources, thus making the diagnosis and treatment of the sources and paths a most comprehensive effort. The aircraft is shown schematically below in Figure 15.

3.2 Test Configurations

The following major configurations of the aircraft were tested:

Engine	Propeller	Interior Trim
Turbocharged	2 blade	None
Turbocharged	3 blade	None
Normal Aspiration	2 blade	Production
Normal Aspiration	3 blade	Production

Flight tests were conducted at normal cruise conditions plus selections of takeoff, climb and a dive with the engine shut down. Flight payloads were similar to those described in Sec. 2.2. Ground tests were also conducted to measure certain acoustic and vibration transfer functions.

3.56 m

10.97 m

208 cm MAX.

2.74 m

2.72 m MAX.

8.72 m
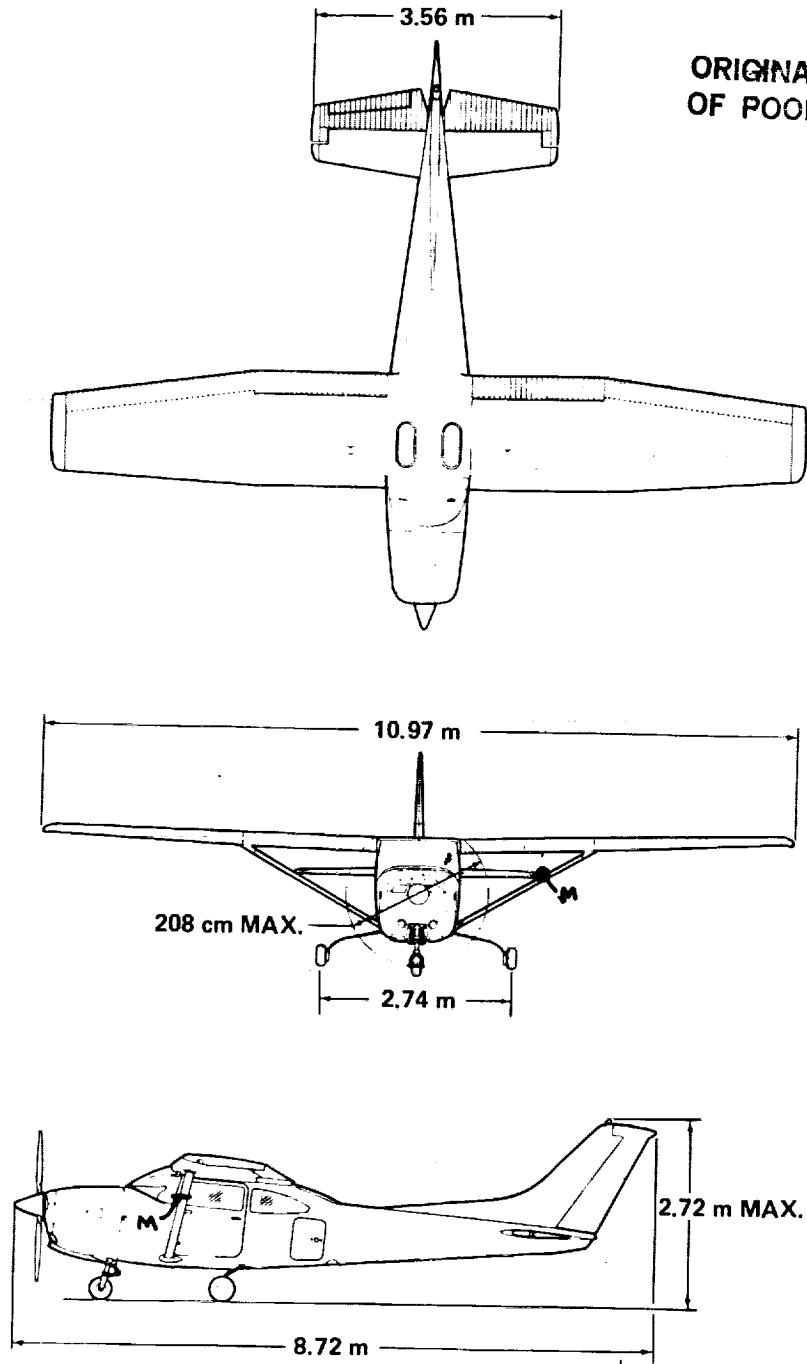
FIG. 15. SCHEMATIC OF AIRCRAFT D SELECTED FOR DIAGNOSTIC
TESTS.

35

3.3 Selection of Transducers and Their Locations

A variety of acoustic and vibration transducers were used to measure noise and vibration source strengths as well as to indicate the paths by which the energy reaches the receiver space.

Location of the transducers for source strength measurements requires that all potential sources be evaluated, and as many of them as are judged significant should be instrumented. The flight survey tests provided an indication that virtually all major source categories might be occurring in roughly similar strengths (i.e., engine, propeller, and nonpropulsive sources). The assessment of the noise paths requires that sensors be located such that the noise can, if possible, be traced from source to receiver. In the case of light aircraft, a generalized source path diagram can be constructed to show the locations of key transducers. Such a diagram is shown in Fig. 16. Specific descriptions follow.

Machinery Space Microphone: A condensor microphone was installed in the engine compartment midway between the rear of the crankcase and the firewall, to measure the noise level on the engine side of the firewall. The microphone was mounted via vibration "isolators" (tape-encased foam pads) onto the airframe. A 7.6 cm (3 in.) diameter foam windscreen was installed since air circulation velocities can be high. The compartment temperatures were measured to ensure that the microphone was not overheated.

Exhaust Microphone: This was installed to measure the fluctuating pressures close to the exhaust pipe discharge. This measurement allows estimates to be made of the sound power level radiated from the exhaust pipe and thus the sound pressure levels incident on the fuselage. The high exhaust gas temperatures require that either a high temperature microphone be used or that thermal isolation be employed with a lower temperature microphone. A piezoelectric pressure sensor (6mm (1/4in) diameter) (having internal electronics) was installed in a tube 10 cm long (4"), which provides thermal isolation. The one quarter wavelength resonant frequency of the tube was approximately 770 Hz and thus the assembly had sufficient useable bandwidth to measure the fundamental engine exhaust frequency of 105 Hz plus the first few harmonics. The microphone is illustrated in Fig. 17.
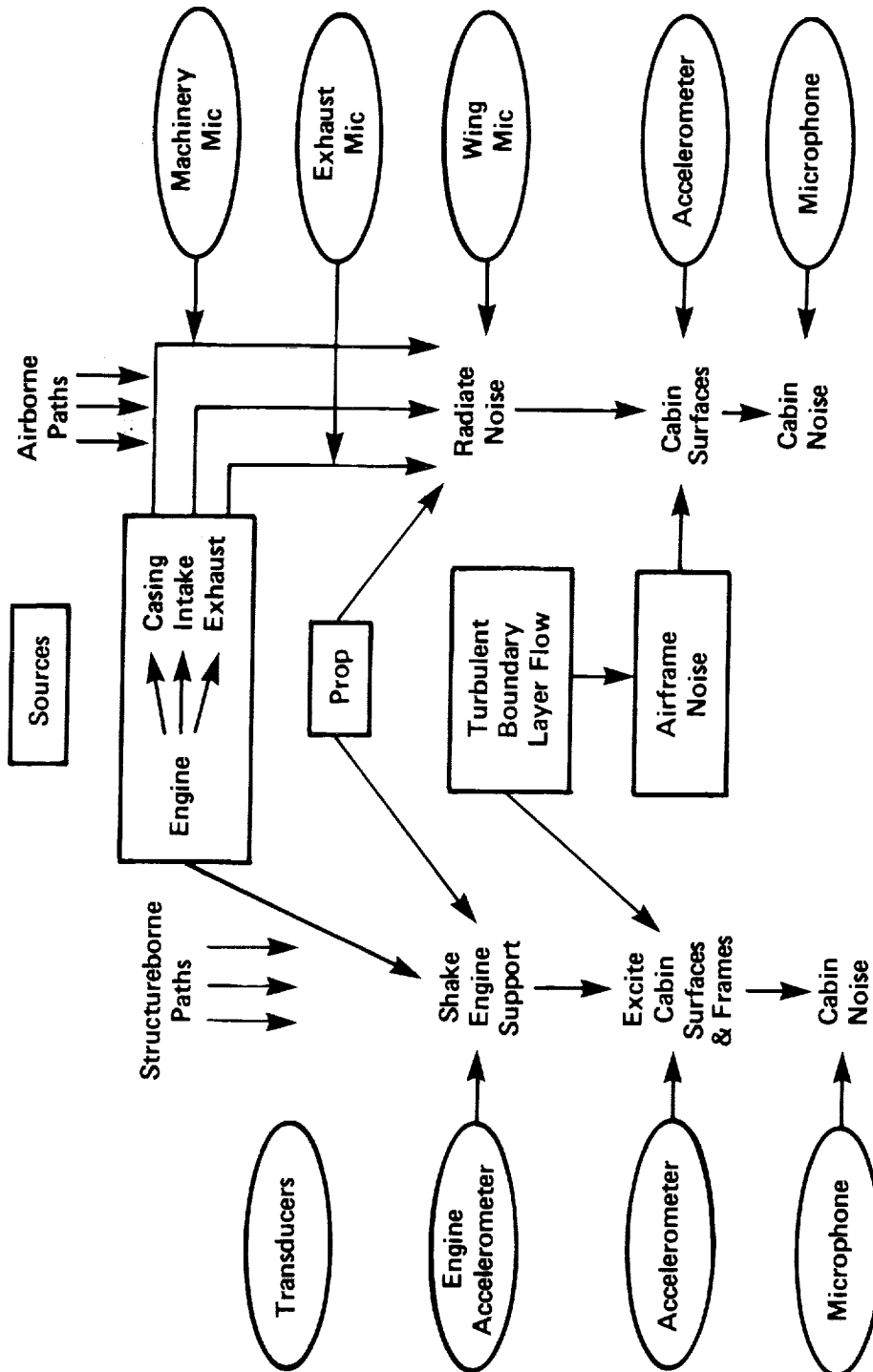
FIG. 16. SCHEMATIC OF TRANSDUCER LOCATIONS FOR SOURCE/PATH DIAGNOSIS
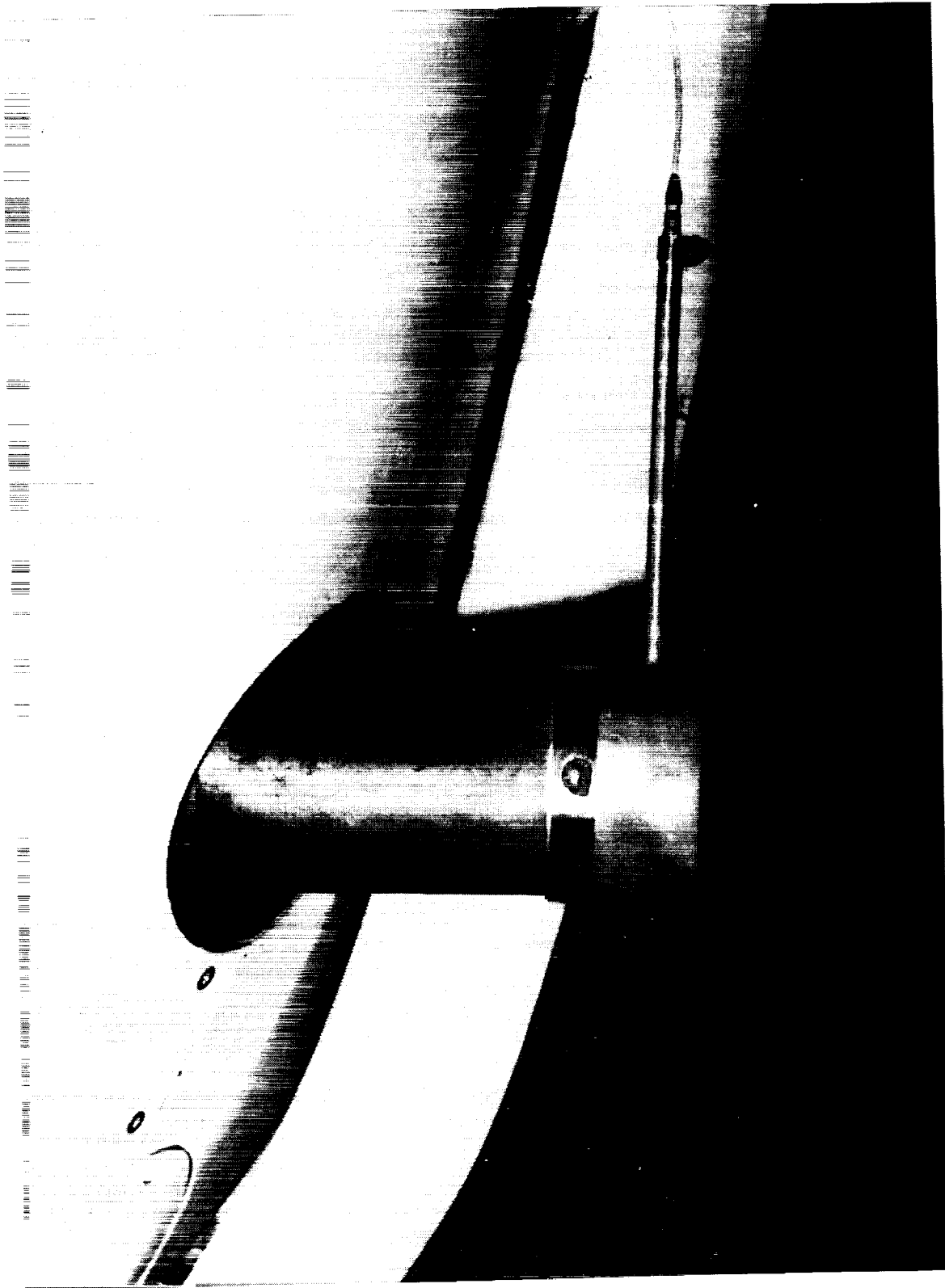
FIG. 17. EXHAUST MICROPHONE INSTALLED ON EXHAUST STACK.

Engine Air Intake Microphone: The location of the air intake in this test aircraft is just behind the propeller. It was considered that the acoustic path from the air intake to the cabin firewall was significantly impeded by the engine and an air-ducting bulkhead. In view of this observation, plus the judgment that the air intake had a low source level, it was decided not to install an intake microphone.

Wing Strut Microphone: Since the propeller rotational noise is known to be a major source, a microphone with a bullet nose cone was installed on a wing strut to measure the amplitude of the blade frequencies. The microphone was placed outside the propeller slipstream area, 1.2 m (48") from the cabin wall as shown in Fig. 18 (see also the location indicated by "M" on Fig. 15). A photograph of the microphone as seen from the cabin is shown in Fig. 19. The measurement of broadband (non-rotational) noise from the propeller was not attempted since it was believed that the proximity of the wing and its strut would control the broadband noise at the microphone location by both direct-radiated noise and by hydrodynamic pressure fluctuations arising from local flow separations at the microphone attachment.

Accelerometers

Point vibration measurements were made at locations which were considered key points in the structure. Given the timewise variability effect observed on one of these aircraft in the flight surveys (see Sec. 2.4) which had been tentatively assoc-iated with engine- and/or propeller-induced vibration, the vibration level induced in the airframe by the engine/propeller combination was of extreme interest. Accelerometers were initially mounted on both the engine-side and the airframe side of the engine isolators, so that the isolator performance could be determined. As will be discussed later, these measurements were not definitive and thus an alternate method was employed to assess engine isolator performance.

Accelerometers were also used in the cabin to measure the vibration levels of the skin panels and fuselage frame members. The vibration measurements were made at the following specific locations:
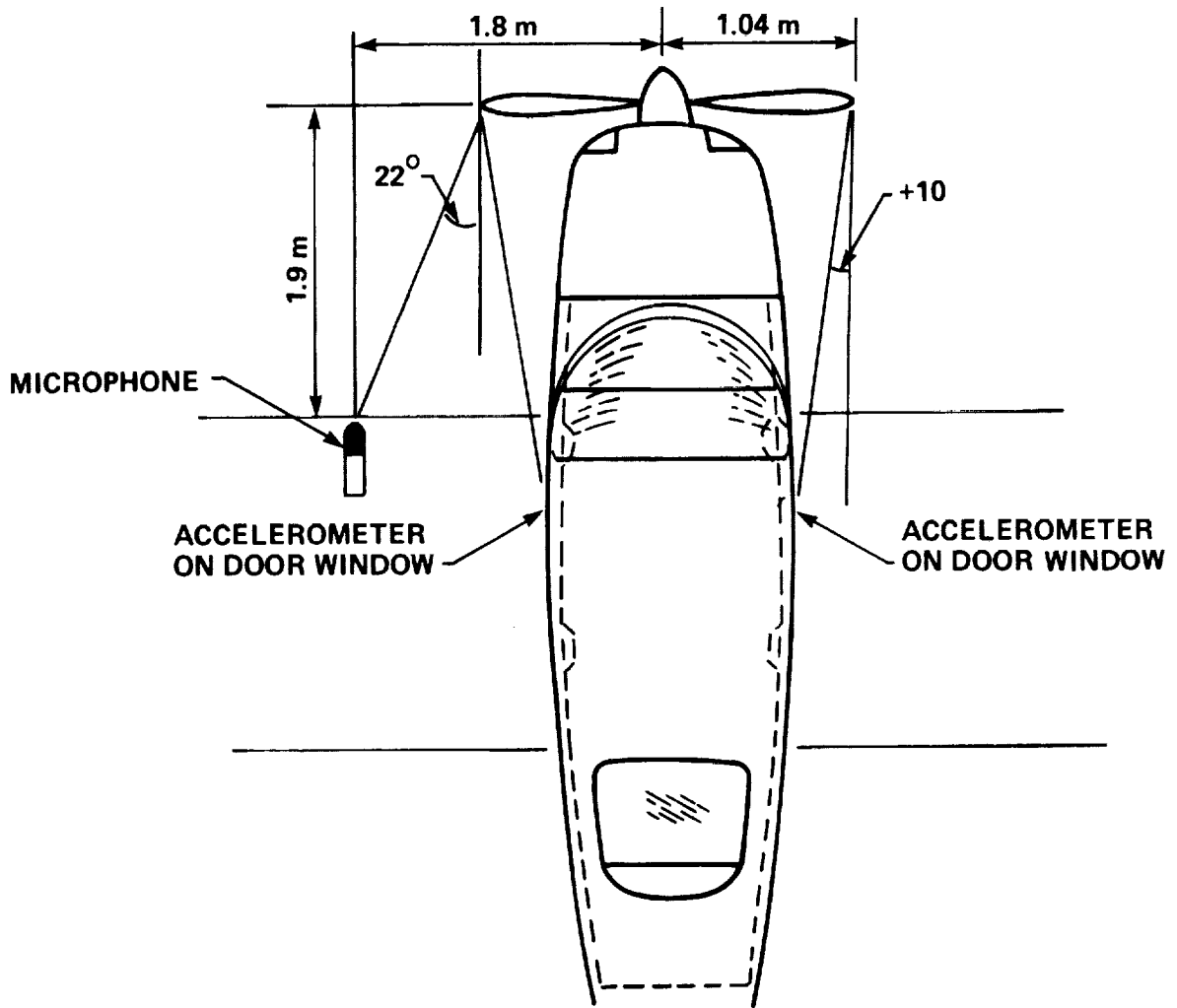
FIG. 18. LOCATION OF WING-STRUT MICROPHONE.

40
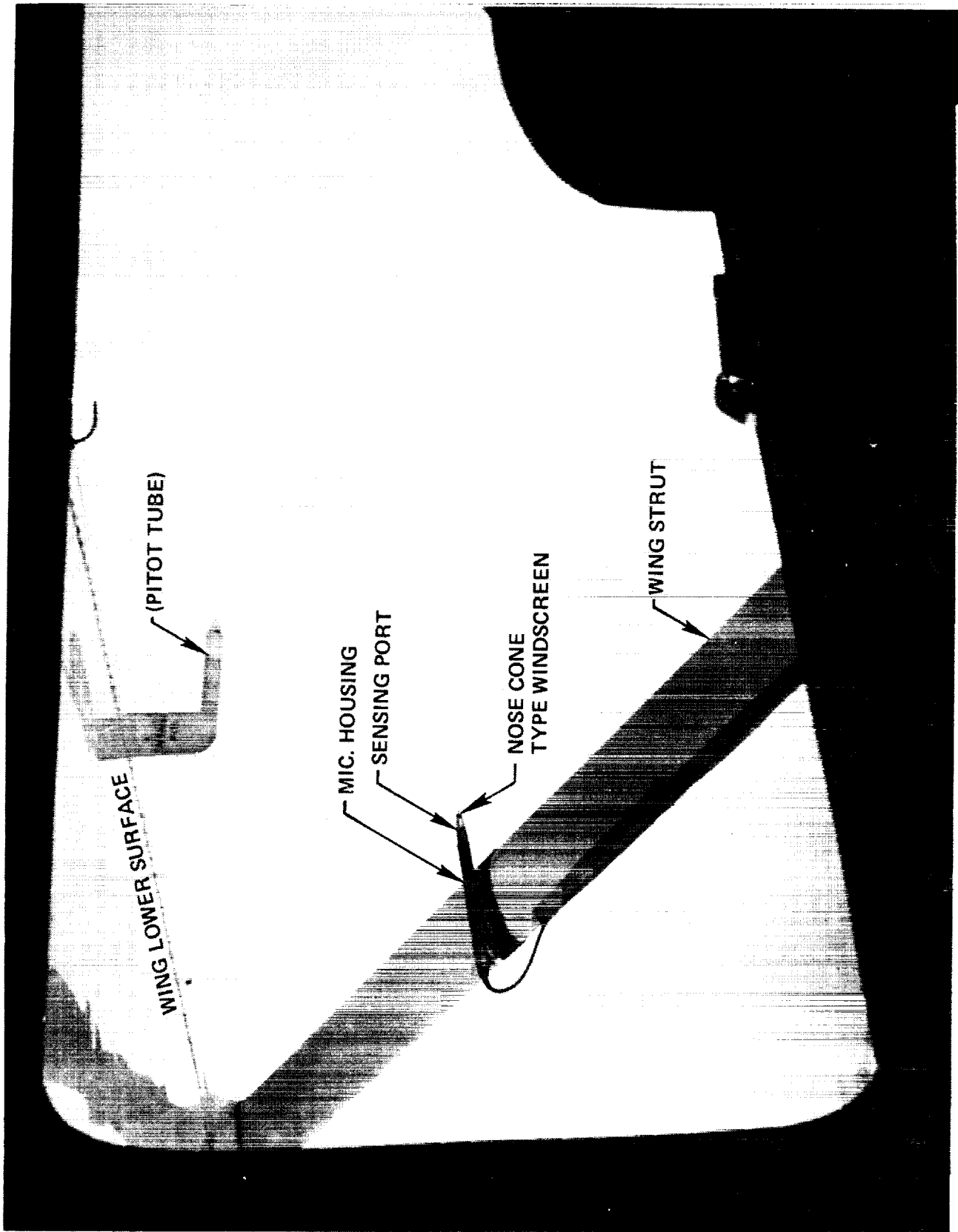
FIG. 19. MICROPHONE CLAMPED TO WING STRUT AS SEEN FROM INSIDE CABIN.

a)   Geometric centers of all windows and the windshield,

b)   Geometric center of the major fuselage skin panels, between frame members and stringers on aircraft with no interiors,

c)   Door frames, seat rails, and wing spars.

As previously mentioned, the accelerometers used were piezoelectric devices weighing 2 grams with internal circuitry, and thus having minimal effect in the vibration of the surfaces being evaluated.

Flight Data Recording System

The signals from all transducers were recorded on magnetic tape for post-flight analysis. The data acquisition system was centered on a 7-track IRIG standard tape recorder with a bandwith DC-10 kHz. The recorder was powered by a rechargeable aircraft battery. Six channels were used for transducer signals and the seventh was allocated to voice recording from the test engineer and conversation with the pilot and flight observer. Precision A.C. data amplifiers were used to increase the voltage level from the transducers to the tape recorder inputs. Test personnel comprised the pilot, front seat observer and rear seat recorder operator. The latter two people had an intercom set which was connected to the recorder so that both could announce test conditions, amplitude settings etc., directly onto the tape.

3.4   Cabin Noise Observations

This section discusses overall characteristics of the cabin acoustics of the test aircraft. Initially, the effects of parametric changes were explored, followed by more detailed studies of the cabin sound field. The reader is also referred to Sec. 2.4 for discussion of the repeatability and timewise variability of levels observed on certain flights of this aircraft.

Two-vs Three-Bladed Propeller

It was found that interior noise levels were somewhat higher when a three-bladed propeller was used as compared to a two-bladed propeller. Figure 20 compares the third octave spectra

from each case. Figure 21 shows the corresponding narrowband spectra upon which recognizable propeller and engine harmonics are identified (refer to Secs. 2.3 and 2.4 for discussion of limitations on frequency separation of different periodic sources). In both cases, the energy at propeller tones is greater than that at engine harmonics. Note that these data apply to the cabin center position for the stripped interior and do not reveal any path information. The major conclusion inferred is that, for this particular aircraft, a three-bladed propeller in combination with a 6-cylinder engine produces slightly higher cabin noise levels than the 2-bladed counterpart. The increases at low frequencies (below 200 Hz) may be attributable to possible rapid changes with frequency in the amount of sound transmitted through structures such as the firewall, windshield, etc., due to low order structural resonances, and/or variations in the degree of propeller-excited structureborne transmission. The increases at higher frequencies between the 3-and 2-bladed cases are broadband in nature and suggest that the prop broadband noise is higher on the three bladed propeller, or that the flow speeds induced over the fuselage are higher. Given the previously-mentioned variability from flight-to-flight, one cannot treat the differences noted here as being highly significant or necessarilty generalizable to all aircraft.

Effect of Production Interior Treatments

Comparison of cabin noise levels with and without the production treatment showed that a 6 - 8 dB reduction is achieved at most frequencies above 300 Hz with the treatment, thus leading to about 6 - 8 dBA reduction. Below 160 Hz, the treatment had inconsistent effects, actually leading to higher levels at some frequencises ans some locations in the cabin. However, low frequency variability was a common phenomenon throughout the study, so one cannot criticize the treatment based on this data. Since the variability was not recognized at the time the treatment evaluation was made, and since the focus of the study was on source-path diagnosis, a more thorough study of production treatments was not made; therefore, the treatment effect quoted above is considered only a general indications,but not a highly reliable figure.

Effect of Turbocharger

When a turbocharger is used on the engine, the exhaust system is manifolded into a single exhaust. No discernable systematic effect of turbocharging on interior noise levels was

43
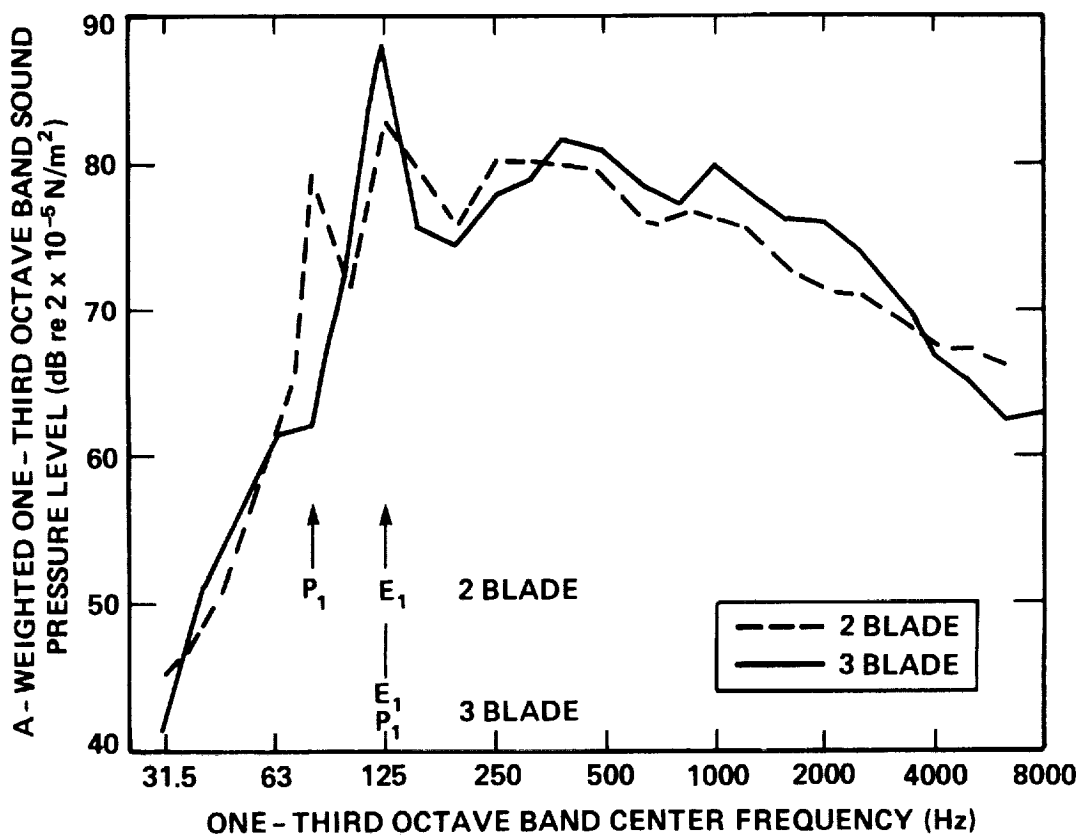
FIG. 20 . COMPARISON OF INTERIOR NOISE WITH 2 AND 3-BLADED
PROPELLER.
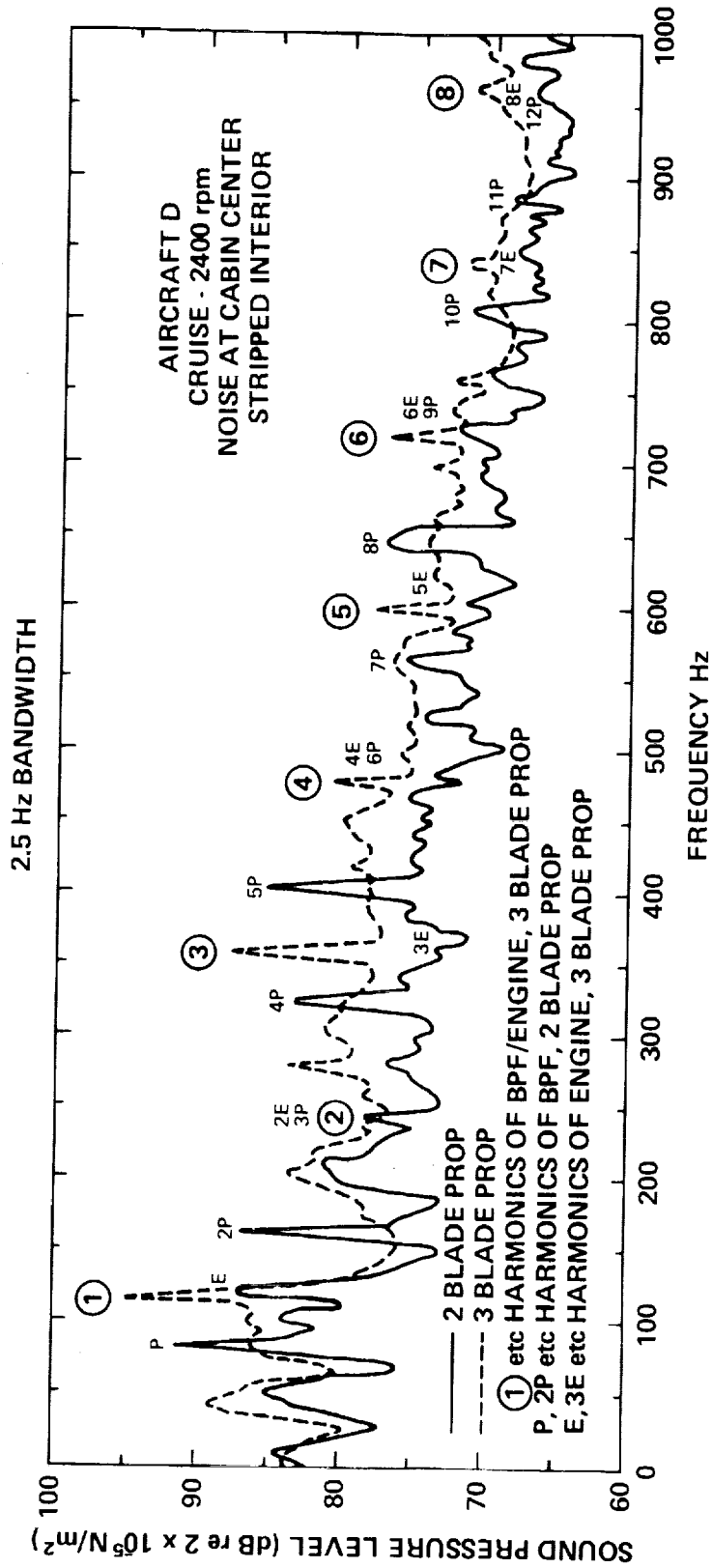
FIG. 21. CABIN NOISE NARROWBAND SPECTRA COMPARING 2 AND 3-BLADED PROPELLERS.

45

found, thus implying that the exhaust airborne levels either change only slightly, or are not a dominant contributor at the cabin center. The question of turbocharging effects can be resolved by exhaust pressure measurements, discussed below.

Spatial Distribution of Levels and Phase Relationships Among Points in Cabin

Other workers have identified acoustic modes within the cabins of light aircraft during static tests [see for example, Ref 29]. Since these modes may lead to amplification of certain discrete frequencies such as the propeller blade tones within the cabin, a survey of the distribution of levels and the phase relationships among various points was conducted during a flight test. Six microphones were arranged in the cabin and recorded simultaneously during steady flight conditions as shown in Fig. 22.

The amplitudes of tones was measured and the phase relationship of each microphone to the other five was determined using a 2 channel F.F.T. analyzer. Cross spectra were measured, and in some cases, coherence. Appendix A contains an in-depth discussion of all tests conducted. Some typical results are presented here.

Figure 22 shows the microphone location used which is arranged to identify longitudinal and lateral modes within the cabin. The SPL measured at each location within the cabin is given for the two major tones, the propeller blade rate and the firing rate. The firing rate SPL is seen to be highest at the front of the cabin, which would suggest that the source of those tones is either airborne sound from the exhaust pipe, or the firewall responding to engine vibration. The propeller blade tone amplitude is observed to be somewhat higher in the cabin center and aft region than at the windshield. This suggests that the propeller blade passage tone may be transmitted primarily through the airborne path through the sidewall rather than structureborne via the firewall. However, the existence of modes in the cabin could confuse that simple logic.

Cross spectra were obtained to determine the phase relationship between pairs of microphones. Appendix A contains phase spectra for all microphone pairs at both engine speeds. Figure 23(b) shows a typical result obtained between microphones spaced 1 m apart along the aircraft longitudinal axis. Figure 23(a) shows a typical result obtained for microphones placed 0.5 m apart across the cabin width. Since the object of the experiment

46

**A - WEIGHTED LEVELS OF
PROPELLER BLADE PASSAGE TONE**

ENGINE SPEED

2100 RPM	75	74	77	78	76	78	(70 Hz)
2400 RPM	75	79	79	78	72	84	(80 Hz)

FORWARD

ENGINE SPEED

2100 RPM	88	85	84	76	84	79	(105 Hz)
2400 RPM	88	87	85	82	85	83	(120 Hz)

**A - WEIGHTED LEVELS OF
ENGINE FIRING FREQUENCY FUNDAMENTAL**
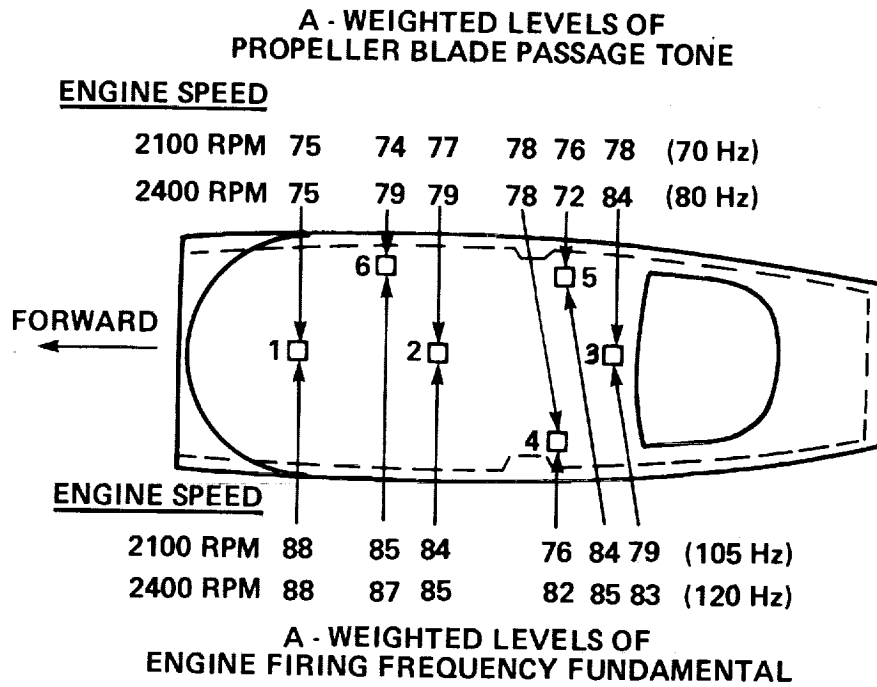
FIG. 22. MICROPHONE LOCATIONS AND SPATIAL DISTRIBUTION OF TONES IN CABIN.

47
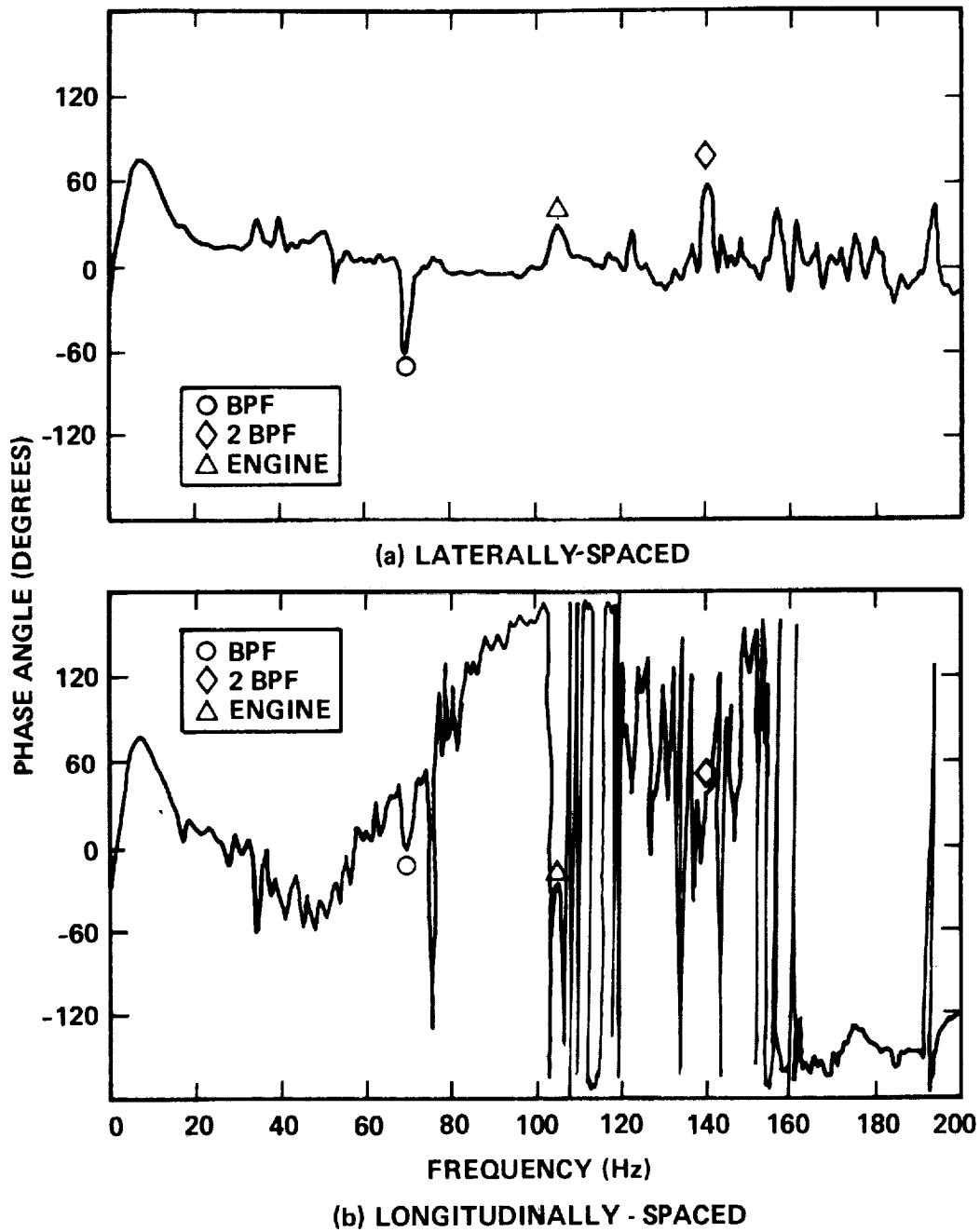
FIG. 23. PHASE OF CROSS SPECTRUM BETWEEN TYPICAL PAIRS OF CABIN MICROPHONES; 2100 RPM (BPF = Blade Passage Frequency)

was to try to detect the presence of standing waves at the main discrete frequencies attention should be given in the figures to 70 Hz (propeller blade rate) and 105 Hz (engine firing rate). If standing waves are dominant, phase relationships of 0° or 180° should be apparent. In the case of the longitudinal microphone spacing zero degree phase angle is seen at 70 Hz and 25° at the firing rate. Thus a mode may exist at 70 Hz based on this evidence. A check of the phase between microphones longitudinally spaced 2 m apart shows a 90° phase angle thus suggesting that no mode exists. Also to be considered is the 60° phase angle which exists at 70 Hz in Fig. 23(a) between the laterally-spaced microphones. Attempts were also made to determine the convection speed between the cabin microphones at blade rate to obtain an understanding of the path direction, but the results of these attempts did not prove conclusive.

In Fig. 23b the slope of phase angle versus frequency is approximately uniform between 50 Hz and 90 Hz at 5.3°/Hz and indicates a propagating wave along the cabin. The convection speed of the wave is related to the phase shift by the following relationship:

$$U_c = \frac{360 \; \Delta f \; d}{\Delta \phi}$$

where U_c is convection velocity in m/sec
f is frequency in Hz
ϕ is phase angle in degrees
d is distance between microphones in meters.

For the case in question,

$$U_c = \frac{360 \; (90-50) \; 0.95}{210} = 65 \text{ m/sec}$$

Since this phase velocity occurs at 0.19 times the local speed of sound, it cannot be associated with an acoustic wave, but it suggests either a hydrodynamic or structureborne effect. The aircraft flight speed was 70 m/sec during these tests which is the same order of magnitude as the derived convection velocity; thus boundary layer excitation may be the cause of the observed phase shift. The flexural wave speed in 6 mm (0.25 in) thick aluminum ranges from about 17.5 m/s at 50 Hz to 25 m/s at 100 Hz, much slower than the measured convection speed. However,

if the structural response involves modal participation, the effective wave velocity in the longitudinal direction would be higher. Detailed vibration measurements on the fuselage would resolve this issue; however, appropriate measurements were not made at the time of the survey.

Although this series of tests did not comprise a proper modal survey due to the number of transducers and the possible variability of the source during the sample interval, several observations are helpful. First, there is some evidence of cabin acoustic modes being excited in the frequency range of interest. Secondly, the clear evidence of an axial phase velocity corresponding roughly to the free stream flight velocity suggests that aerodynamic disturbances in the boundary layer (which includes propwash) may be a dominant source of excitation of the cabin structure and subsequent radiation into the interior. This latter observation supports the dive test results in the survey phase.

3.5 Definition of Source Levels

Propeller and Engine Exhaust Airborne Levels

An opportunity arose to mount a microphone with bullet nose cone on the wing strut of Aircraft D (see Figs 18 and 19). The "wing strut" microphone provides a means of measuring at least the tonal noise from the propeller and engine for comparison with propeller noise prediction methods, as well as providing an estimate of the sound pressure exciting the fuselage skin. The wing microphone and fuselage are in the geometric near field of the propeller and in strong diffraction region of the wing; thus, the measurements must be interpreted with great care as to their general applicability to other areas of the aircraft. Shown in Figure 24 are data from two different propellers which are virtually identical in their broadband levels. A calculation of the propeller noise using Succi's propeller noise program [25,26] with the mean load distribution and thickness distributions of the propeller as inputs. This calculation underestimated the level measured near the strut by about 4 dB, probably due to the lack of detailed data on the inflow environment (no distortion assumed) or to the focussing effect of the wing/fuselage junction (none accounted for). Therefore, the measured data were used as the representative exterior propeller airborne levels in the mid-region of the fuselage.

50
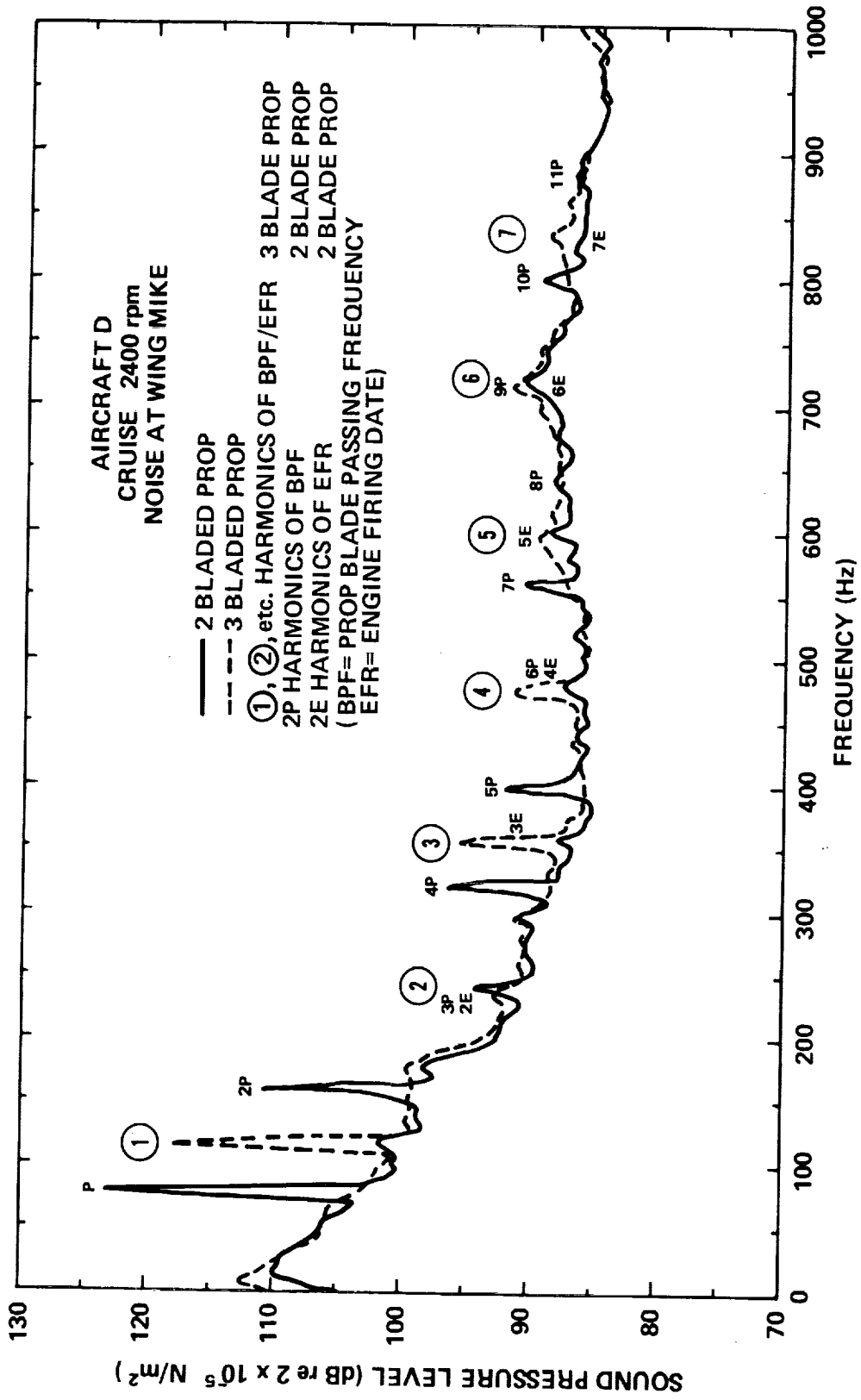
FIG. 24. MEASURED NOISE AT WING STRUT MICROPHONE.

Machinery Noise Spectra

Noise spectra measured in the engine compartment of Aircraft D (turbocharged version), fitted with 2- or 3-bladed propellers, are shown in Figures 25 and 26. It is interesting to note that the noise levels at firing rate are considerably lower than those at propeller blade rate. The engine noise sensed by this microphone is believed to be mainly casing-radiated noise with some contamination by intake noise. The engine compartment is open to the outside through the engine cooling fins and cowl flaps and this is presumably the path by which prop noise enters the space (in addition to acoustic transmission through the cowl skin). The propeller levels are comparable to those measured at the wing microphone. The levels in Figs. 25 and 26 are to be used as typical in the forward part of the aircraft. Both propeller-and engine-generated levels could enter the cabin through air handling ducts if they were under-designed acoustically, as well as directly through the firewall.

Exhaust Noise Spectra

The ported microphone described earlier was used to obtain pressure spectra at the exit of the exhaust stacks on Aircraft C (normally aspirated, dual exhaust) and D (turbocharged, single exhaust). The results are shown in Fig. 27. From these measurements, the radiated acoustic power level may be calculated, given the exhaust stack area, if it may be assumed that end reflections are not appreciable at the frequency of interest. The exhaust microphone may not be used to estimate the high frequency exhaust noise because of the probe tube resonance (shown in Fig. 28), a narrowband analysis of the exhaust pressures for Aircraft D.

The measured spectrum inside the exhaust pipe near the exist is shown in Fig. 28(b), in which a series of discrete frequencies are seen at increments of 20 Hz, which is one half the rotation rate of the engine (i.e., equal to the firing rate of each individual cylinder). Pronounced peaks occur only at certain multiples of 20 Hz commencing at 1/2 net firing rate. A broad peak is seen centered at about 770 Hz which is the quarter wave resonance of the microphone tube and is therefore a measurement artifact.

52
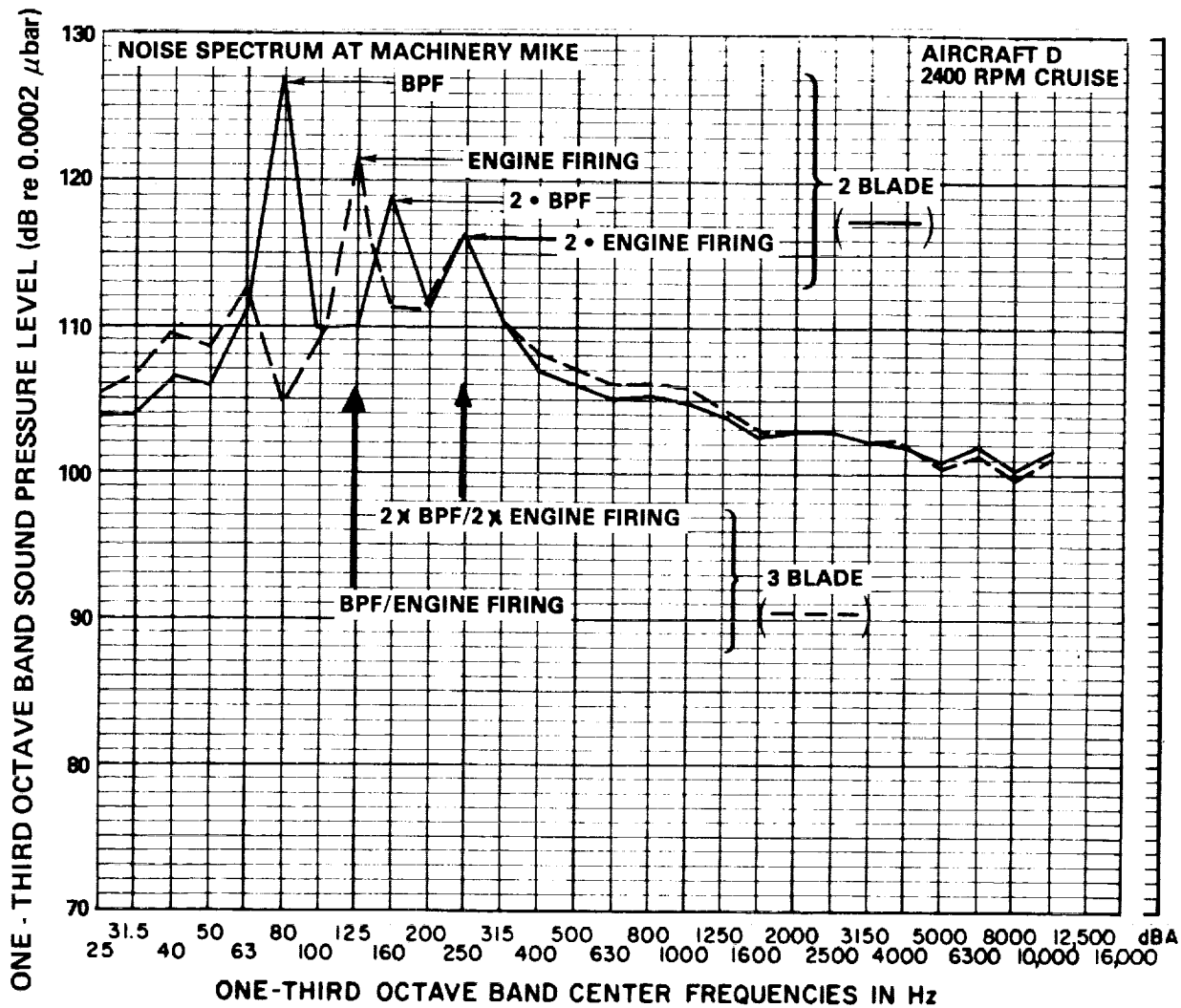
FIG. 25. MEASURED NOISE BETWEEN ENGINE AND FIREWALL IN ENGINE
COMPARTMENT FOR 2 AND 3-BLADED PROPS.
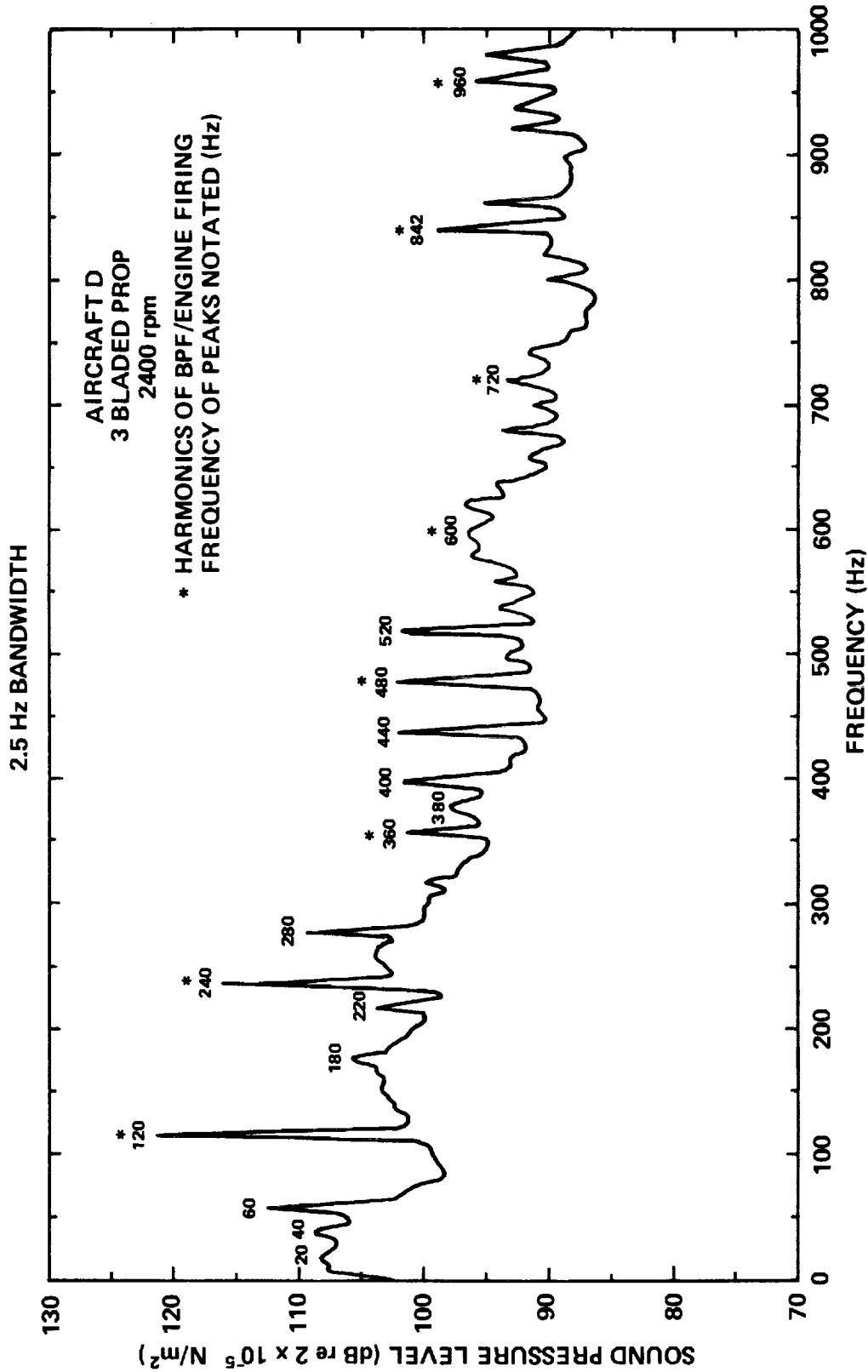
FIG. 26. NARROWBAND ANALYSIS OF MACHINERY COMPARTMENT NOISE.

54
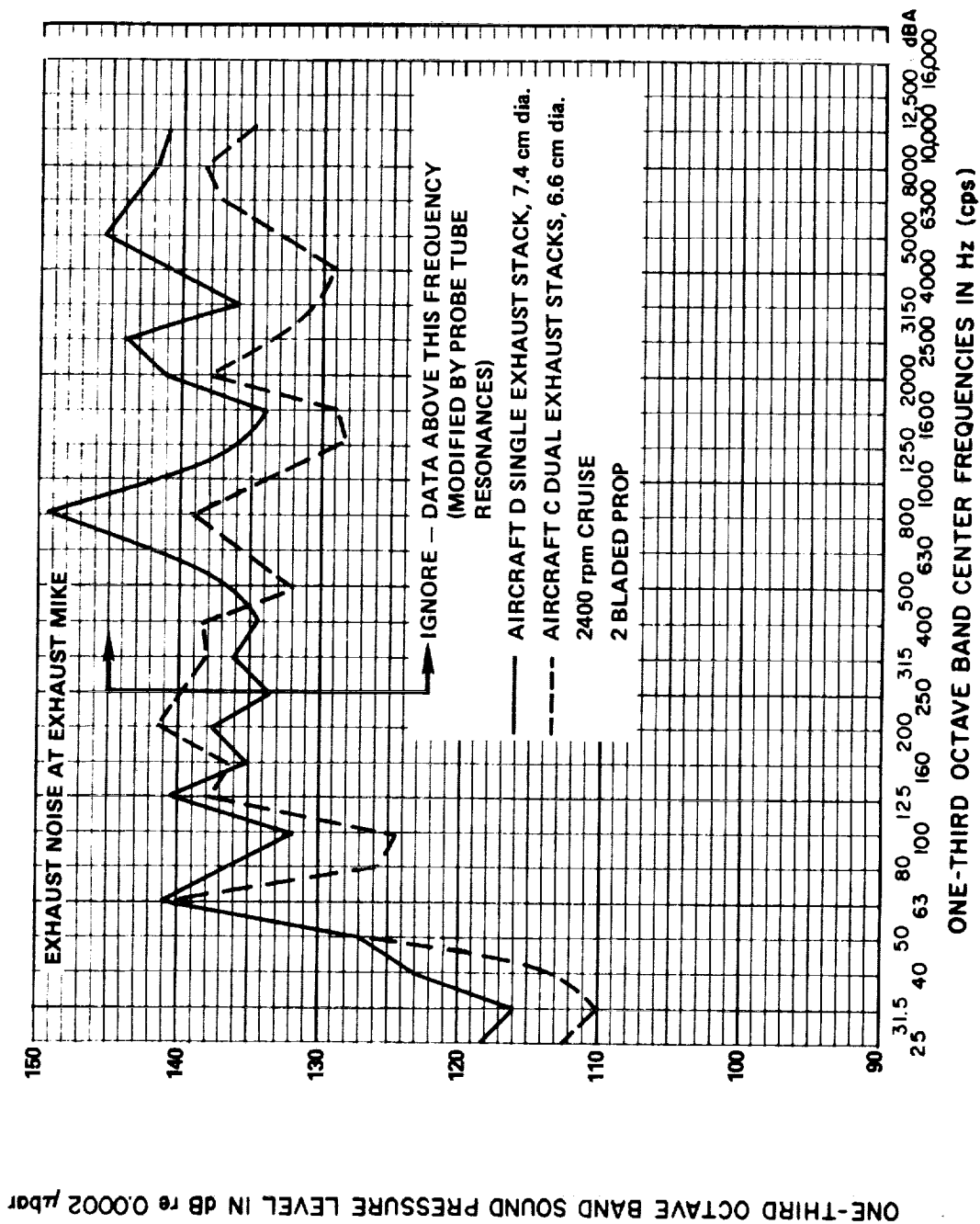
FIG. 27. EXHAUST NOISE SPECTRA FOR SINGLE AND DUAL EXHAUST STACKS.

55

(a) WING MICROPHONE

(b) EXHAUST MICROPHONE
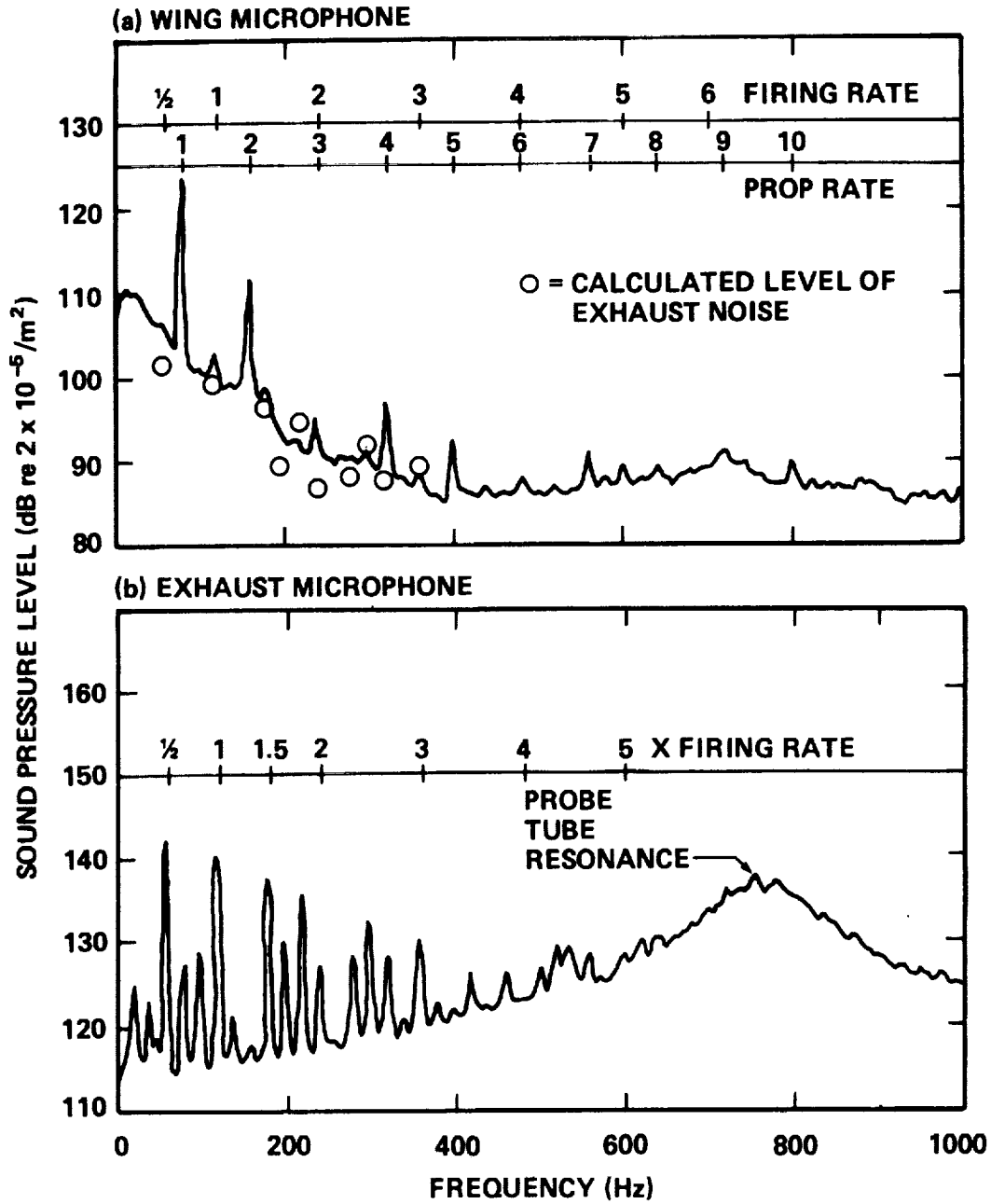
FIG. 28. NARROWBAND ANALYSIS OF EXHAUST NOISE AT STACK AND AT WING STRUT MICROPHONE.

56

The sound radiated by the exhaust can be calculated based on the pressure spectrum. Since the microphone is very close to the end of the pipe it is assumed that it measures the radiated acoustic pressure of a simple (monopole) source in a pipe. Thus, the radiated sound was estimated assuming spherical spreading (no account was taken of the possible effects of flow on the acoustic impedance of the pipe, and thus its radiation efficiency). Such a calculation was performed to compare estimates with the wing-strut-measured levels shown in Fig. 28(a). The results of the calculation are shown in Fig. 28(a) and are indicated by the circles. Good agreement is seen where the engine peaks are evident. Thus, it should be possible to estimate (or simulate in the laboratory) the distribution of exhaust noise over the fuselage, based upon the exhaust pipe measurements. Although the exhaust noise levels shown in Fig. 28(a) appear low with respect to the propeller airborne levels, the exhaust is a concentrated source and therefore may produce high levels near the forward and lower part of the fuselage, closer to the exhaust pipe opening. If so, the significant transmission would be localized and could be treated close to the source by stiffening individual panels, or increasing their mass.

Airflow Noise

In order to determine the noise associated with the airflow over the fuselage, such as that induced by the turbulent boundary layer and edge noise from the wings and their struts, a test was made in which the engine was shut down and the plane was dived at cruise speed. As discussed in Sec. 2, the engine rotation did not stop during the dive due to safety mechanisms on the air-craft. Figure 29 shows the result obtained in the cabin center position, from which it can be seen that the aerodynamic noise in dive approaches the cruise noise spectrum, except at the pro-pellers' lowest frequencies. In an effort to determine the residual noise due to engine rotation and propeller wake impingement, narrowband analyses were performed at three locations, as shown in Fig. 30. Engine and propeller influence is evident below 150 Hz, but the broadband levels elsewhere are consistent, actually increasing at low and high frequencies toward the aft part of the cabin.

To extend these dive results to cruise, one must at least take into account the acceleration of the flow near the aircraft relative to the free stream airspeed, due to the propeller slipstream. At cruise, we estimate, using simple acuator disc theory, that the mean velocity of the airflow near the

57
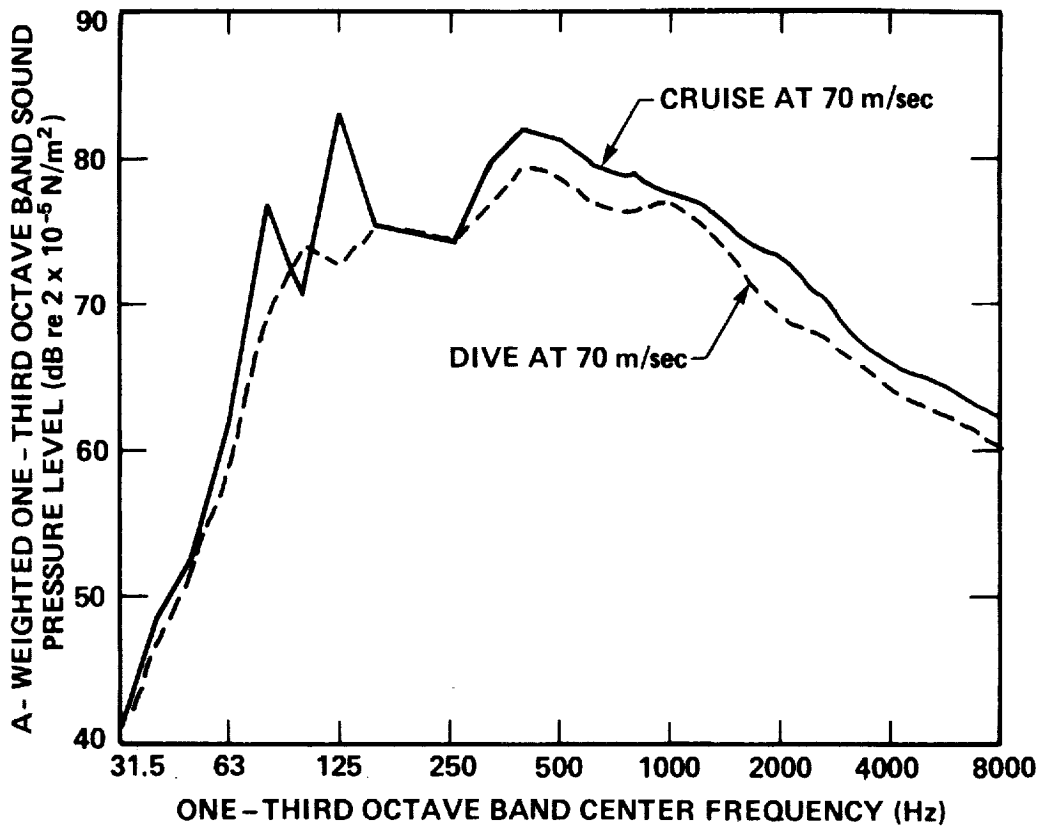
FIG. 29 . COMPARISON OF CABIN NOISE IN CRUISE AND DIVE.

58
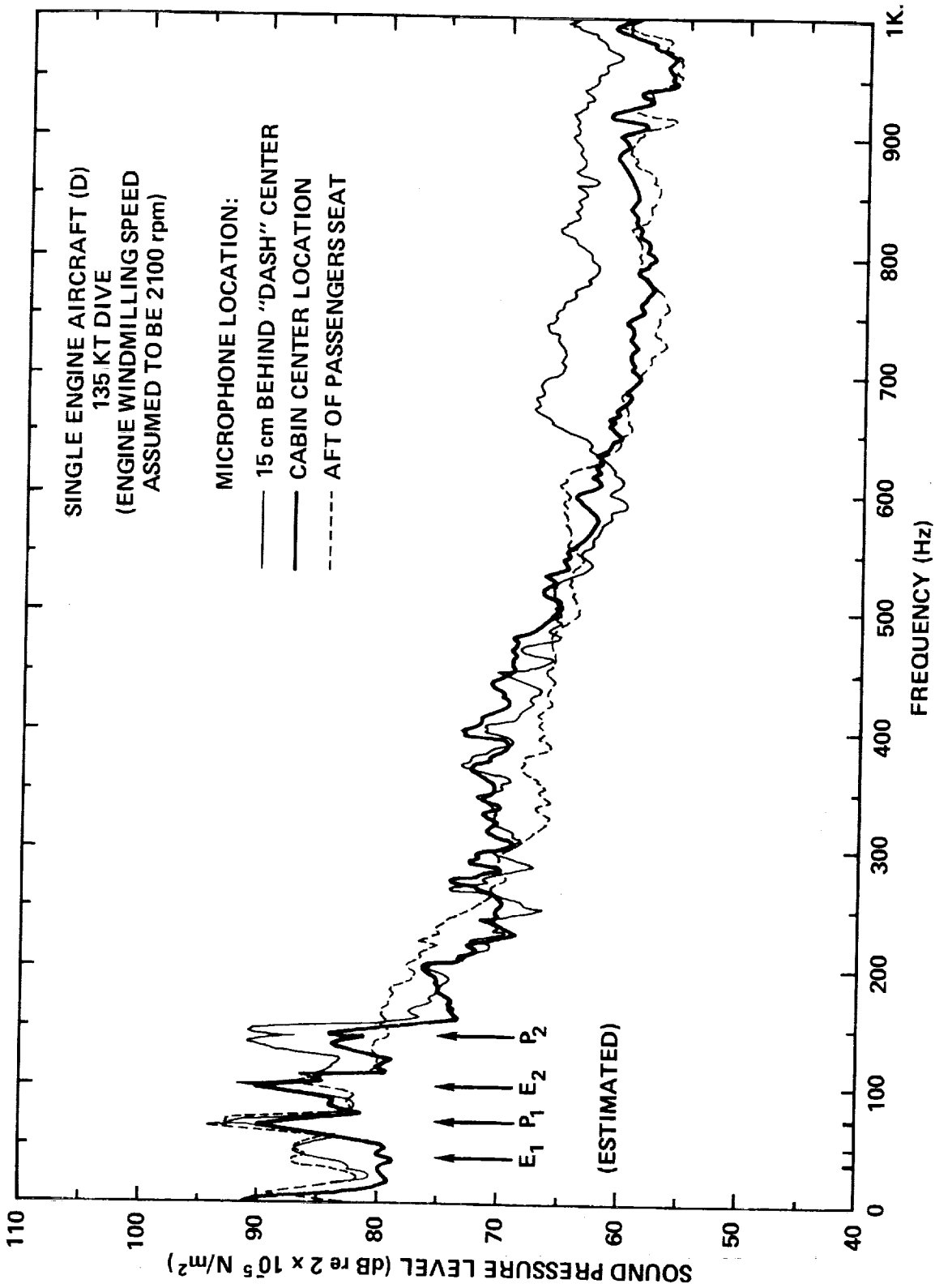
FIG. 30 . NARROWBAND SURVEY OF VARIOUS CABIN LOCATIONS DURING DIVE.

59

fuselage is approximately 110% of the flight speed. Thus, as a first approximation, the results in Fig. 29 should be corrected to account for this, by assuming a V^4 scaling relationship. Thus, the "dive" noise in Fig 29 could be raised by 40 log (1.1), or 1.7 dB, which effectively superimposes the two results except at the propeller fundamental and first harmonic. This result will later be used in forming a composite noise prediction of all sources.

This result, coupled with the dive test results on the twins and the cross-spectra measured in the cabin which showed a phase speed of the pressure field to be approximately that of the cruise speed, are evidence that aerodynamic sources may be responsible for a significant contribution to interior noise above the lowest machinery tones. If this can be confirmed (the implication on treatment design could be substantial. In particular, damping is the most effective way to control the resonant response of panels excited by a turbulent boundary layer; unless areas near the wing/fuselage junction are found to dominate the flow noise process (due to separated flow in these regions), then the damping would be needed over a large area of the fuselage.

3.6 Characterization of Transmission Paths

Fuselage Noise Reduction

The overall relationship between exterior airborne and interior noise was established during a ground test. The aircraft was parked in a large hangar and a loudspeaker placed about 10 meters from the port side of the fuselage. The exterior noise was monitored at the wing microphone, whose position has been described already, and at positions close to the cabin surfaces on the port side and at the windshield and the rear window. The interior noise was measured at the cabin center.

The exterior spectra shown in Fig. 31 were obtained for the aircraft when exposed to primarily a direct field propagating normally to the aircraft axis. The major point to note is that the windshield and rear window exterior SPL's are lower than those on the port side of the aircraft. Thus it is assumed also that the incident (diffracted and reverberant) levels on the starboard side will also be lower than on the port side. Thus, the fuselage noise reduction measure obtained is across one side of the aircraft fuselage only, for roughly normal incidence. A somewhat higher noise reduction would be expected for grazing incidence at some frequencies, while sound incident on the windshield at angles normal to its surface might result in less noise reduction of that part of the aircraft.

60
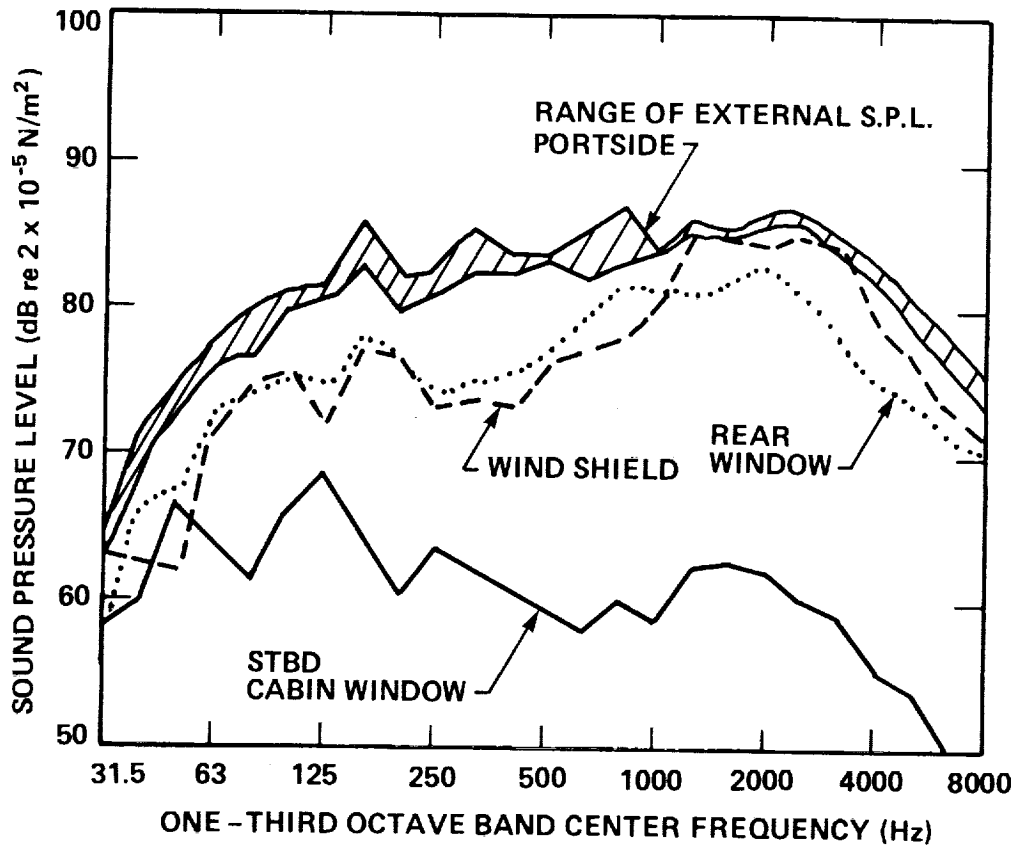
FIG. 31. SPECTRA OF EXTERNAL SOUND PRESSURE DURING SIDEWALL
NOISE REDUCTION TEST.

Figure 32 summarizes the measured fuselage noise reduction for aircraft with both types of interiors tested. Consistent and significant acoustic benefits due to the furnishings are limited to frequencies above 630 Hz. Figure 32 also shows for comparison the results obtained on a single engine aircraft [14] which was tested in a reverberent room. Since that test produced a nominally uniform sound field around the fuselage, the aircraft tested in that environment will tend to show a lower noise reduction when compared to the results obtained in this study. An improved technique over both the test done in this study and that of Ref. 14 would be to place controllable airborne sources at the propeller, engine case, and exhaust source locations and measure the noise reduction spectrum for each source location. This could be extended further by carefully covering panels or windows with a high noise reduction material to derive the noise reduction not only on a source-by-source basis, but also on a panel-by-panel basis, thus helping to localize treatment.

Fuselage Panel and Window Response

During the noise reduction tests, measurements were made of the relationship between the acoustic field and the resultant motion of the fuselage wall components. A microphone was placed close to the exterior surface at the geometric center of the panel or window in question. A 2 gram accelerometer was mounted on the surface close to the microphone position. The relationship between the acoustic level and acceleration was then determined during the application of noise from the loudspeaker system. The experiment included checks for background noise so that this would not contaminate the results.

Figure 33 shows the 1/3 octave band results obtained from the window tests and Fig. 34 for certain skin panels. The data show the acceleration level AL(dB re 1g) resulting from an external sound pressure level (SPL) of 0 dB (2×10^{-5} N/m^2). The response of the panels and windows to acoustic signals is significantly greater than that of an equivalent limp mass. Resonant behavior of these surfaces is therefore indicated. However, if sound transmission through the panels is mass law dominated, use of the above data must be undertaken with care, since:

(1) radiation efficiency effects must be considered both in estimating the panel response to a given exterior field, and in estimating subsequent radiation into the cabin.
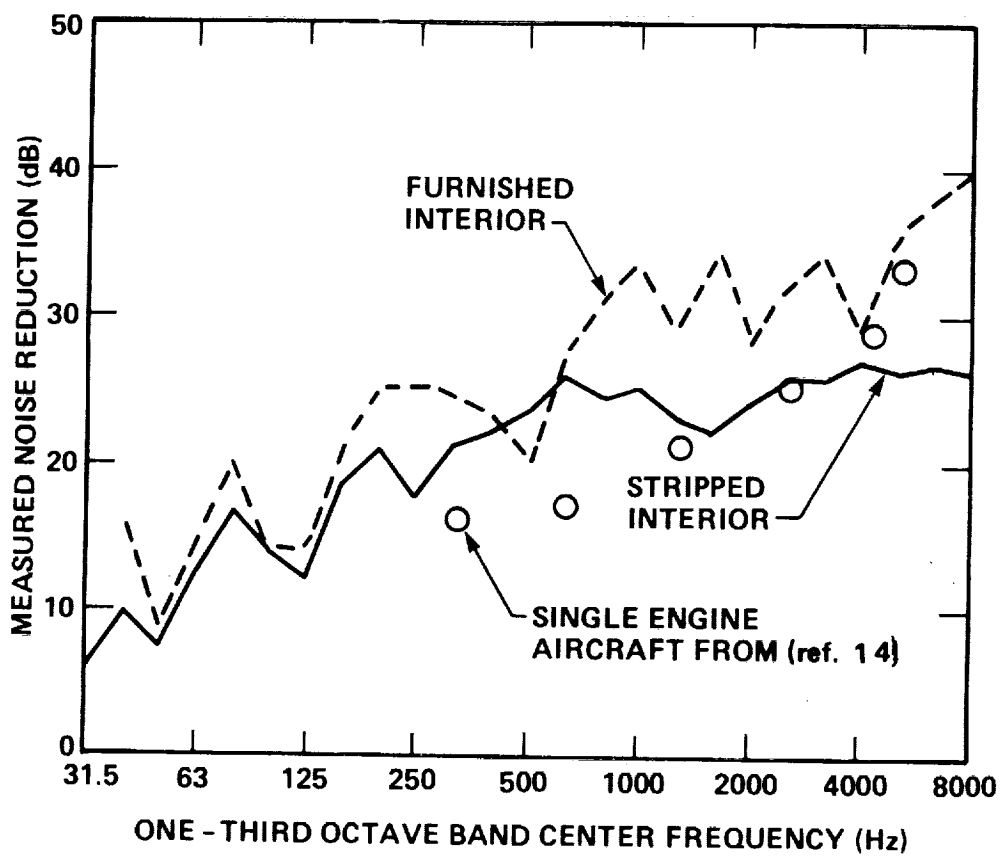
FIG. 32 . FUSELAGE NOISE REDUCTION WITH STRIPPED AND PRODUCTION
INTERIORS.
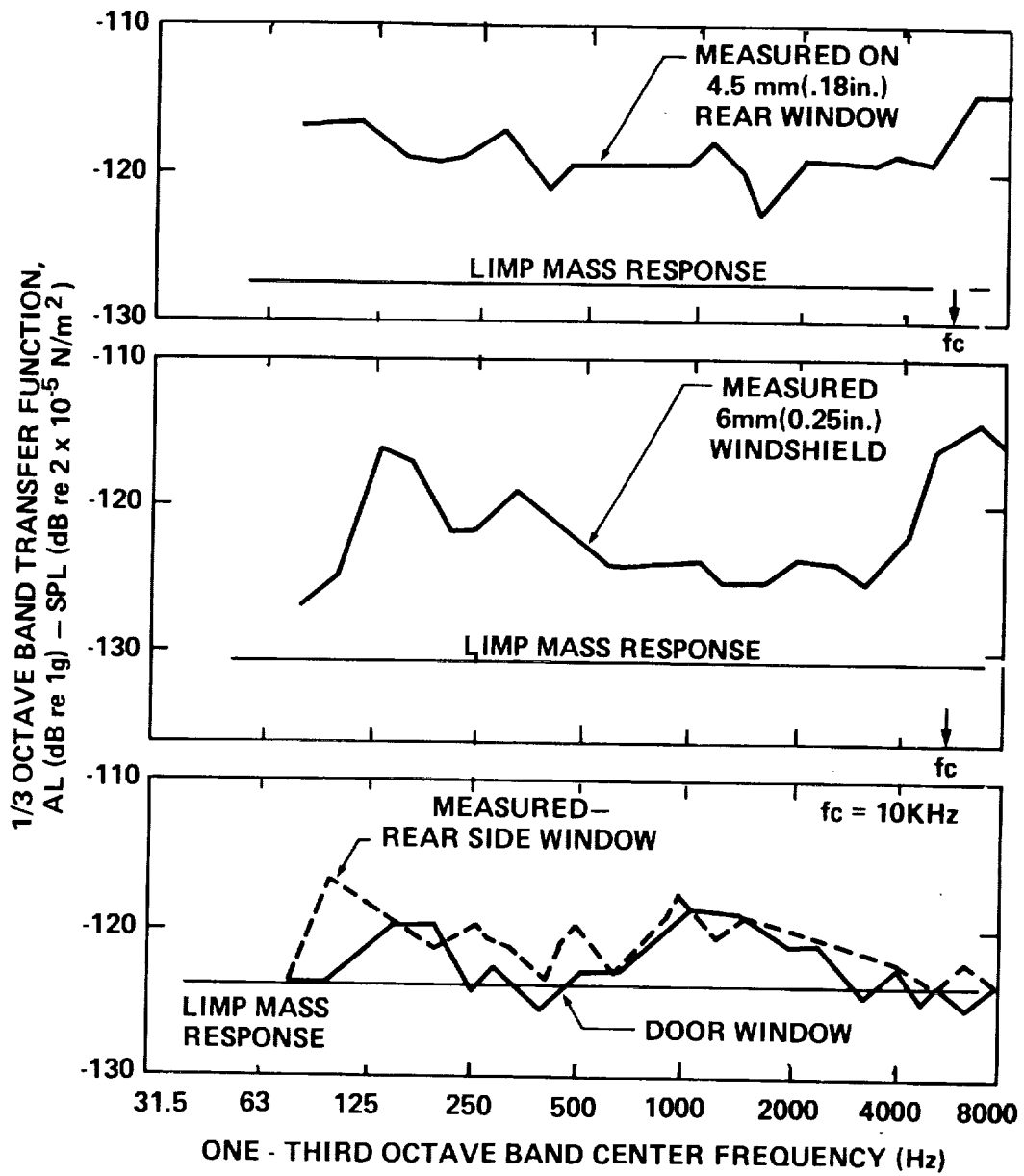
FIG. 33.   RESPONSE OF WINDOW ELEMENTS TO FREEFIELD
ACOUSTIC EXCITATION.
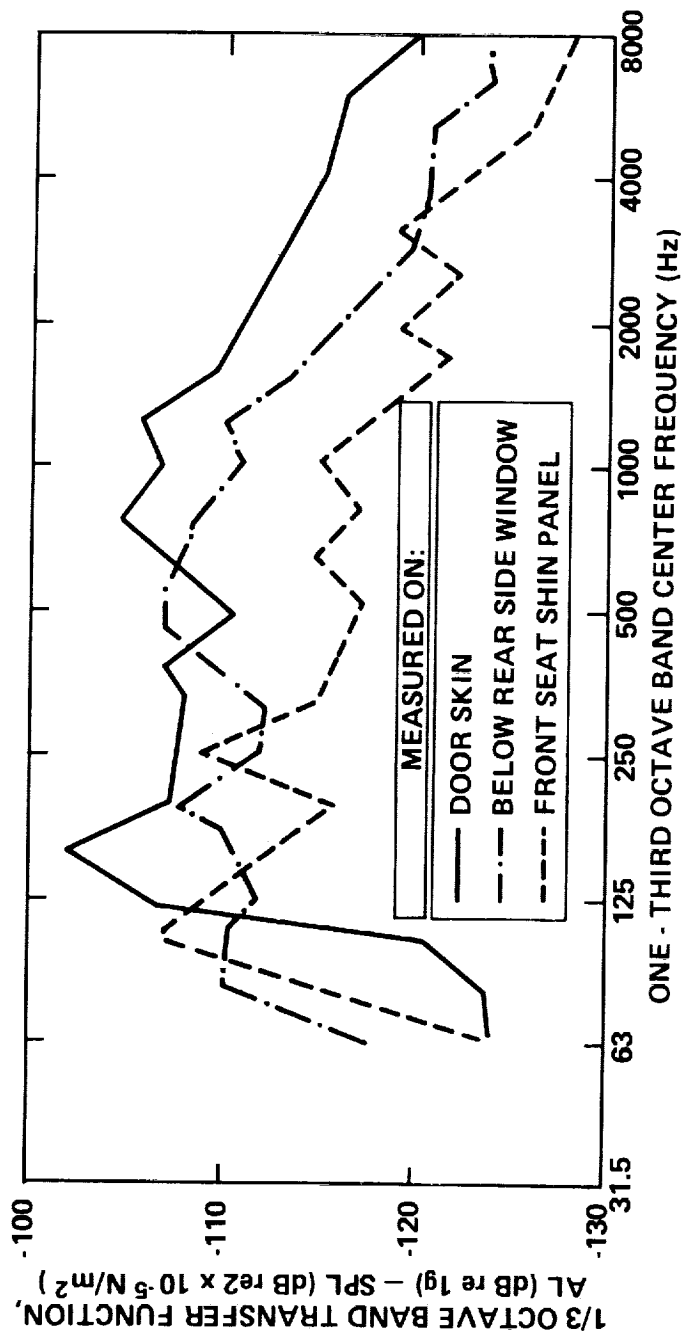
FIG. 34. RESPONSE OF PANELS TO FREEFIELD EXCITATION.

(2)   the given data apply only to an acoustic field at
       roughly normal incidence, and the transfer function will
       vary depending upon details of the excitation.

    Thus, these data are not used further quantitatively in this
study.

Structureborne Path from the Engine/Propeller Combination

    After flight observations of significant vibration at the
engine mounts, a series of ground tests were conducted to derive
the energy-averaged insertion loss of the mount system. Given
the insertion loss, engine mount vibration levels could then be
monitored and used in conjunction with a transfer function
(derived below) to predict interior noise contribution of engine-
transmitted vibrations. The insertion loss tests are described
in detail in Appendix A. Figure 35 shows the essential result
and indicates that very consistent mount performance is found
above 160 Hz, but that the behavior at lower frequencies is
erratic indicating possible resonant behavior.

    To estimate the contribution to the cabin acoustic levels of
vibration transmitted from the engine/propeller combination
through the mounts, a series of ground and flight experiments
were performed (see also Appendix A.) In one test, cabin noise
was measured in flight, with the normal mounts replaced by solid
aluminum blocks. The resultant difference is shown in Fig. 36,
wherein increases are seen out to almost 4 kHz. Also shown by
the dashed line is the change in level which would occur if all
cabin noise was due to vibration at the mounts and if the effect
of the solid mounts was to increase levels as derived above. If
these two experiments can be legitimately combined in this way,
then one concludes that the vibration of the particular mount
monitored increases more rapidly than the interior noise, and
thus either other mounts or other sources are contributing more
to the interior noise levels.

    A ground test was also conducted to derive the transfer
function necessary to quantitatively convert flight vibration
data at the mounts into interior noise levels. The difference in
noise between the "hard" and "soft" mount tests is assessed in
terms of the associated change in vibration (on the assumption of
linear relationship between structural vibrations and cabin
noise). Within the limitations of dissimilarity of relative
source contributions between ground run-up and flight, a transfer
function can be thusly developed. A specific example of the
method used to arrive at the transfer function is presented
below. The following results were obtained during the ground run
at an engine speed of 2400 RPM and a manifold pressure of 69 cm
(27 in) Hg. The results are presented for the 800 Hz one-third
octave band.

66
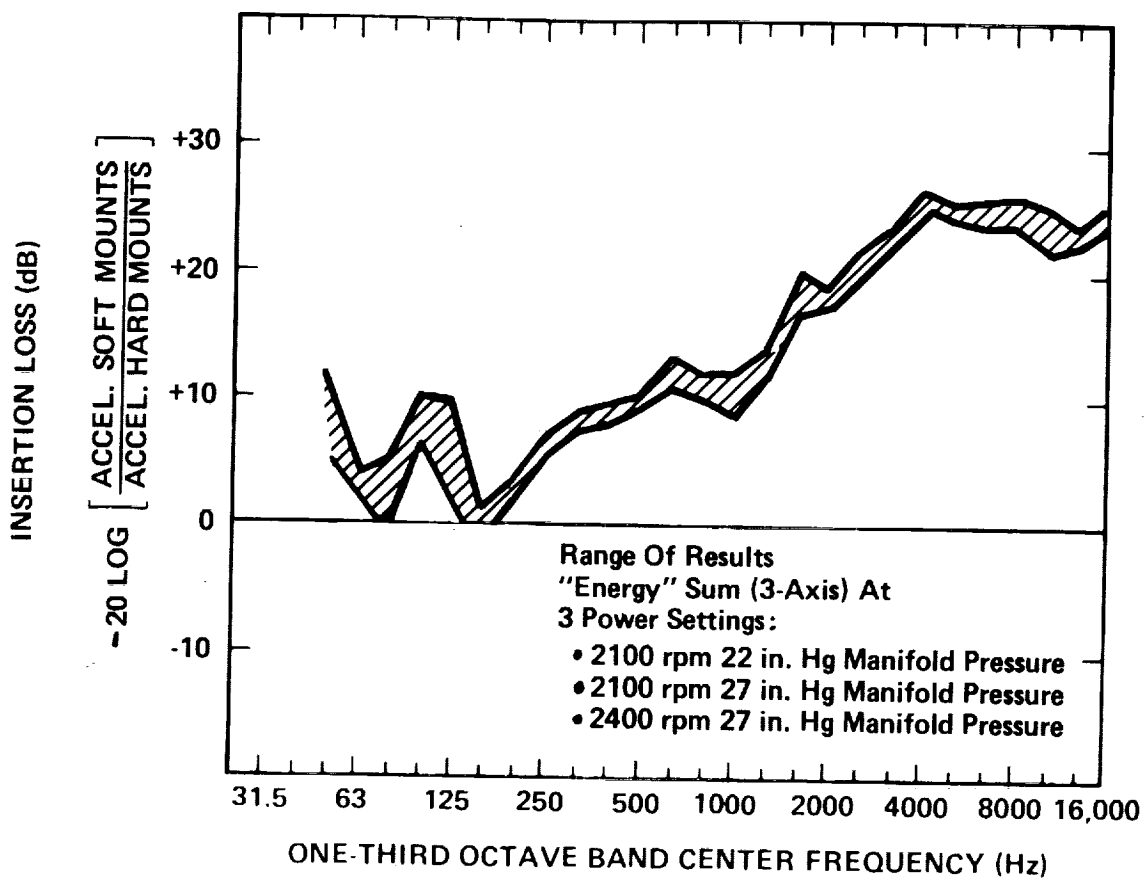
FIG. 35. INSERTION LOSS OF ENGINE MOUNTS.
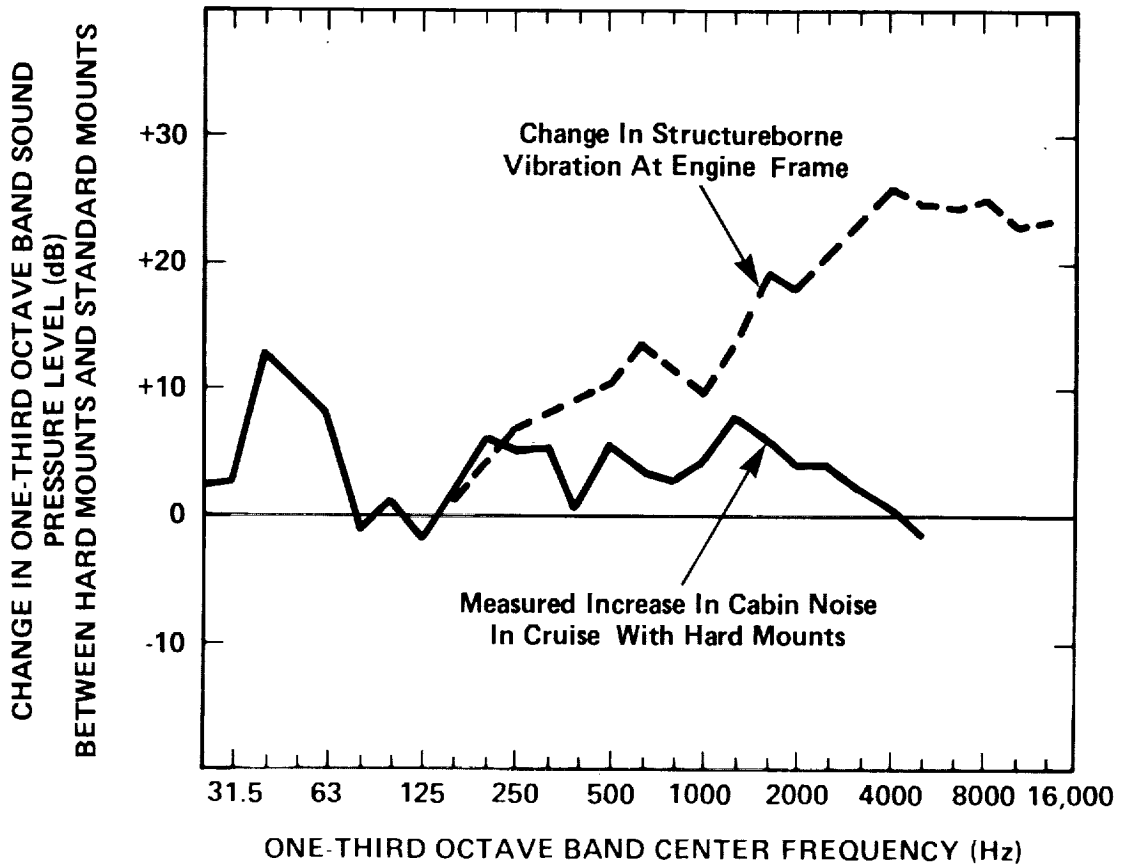
FIG. 36. CHANGE IN CABIN NOISE LEVELS WITH HARD MOUNTS.

	Average Mount Accelerations (dB re 1g):	Cabin Noise (dB re 2×10^{-5} N/m^2)
Hard Mounts	+10dB	88
Soft Mounts	− 3dB	84

Thus, at this particular frequency, a 13 dB increase in mount acceleration produced a 4 dB increase in cabin noise.

The airborne and structureborne contribution can be estimated according to the following relationship.

$$\overline{p^2}_{cabin} = \overline{p^2}_{air} + (Ka)^2$$

where K = transfer function (in N/m^2 per g)

a = acceleration (in g)

$\overline{p^2}_{cabin}$ = cabin mean square acoustic pressume (N^2/m^4)

$\overline{p^2}_{air}$ = airborne mean square acoustic pressure (N^2/m^4)

Substituting the measured values stated above, the following two equations are generated.

Hard Mount: $\overline{p^2}_{cabin} = 5.02 \times 10^{-1}$ N/m^2 = $\overline{p^2}_{air}$ + (K × 3.16)^2

Soft Mount: $\overline{p^2}_{cabin} = 3.17 \times 10^{-1}$ N/m^2 = $\overline{p^2}_{air}$ + (K × .707)^2

Solving these two equations yields the following results:

K = .126 N/m^2 per g (i.e., $SPL_{cabin} - AL_{mount}$ = 76dB)

$\overline{p^2}_{air}$ = .0935 N^2/m^4 (i.e., SPL_{air} = 83.7 dB re 2×10^{-5}N/m^2)

Thus, the contribution of airborne and structureborne noise at 800 Hz are as follows:

	Airborne	Structureborne
Hard Mount	83.7 dB	76+10 = 86 dB
Soft Mount	83.7 dB	76-3 = 73 dB

In those cases where there is at least a 3 dB increase in the cabin noise when hard mounts rather than soft mounts were used, the above estimating method is accepted. Figure A.46 shows the comparison of cabin noise levels with and without the hard mounts for all runs. This figure serves as the basis for deriving a complete spectrum of transfer functions. Increases of at least 3dB were noted for all frequencies between the 160 Hz and 4 kHz bands, except for the 2400 RPM ground run where the "3 dB increase" threshold is not reached below 400 Hz.

Figure 37 shows the values of the transfer functions (SPL – AL) calculated in the manner shown above for frequencies between 160 Hz and 4000 Hz using the ground runs; thus by knowing the average mount acceleration, the structureborne contribution to cabin noise can be estimated.
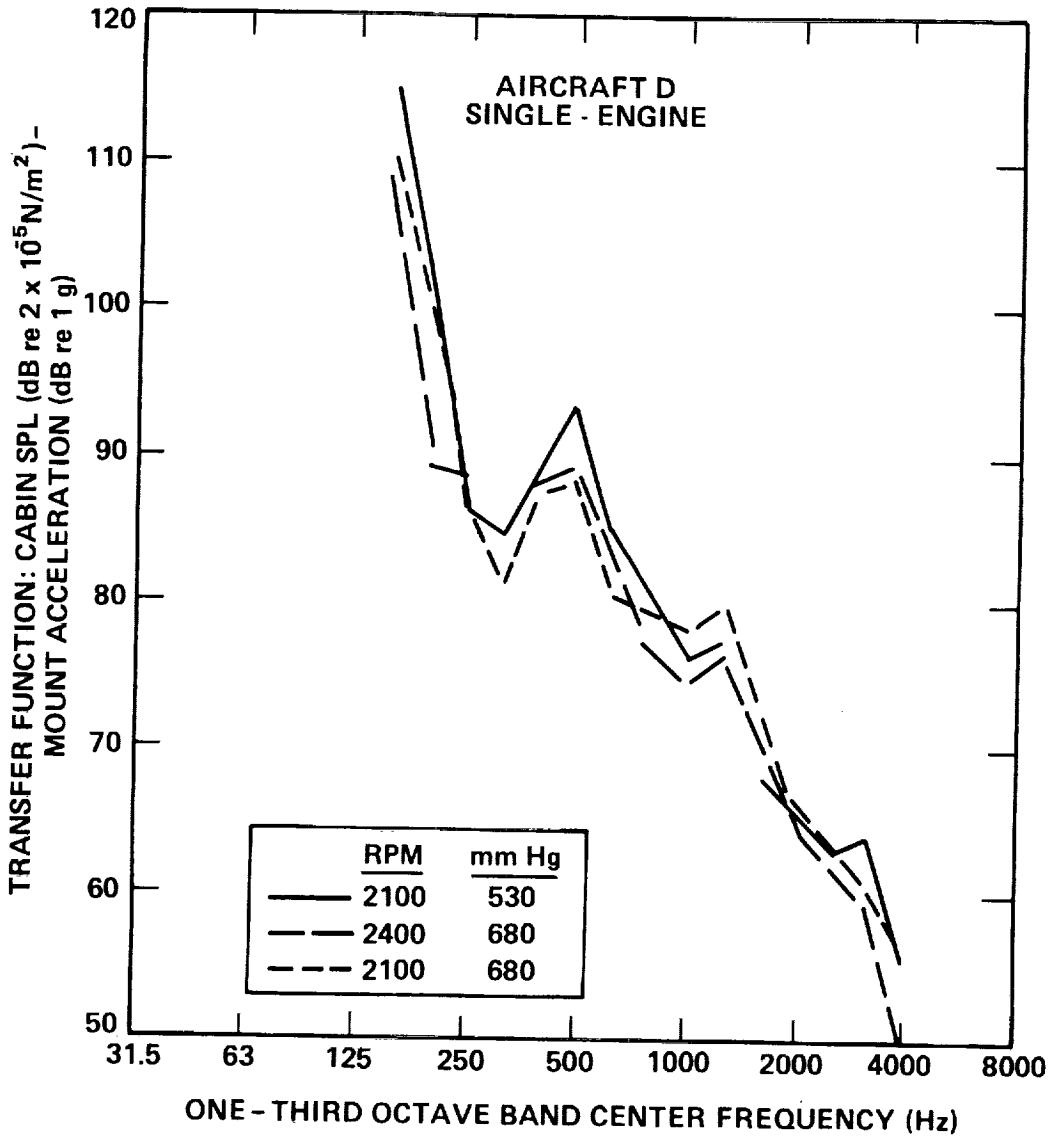
FIG. 37. TRANSFER FUNCTION BETWEEN AVERAGE MOUNT ACCELERATION
AND CABIN NOISE. (DERIVED FROM GROUND TIE-DOWN TEST).

3.7 Synthesis of Cabin Noise Spectrum from Source and Path Information

The foregoing data are used directly to estimate the interior noise contributed by the various sources and paths.

Airborne Sources

The calculation of airborne propeller and engine exhaust source contributions is done by combining exterior levels measured at the wing-strut and machinery space microphones with the sidewall and windshield noise reduction data derived from the ground test (Figs. 24-28). This approximation utilizes spatial averages of the propeller and exhaust sound field and of the localized transmission variations. Therefore, the approach may overlook source or transmission path "hot spots", such as may occur near the exhaust pipe.

Non-propulsive Sources

The dive test results which were shown earlier in Fig. 29, increased by 1.7 dB to account for propeller slipstream velocity increase, are used as the estimate of interior noise due to nonpropulsive sources.

Structureborne Sources

Figure 38 presents the energy-averaged spectrum of the accelerometer on the aircraft side of the four engine mounts, taken from a ground runup test. Each mount was instrumented with a 3-axis accelerometer and the spectrum from each recorded. Obviously individual mounts will have a spectra different from the averaged spectrum shown, and flight acceleration spectra may differ from those on ground tests. Since flight spectra were not monitored on all four mounts simultaneously and since the ground transfer function tests provided the most complete mount vibration survey, the energy-averaged spectra are used below to deduce the approximate contribution of engine-and propeller-induced structureborne noise for the flight cases. It should be noted that the vibration spectra measured in flight on the one mount which could be monitored fell within the band of 12 individual spectra included in the ground test; therefore, the approach used in calculating the noise seems justified, given the level of detail available.
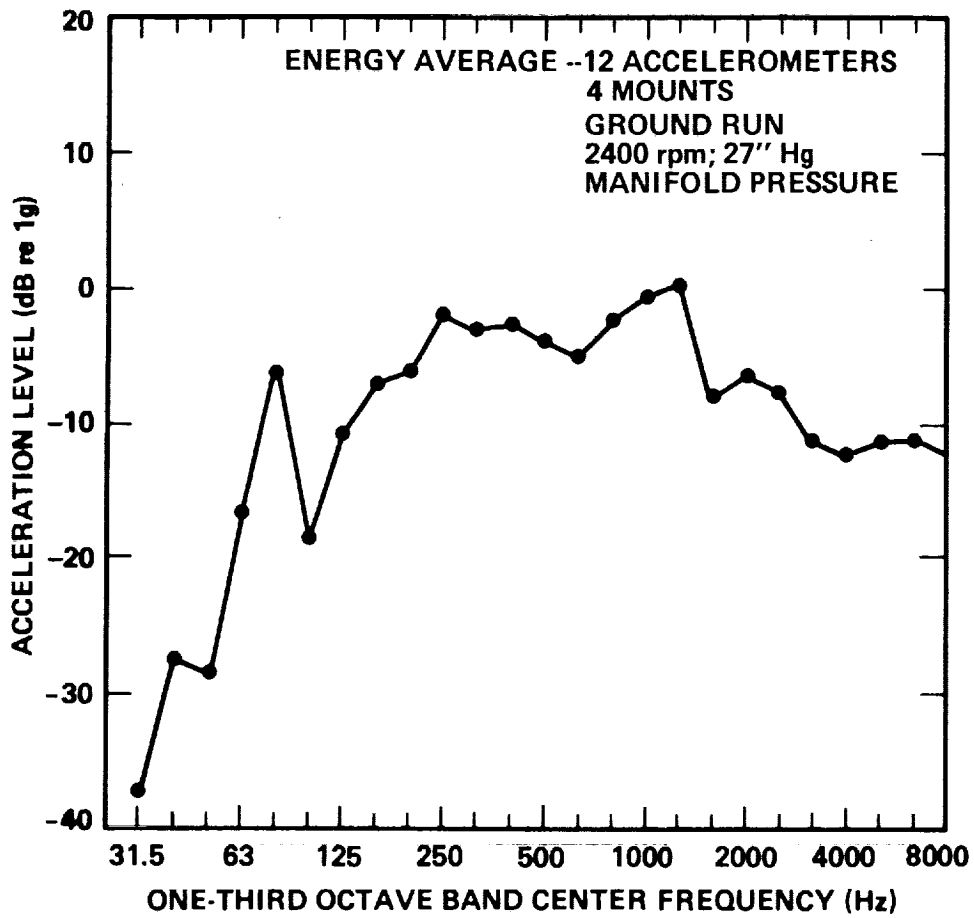
FIG. 38.   ENERGY-AVERAGE SPECTRUM OF 12 ACCELEROMETERS ON
ENGINE MOUNTS; GROUND RUNUP - 2400 RPM

Calculation of Structureborne Contribution to Cabin Noise

Figure 39 shows the structureborne contribution to the cabin noise spectrum (in ground runup) deduced by combining the appropriate transfer function from Fig. 37 with the energy-averaged acceleration spectra for two engine power settings. The structureborne noise is predicted to be either dominant or contributing strongly at frequencies from 160 Hz (the lower freuency limit of the valid data) and 1250 Hz, above which the contribution falls off rapidly. Note that in the data shown in Fig. 39, the other principal noise sources – especially the propeller airborne and airflow noise – do not have the same characteristics during a ground runup as in flight, and the presence of the ground plane alters the airborne transmission path of propeller and engine airborne noise by providing a reflecting surface below the aircraft. The curve for the 2400 RPM case is used in the source-path composite calculation below, for the reasons previously cited.

Summation

The previously-derived source-path contributions are summarized on the top half of Figure 40. It can be seen that the predictions show dominant contributions from each of the several major source-path combinations:

- Propeller airborne sound transmitted through the various exterior surfaces appears to dominate the low frequency part of the spectrum (below the 100 Hz band), and contributes measurably to the 160 Hz band (2P).

- Structureborne sound from the engine/propeller combination transmitted through the mounts and engine support structure into the airframe is a strong contributor from the 160 Hz band (twice prop rate) to the 1250 Hz band, above which its contribution drops rapidly.

- Noise due to sources unrelated to the propeller or engine provide a significant contribution to broadband levels above 100 Hz, being dominant in many frequency bands.

- Engine airborne sound is not predicted to be dominant in any frequency band.

74
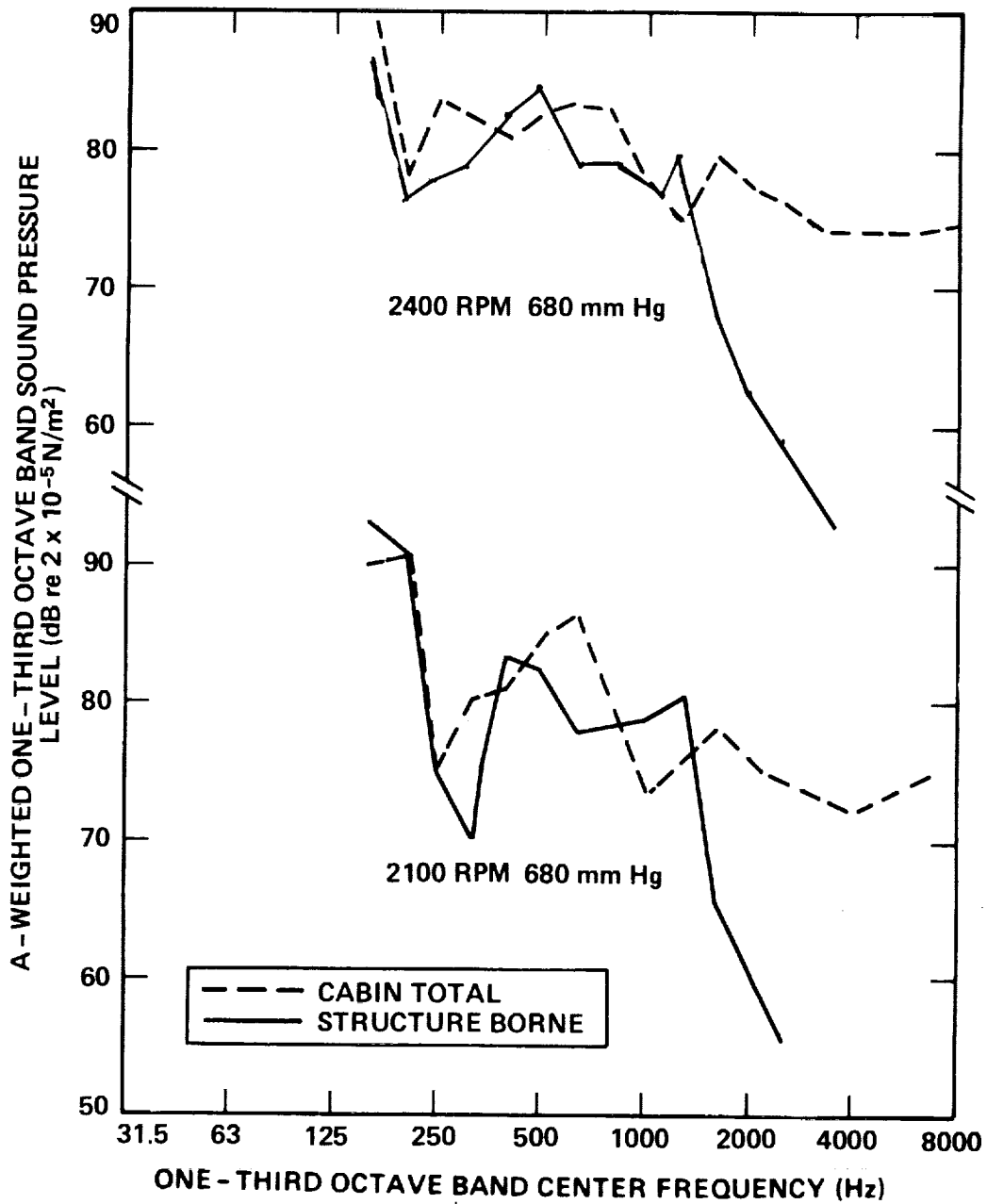
FIG. 39 . DEDUCED STRUCTUREBORNE CONTRIBUTION TO CABIN NOISE
DURING GROUND RUNUP.
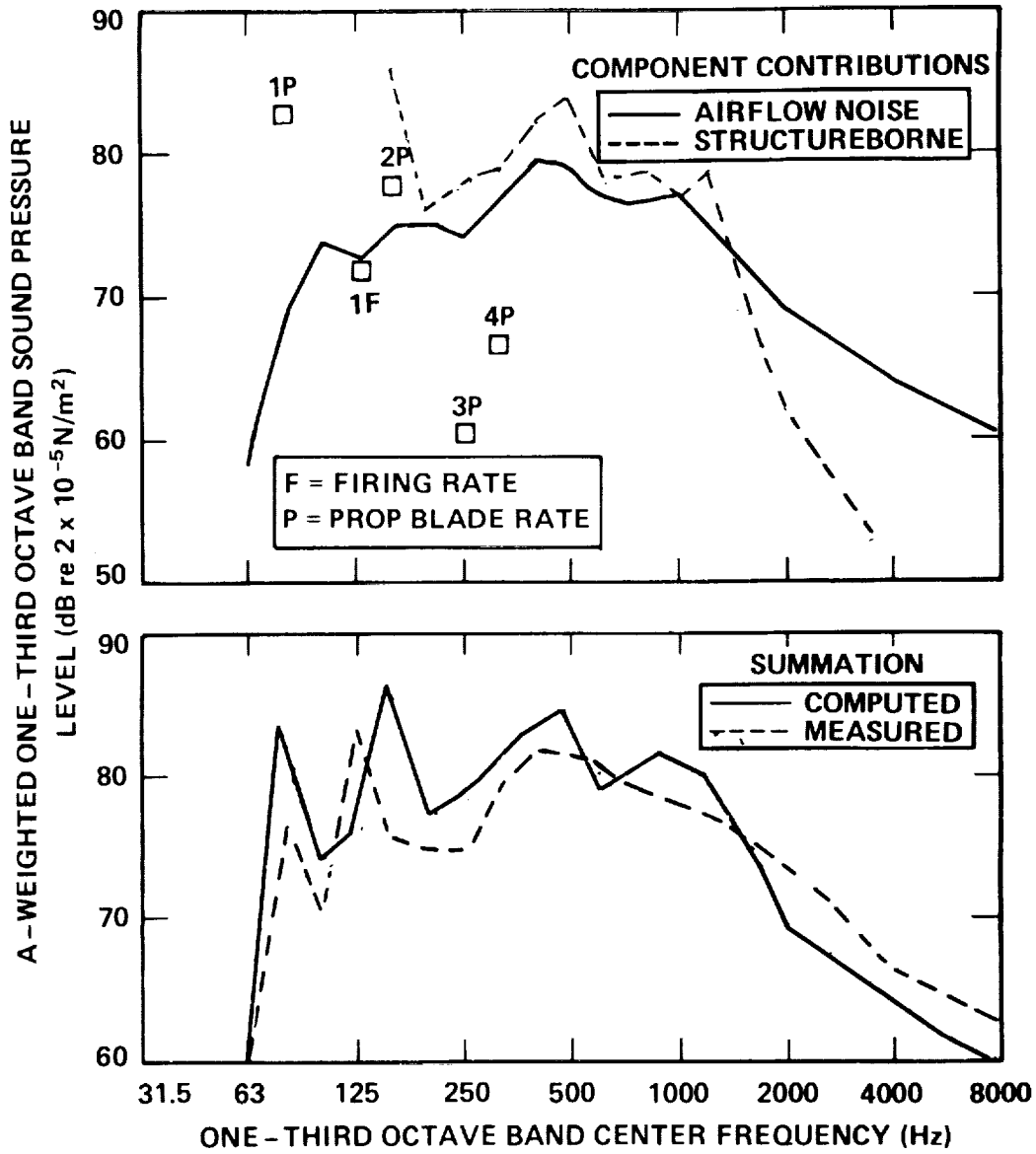
FIG. 40.   ESTIMATE OF CABIN NOISE CONTRIBUTION FOR CRUISE
CONDITION: 2400 RPM; 70M/SEC.

76

The contributions predicted for the structureborne sound and the airflow should be viewed as probable upper limits for the following reasons:

- The transfer function approach used to determine the contributions of the energy transmitted through the mounts did not account for coupling between the mounts and attachment points on the structure. If the mounts are well coupled via the engine or the spider (support) structures, the energy flow within the mount structure will produce several transmitting contributions from one source of vibration, thus overestimating the transfer function when derived in the manner shown above. This problem is likely to be greatest at low frequencies where vibrational modal behavior will exist.

- The airflow contribution was derived from a dive test, which included the contributions of residual propeller and engine airborne sound, and structureborne contributions. However, the prop-wash effect on flow-induced noise was not well simulated and that effect may actually increase the true contribution of the nonpropulsion sources.

The predicted cabin noise spectra from individual source-path combinations are added up in an energy sense as incoherent sources to obtain a composite predicted spectrum, which is shown in the lower half of Fig. 40, and which is also compared with measured data. The overall agreement between prediction and measurement is good, except at the frequency corresponding to the engine firing frequency (1F) and at twice propeller rate. The general overestimate of the interior levels is not great enough to cause concern, considering the previously-described variability in the cabin levels and in the vibration of individual mounts during a flight, and thus considering that some of the data used to derive the predicted levels was taken from different flights and from ground tests. The large discrepancy at 1F may be due to locally high levels near the exhaust pipe exit transmitting through a hot-spot in the fuselage, rather than a more generally distributed transmission of much lower levels, through the whole fuselage structure, as was assumed. The overestimate at 160 Hz is dominated by the calculated structureborne contribution; as mentioned above, there may be coupling within the engine-mount system which causes an overestimate of the transfer function using the techniques described herein.

77

4. SUMMARY AND CONCLUSIONS

Summary

This study consisted of a systematic survey of the interior noise levels and spectral characteristics of 18 single- and twin-engin propeller-driven light aircraft, as well as an in-depth source-path diagnosis of a single-engine aircraft which was considered representative of a large part of the fleet.

The technical efforts began with a survey of all propeller-driven general aviation aircraft of US manufacture to determine their relative performance ranges, their impact on the total fleet (both present and future), and their internal noise characteristics. From these aircraft, 18 were selected for flight surveys. The purpose of the flight surveys was to measure internal noise levels and identify principal noise sources and paths under a carefully-controlled and standardized set of flight procedures. Once the survey had been completed and the results analyzed, one aircraft model was chosen for more detailed application of advanced noise source and path diagnosis. This aircraft was subjected to a second round of flight tests in which more detailed measurements of sources and paths were made and additional diagnostic ground tests were performed.

The detailed diagnostic tests consisted of flights and ground tests in which various parts of the aircraft, such as engine mounts, the engine compartment, exhaust pipe, individual panels, and the wing strut were instrumented to determine source levels and transmission path strengths using the transfer function technique. The tests were limited to those which could be conducted on flightworthy aircraft in an operational environment (i.e., at an airfield, in a hangar, or in-flight), but the results were suitably conclusive to provide identification of predominant source and path combinations.

Conclusions

The objectives of the flight survey were fulfilled. Surveys of 18 production aircraft produced consistent trends of cabin noise levels, which fall in the range of previously-reported results. Standardizing the flight test procedures allowed meaningful direct comparisons to be made. The survey also identified some potential pitfalls of flight testing, namely variability in levels among nominally-similar operations. Previously-observed variations in sound and vibration levels among different cabin locations were consistently found in all aircraft. Pressurization effects generally provided reduced levels of broadband noise and reduced levels of propeller harmonics.

The results of the flight survey phase of the work confirmed that the presently-produced designs of both single- and twin-engine aircraft produce cabin noise levels which, when compared with results of careful psychoacoustic tests, would be considered highly annoying to a large percentage of the population. The flight surveys also produced consistent evidence of propeller noise as a primary contributor to cabin noise in all types of aircraft, as well as revealing some evidence of engine and airflow noise being of considerable importance in most aircraft.

Energy at propeller blade rate and its harmonics was dominant in all 18 aircraft tested, while the apparent contribution of engine-related noise varied widely; therefore propeller sources and paths must be controlled in all aircraft, but the engine-related sources may not control cabin levels in all aircraft, especially large twins. One finding that is perhaps new to the light aircraft community is the apparently strong role of nonpropulsion noise in determining the cabin A-weighted noise levels of single-engine aircraft. Inasmuch as treatments for turbulence-excited panel vibration may be different from those which are best-suited for controlling sound-induced vibration (and reradiation), a more detailed under-standing of this source is needed.

The diagnosis of one single-engine aircraft illustrated that to successfully separate the contributions of all sources and paths, extensive ground and flight measurements are required, and that further component-by-component testing is desirable in order to isolate the contributions of various paths by which the energy from a given source reaches the cabin. However, within the context of the tests and analyses carried out, a source-path model was constructed which, in composite form, produced predicted noise levels which agreed quite well with measurements and predicts the following major trends:

- Propeller airborne sound transmitted through the various exterior surfaces appears to dominate the low frequency part of the spectrum (below the 100 Hz band), and contributes measurably to the 160 Hz band (2P).

- Engine airborne sound was not predicted to be dominant in any frequency band, but appeared clearly in the measured spectrum at firing rate, probably due to an undiagnosed airborne path, and/or to the locally high levels near the exhaust pipe exit.

- Noise due to sources unrelated to the propeller or engine (i.e., airflow over the airframe) provide a significant contribution to broadband levels above 100 Hz, being dominant in many frequency bands.

79

- Structureborne sound from the engine/propeller combination transmitted through the mounts and engine support structure into the airframe is a strong contributor from the 160 Hz band (twice prop rate) to the 1250 Hz band, above which its contribution drops rapidly.

Further refinements in the diagnosis will probably not change the overall trends predicted above, but would be helpful to isolate critical paths. The major uncertainties which could be resolved by further diagnosis are:

- coupling between vibration transmitted through the four mounts;

- isolation of airborne sound transmitted through individual panels, the windshield, windows, and firewall;

- localization of airflow noise (if possible).

The transfer function approach was found to be most useful in developing predictions of the various source-path contributions to the interior noise. This approach provides a direct means of quantifying the benefits which could be achieved by source reductions and/or path treatments, and thus helps to set goals for the analysis of either class of noise reduction approaches.

Noise control treatments which are applicable to the dominant source-path combinations include:

Source	Path	Treatment Concepts
Propeller Blade (due to steady and unsteady sources)	Airborne through exterior surfaces	(1) Locally-stiffened panels with resonances at frequencies other than blade frequencies
		(2) Increased thickness of windshield and windows, where appropriate
		(3) Tuned dynamic absorbers on structural elements showing high response at prop frequencies

80

Source	Path	Treatment Concepts
Propeller unsteady loads	Structureborne through engine mounts	(1) Improved mounts (2) Stiffer mounting points at firewall (3) Redesigned engine suspension to optimize (1) and (2) (4) Damping of transmitting and radiating surfaces
Engine radiated noise	Airborne through aircraft exterior	(1) Exhaust muffler (2) Exhaust extension to move source away from critical areas (3) Same as (1)-(3) for propeller airborne
Engine vibration	Structureborne through engine mounts	Same as Propeller structureborne
Flow over exterior surfaces	Excitation of panels and windows causing radiation into cabin	(1) Damping (2) Alteration of panel or window properties (thickness or material) to separate predominant response spectrum from excitation spectrum
Flow over exterior	Interaction with surface discontinuities (cracks, cutouts, etc.)	(1) Minimize excitation by careful microscale aerodynamic cleanup (2) Ensure adequate seals

In addition to the specific concepts mentioned above, good noise control engineering practice dictates careful attention to all flanking paths, such as untreated air vent ducts, inadequate structure between tail cone and passenger compartment, etc. It is also vital to ensure that treatment is balanced among all dominant sources in a way that will bring all contributions to an equal level in each frequency band of interest.

APPENDIX A

SUMMARY OF FLIGHT DATA

A.1 Introduction

This appendix provides a detailed summary of flight tests conducted in both the fleet survey and preliminary diagnostic studies. The appendix is written to stand alone, so some of the material may repeat what is written in the main body of the report. The aircraft surveyed are not identified by manufacturer or model number inasmuch as the objectives of the study are to develop generally applicable data and techniques. However, where important phenomena are illustrated by the data, the pertinent features of the aircraft are provided to assist in analysis and understanding.

The methods and equipment used in the data acquisition process were described in the main body of the report (Secs. 2 and 3). This appendix is a summary of all noise and vibration data gathered during the test program. While it is not practical to include graphs of every datum measured, the major data packages are reported in detail. In this appendix, no attempt is made to link the various data into a description of the role of each noise source and path for interior noise. Rather, the available "raw material" used for this task is summarized. The text is generally brief because most of the information is provided in tables and graphs.

A-1

A.2 Data Matrix

Shown in Table A.1, Parts A through D, is a listing of all data gathered during the flight test program. The following information is given for each aircraft tested:

- a) Aircraft type identification (by code letter)

- b) Number of propeller blades

- c) Engine operating conditions (RPM, manifold pressure, synchronized or unsynchronized engines for twins)

- d) Position and type of each transducer for which data are available. Note that not all transducers were operating simultaneously, i.e., some data samples were taken sequentially using a single transducer.

A.3 Table of A-weighted Sound Levels and Speech Interference Levels

Listed in Table A.2, are the measured values of A-weighted sound pressure levels and speech interference levels [SIL (0.5, 1, 2, 4)] for each aircraft. All measurements were made at or near the center of the cabin (i.e., between the pilot and co-pilot) at head height, except for the case of turbine-powered twins. In these larger aircraft, the results shown are the range of levels measured in the passenger cabin (as differentiated from the cockpit). As was noted in Sec. 2 of this report, sound levels may vary significantly with position inside the aircraft, even in small aircraft cabins. This fact is clearly demonstrated in Sec. A.4 below.

TABLE A.1. SUMMARY OF DATA MEASURED IN FLIGHT SURVEYS.

A. SINGLES WITH PRODUCTION INTERIORS

Reference: FLIGHT TEST SURVEY

Notes: Job 08108
NASA LaRC

TRANSDUCERS

MICROPHONES columns: Cabin Center, Windshield, Copilot Side Window, Pilot Side Window, 2nd RHS Window, 3rd RHS Window, 2nd LHS Window, 3rd LHS Window, Rear Wind./Compart., Rear Passenger, 4th RHS Window, 1st LHS Passenger, 1st RHS Passenger, Pilot Weather Window

ACCELEROMETERS columns: Windshield, Seat Rail, Wing Spar, Copilot Side Window, Copilot Door Skin Trim, 2nd RHS Window, 3rd RHS Window, Rear Window, Overhead Window, Door Frame (Axial), Overhead Trim Panel Center Cabin, Overhead Trim Panel-RHS Copilot, Overhead Trim Panel-RHS Rear, 2nd LHS Window, 3rd LHS Window, Center Console, Windshield Frame, 4th RHS Window, Window Trim-Rear

AIRCRAFT DESCRIPTION	Test Date
AC. A, 2 blade; piston 2550 RPM	7/18
AC. B, 2 blade; piston 2600 RPM, 104 kts / 2300 RPM, 90 kts	7/17
AC. E, 3 blade Turboch; piston 2450 RPM, 140 kts, Unpressured (1) / 2450 RPM, 140 kts, Unpressured (2) / 2450 RPM, AirCond, Pressurized 1.5 psi / 2450 RPM, No AC, Pressurized 1.5 psi / 2350 RPM, AC, Pressurized 1.5 psi	7/17
AC. D, 2 blade 2400 RPM, 135 kts / 2100 RPM, 120 kts	7/17
AC. I, 3 blade 2450 RPM, 160 kts, 23" Hg / 2300 RPM, 155 kts, 23" Hg	11/6
AC. J, 3 blade Turbo 2400 RPM, 158 kts, 29" Hg / 2200 RPM, 145 kts 27" Hg	11/5
AC. H, 3 blade 2500 RPM, 140 kts / 2300 RPM, 140 kts	10/22
AC. G, 2 blade 2380 RPM, 130 kts / 2200 RPM, 137 kts	10/22

NOTATION CODE

X = HAVE DATA
? = DATA QUESTIONABLE
-- = BAD DATA
1 = DATA AT LEFT RATHER THAN RIGHT SIDE

TABLE A.1. (Cont.) SUMMARY OF DATA MEASURED IN FLIGHT SURVEYS.

B. PISTON-POWERED TWINS

Reference: Flight Survey

The table columns are grouped under three major headings: **CABIN MICROPHONES** and **TRANSDUCERS** (sub-column: Pilot Weather Window, 2nd/3rd/4th RHS Window, Pilot Weather Window) and **CABIN ACCELEROMETERS**.

Cabin Microphone columns: Tape Reel, Cabin Center, Windshield, Copilot Side Window, Copilot Head, Pilot Side Window, Pilot Head, 1st LHS Passenger, 1st RHS Passenger, Rear Passenger, Baggage/Tailcone.

Cabin Accelerometer columns: Windshield, Seat Rail-Pilot/Copilot, Copilot Side Window, Pilot Side Window, Pilot Weather Window, 2nd RHS Window, 3rd RHS Window, 4th RHS Window, Copilot Entry Door, Overhead Trim Panel-Btw. Pilot/Copilot, Trim Btw. 2nd-3rd RHS Window, Trim @ 2nd RHS Window, Trim @ 3rd RHS Window, 1st RHS Pass. St. Rail, Trim @ 4th RHS Window, 2nd LHS Window, Trim on Rear Entry Door, HH Trim Passenger Area, Frame of 4th RHS Window, Frame of 2nd RHS Window.

AIRCRAFT DESCRIPTION	Test Date
AC. K, 3 blade 2400 RPM, 178 kts, 23" Hg, synchron 2200 RPM, 165 kts, 23" Hg, synchron 2400 RPM, 178 kts, 23" Hg, unsynch 2400 RPM, 140 kts, 23" Hg, port eng. only Dive, 110 kts, engines off	11/6
AC. L, 3 blade, Turbo 2400 RPM, 175 kts, 32" Hg, synchron 2200 RPM, 153 kts, 26" Hg, synchron Dive, 110 kts, engines off Dive, 150 kts, engines off	11/7
AC. M, 3 blade, Turbo pressure 2400 RPM, 185 kts, 23" Hg, synchron 2100 RPM, 148 kts, 21" Hg, synchron	11/5
AC. N, 3 blade 2500 RPM, 163 kts, 23" Hg, synchron 2300 RPM, 148 kts, 21" Hg, synchron	11/7
AC. O, 3 blade 2500 RPM, 190 kts, 25" Hg, synchron 2300 RPM, 185 kts, 23" Hg, synchron	11/5
AC. P, 3 blade Turbo 2700 RPM, pressurized synchron 2500 RPM, pressurized synchron pressurized unsynchron	11/5
AC. F, 2 blade, stripped 2400 RPM, 25" Hg, synchron 2100 RPM, 23" Hg, synchron	7/18
AC. F, 3 blade, stripped, prototype 2400 RPM, 25" Hg, synchron 2100 RPM, 22" Hg, synchron	7/18

Under the TRANSDUCERS section: "SEE ALSO NOTE 1" (applies to AC. P rows).

Under CABIN ACCELEROMETERS, AC. F rows note: "(+ Addit. Structural Members)".

Notes: 1. Data on left side.

A-4

TABLE A.1. (Cont.) SUMMARY OF DATA MEASURED IN FLIGHT SURVEYS.

C. TURBINE-POWERED TWINS

Reference: Flight Survey

DESCRIPTION	Test Date	Tape Reel	Center Cockpit	1st LHS Passenger	1st RHS Passenger	2nd LHS Passenger	2nd RHS Passenger	3rd LHS Passenger	3rd RHS Passenger	Behind Rear Bulkh at Entry Door	LHS Passenger @ Entry Door	RHS Passenger @ Entry Door	LHS Passenger in Baggage Area	Pilot/Copilot Seat Rail	Passenger Seat Rail	Wing Spar	Overhead Trim Panel @ Pilot/Copilot	Overhead Trim Panel @ Midcabin	1st RHS Window	2nd RHS Window (1st Porthole)	3rd RHS Window (2nd Porthole)	4th RHS Window (3rd Porthole)	1st LHS Window	2nd LHS Window	3rd LHS Window	4th LHS Window	5th LHS Window	5th LHS Window Frame	5th RHS Window (4th Porthole)	1st RHS Window Frame	6th RHS Window (5th Porthole)
AC. Q, 4 blade 1950 RPM, 214 kts, synch., press 1930 RPM, 215 kts, synch., press	11/3		X X	X X	X X	X X	X X	X X	X X	X X				X	X X	X X	X	X		X	X										
AC. R, 3 blade 1690 RPM, 215 kts, synch. press	11/4		X	X	X	X	X	X	X	X					X	X	X	X		X	X	X			X X	X X			X		
AC. S, 3 blade 2000 RPM, 162 kts, synch., press. 1900 RPM, 155 kts, synch., press.	11/6		X X	X X	X X	X X	X X			X		X X	X	X	X X		X		X X		X				X						
AC. T, 4 blade 1710 RPM, 205 kts, synch., press.	11/4		X	X	X	X	X	X	X	X	X		X		X X X	X X X	X X X	X X	X	X	X	X			X		X		X		X

A-5

TABLE A.1. (Cont.) SUMMARY OF DATA MEASURED IN FLIGHT SURVEYS.

D. DETAILED DIAGNOSTIC TESTS

Reference: Flight Survey

TEST DESCRIPTION	Date	Tape Reel #
AC. C, PARTIAL PRODUCTION INTERIOR		
3BL, 2400 RPM, 130 kts, 21.5" Hg	7/17	6
Shake test-shaker on eng. support	7/17	6
Shake test-shaker on eng. support	7/17	6
Acoustic NR-Loudspeaker		7
2BL, 2400 RPM, 130 kts, 22.5" Hg	7/18	7
2BL, 2100 RPM, 128 kts, 22.5" Hg		7
2BL, 2400 RPM, 138 kts, 22.5" Hg		8
2BL, 2100 RPM, 130 kts, 22.5" Hg	9/16	8
Ground Run 2100, 2400 RPM		9
Vibration Isolator 1L Test	9/17	10
2BL, 2400 RPM, 27" Hg Static at		
2100 RPM, 27" Hg reels q & 10		
2100 RPM, 22" Hg		
AC. D, STRIPPED INTERIOR		
3BL, 2400 RPM, 140 kts, 25.5" Hg	7/15	1
3BL, 2400 RPM, 140 kts, 26" Hg		1
3BL, 2100 RPM, 125 kts, 25" Hg		1
3BL, 2100 RPM, 125 kts, 25" Hg		2
3BL, 2400 RPM, 140 kts, 26" Hg		2
3BL, 2100 RPM		2
3BL, 2400 RPM, 130 kts, 26" Hg	7/16	3
3BL, 2400 RPM, 130 kts, 26" Hg		3
3BL, 2100 RPM, 128 kts, 25" Hg		3
2BL, 2425 RPM, 130 kts, 25" Hg	7/16	4
2BL, 2100 RPM, 135 kts, 25" Hg		4
2BL, 2400 RPM, 140 kts, 25" Hg		4
Shake test-shaker on Eng. support		5
Acoustic Xfer-loudspeaker, NR		
AC. D, PRODUCTION INTERIOR		
2BL, 2400 RPM, 135 kts, 25" Hg		
2BL, 2100 RPM, 120 kts, 25" Hg		

*Upper
**Lower

SOFT MOUNTS — 2 runs of 6 accelerometers describing
HARD MOUNTS — 3 axes on 4 engine mounts

CABIN MODE SURVEY
CABIN MODE SURVEY
CABIN MODE SURVEY

TABLE A.1. (Cont.) SUMMARY OF DATA MEASURED IN FLIGHT SURVEYS.

| | | | CABIN MICROPHONES | | | | | | STRUCTURE ACCELEROMETERS | | | ENGINE ACCELEROMETERS | | |
PISTON POWERED TWINS (cont'd) Reference: Flight Survey DESCRIPTION	Test Date	Tape Reel	Cabin Center #1	#2	#3	#4	#5	#6	#4 Longitudinal	#4 Lateral	#3 Longitudinal	#4 Longitudinal	#4 Lateral	#3 Longitudinal
AC. F, 2 blade, stripped prototype	9/18													
2400 RPM, 155 kts, synchronized			X	X	X	X	X		X	X	X	X	X	X
2100 RPM, 147 kts, synchronized			X	X	X	X	X		X	X	X	X	X	X
2400 RPM, 150 kts, unsynchronized			X	X	X	X	X		X	X	X	X	X	X
2100 RPM, 143 kts, unsynchronized			X	X	X	X	X		X	X	X	X	X	X
AC. F, 2 blade, stripped prototype	9/18		X	X	X	X	X							
2400 RPM, 146 kts, synchronized			X	X	X	X	X	X						
2100 RPM, 147 kts, synchronized			X	X	X	X	X	X						
2400 RPM, 152 kts, unsynchronized			X	X	X	X	X	X						
2100 RPM, 147 kts, unsynchronized			X	X	X	X	X	X						
Dive, 150 kts, Engines off														

TRANSDUCERS

CABIN ACOUSTIC MODE SURVEY

TABLE A.2.   A-WTD SOUND LEVELS AND SPEECH INTERFERENCE LEVELS FOR AIRPLANES TESTED

A. PISTON POWERED AIRCRAFT

Aircraft	Engine	Turbo	No. Prop Blades	RPM	Interior Configuration	A-wtd SPL at Cabin Center	SIL**	Comments
A	4 cyl 112 HP	No	2	2300 2550	Production	89 93	79 83	
B	4 cyl 160 HP	No	2	2300 2600	Production	86 90	76 80	
C	6 cyl 235 HP	No	2	2100 2400	Partial Production	93,92 90,90	79	2 flights
C	6 cyl 235 HP	No	3	2400	Partial Production	92	81	
D	6 cyl 235 HP	Yes	2	2100 2400	Production	89 90	78 79	
D	6 cyl 235 HP	Yes	3	2100	Stripped	89,89,94 90,92,96,96	86	4 flights
D	6 cyl 235 HP	Yes	2	2400	Stripped	95	86	
E	6 cyl 300 HP	Yes	3	2450	Production	85	74	10K ft Pres.
F	Twin 6 cyl 250 HP	Yes	2	2100 2400	Stripped Prototype	98 102	90 94	12,400 ft
F	Twin 6 cyl 250 HP	Yes	3	2100 2400	Stripped Prototype	97 97	89 89	12,400 ft

Brackets indicate same test vehicle used for paired flight conditions; altitude = 5000 ft. unless noted

**SIL (0.5, 1, 2, 4) at Cabin Center

A-8

TABLE A.2 (Cont.)   TABLE OF A-WTD SOUND LEVELS AND SPEECH INTERFERENCE LEVELS FOR AIRPLANES TESTED

Aircraft	Engine	Turbo	No. Prop Blades	RPM	Interior Configuration	A-wtd SPL at Cabin Center	SIL	Comments
G	6 cyl 235 HP	No	2	2200 2380	Production	89 89	77 75	
H	6 cyl 200 HP	Yes	3	2300 2500	Production	89 87	76 76	
I	6 cyl 285 HP	No	3	2300 2450	Production	89 91	77 78	
J	6 cyl 300 HP	Yes	3	2200 2400	Production	95 92	79 80	
K	Twin 6 cyl 300 HP	No	3	2200 2400	Production	90 96	74 77	
L	Twin 6 cyl 325 HP	Yes	3	2200 2400	Production	87 95	74 78	
M	Twin 6 cyl 325 HP	Yes	3	2400	Production	92	76	Pressurized (Cabin Alt 4k ft)
N	Twin 6 cyl 260 HP	No	2	2100 2300	Production	88 90	75 77	
O	Twin 6 cyl 285 HP	No	3	2300 2500	Production	93 93,92	78 80	
P	Twin 6 cyl 380 HP	Yes	3	2500 2700	Production	87 91	72 75	Pressurized (Cabin Alt 2k ft)

TABLE A.2B. A-WTD SOUND LEVELS AND SPEECH INTERFERENCE LEVELS FOR AIRPLANES TESTED

TURBINE POWERED AIRCRAFT — TWIN ENGINES

Aircraft	Engine	No. Prop Blades	Prop RPM	Range of A-wtd SPLs in Passenger Cabin	SIL	Flight Conditions
Q	715 SHP*	4	1930	86-89	69-73	8k ft, 215 kts / 3k ft cabin altitude
			1950	84-91	69-77	12k ft, 214 kts / 3k ft cabin altitude
R	850 SHP	3	1690	82-84	69-70	12.5k ft, 215 kts / 2k ft cabin altitude
S	550 SHP	3	1900	82-86	66-69	16k ft, 160 kts / 2k ft cabin altitude
T	750 SHP	4	1710	82-90	68-74	12.5k ft, 203 kts / 2k ft cabin altitude

*SHP = Shaft Horsepower

A-10

A.4 Cabin Noise Surveys for Aircraft with Production Interiors

Shown in Figure A.1 through A.18, are the results of cabin noise surveys performed in all aircraft which had full production interiors. The blade passage frequency and engine firing frequencies are indicated. The microphone positions most used were:

a)   Center cabin between pilot and copilot at head height,

b)   Windshield,

c)   Right passenger window at copilot's right ear,

d)   Right rear side window - usually even with the second row of seats (if present), and

e)   Rear baggage area or rear seats, depending on the layout of the cabin.

Results for a second engine speed are available for most aircraft but are not shown. Data for aircraft with partial or no interior furnishings are presented later in the appendix in connection with source/path diagnosis tests.
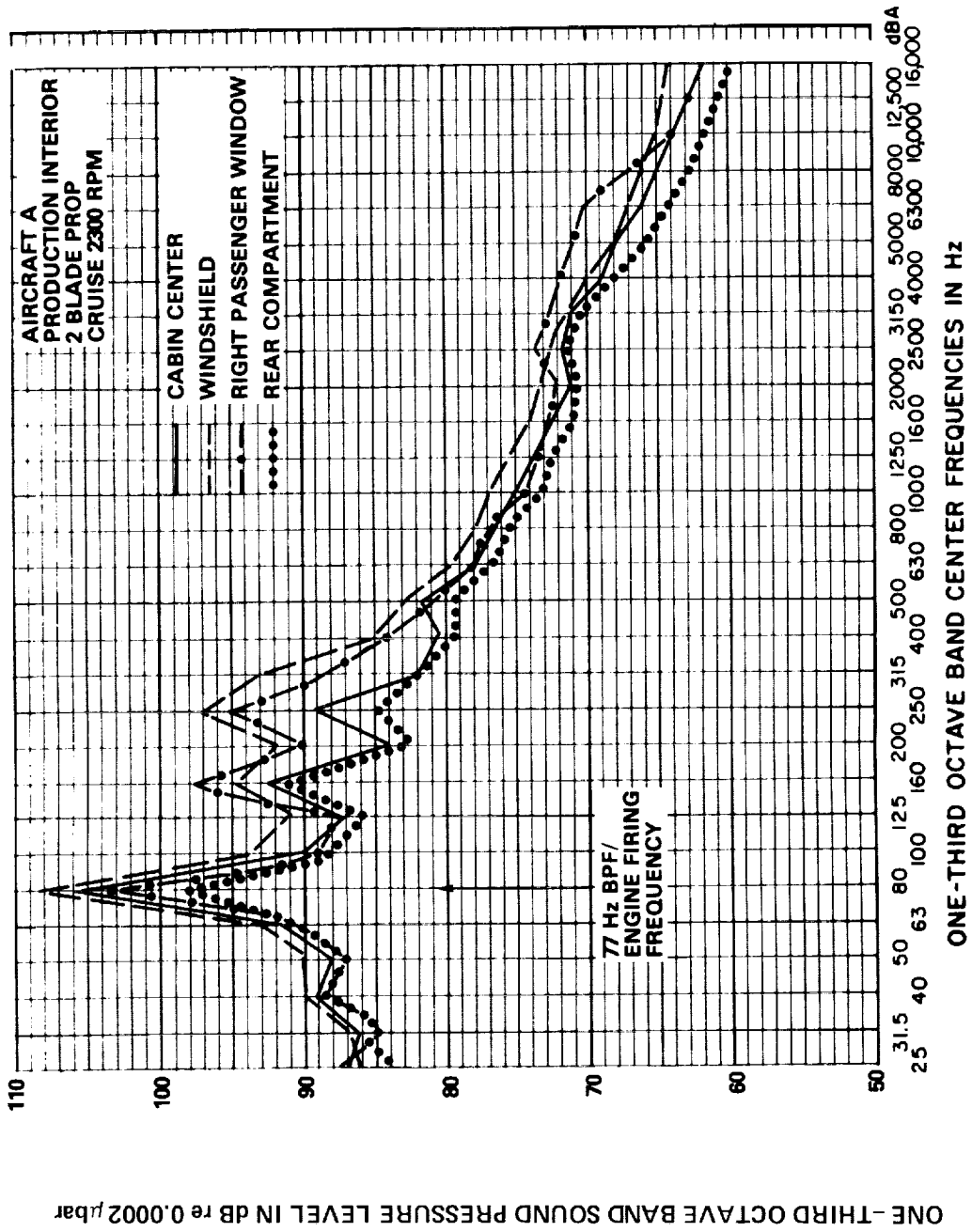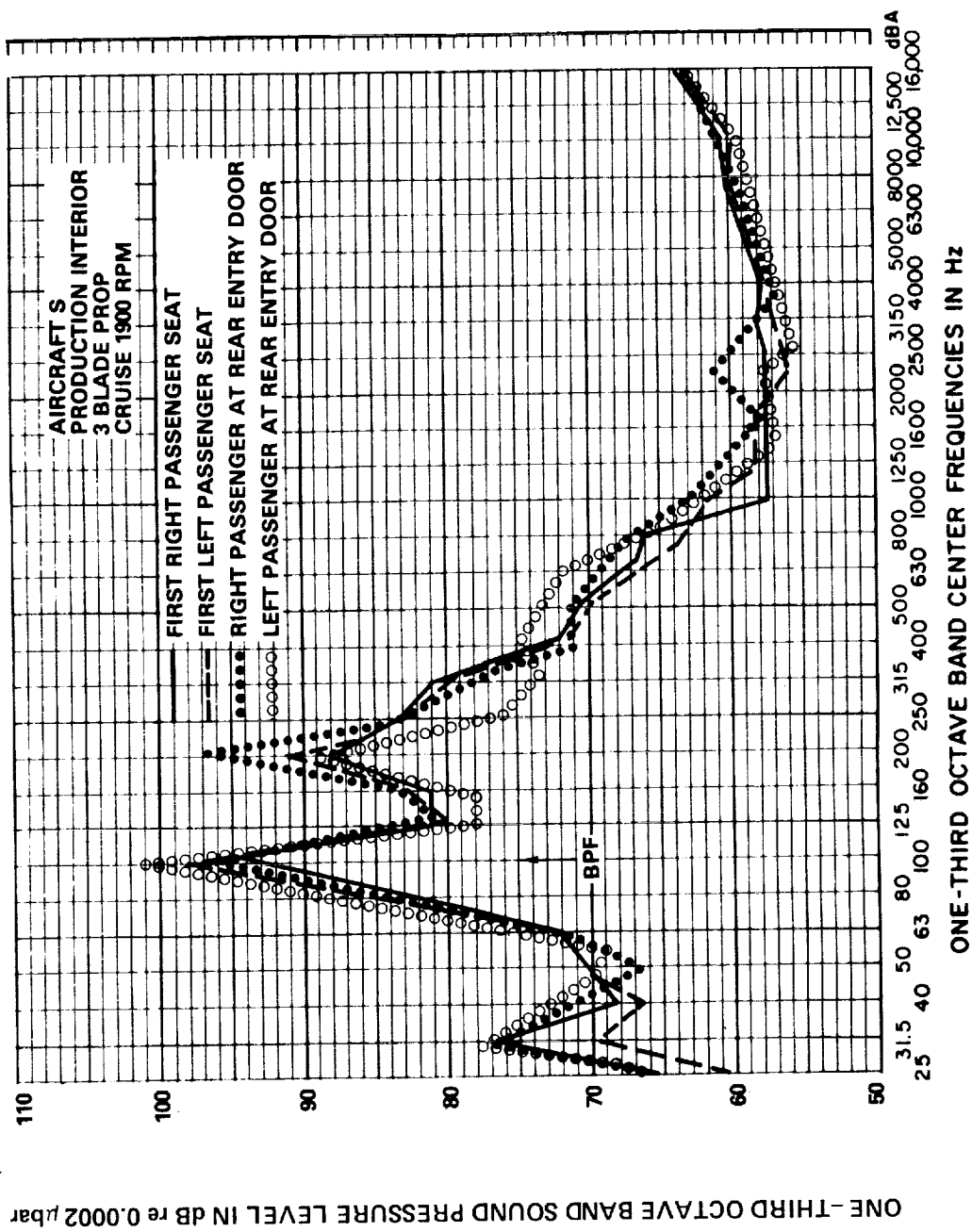
FIG. A.1. CABIN NOISE SURVEY IN AIRCRAFT A IN CRUISE CONDITION
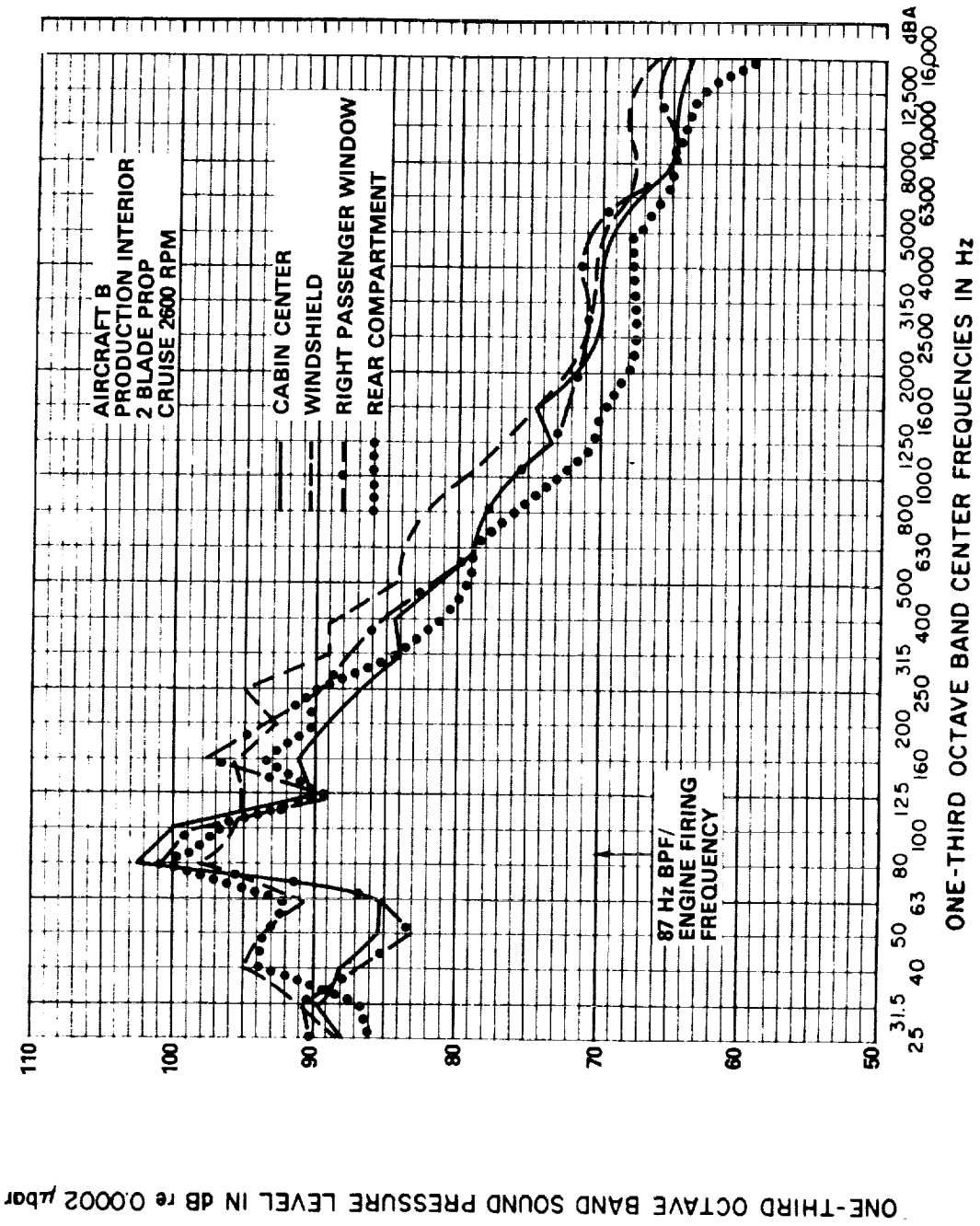
FIG. A.2. CABIN NOISE SURVEY IN AIRCRAFT B IN CRUISE CONDITION
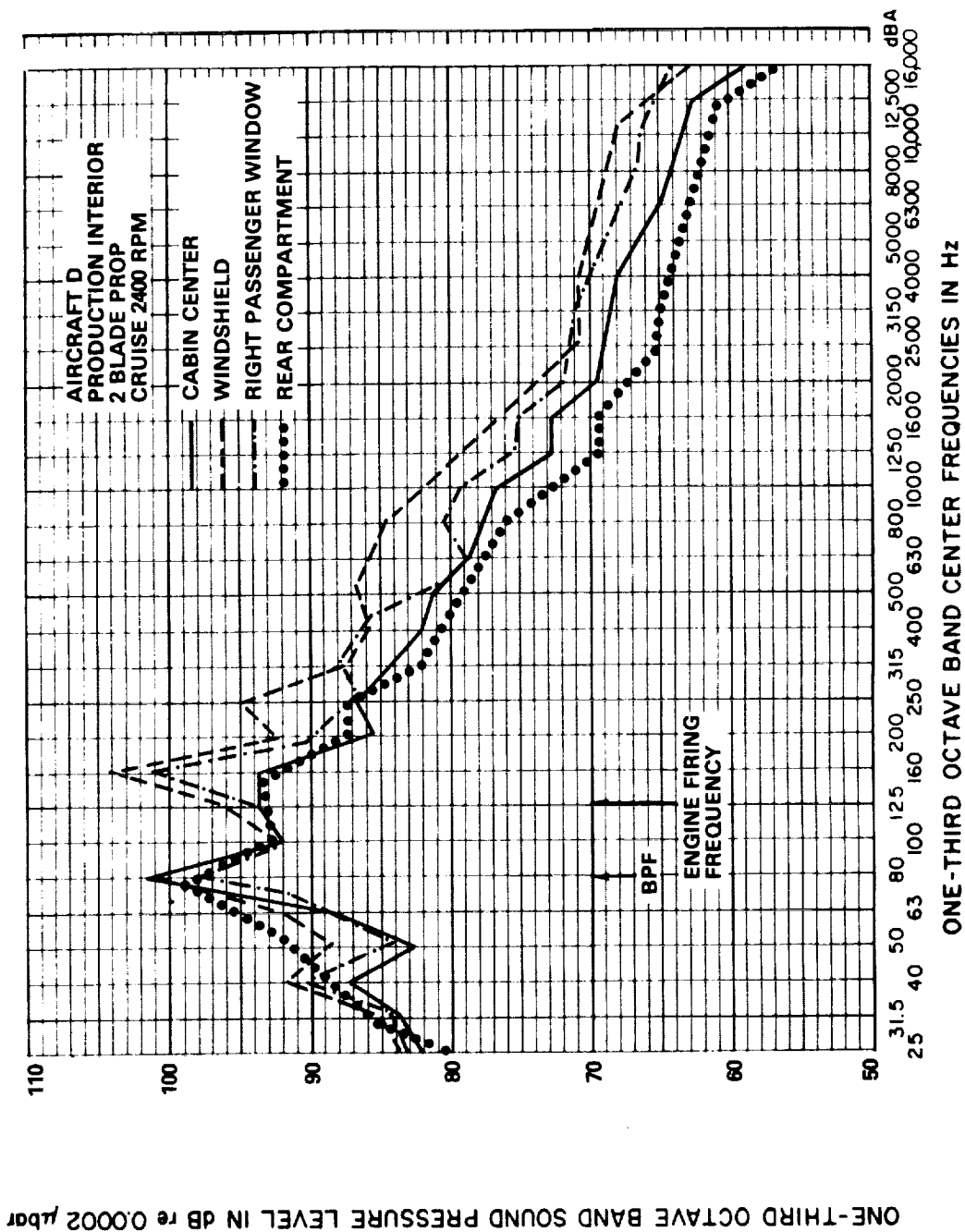
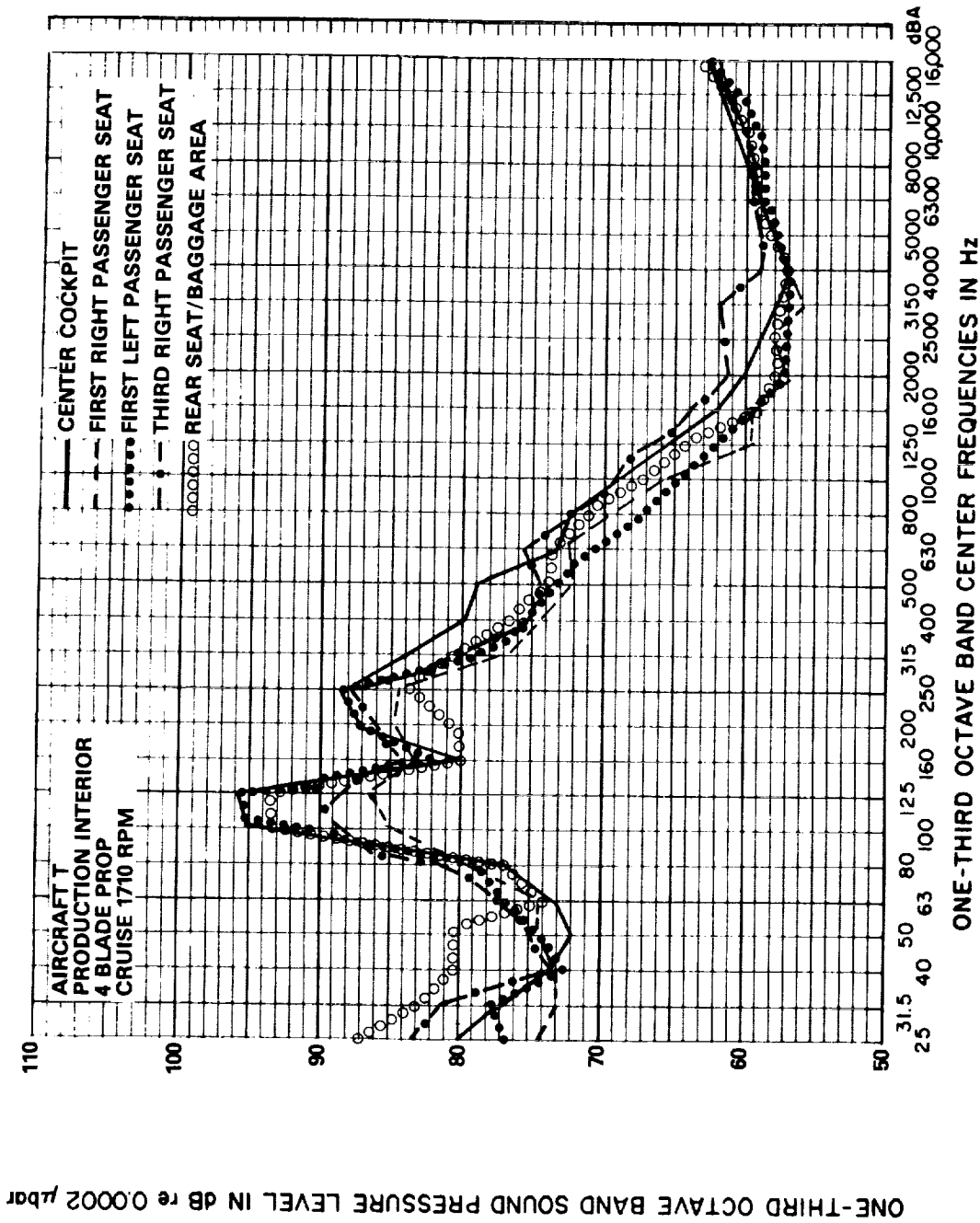FIG. A.3. CABIN NOISE SURVEY IN AIRCRAFT D IN CRUISE CONDITION
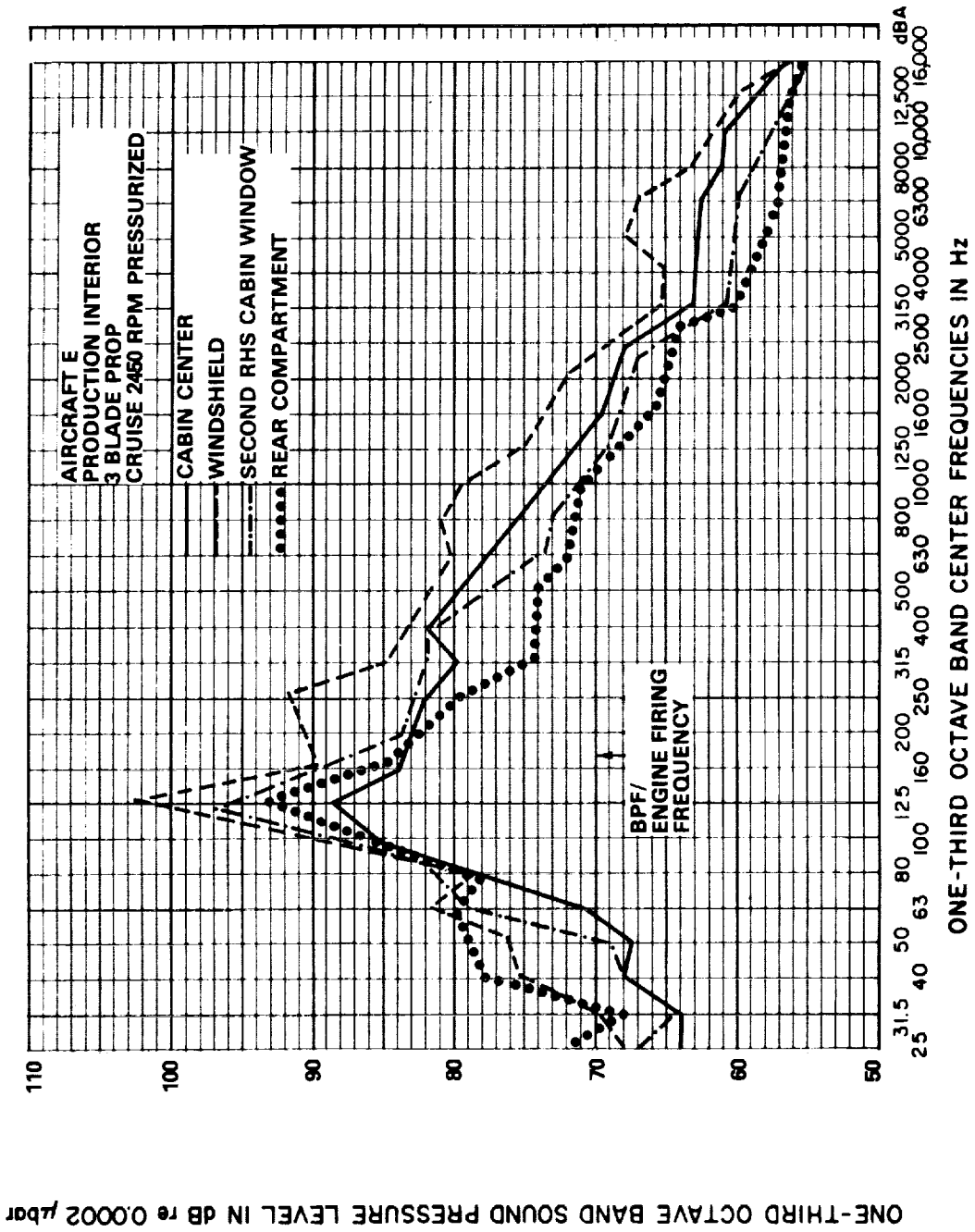
FIG. A.4 CABIN NOISE SURVEY IN AIRCRAFT E IN CRUISE CONDITION
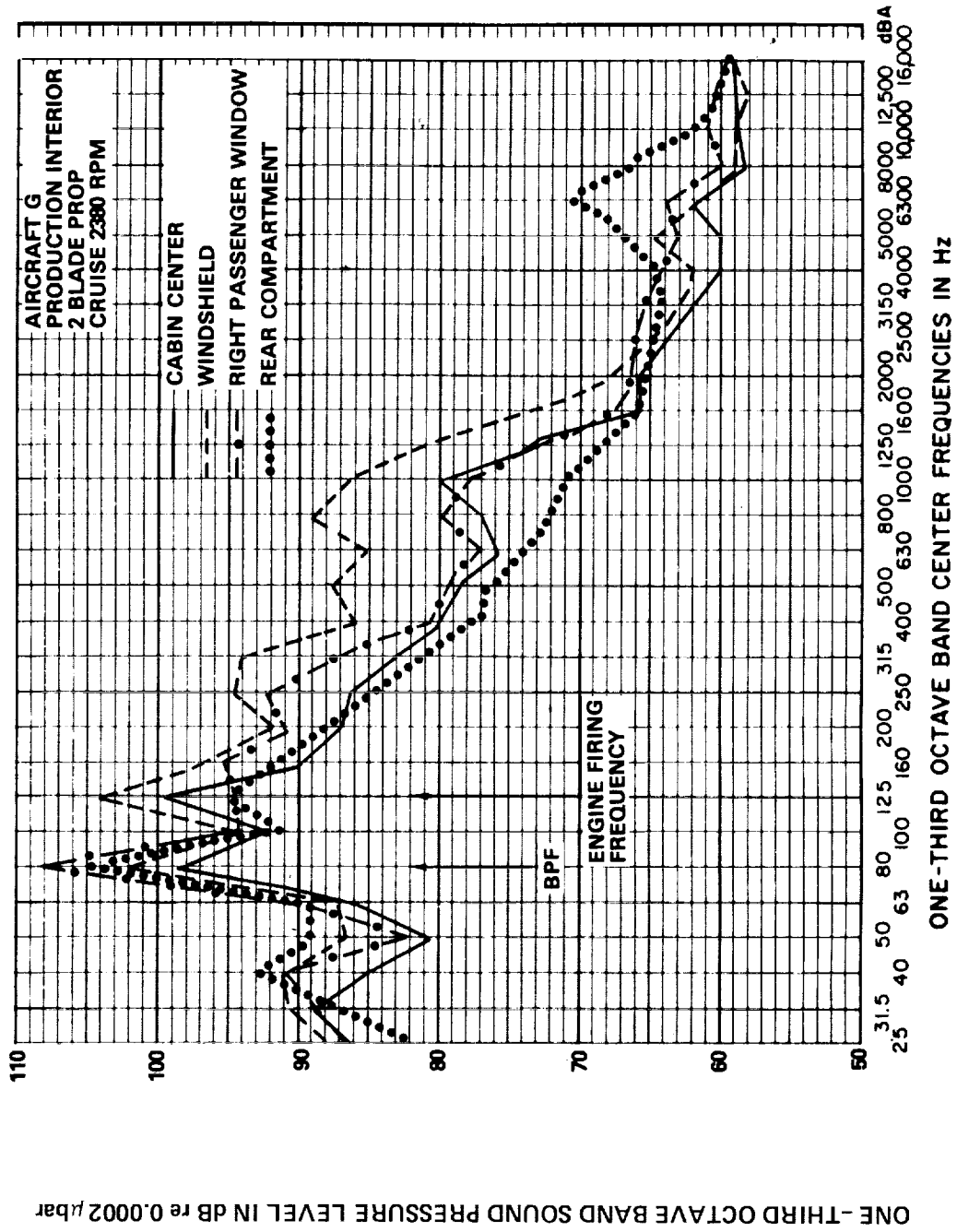
FIG. A.5. CABIN NOISE SURVEY IN AIRCRAFT G IN CRUISE CONDITION
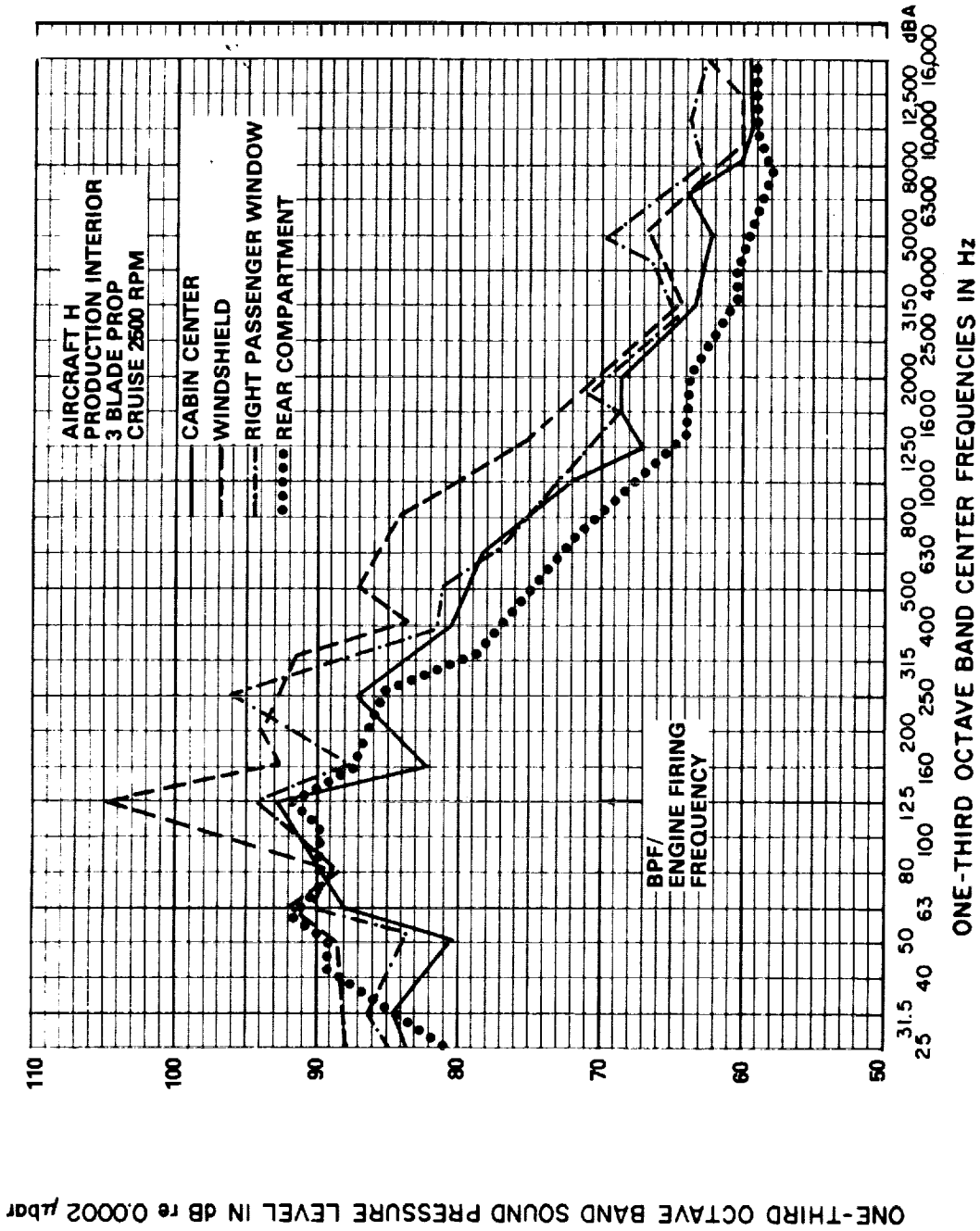
FIG. A.6. CABIN NOISE SURVEY IN AIRCRAFT H IN CRUISE CONDITION

ONE-THIRD OCTAVE BAND SOUND PRESSURE LEVEL IN dB re 0.0002 μbar
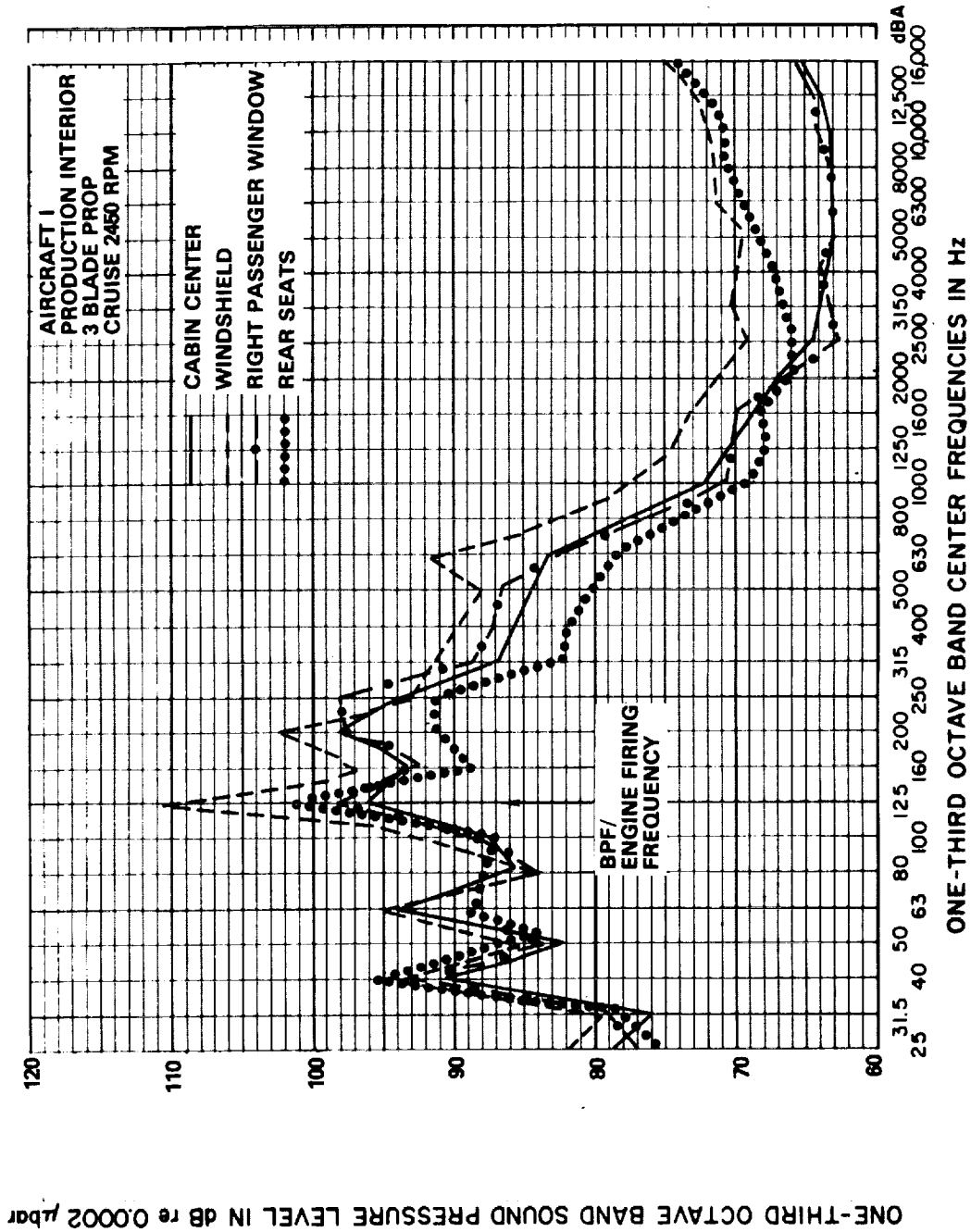
FIG. A.7. CABIN NOISE SURVEY IN AIRCRAFT I IN CRUISE CONDITION
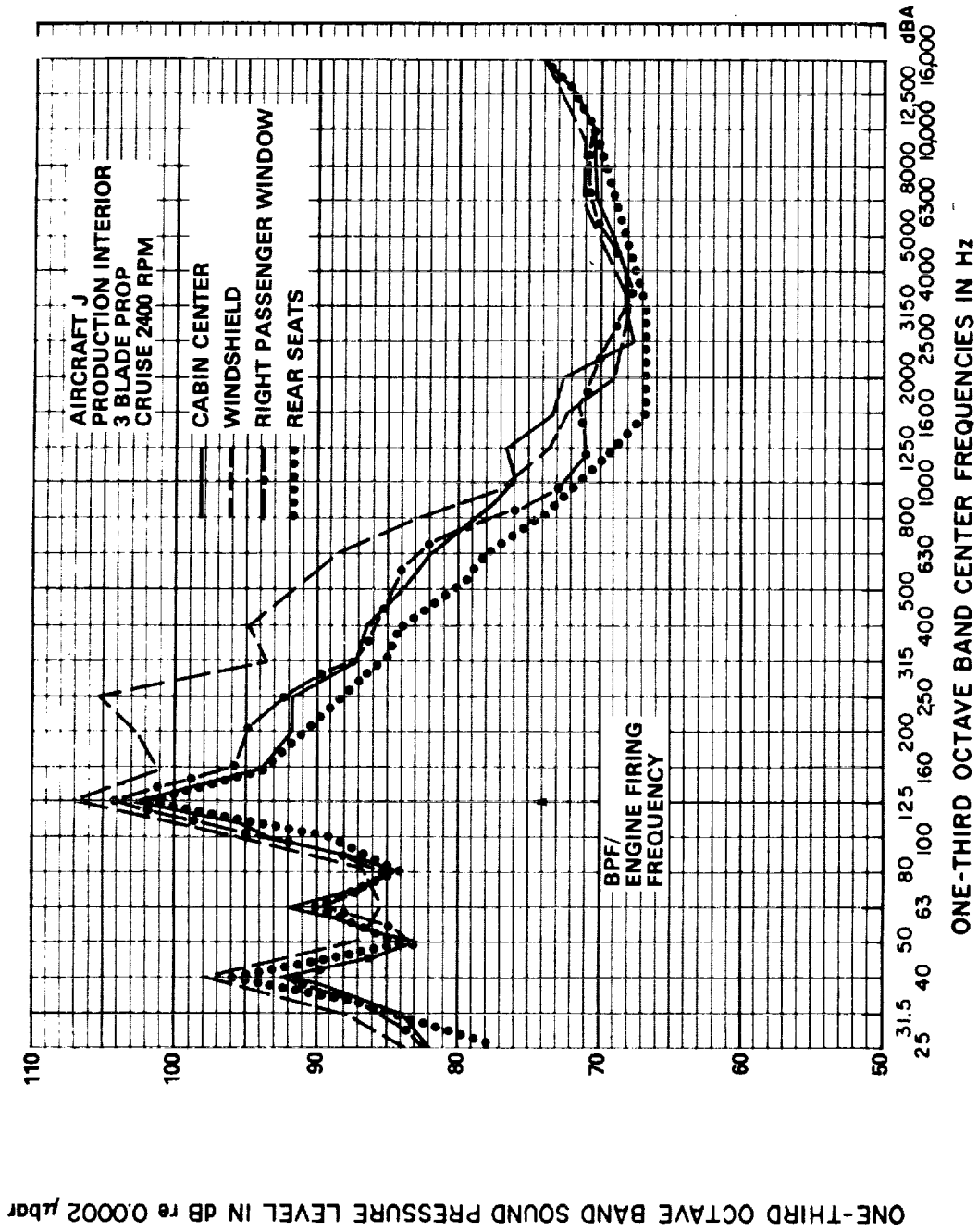
FIG. A.8. CABIN NOISE SURVEY IN AIRCRAFT J IN CRUISE CONDITION'

AIRCRAFT K
PRODUCTION INTERIOR
3 BLADE PROP
CRUISE 2400 RPM

CABIN CENTER
WINDSHIELD
RIGHT PASSENGER WINDOW
BAGGAGE AREA/TAILCONE

BPF/
ENGINE FIRING
FREQUENCY

ONE-THIRD OCTAVE BAND CENTER FREQUENCIES IN Hz

dBA

31.5 40 50 63 80 100 125 160 200 250 315 400 500 630 800 1000 1250 1600 2000 2500 3150 4000 5000 6300 8000 10,000 16,000
25   12,500

120 110 100 90 80 70 60

ONE-THIRD OCTAVE BAND SOUND PRESSURE LEVEL IN dB re 0.0002 μbar
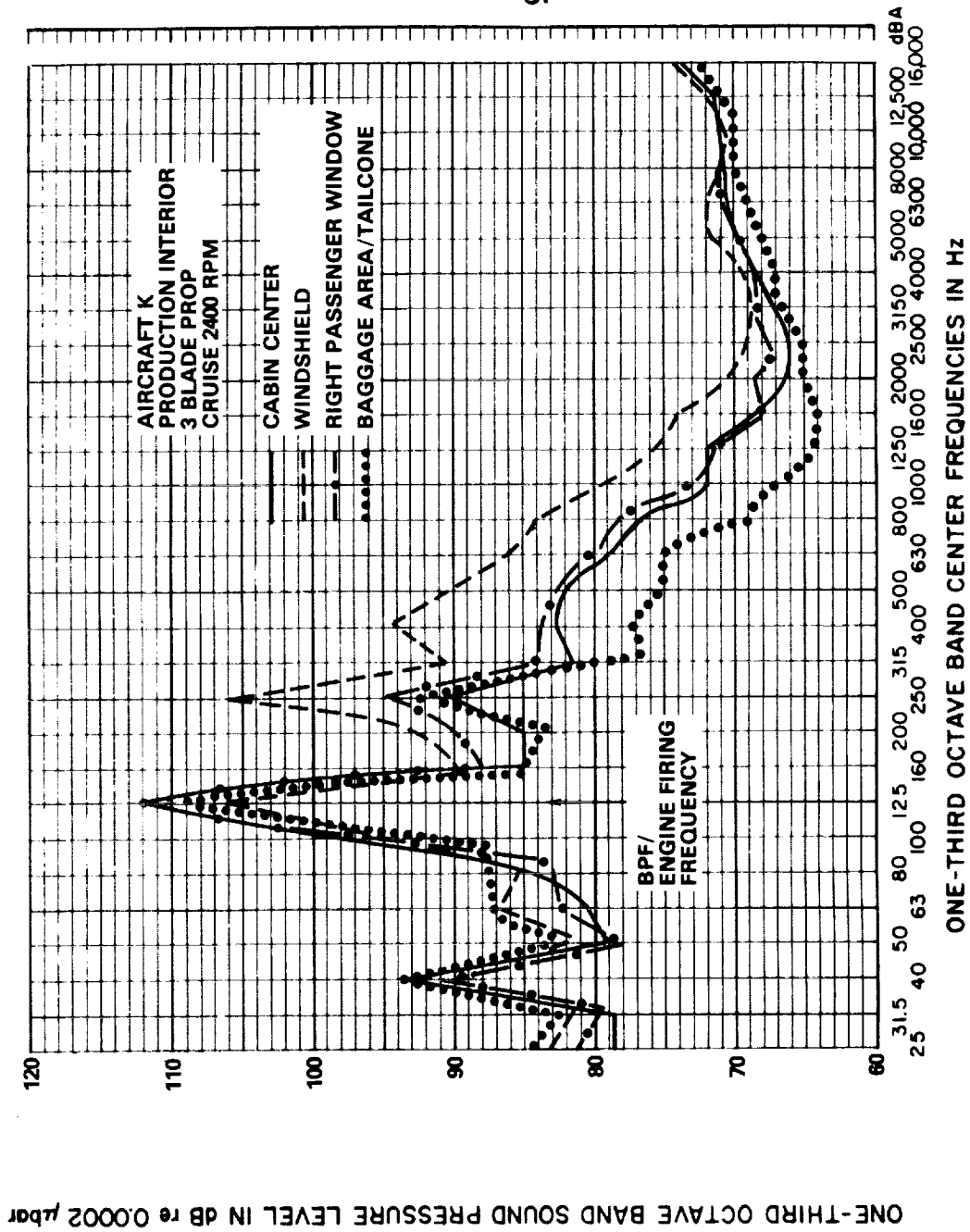
FIG. A.9.   CABIN OISE SURVEY IN AIRCRAFT K IN CRUISE CONDITION
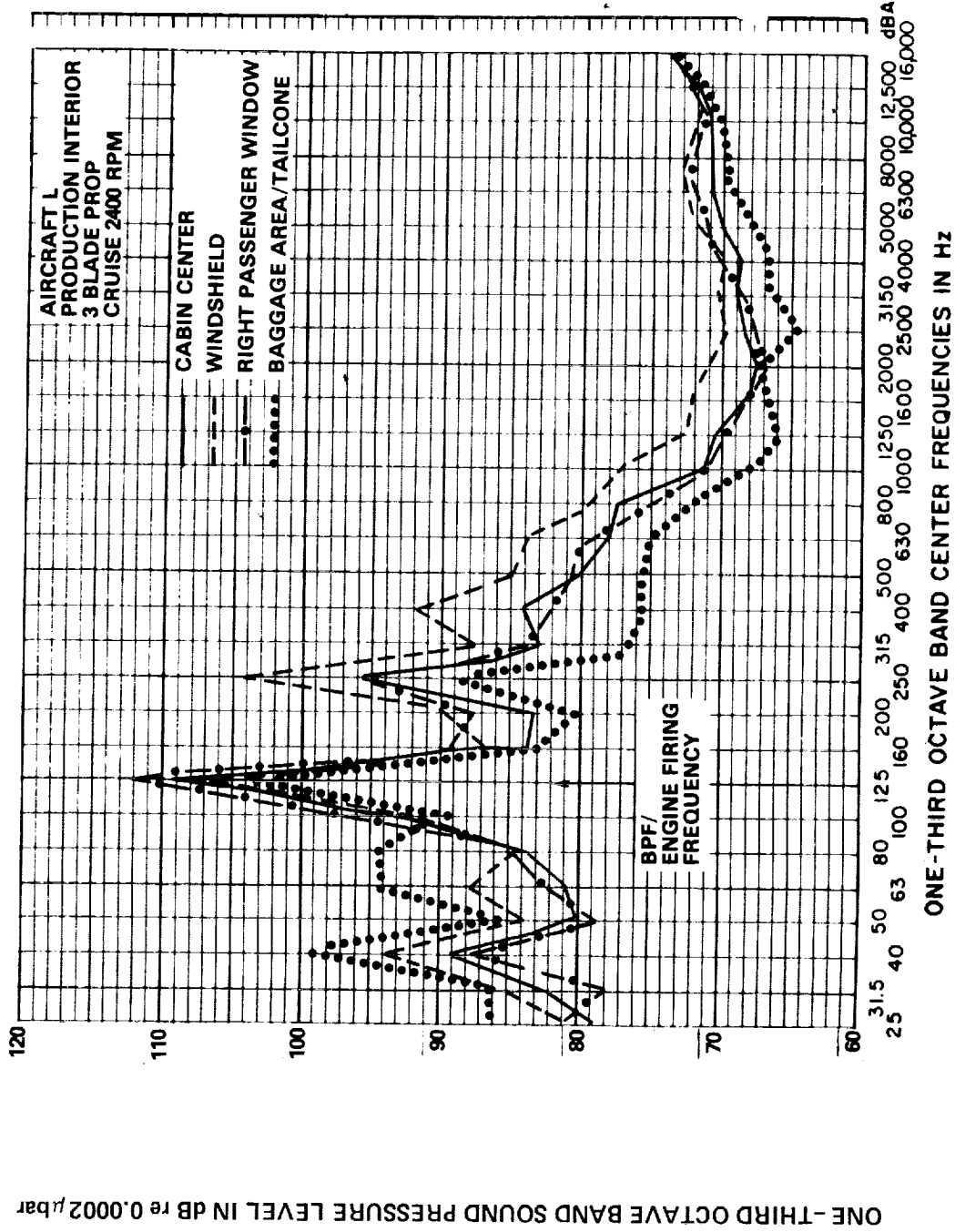
FIG. A.10. CABIN NOISE SURVEY IN AIRCRAFT L IN CRUISE CONDITION

AIRCRAFT M
PRODUCTION INTERIOR
3 BLADE PROP
CRUISE 2400 RPM

PILOT'S HEAD POSITION
WINDSHIELD
RIGHT PASSENGER WINDOW
RIGHT REAR SEAT

BPF/
ENGINE FIRING
FREQUENCY

ONE-THIRD OCTAVE BAND CENTER FREQUENCIES IN Hz

ONE-THIRD OCTAVE BAND SOUND PRESSURE LEVEL IN dB re 0.0002 μbar
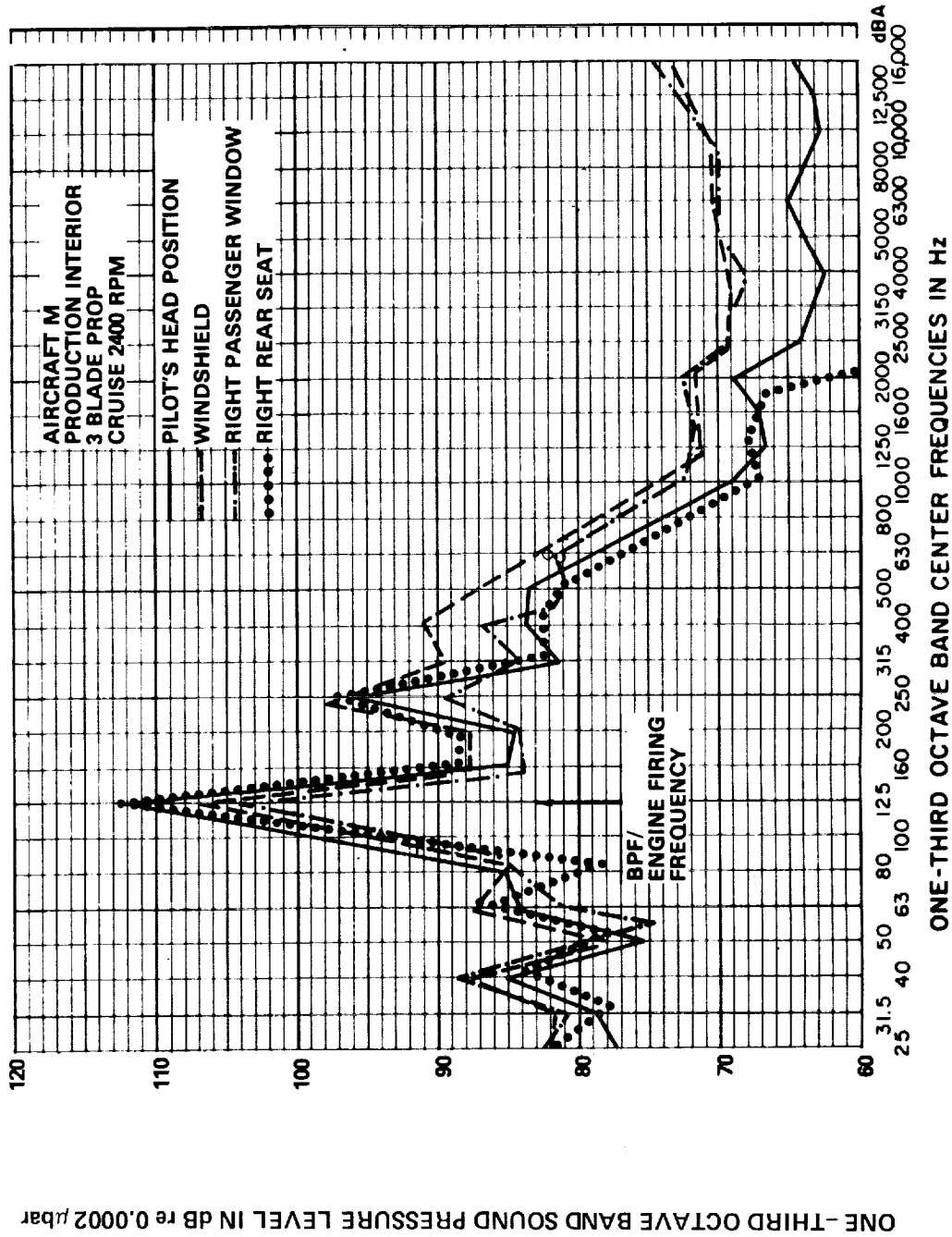
FIG. A.11. CABIN NOISE SURVEY IN AIRCRAFT M IN CRUISE CONDITION

A-22
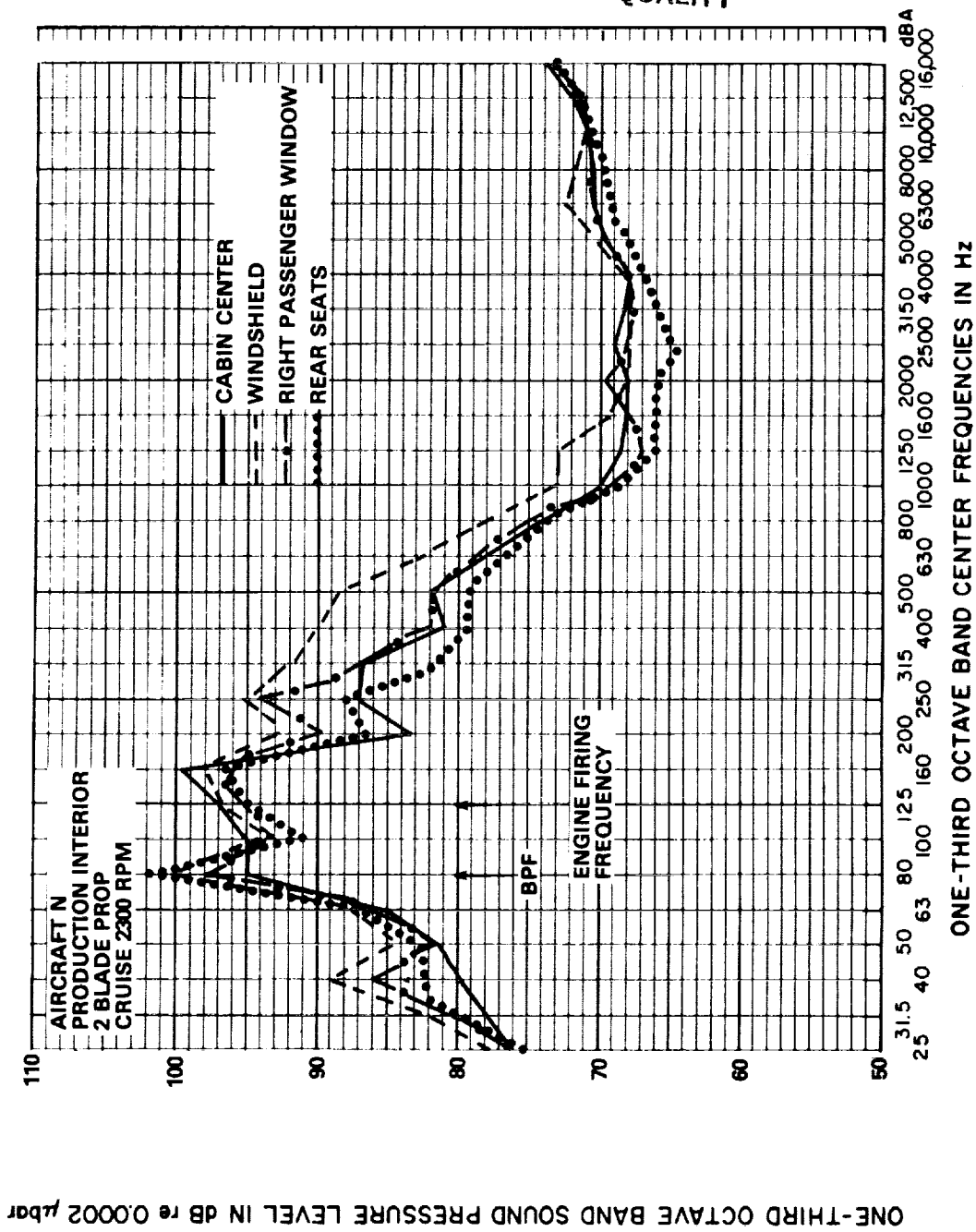
FIG. A.12. CABIN NOISE SURVEY IN AIRCRAFT N IN CRUISE CONDITION
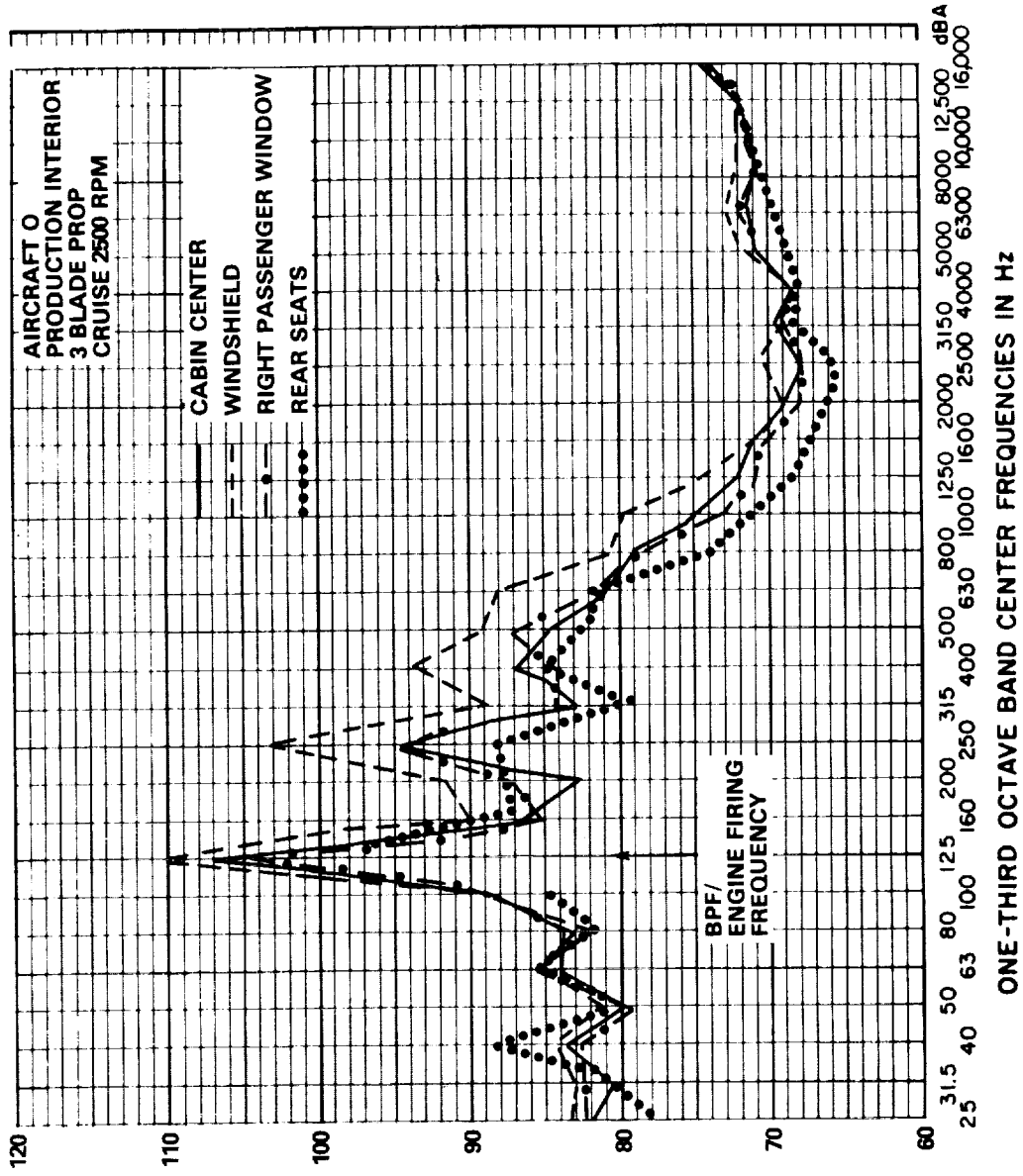
FIG. A.13. CABIN NOISE SURVEY IN AIRCRAFT O IN CRUISE CONDITION
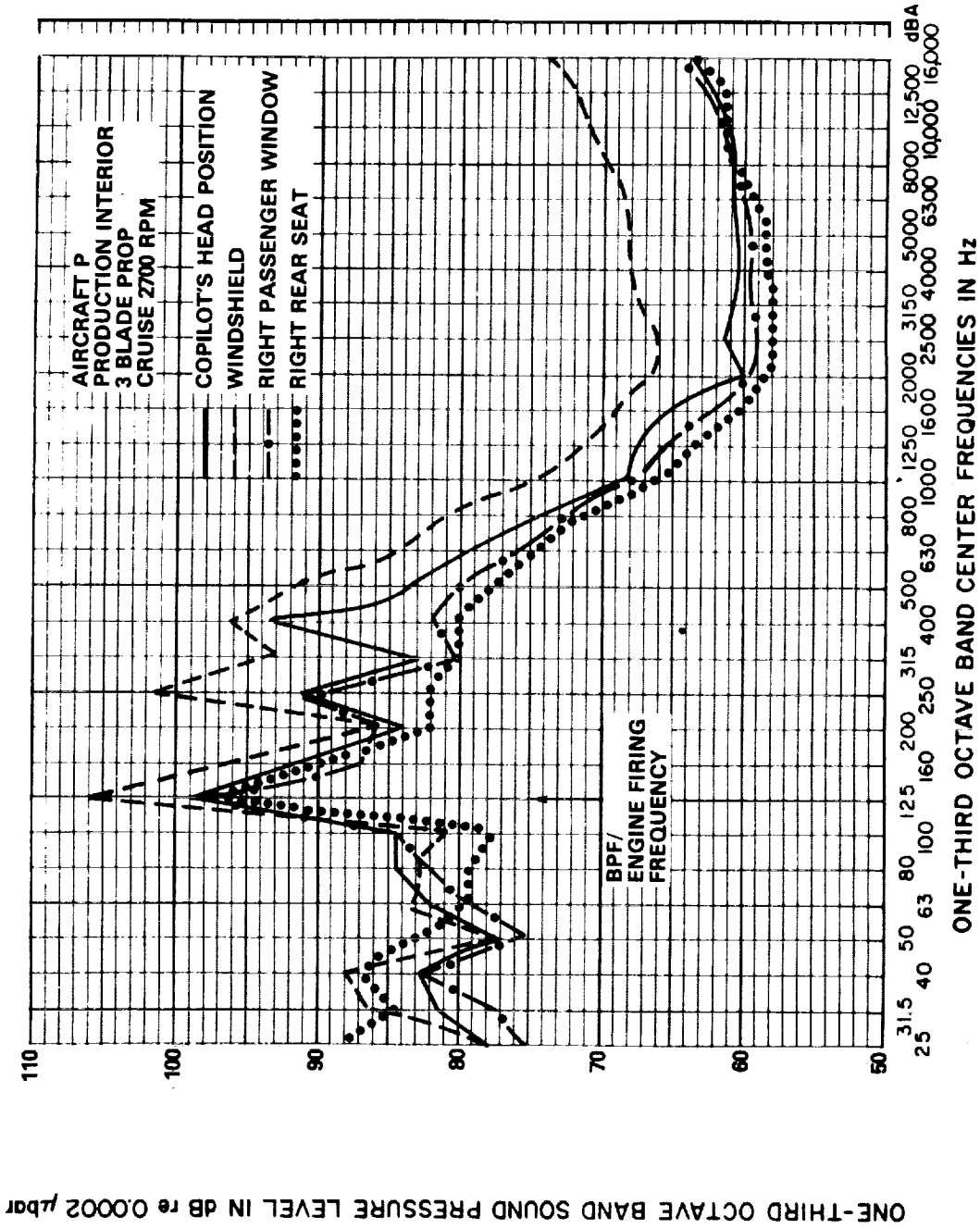
FIG. A.14. CABIN NOISE SURVEY IN AIRCRAFT P IN CRUISE CONDITION

ONE-THIRD OCTAVE BAND SOUND PRESSURE LEVEL IN dB re 0.0002 µbar

ONE-THIRD OCTAVE BAND CENTER FREQUENCIES IN Hz

AIRCRAFT Q
PRODUCTION INTERIOR
4 BLADE PROP
CRUISE 1960 RPM

CENTER COCKPIT
FIRST RIGHT PASSENGER SEAT
FIRST LEFT PASSENGER SEAT
THIRD RIGHT PASSENGER SEAT
THIRD LEFT PASSENGER SEAT
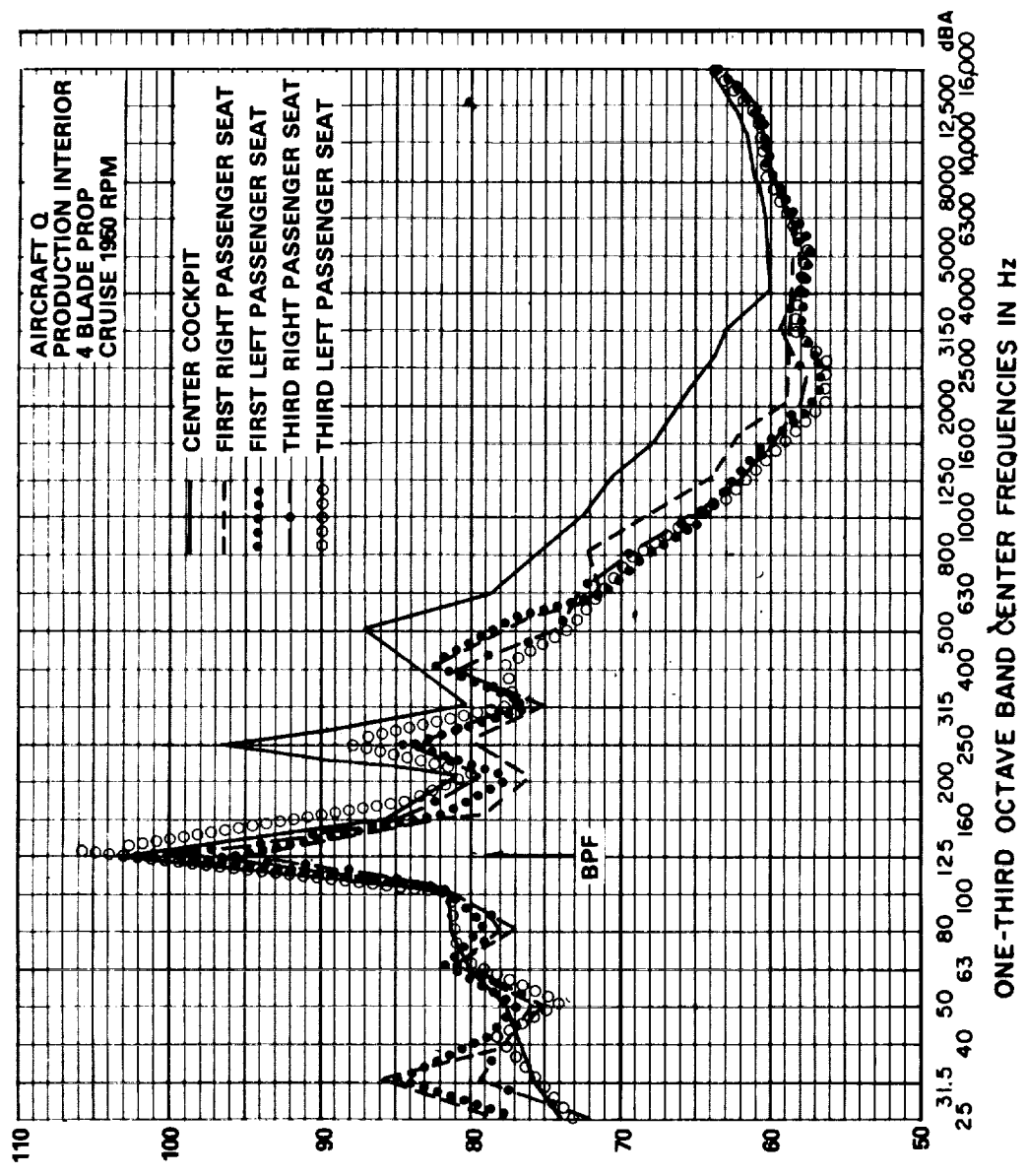
FIG. A.15. CABIN NOISE SURVEY IN AIRCRAFT Q IN CRUISE CONDITION
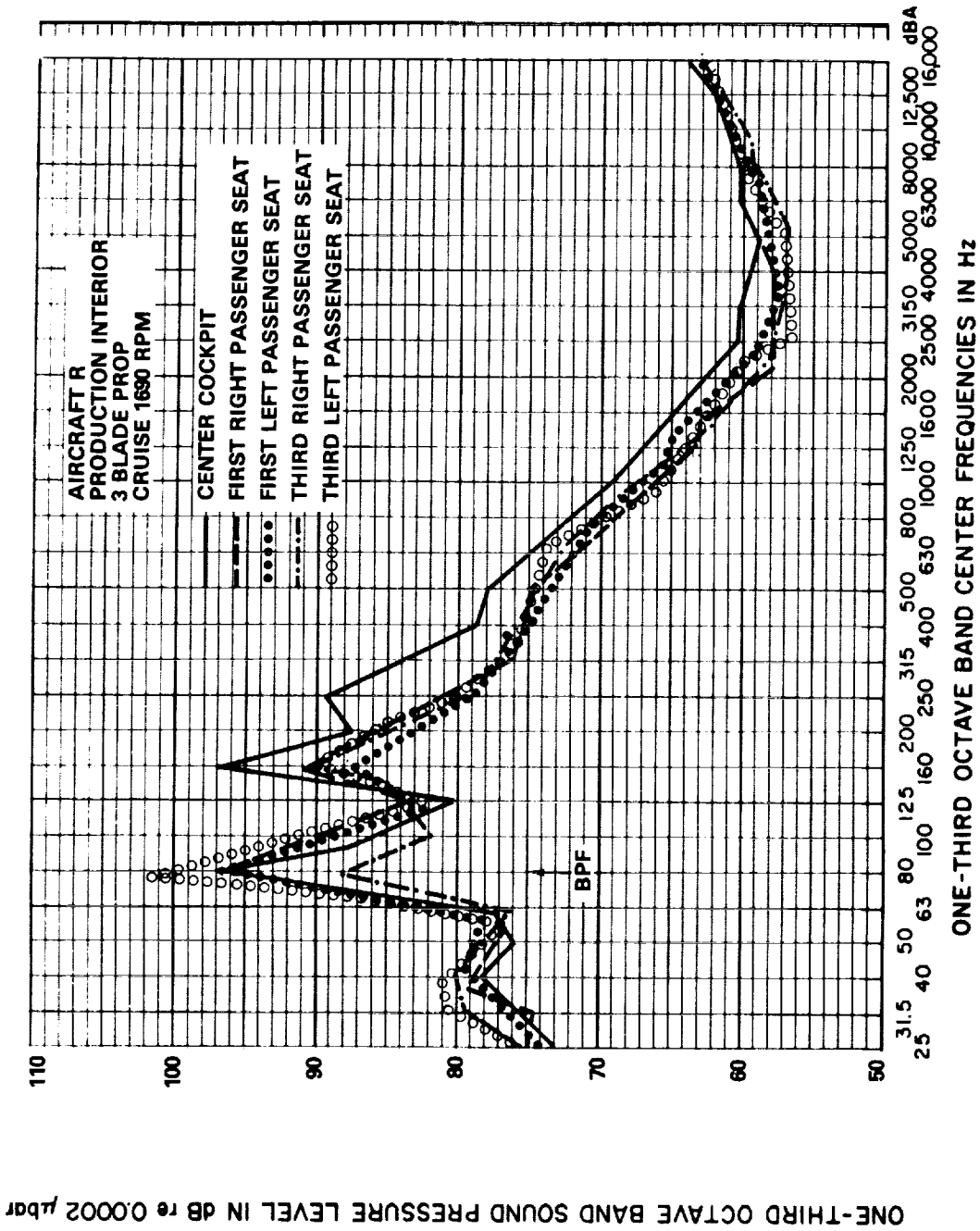
FIG. A.16. CABIN NOISE SURVEY IN AIRCRAFT R IN CRUISE CONDITION

A-27

AIRCRAFT S
PRODUCTION INTERIOR
3 BLADE PROP
CRUISE 1900 RPM

FIRST RIGHT PASSENGER SEAT
FIRST LEFT PASSENGER SEAT
RIGHT PASSENGER AT REAR ENTRY DOOR
LEFT PASSENGER AT REAR ENTRY DOOR

ONE-THIRD OCTAVE BAND CENTER FREQUENCIES IN Hz

ONE-THIRD OCTAVE BAND SOUND PRESSURE LEVEL IN dB re 0.0002 μbar

FIG. A.17. CABIN NOISE SURVEY IN AIRCRAFT S IN CRUISE CONDITION

A-28

FIG. A.18. CABIN NOISE SURVEY IN AIRCRAFT T IN CRUISE CONDITION

A.5 Cabin Vibration Surveys for Aircraft with Production Interiors

Shown in Figures A.19 through A.36 are the results of cabin vibration surveys performed in all aircraft with production interiors. The blade passage and engine firing frequencies are indicated. The minimum set of accelerometer positions used was:

a) Center of windshield or center of right windshield half if the windshield is split,

b) Center of right passenger window,

c) Center of right rear side window,

d) Center of back window (if present), and

e) Seat rail and/or wing spar (vertical direction).

The survey was intended to define the vibration of the largest radiating surfaces in the cabin. The vibration of large pieces of rigid trim material was also measured when possible. Many furnished cabins have few "rigid"* interior surfaces except for the windows. The seat rail and wing spar positions were chosen to define the vibration of the airplane's structural members (as opposed to skin panels) because these points are some of the most rigid areas of the airframe.

The point vibration spectra must be carefully interpreted in terms of their quantitative contribution to the sound radiated into the cabin space, since some of the point vibration is dominated by resonant response at many frequencies, and the space-averaged levels which one would use to estimate radiation (in conjunction with radiation efficiency estimate), will be lower. However, these surveys lead one to areas where significant radiation might be found.

---

*"Rigid" is used in the sense that the surface is either part of the airframe or securely connected to it.
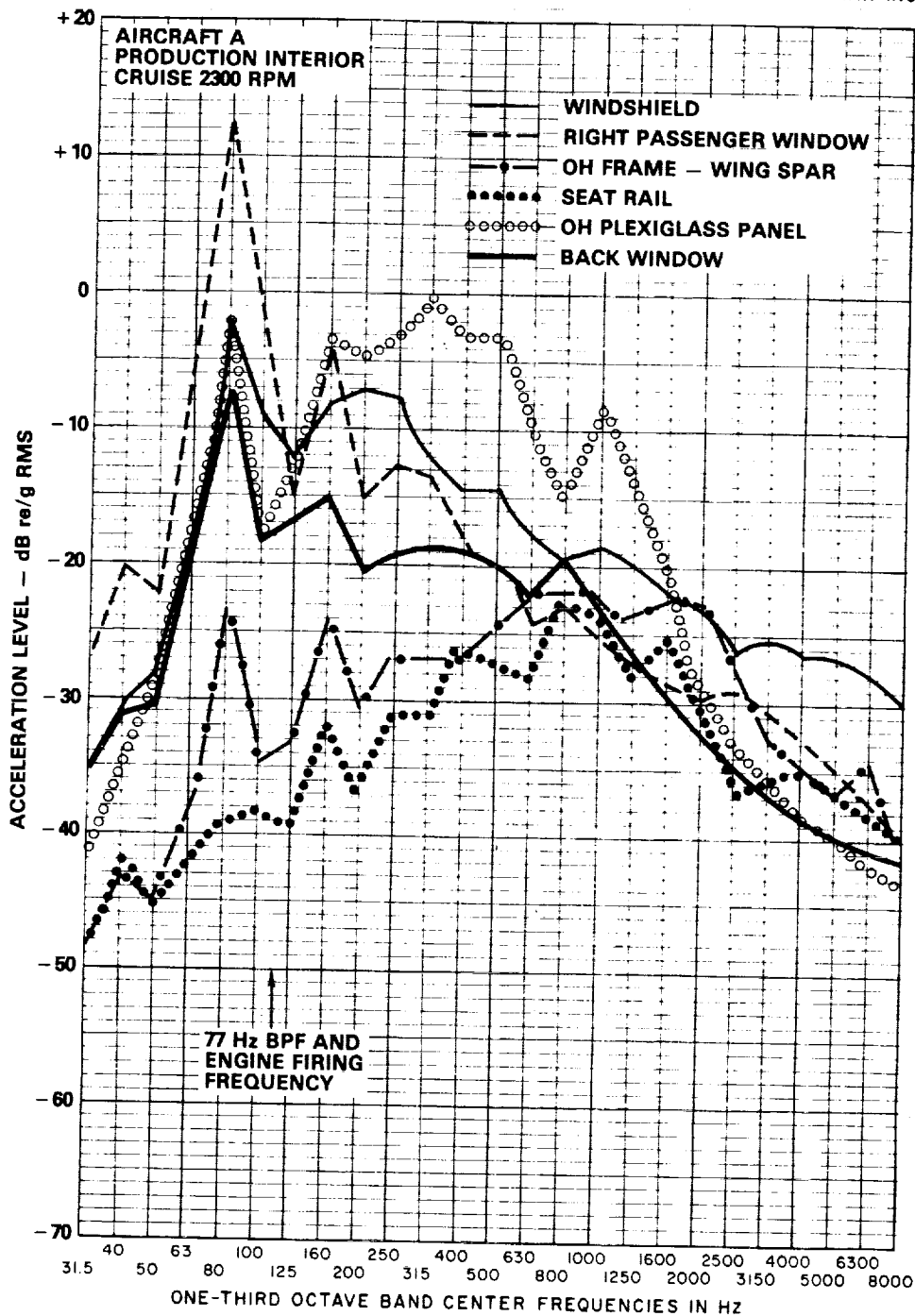
FIG. A.19 VIBRATION SURVEY ON INTERIOR SURFACES IN AIRCRAFT A
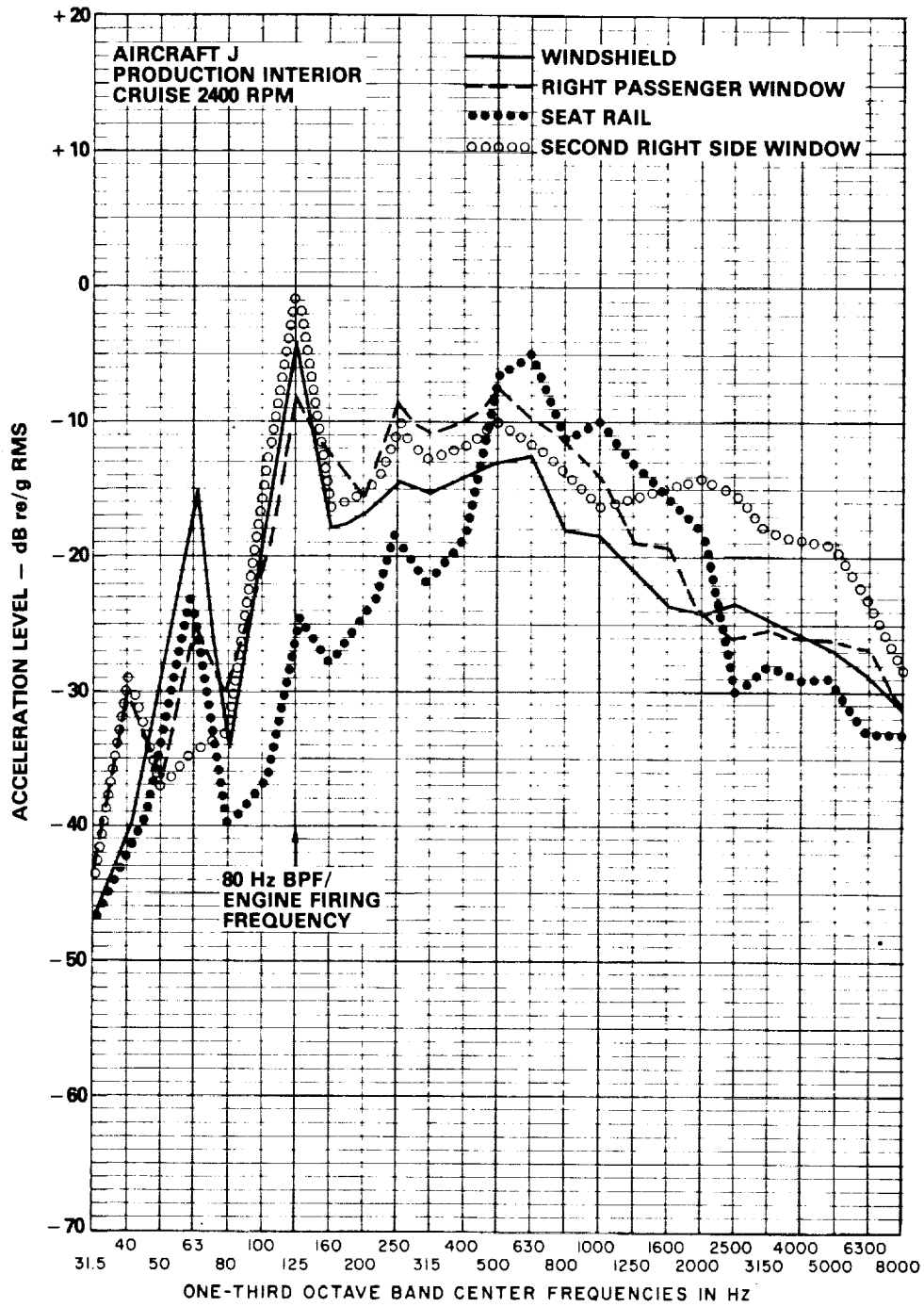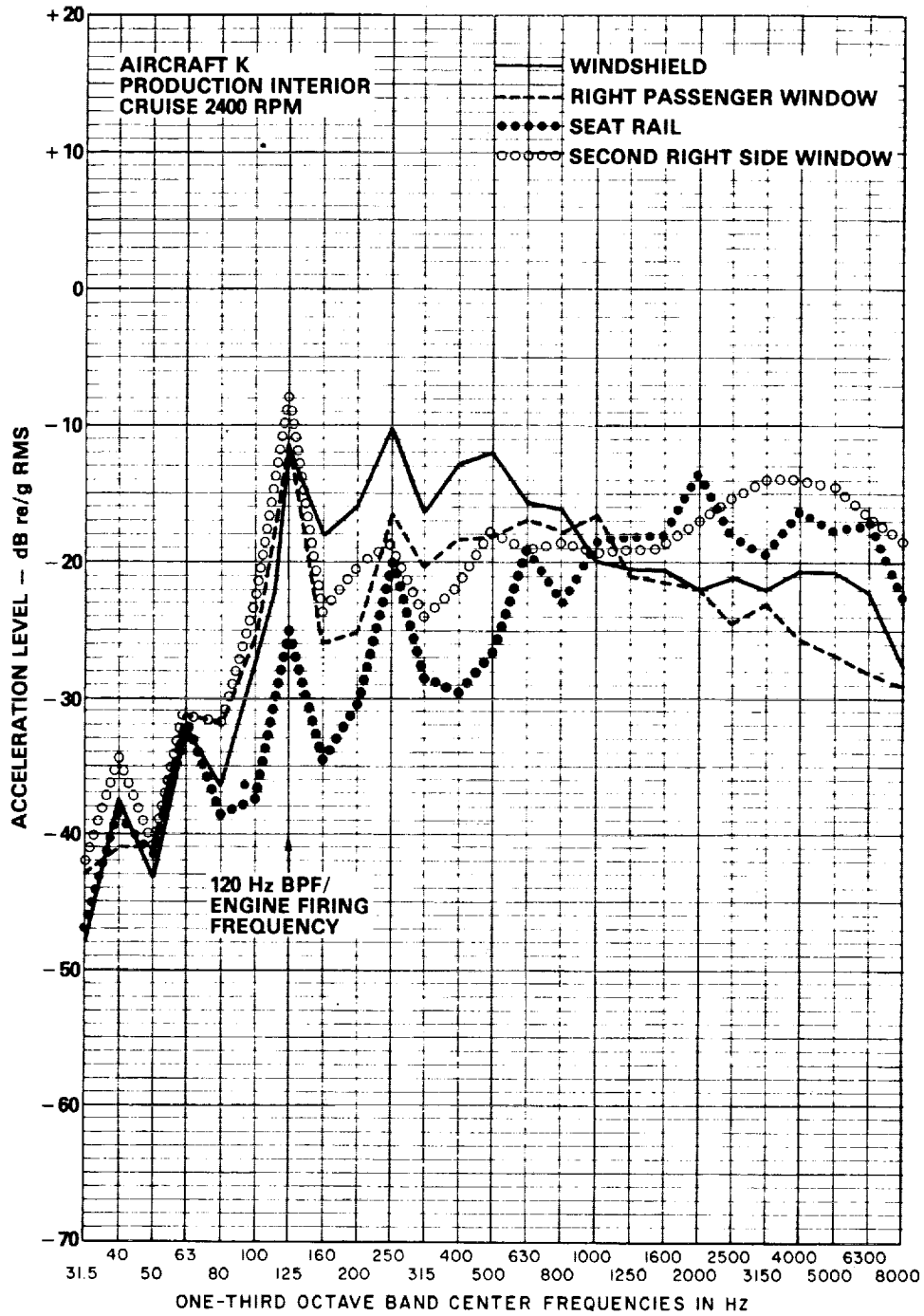IN CRUISE CONDITION

BOLT BERANEK & NEWMAN INC
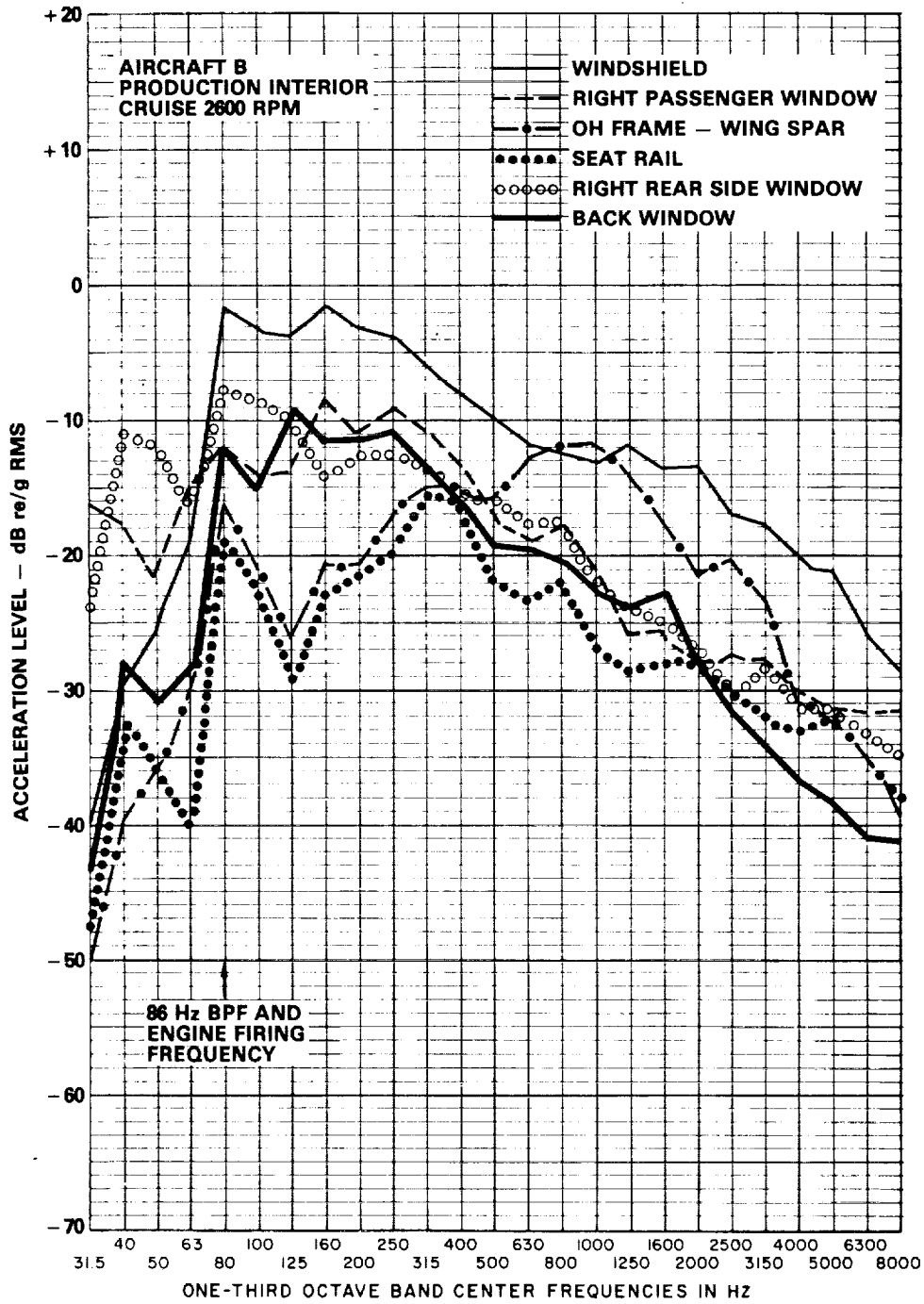
FIG. A.20. VIBRATION SURVEY ON INTERIOR SURFACES ON AIRCRAFT B
IN CRUISE CONDITION
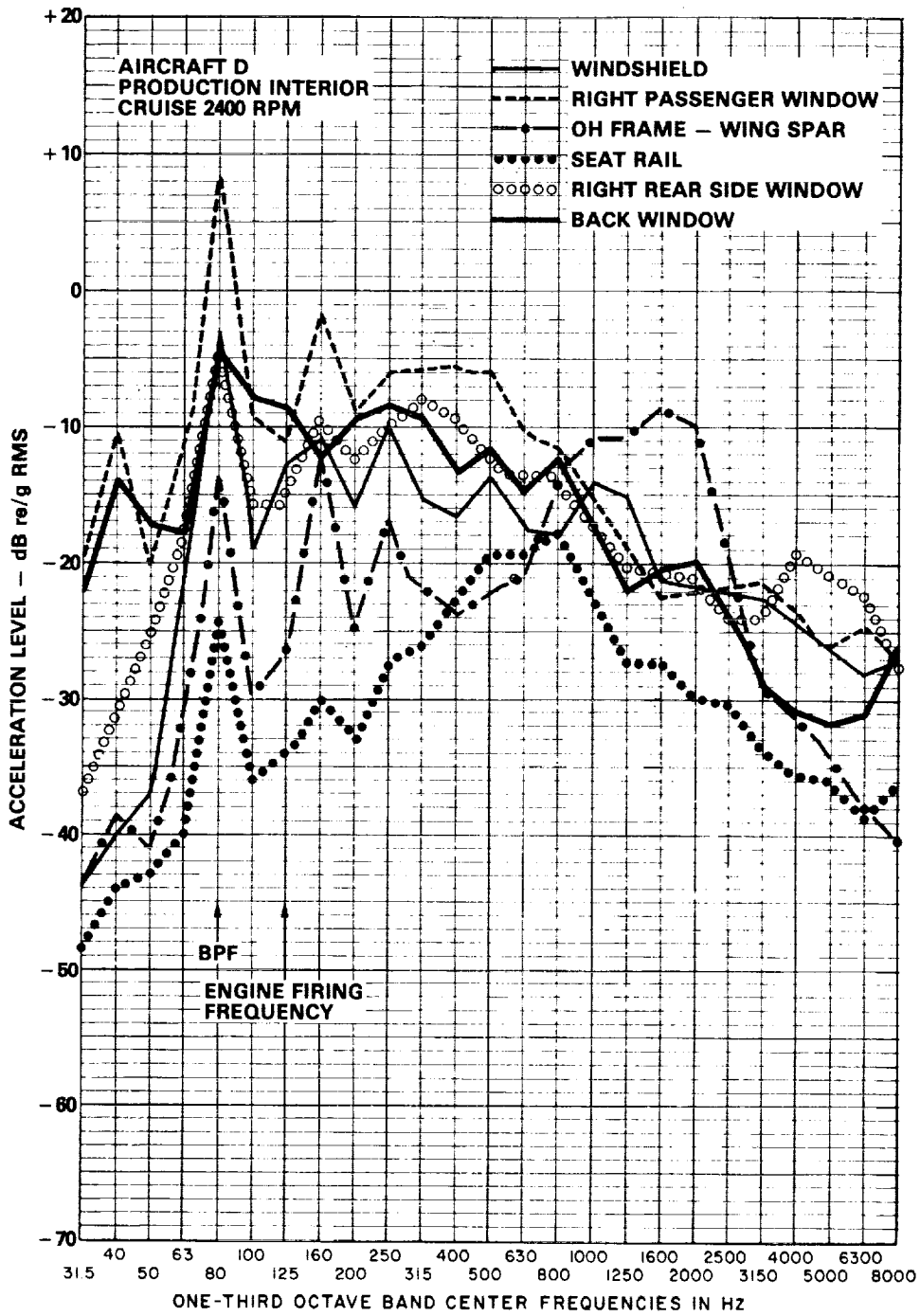
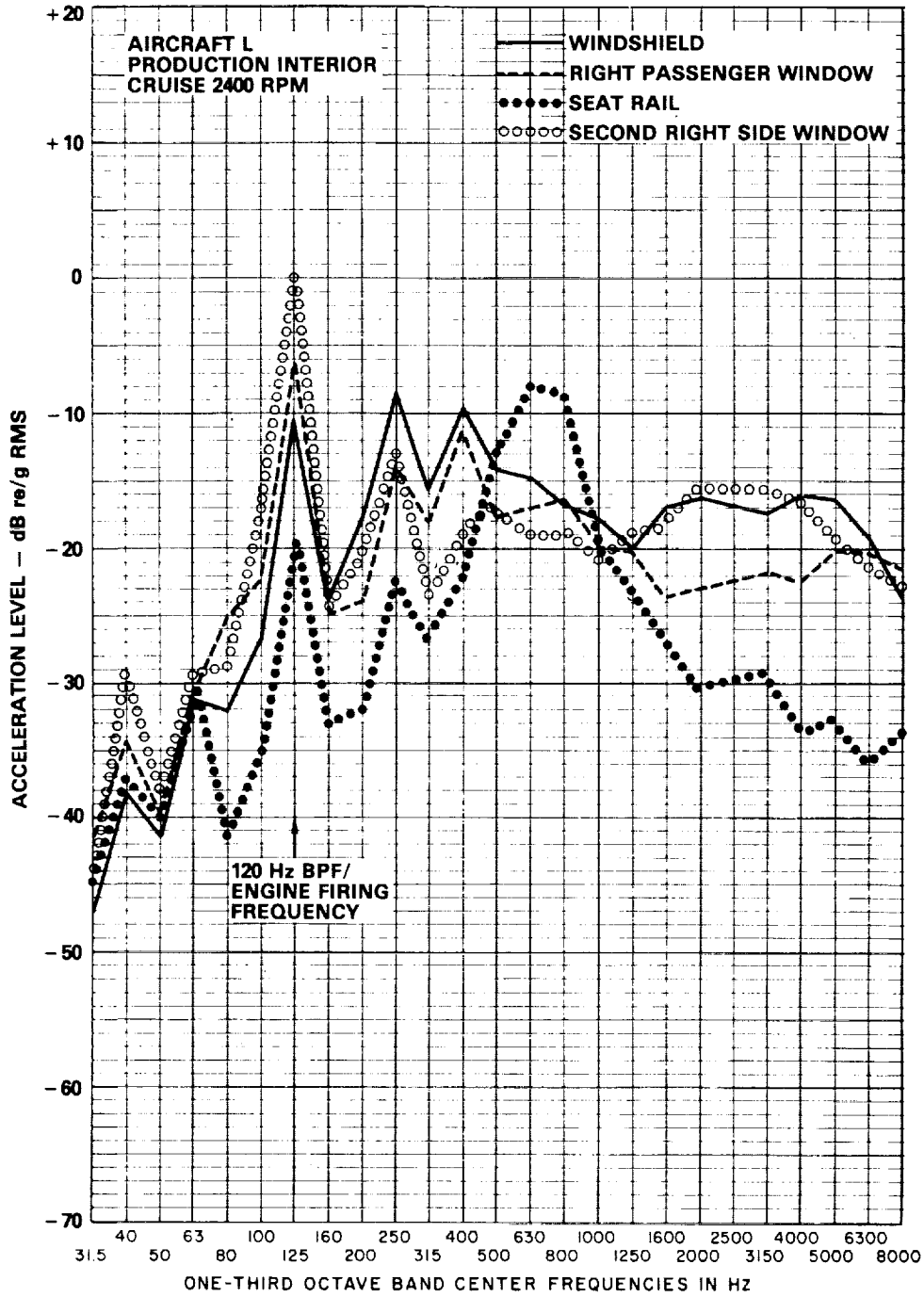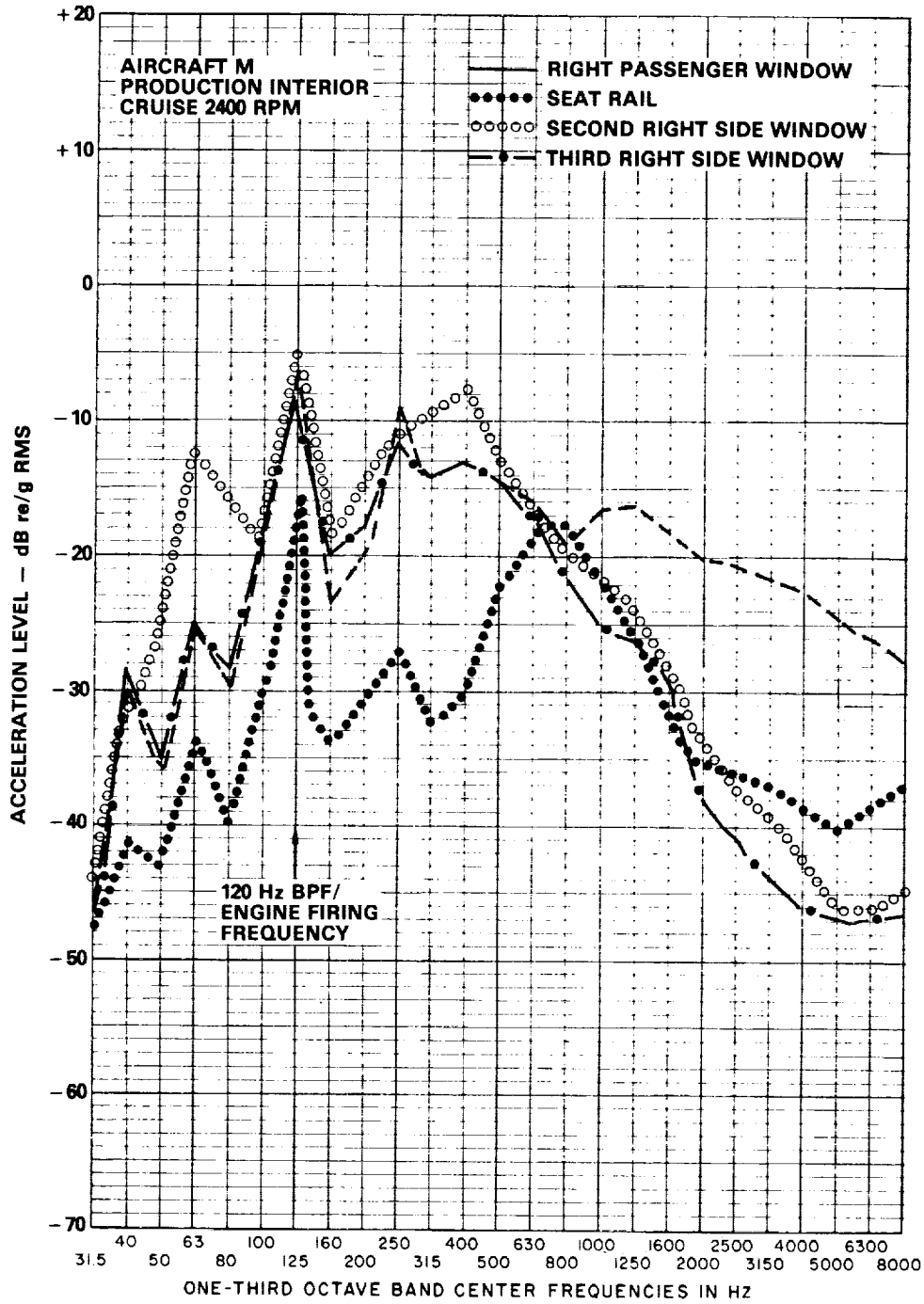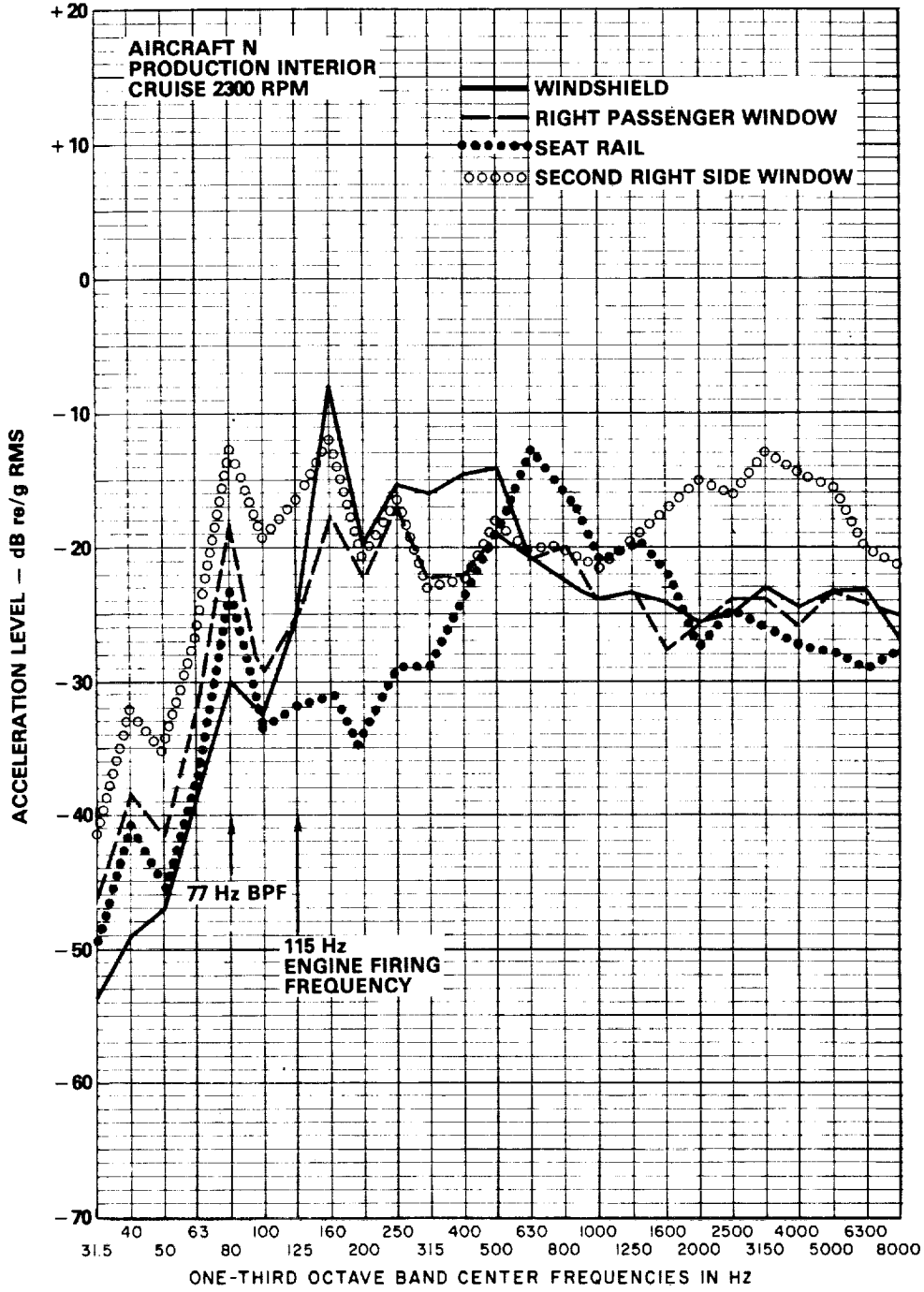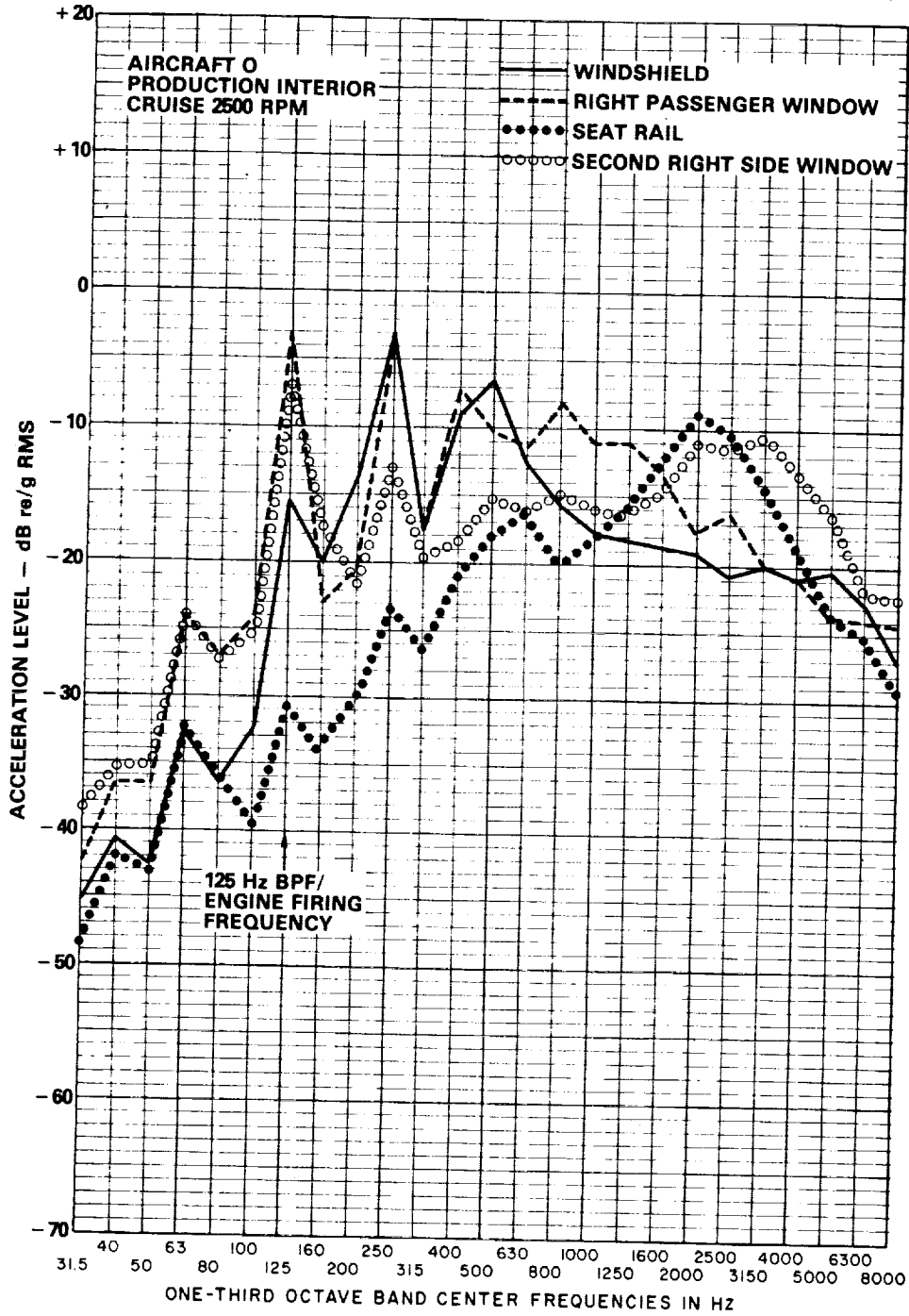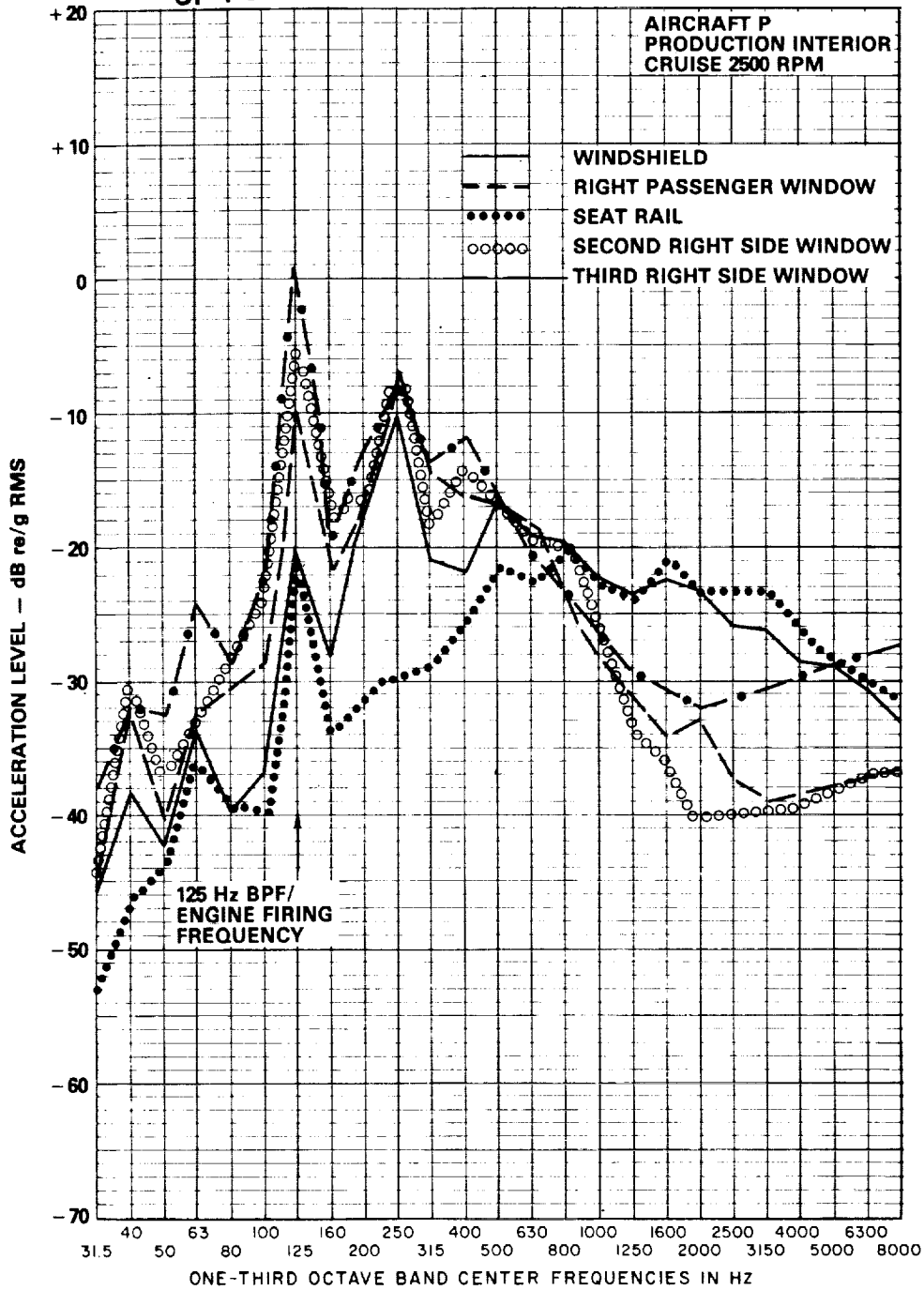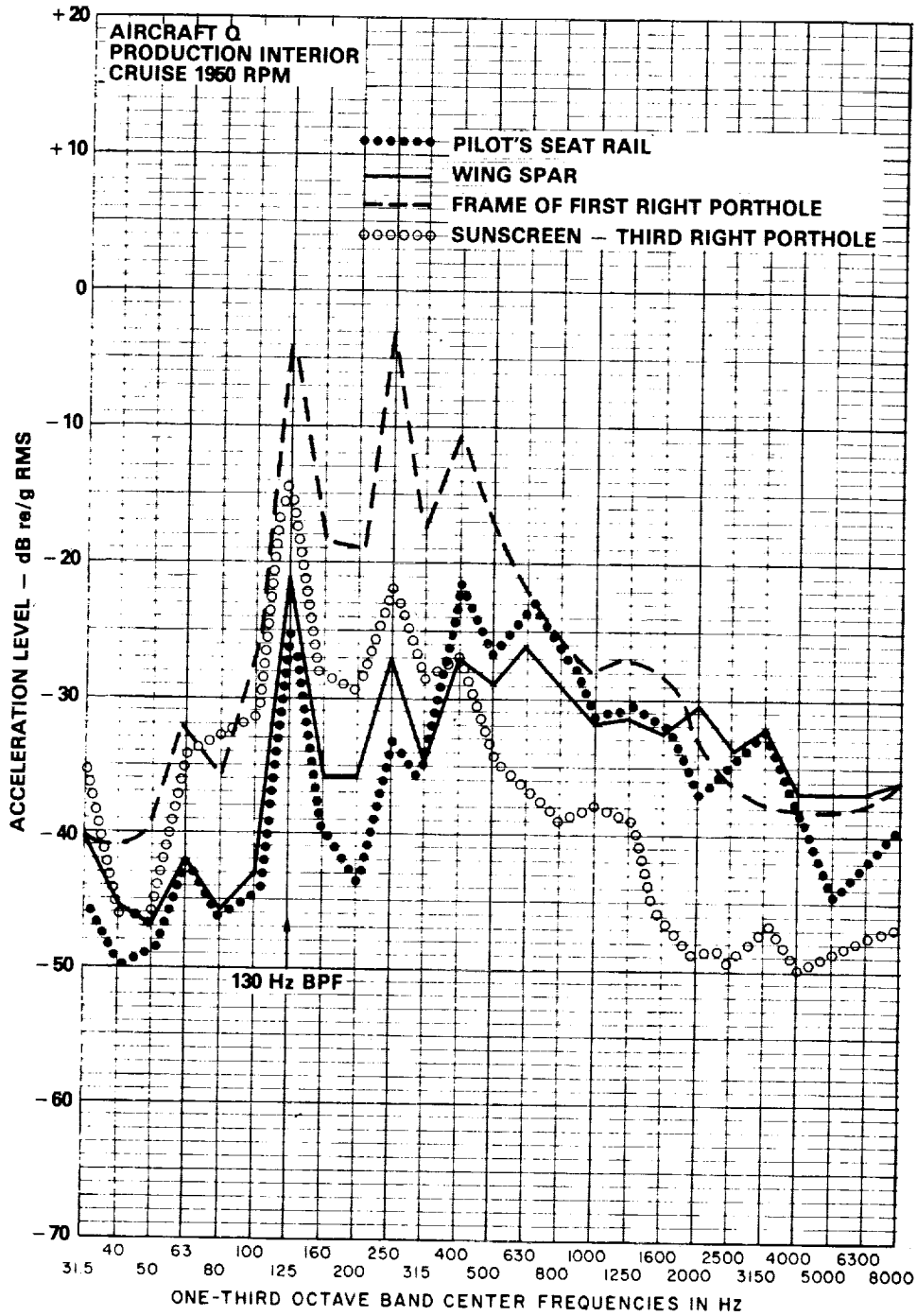FIG. A.21. VIBRATION SURVEY ON INTERIOR SURFACES ON AIRCRAFT D
IN CRUISE CONDITION

BOLT BERANEK & NEWMAN INC
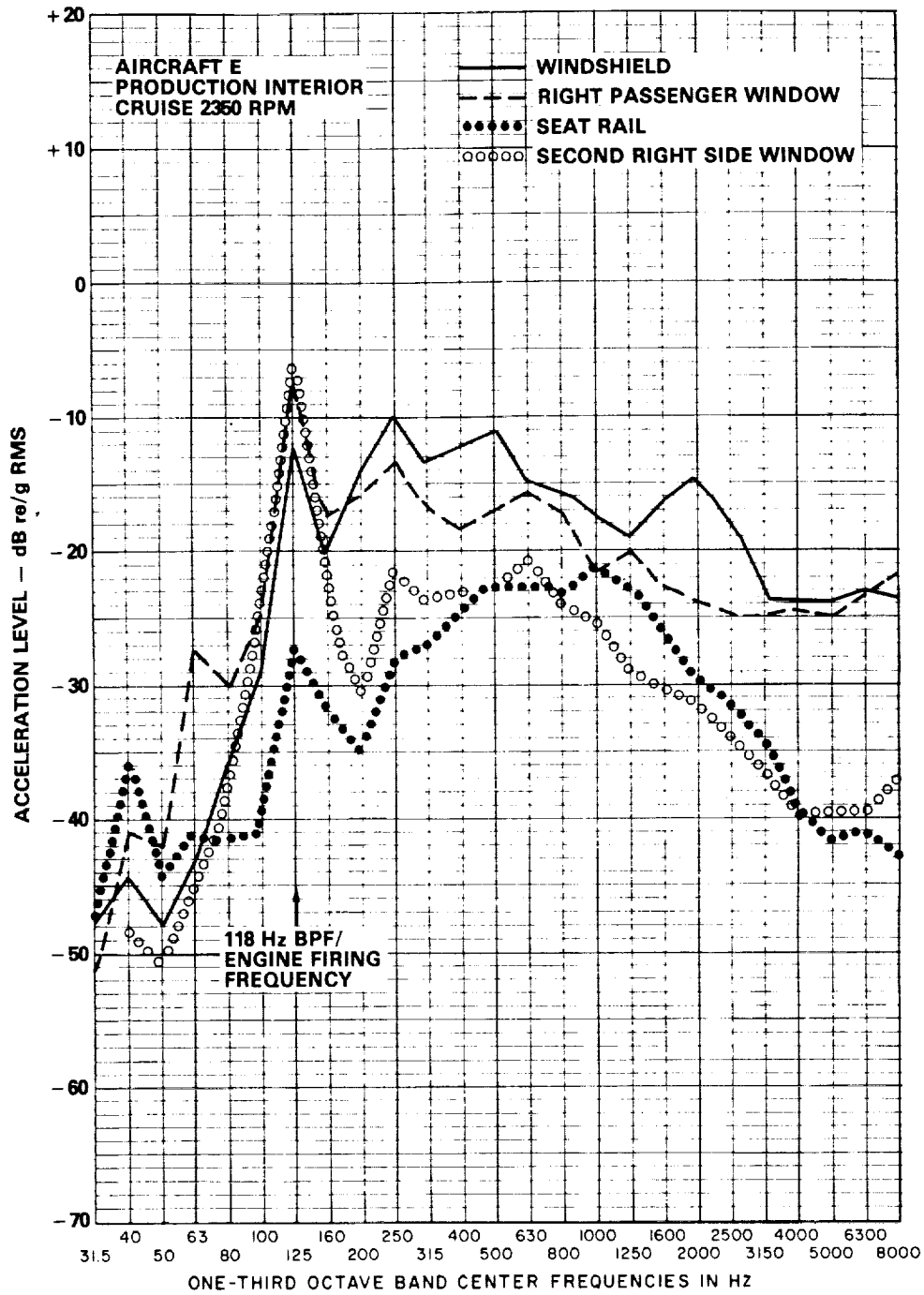
FIG. A.22. VIBRATION SURVEY ON INTERIOR SURFACES ON AIRCRAFT E
IN VRUISE CONDITION

BOLT BERANEK & NEWMAN INC
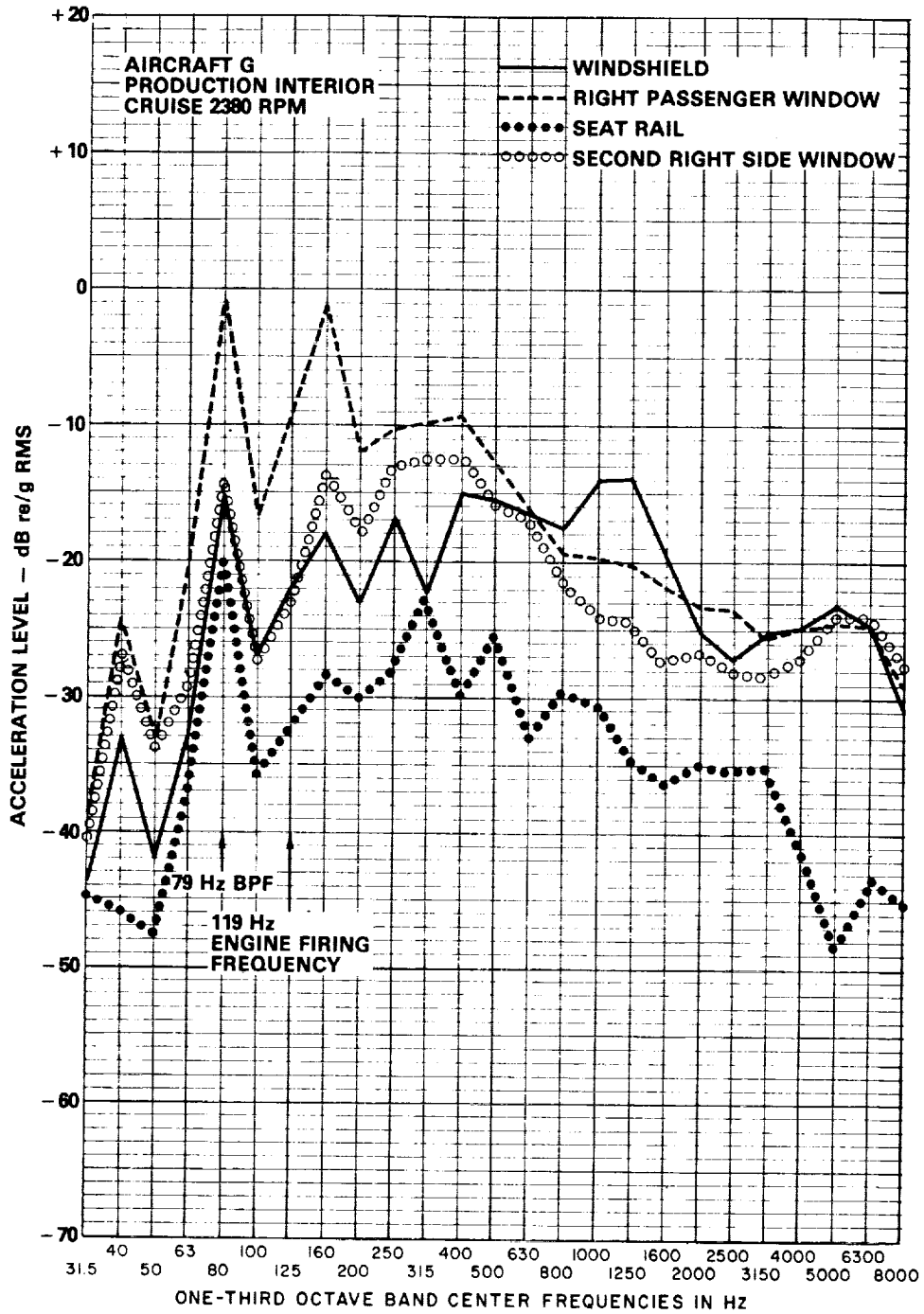
FIG. A.23.   VIBRATION SURVEY ON INTERIOR SURFACES ON AIRCRAFT G
IN CRUISE CONDITION
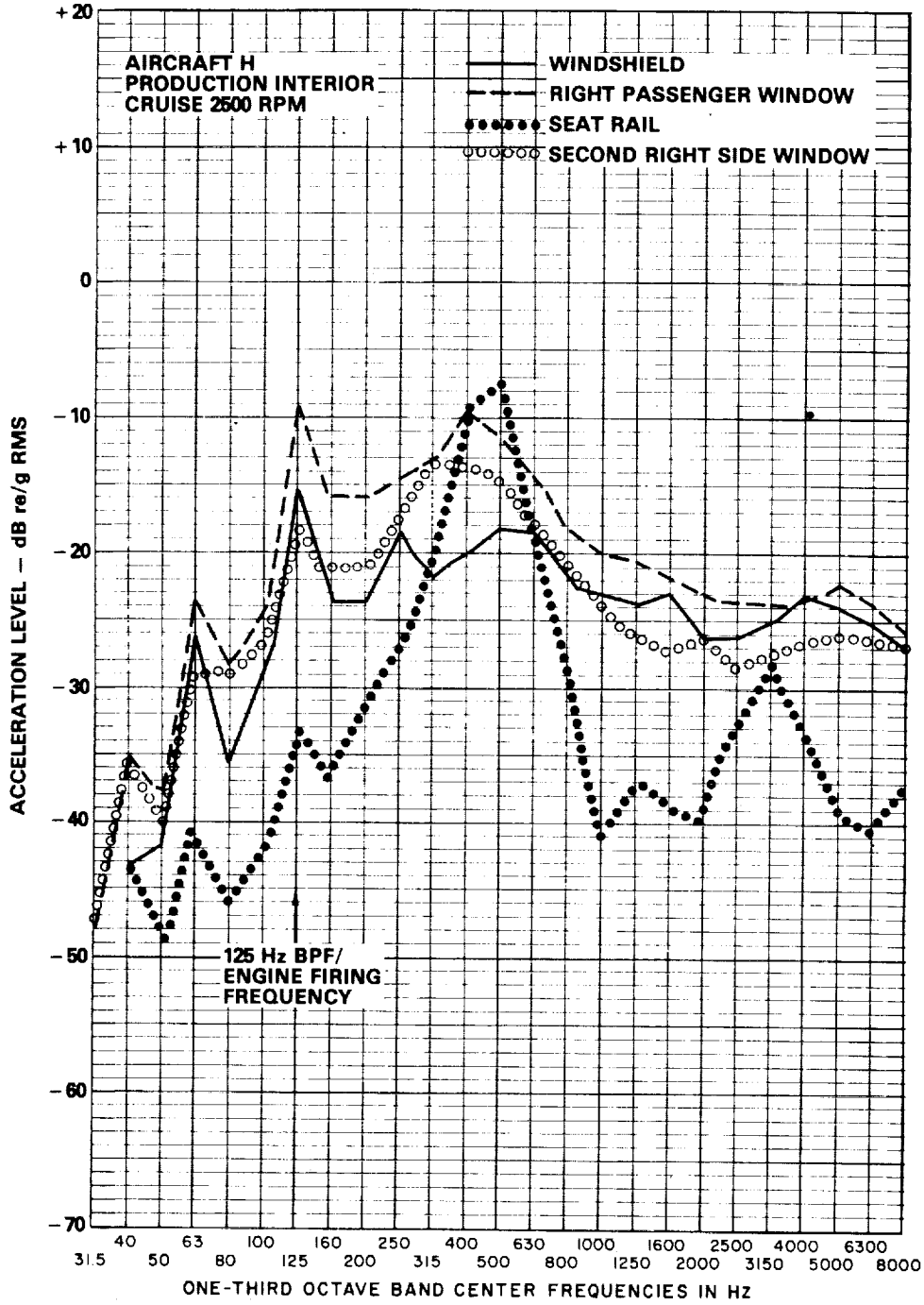
FIG. A.24. VIBRATION SURVEY ON INTERIOR SURFACES ON AIRCRAFT H
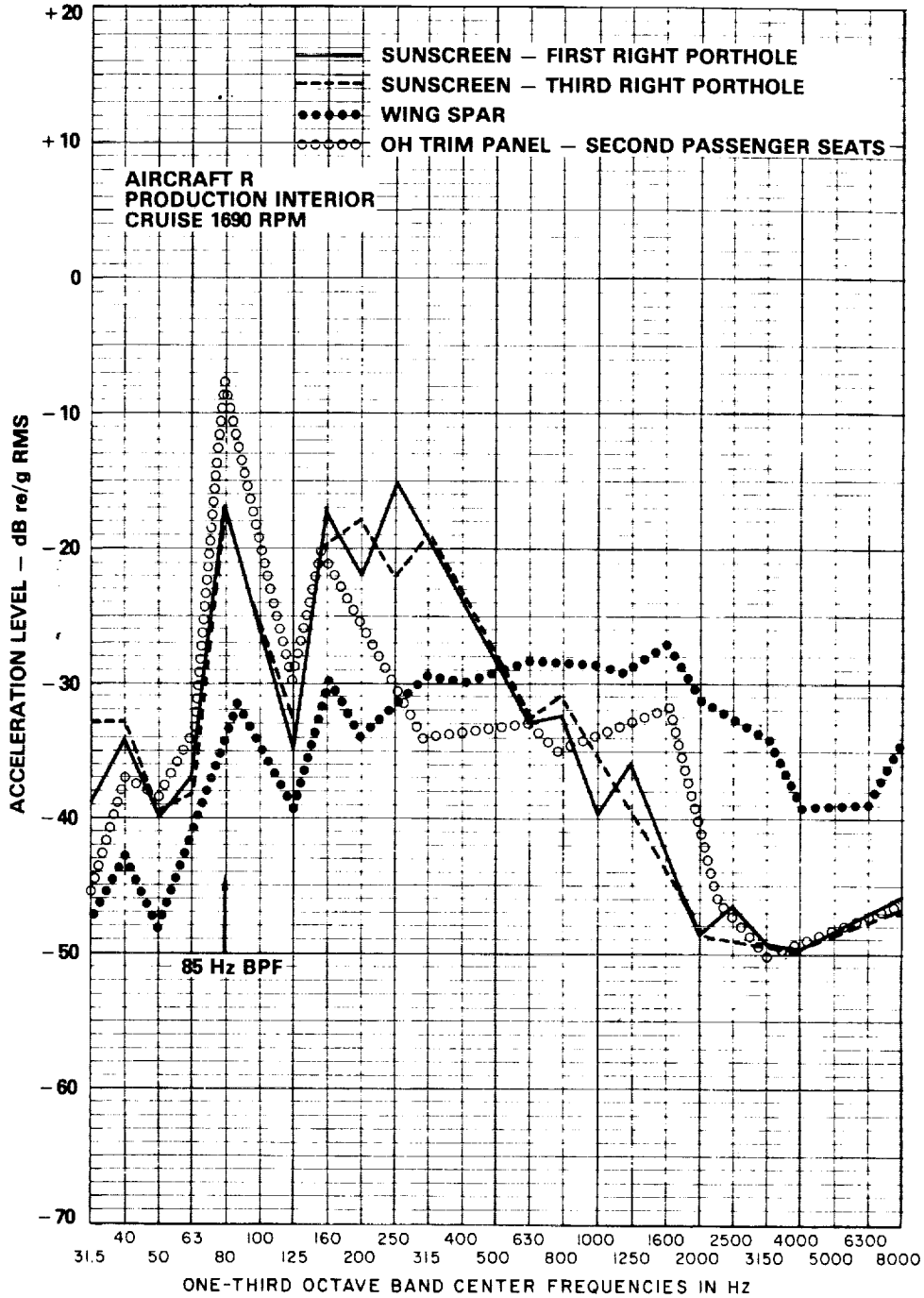IN CRUISE CONDITION
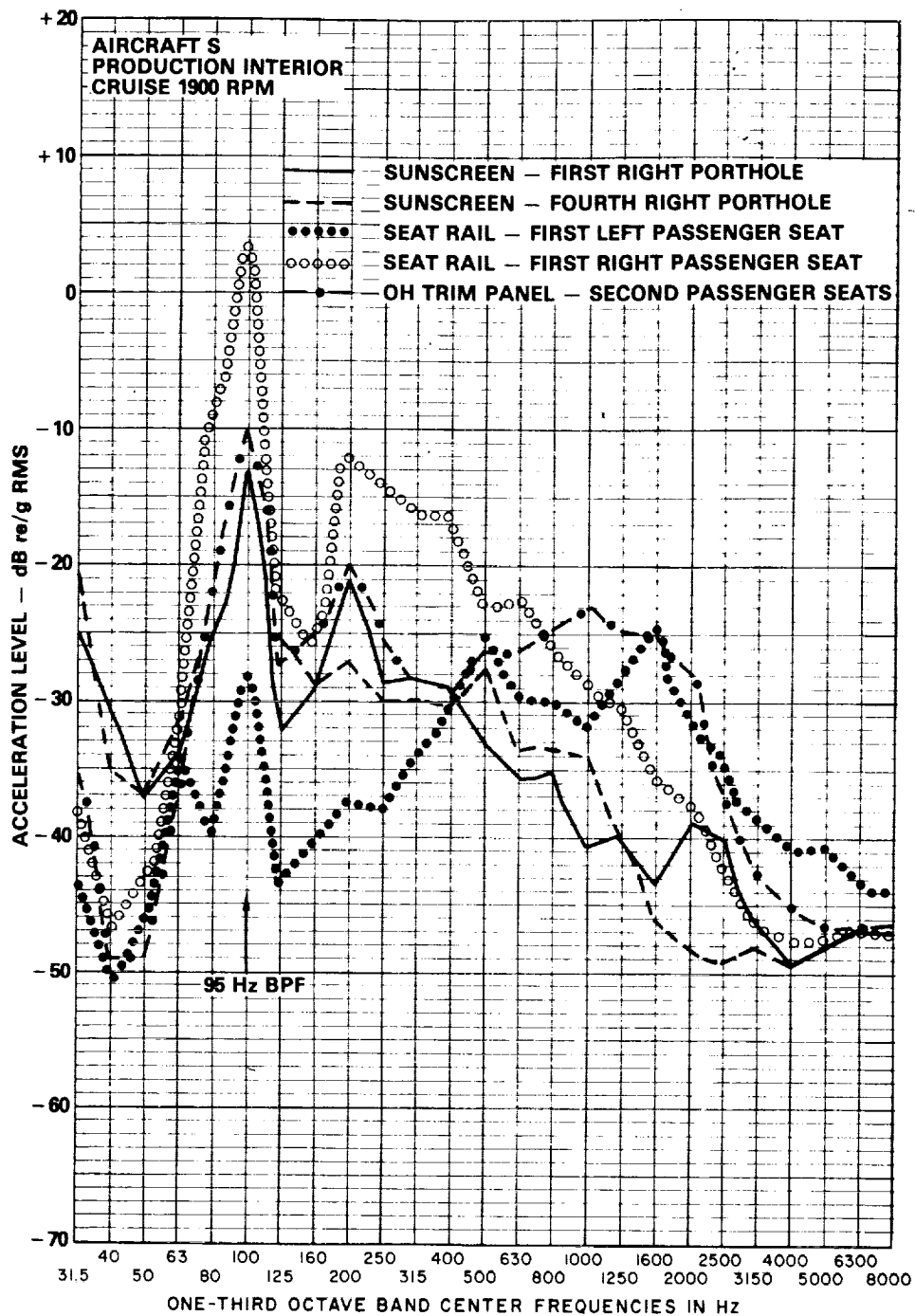
BOLT BERANEK & NEWMAN INC
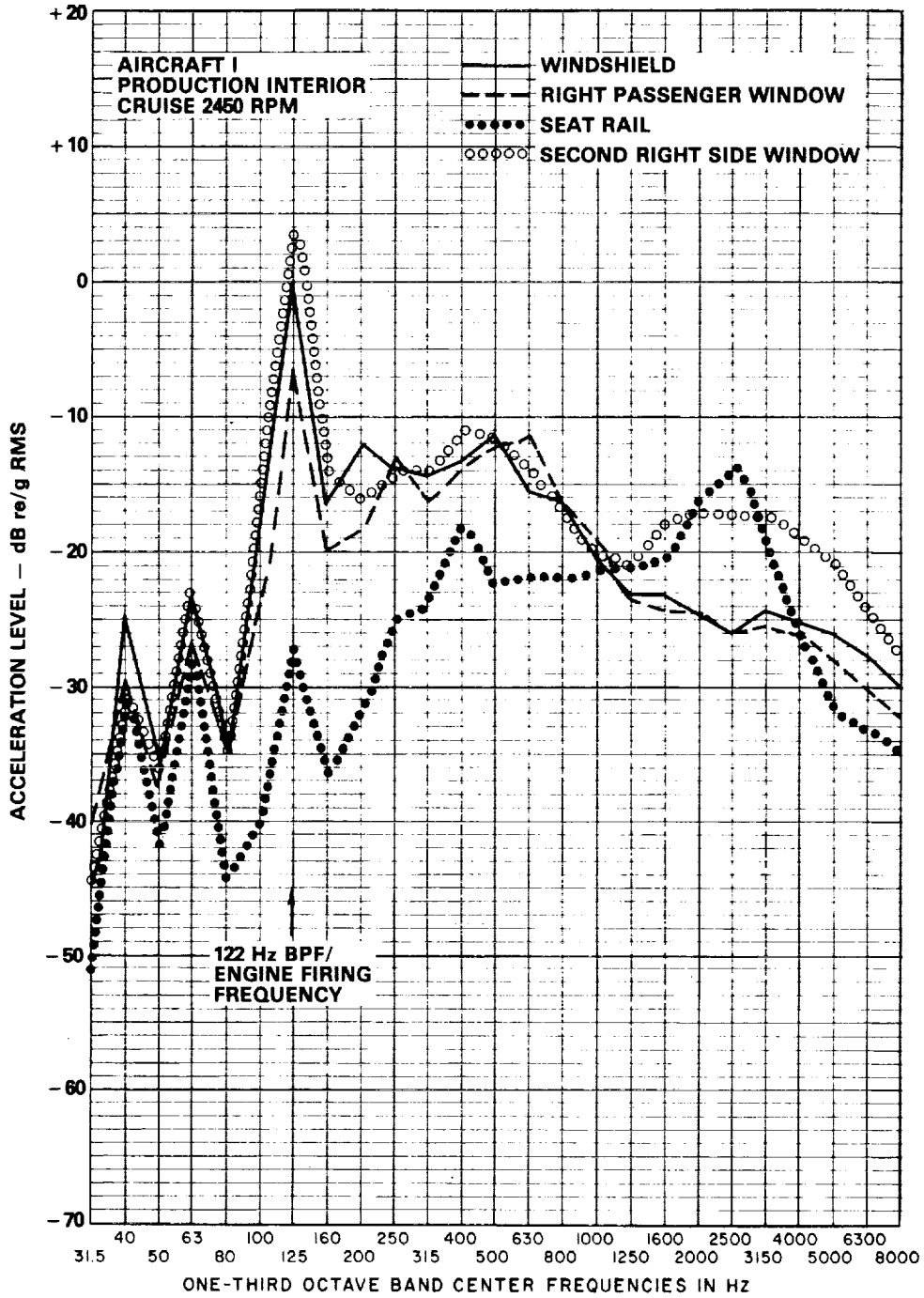
FIG. A.25. VIBRATION SURVEY ON INTERIOR SURFACES ON AIRCRAFT I
IN VRUISE CONDITION'

FIG. A.26. VIBRATION SURVEY ON INTERIOR SURFACES ON AIRCRAFT J IN CRUISE CONDITION

BOLT BERANEK & NEWMAN INC

FIG. A.27. VIBRATION SURVEY ON INTERIOR SURFACES ON AIRCRAFT K
IN CRUISE CONDITION

BOLT BERANEK & NEWMAN INC

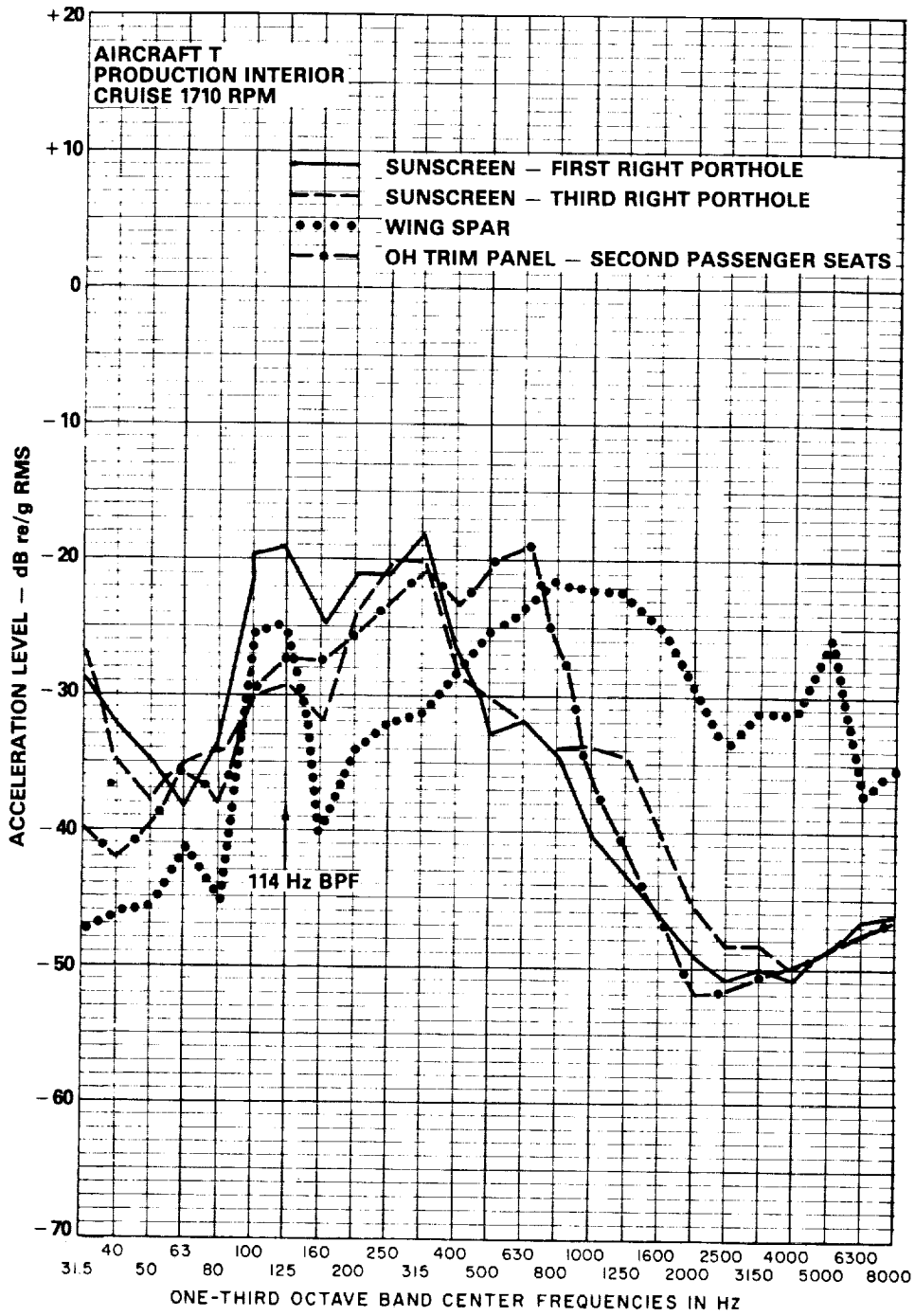
FIG. A.28. VIBRATION SURVEY ON INTERIOR SURFACES ON AIRCRAFT L
IN CRUISE CONDITION

A-40

BOLT BERANEK & NEWMAN INC

FIG. A.29 VIBRATION SURVEY ON INTERIOR SURFACES ON AIRCRAFT M
IN CRUISE CONDITION

FIG. A.30. VIBRATION SURVEY ON INTERIOR SURFACES ON AIRCRAFT N
IN VRUISE CONDITION

FIG. A.31. VIBRATION SURVEY ON INTERIOR SURFACES ON AIRCRAFT O
IN CRUISE CONDITION

BOLT BERANEK & NEWMAN INC

FIG. A.32. VIBRATION SURVEY ON INTERIOR SURFACES ON AIRCRAFT P
IN CRUISE CONDITION

FIG. A.33. VIBRATION SURVEY ON INTERIOR SURFACES ON AIRCRAFT Q
IN CRUISE CONDITION

BOLT BERANEK & NEWMAN INC

FIG. A.34.   VIBRATION SURVEY ON INTERIOR SURFACES ON AIRCRAFT R
IN CRUISE CONDITION

BOLT BERANEK & NEWMAN INC

AIRCRAFT S
PRODUCTION INTERIOR
CRUISE 1900 RPM

SUNSCREEN — FIRST RIGHT PORTHOLE
SUNSCREEN — FOURTH RIGHT PORTHOLE
SEAT RAIL — FIRST LEFT PASSENGER SEAT
SEAT RAIL — FIRST RIGHT PASSENGER SEAT
OH TRIM PANEL — SECOND PASSENGER SEATS

95 Hz BPF

ACCELERATION LEVEL — dB re/g RMS

ONE-THIRD OCTAVE BAND CENTER FREQUENCIES IN HZ

FIG. A.35.   VIBRATION SURVEY ON INTERIOR SURFACES ON AIRCRAFT S
IN CRUISE CONDITION

BOLT BERANEK & NEWMAN INC

**AIRCRAFT T
PRODUCTION INTERIOR
CRUISE 1710 RPM**

SUNSCREEN — FIRST RIGHT PORTHOLE
SUNSCREEN — THIRD RIGHT PORTHOLE
WING SPAR
OH TRIM PANEL — SECOND PASSENGER SEATS

114 Hz BPF

ACCELERATION LEVEL — dB re/g RMS

ONE-THIRD OCTAVE BAND CENTER FREQUENCIES IN HZ

FIG. A.36. VIBRATION SURVEY ON INTERIOR SURFACES OF AIRCRAFT T
IN CRUISE CONDITION

A.6 Twin-Engine Aircraft Dive Tests

A complete source/path diagnosis for interior noise must include noise sources other than the prime mover (engines and propellers). The most significant additional noise sources are the turbulent flow over the fuselage caused by the boundary layer and the propeller slipstream (on single engine aircraft). During the flight test program, three opportunities arose to examine interior noise caused by turbulent boundary layer excitation and airframe-radiated noise. The test procedure was to shut down the engines, feather the props, and dive at a representative speed, recording cabin noise once the aircraft had reached a steady speed. Since twin-engine aircraft are normally fitted with full-feathering propellers, the data presented below are confined to twins. Data from single-engine aircraft in dive mode also contain noise from engine-related sources and from the wake from the windmilling prop. Some of the data was discussed in Secs. 2 and 3 of the main body of the report.

The first test was performed on the prototype, Aircraft F, before an interior had been fitted. The cabin noise level in this aircraft was very high because of the stripped interior and whistling from many air leaks near the rudder pedals. The results of the dive test are shown in Figure A.37, where it is seen that that the dBA level is decreased by only 2 dBA (108.5-106.5) by shutting down the engines. The subjective impression of the test team was that much of the noise was due to air leaks. The results of this test were therefore of little help in quantifying the role of turbulent boundary noise, other than to point up the importance of sealing all air leaks.

The results of two more useful tests are shown in Fig. A.38 and A.39. Aircraft K and L, with furnished interiors, were flown

with and without the engines operating. The decrease in noise
which occurs when the engines are shut down gives an indication
of the role of airborne and structureborne noise from the engine/
propeller combination. The remaining noise is therefore only due
to the turbulent boundary layer's direct excitation of the struc-
ture, and turbulent boundary layer and wake interaction with
control surfaces and struts (which generates airborne noise and
structural vibration). The large increment in tonal noise
observed between one- and two-engine operation (Fig. A.38), is
presumably due to the asymmetric acoustic field induced by the
propellers, caused by the different relative rotation sense with
respect to the airframe. In order to compare the propulsion- and
nonpropulsion-related contributions, the data must be scaled to the
same speed. Figure A.40 shows narrowband data corresponding to
the engine-off conditions in Fig. A.39. Increasing the amplitude
of the 110 kt data by 10 log V^4 produces a reasonable agreement
with the measured data at 150 kt. It was not possible to achieve
the 175 kt cruise speed in a dive, so the 150 kt data must be
scaled to 175 kt for assessment of the nonpropulsion contri-
butions. This comparison is shown in Fig. A.41.

A vibration measurement made on a window during a dive can
provide further assessment of nonpropulsion noise. Such a
measurement is shown in Fig. A.42. As shown in Fig. A.43, the
broadband vibration of the window is only slightly changed by
shutting down the engines when account is taken for the change
in flight speed using a V^4 scaling relationship. Thus, the
turbulent boundary layer excitation seems to be an important
cause of window vibration.
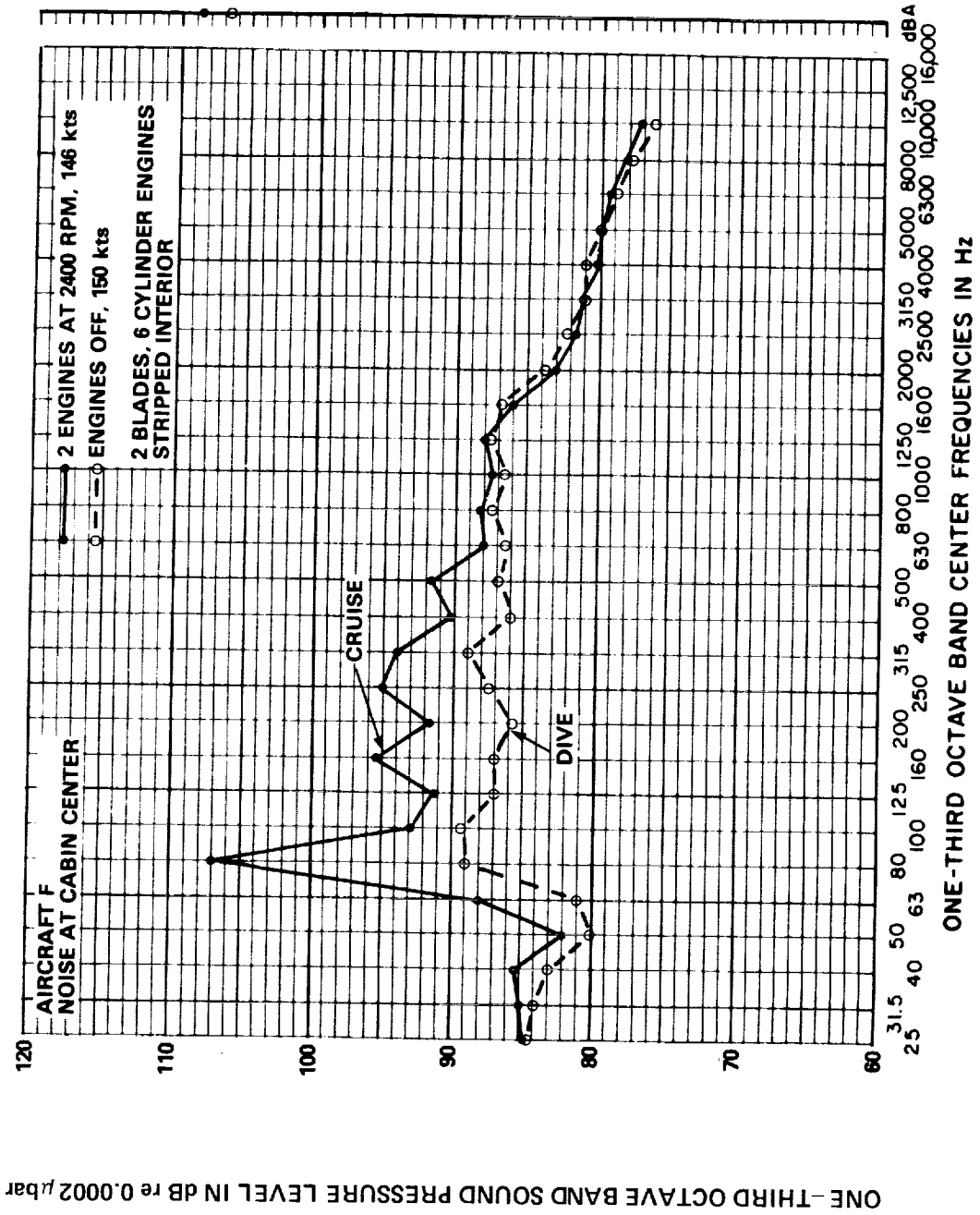
FIG. A.37. COMPARISON OF NOISE AT CABIN CENTER IN UNFURNISHED TWIN IN CRUISE AND DIVE CONDITIONS
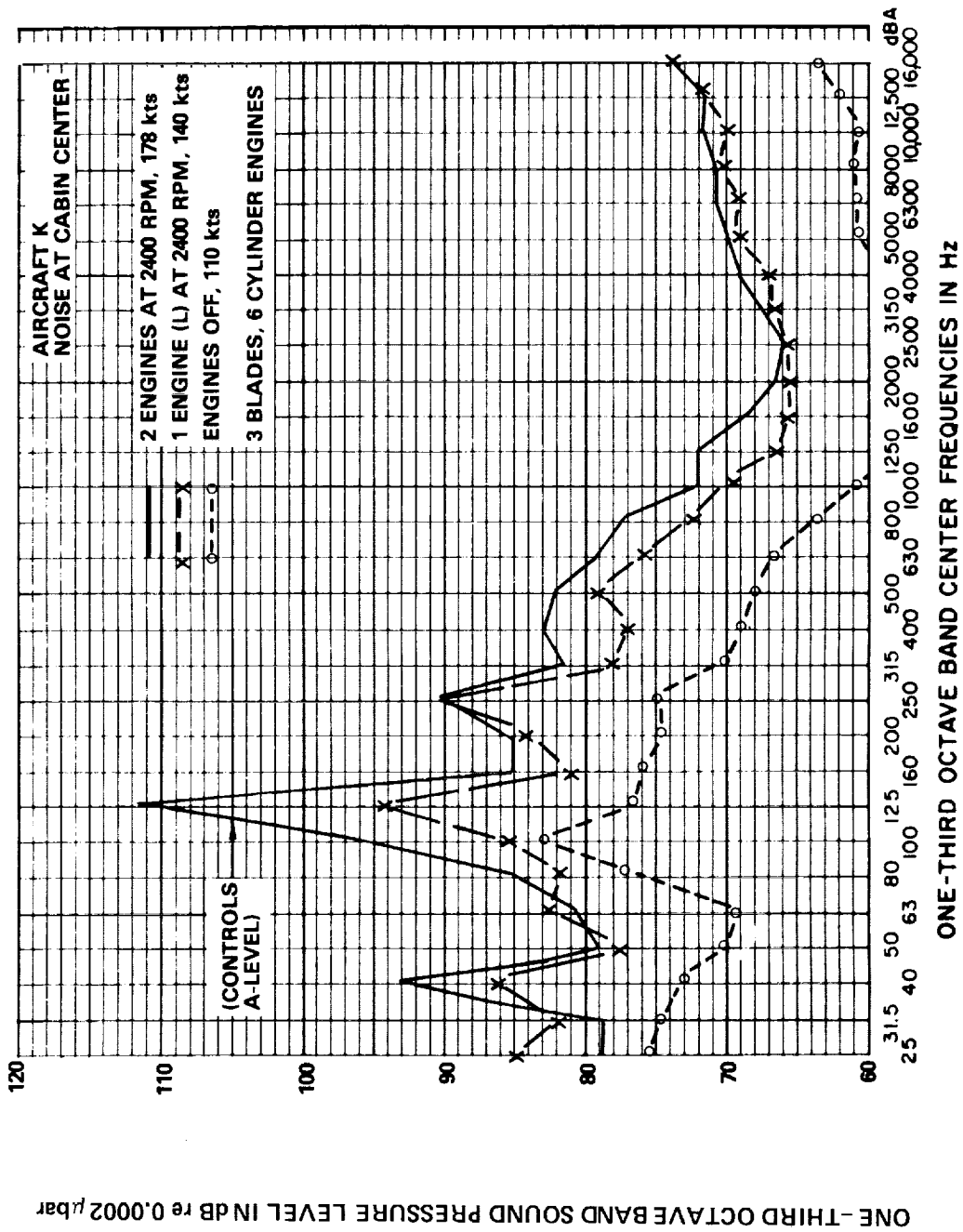
A-51

AIRCRAFT K
NOISE AT CABIN CENTER

2 ENGINES AT 2400 RPM, 178 kts	
1 ENGINE (L) AT 2400 RPM, 140 kts	x—x
ENGINES OFF, 110 kts	o- -o
3 BLADES, 6 CYLINDER ENGINES	

ONE-THIRD OCTAVE BAND CENTER FREQUENCIES IN Hz

ONE-THIRD OCTAVE BAND SOUND PRESSURE LEVEL IN dB re 0.0002 μbar

(CONTROLS
A-LEVEL)

FIG. A.38. COMPARISON OF NOISE IN A FURNISHED TWIN (AIRCRAFT K) WITH TWO ENGINES, ONE ENGINE, AND NO ENGINES RUNNING

A-52
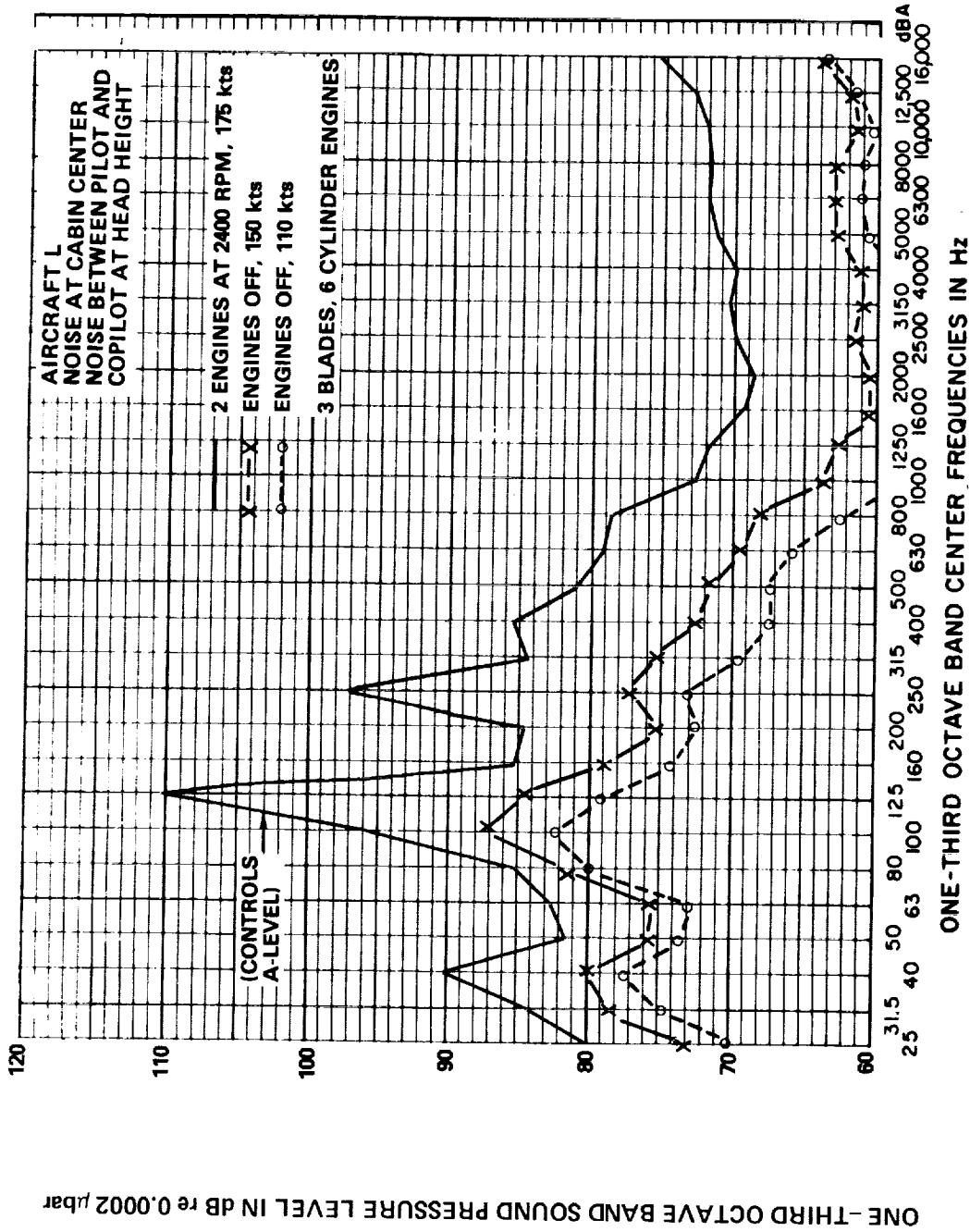
FIG. A.39. COMPARISON OF NOISE IN A FURNISHED TWIN (AIRCRAFT L) WITH ENGINE ON, AND DIVING AT TWO DIFFERENT SPEEDS
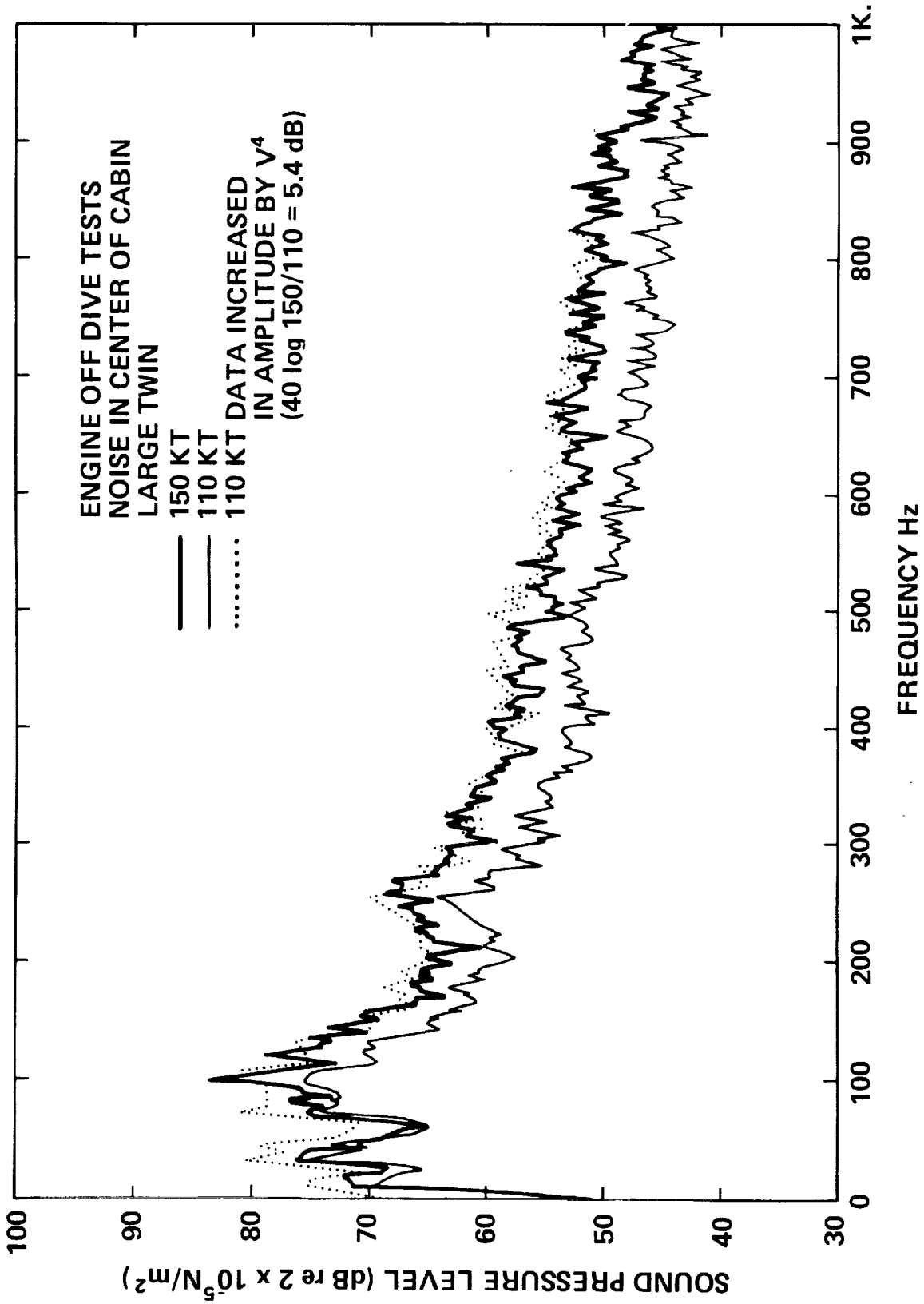
FIG. A. 40. NARROWBAND ANALYSIS OF SPEED DEPENDENCE OF NONPROPULSION NOISE
IN AIRCRAFT I
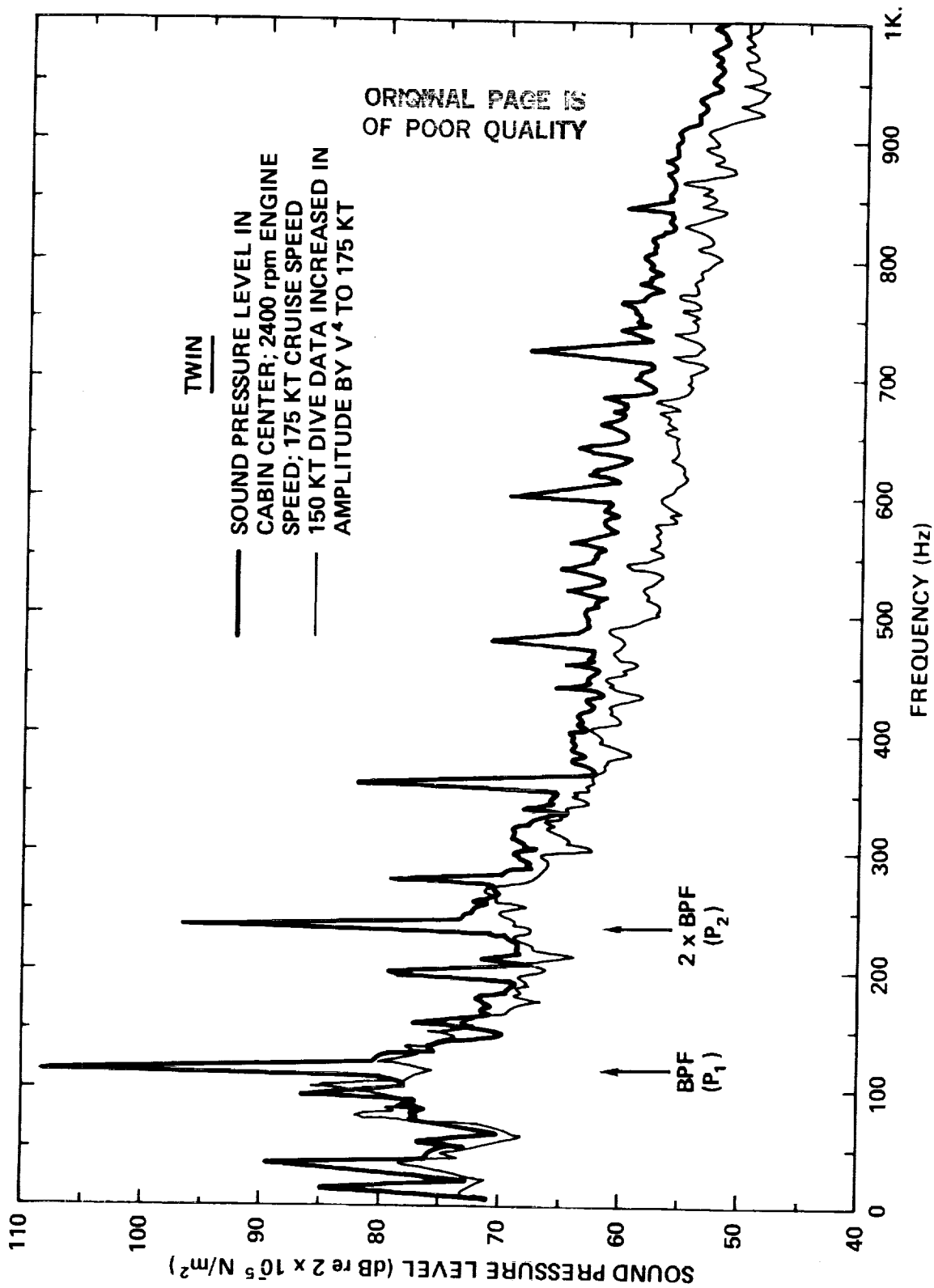
FIG. A.41. NARROWBAND COMPARISON OF CABIN NOISE IN AIRCRAFT L AT CRUISE AND NONPROPULSION NOISE CALED BY V^4
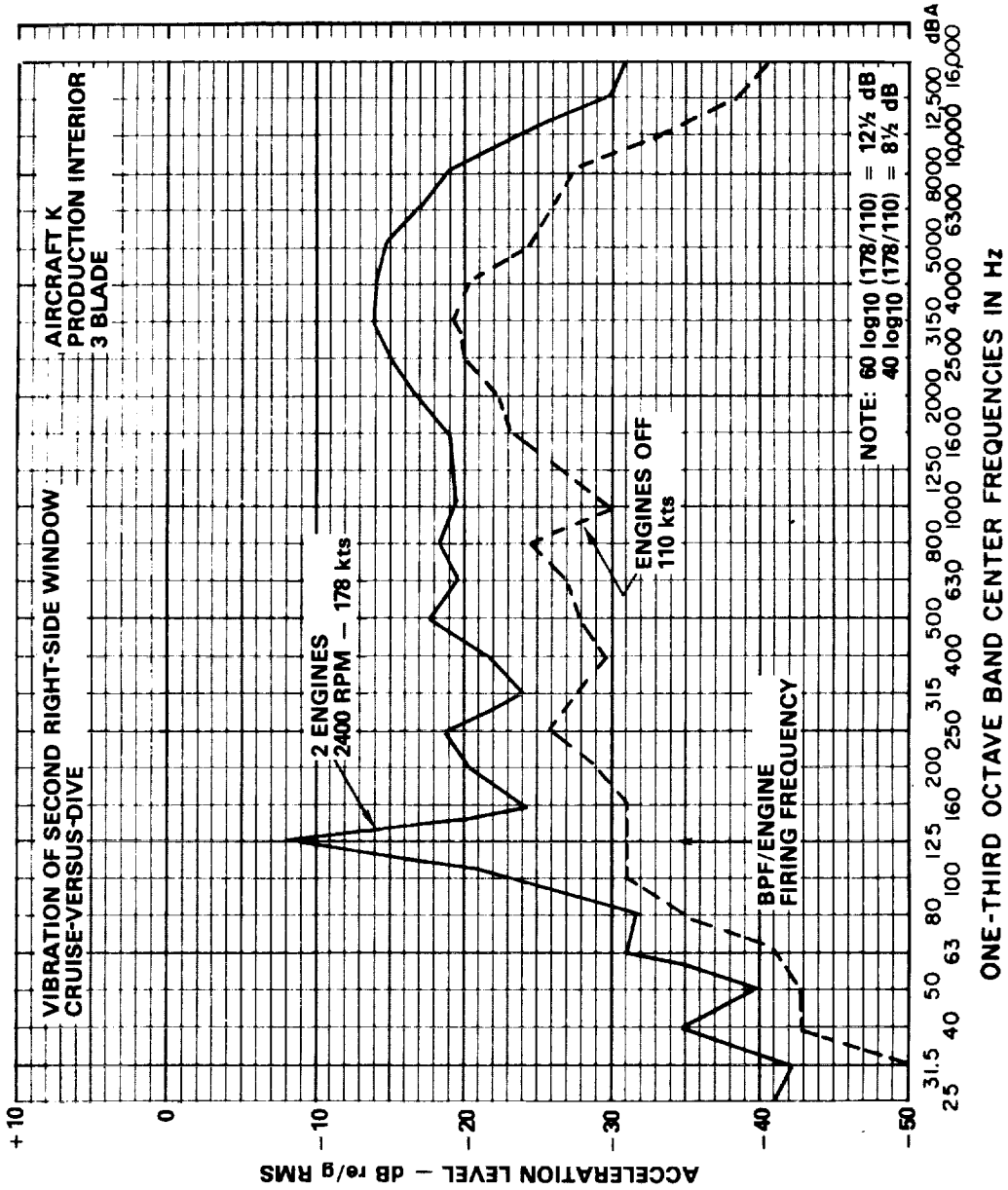
FIG. A.42. VIBRATION RESPONSE OF SIDE WINDOW OF TWIN (AIRCRAFT K) DURING POWERED AND UNPOWERED FLIGHT

A-56

POINT ACCELERATION ON TWIN ENGINE AIRCRAFT
2nd RIGHT HAND SIDE WINDOW

MEASURED VIBRATION ON WINDOW
AT 178 KT CRUISE 2400 rpm

MEASURED VIBRATION FROM 110 KT DIVE
SCALED TO 178 KT BY V^4 IN AMPLITUDE
(NO FREQUENCY SHIFT)

ACCELERATION LEVEL (dB re 1g rms)

FREQUENCY (Hz)
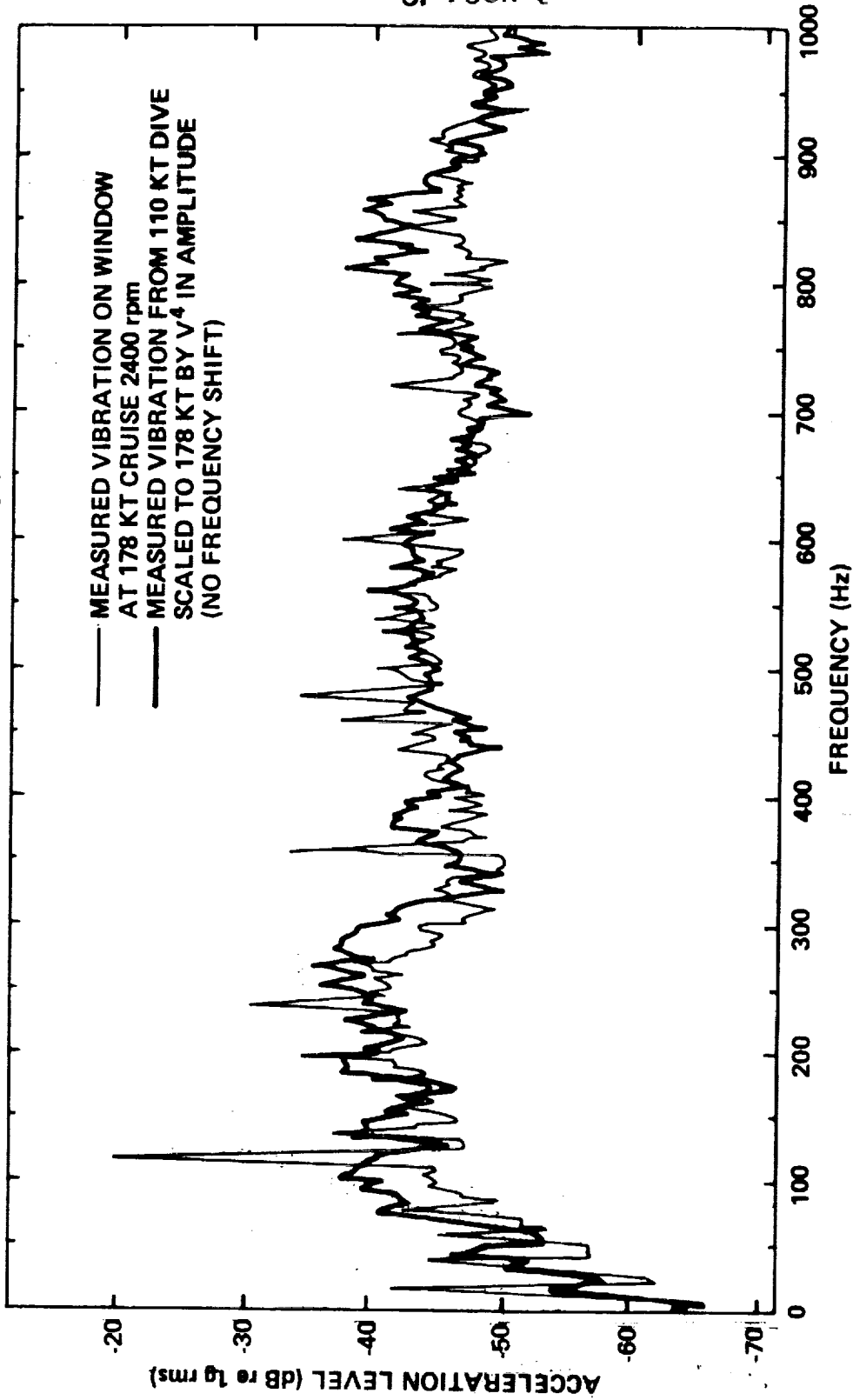
FIG. A.43. NARROWBAND SPECTRUM OF WINDOW VIBRATION DURING POWERED AND UNPOWERED
FLIGHT WITH 110 KT DIVE DATA SCALED TO 178 KT CRUISE

A.7 Diagnostic Tests

In addition to the previously-described dive tests, several ground and flight tests were conducted to attempt to isolate a particular source or path, or to characterize a particular phenomenon. The data supporting these tests are discussed below.

a) Engine Vibration Isolator Performance

Central to the issue of structural coupling of vibration of the propeller/engine combination is the behavior of the engine mounts. Flight and ground experiments were conducted to measure their performance. In the early stages of the diagnostic work, the experiments consisted of measuring the acceleration of each side of the mount, and simply taking the difference in mean-squared amplitude as a measure of the isolation provided. This is recognized as being a superficial test since the mount itself will couple the structural components and thus influence the mean-square acceleration on both sides of the mount, thereby causing an underestimate of the mount's isolation performance.

However, the flight data are presented for informational purposes, as they do point up some trends. Fig. A.44 shows the results obtained by taking the time-averaged difference in third octave bands between accelerometers aligned on either side of the mounts, during flight tests. The curves show significant fluctuations. Also to be noted is that at the lower frequencies the isolator performance is not consistent at the two tested speeds.

The complex nature of the flight results obtained led to the decision to conduct a formal "insertion loss" experiment. Since insertion loss can be defined as the effect of installing the isolators on the structural vibrations of the fuselage, a test was conducted to measure
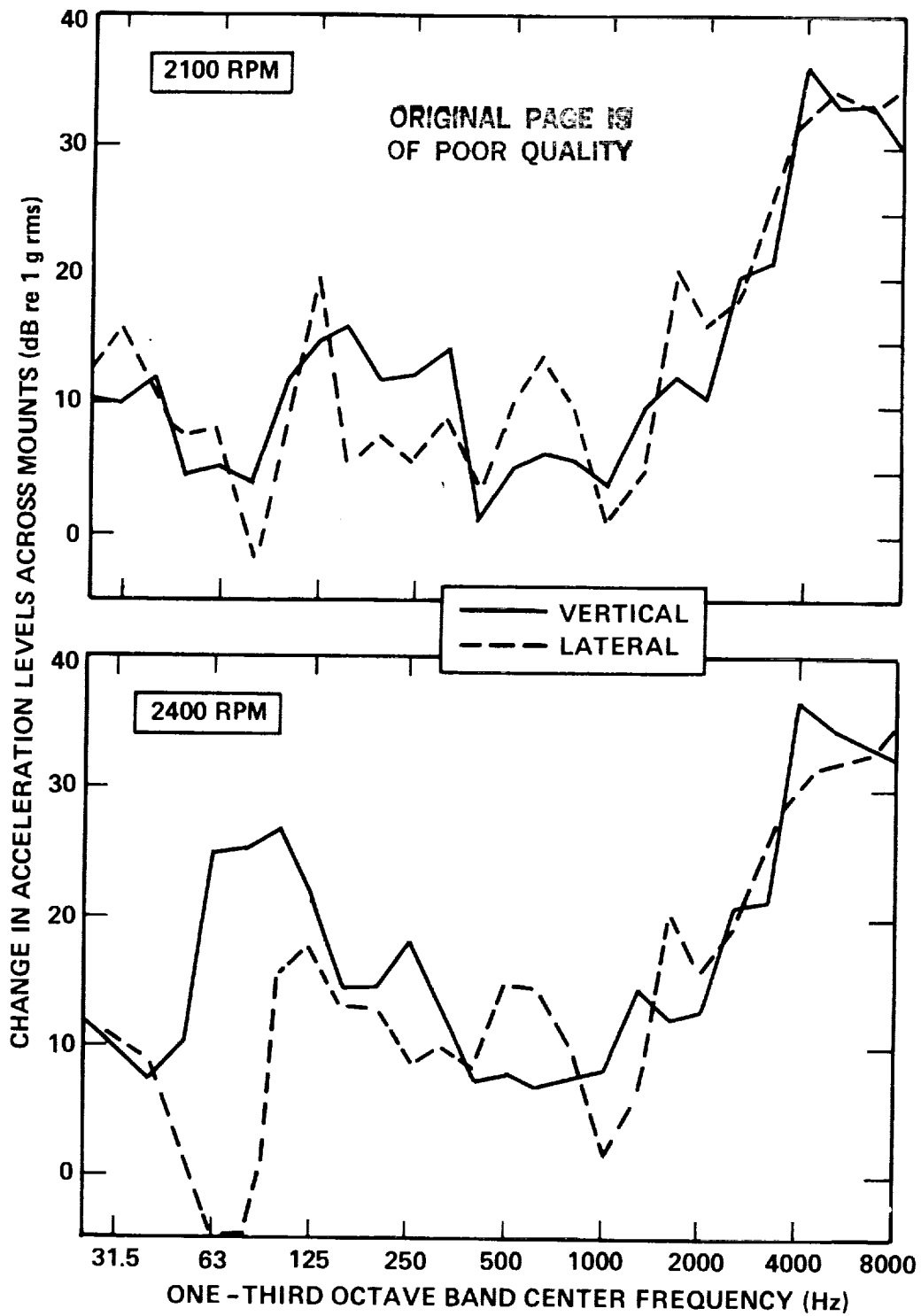
FIG. A.44. FLIGHT TEST MEASUREMENTS OF SINGLE AXIS ACCELERATION
DIFFERENCES ACROSS ENGINE MOUNTS. (AIRCRAFT D)

A-59

this directly. Two mount configurations were tested: one
of the standard design and one in which solid aluminum
blocks were installed in place of the isolator. The
aluminum blocks were similar in form and fit to the rubber
elements of the standard mount. Vibration tests with this
configuration would thus simulate the "no isolator" case and
by comparison with the standard arrangement would determine
the insertion loss of the engine mounts.

Shown in Figures A.45 and A.46 are the results of the ground
test of the engine vibration isolators for Aircraft C.
Three different engine power settings were used with the
wheel brakes locked to load the isolators. The insertion
loss was determined by the 3-axis energy-averaged change in
acceleration level across each mount. The results for the
three tests are very consistent. It is also instructive to
compare the result with the previous simple flight experi-
ment whose results are presented in Fig. A.44. Both sets of
results show that the isolation performance peaks at 4000
Hz, but that the magnitude of isolation is 5-10 dB
difference between them. The trend of isolation versus
frequency is completely different, with the hard/soft mount
test producing the most consistent behavior.

The increase in noise level for a hard-mounted engine
(Figure A.46), is much less than the insertion loss of the
mounts at high frequencies, thus suggesting that the
frequency range over which the engine structureborne noise
is important is below 2 kHz.
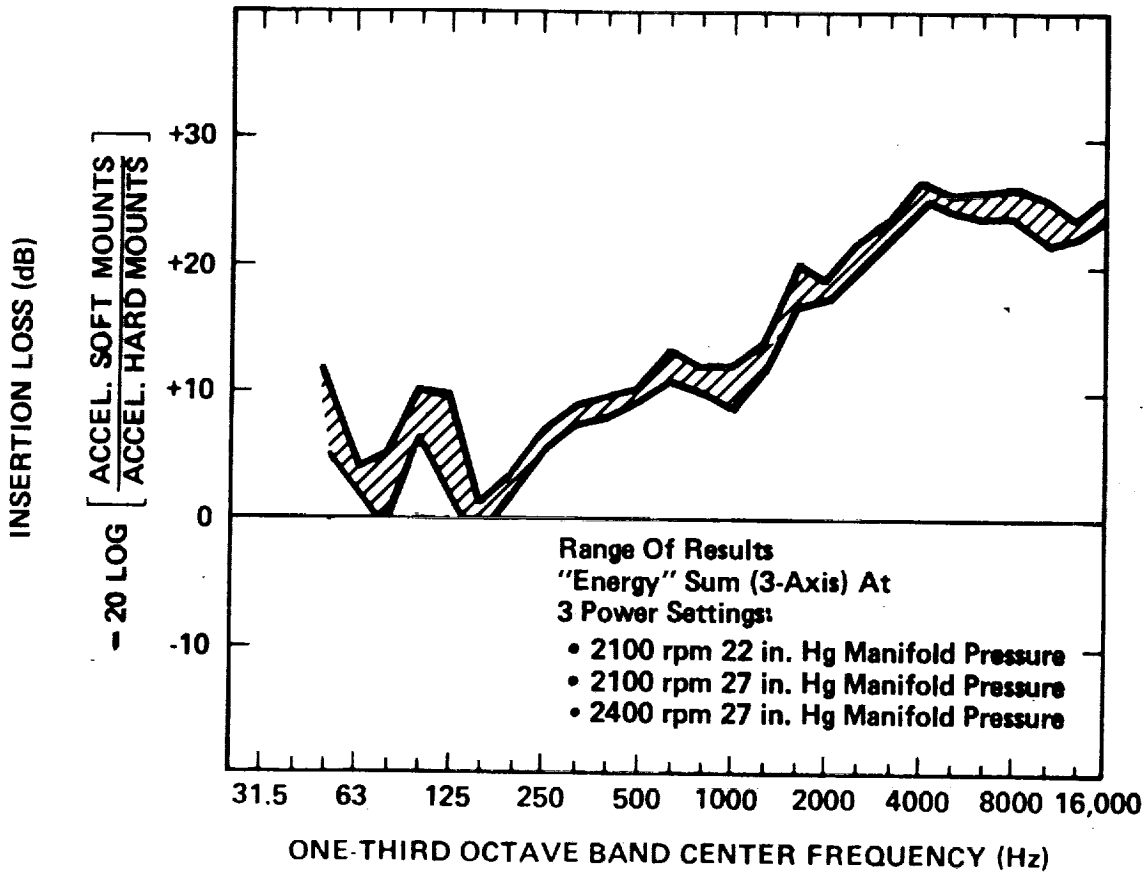
FIG. A.45.   DEDUCED INSERTION LOSS OF STANDARD ENGINE MOUNTS
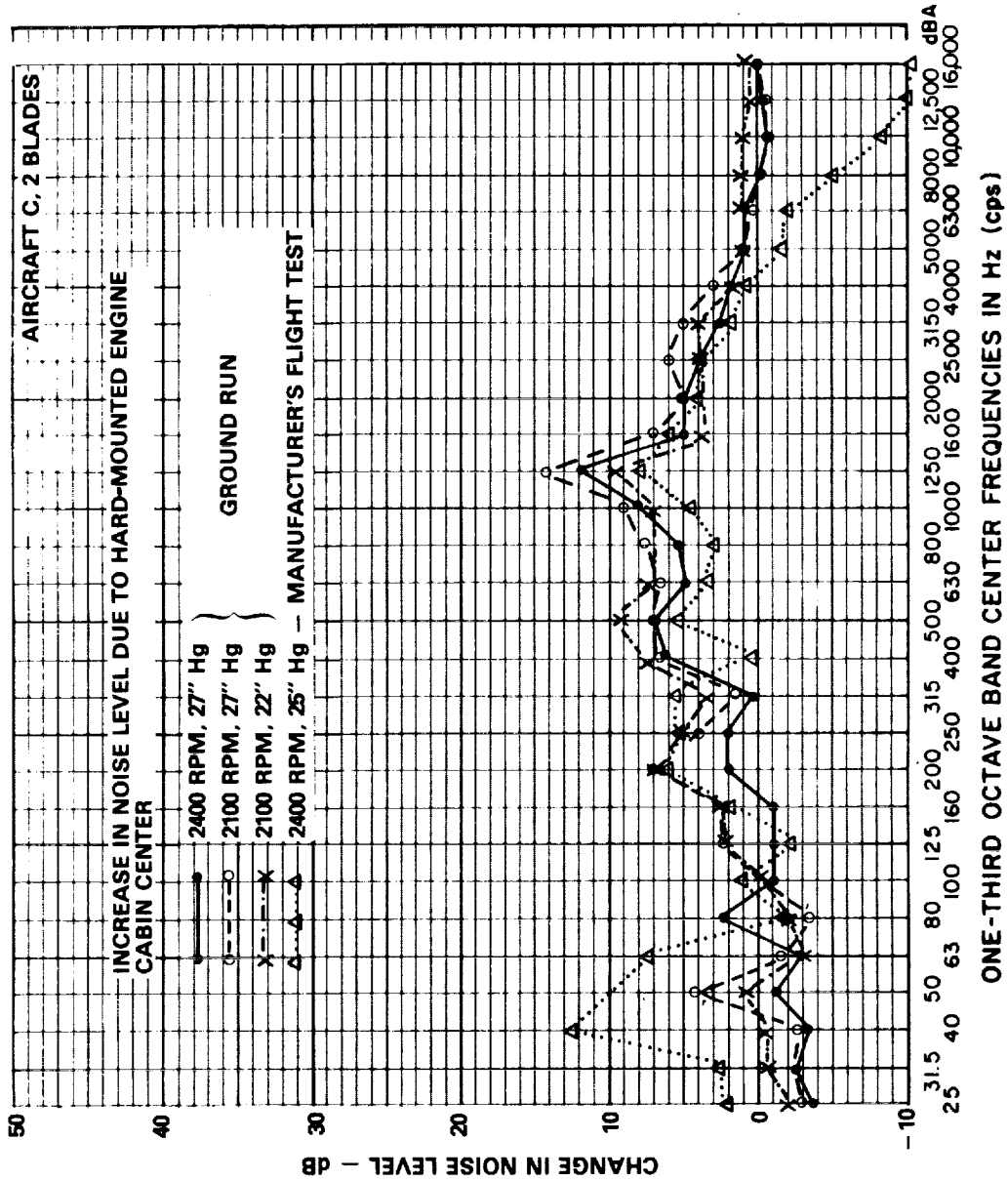
FIG. A.46. MEASURED INCREASE IN NOISE LEVEL WHEN RIGID MOUNTS ARE INSERTED IN PLACE OF STANDARD MOUNTS

b) In-Flight Survey of Cabin Cross Spectra ("Mode" Surveys)

Aircraft C and F were outfitted with microphones arranged to measure cross spectra between various points in the cabin to try to detect the presence of cabin acoustic modes in flight. The microphone positions for the mode survey of Aircraft C are given in Figure A.47. Plotted in Figure A.47(b) and (c) are the one-third octave band sound levels containing the blade passage tone as functions of position. The level at Location 3 (near the rear window) is much higher than elsewhere in the cabin at the 2400 RPM setting, indicating the likelihood of a strongly excited acoustic mode in the cabin at that 1/3 octave frequency. This notion is supported by the phase plots which follow. Figures A.48-A.58 show plots of the phase of the cross spectra between pairs of cabin microphones. The reference microphone (defining 0°) is always the first microphone number cited in the caption of each figure. The blade passage frequency, its second harmonic, and the engine firing frequency are indicated on each plot. Several characteristics of such phase plots should be pointed out. First, if there is low coherence between the two signals, then the phase between them may be random and will vary rapidly, as for example, in Figure A.48 above about 150 Hz. Second, a traveling wave will register as a line with constant slope (phase proportional to frequency) as in Figure A.50 between 90 and 115 Hz. Standing waves (cabin modes) should register as phase differences of 180° for microphones separated by a single node line and should occupy a fairly narrow frequency regime (depending on the Q* of the mode). Dramatic phase shifts occurring only at
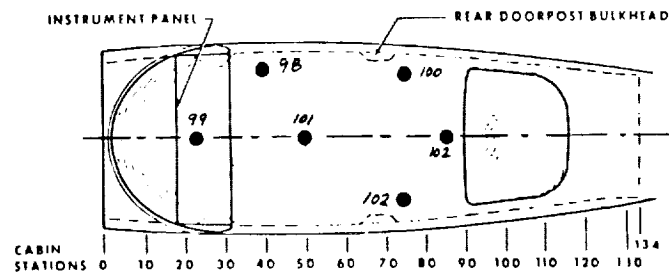
---

*Q = damping ratio.
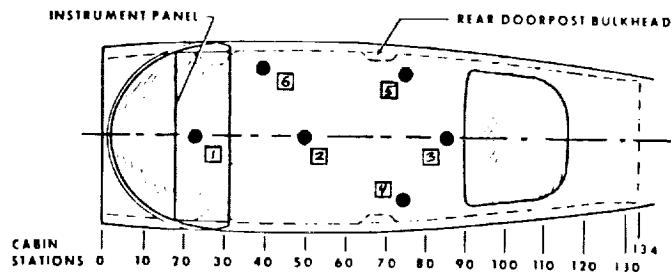
A. Microphone Numbers and Positions (to scale) in Aircraft C
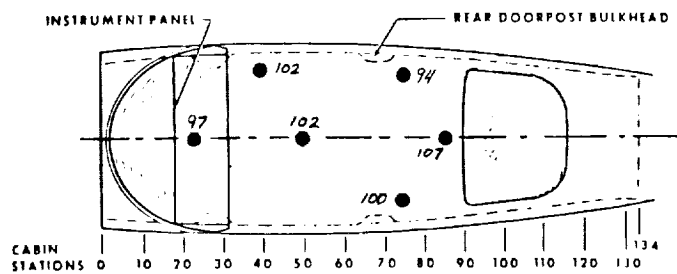
B. One-third Octave Band Sound Pressure Levels at Blade Passage Frequency, 2400 RPM Cruise

C. One-third Octave Band Sound Pressure Levels at Blade Passage Frequency, 2100 RPM Cruise

FIG. A.47. LOCATIONS OF CABIN MICROPHONES FOR MODE SURVEY AND DISTRIBUTION OF BLADE PASSAGE RATE THIRD OCTAVE BAND LEVELS THROUGHOUT CABIN (AIRCRAFT C)

multiples of engine or propeller rotation rate should be interpreted cautiously. In such a case, comparison of the results with those from a different engine speed may be helpful. Another caveat is that the analyzer may register a small deviation about ±180° as a sudden shift to 180°. The first longitudinal mode in the cabin would be expected to occur near 50 Hz. The first transverse mode should occur near 140 Hz. The inspection of Figures A.48-A.57 shows traveling waves running back through the cabin on microphones 1-3.

The pressures at microphones 1 and 3 are 180° out of phase between about 40 to 90 Hz, which may be due to a standing wave in the cabin. Microphones 4 and 5 are in phase below about 140 Hz as would be expected if the main noise sources are axially symmetric. Above 140 Hz, the "hash" registering between microphones 4 and 5 may hide a transverse mode. A coherence computation for this microphone pair should help settle the question. In general, then the phase plots do not rule out the existence of important cabin modes in Aircraft C at low frequencies, but neither are any modes clearly identified for the engine speeds examined.
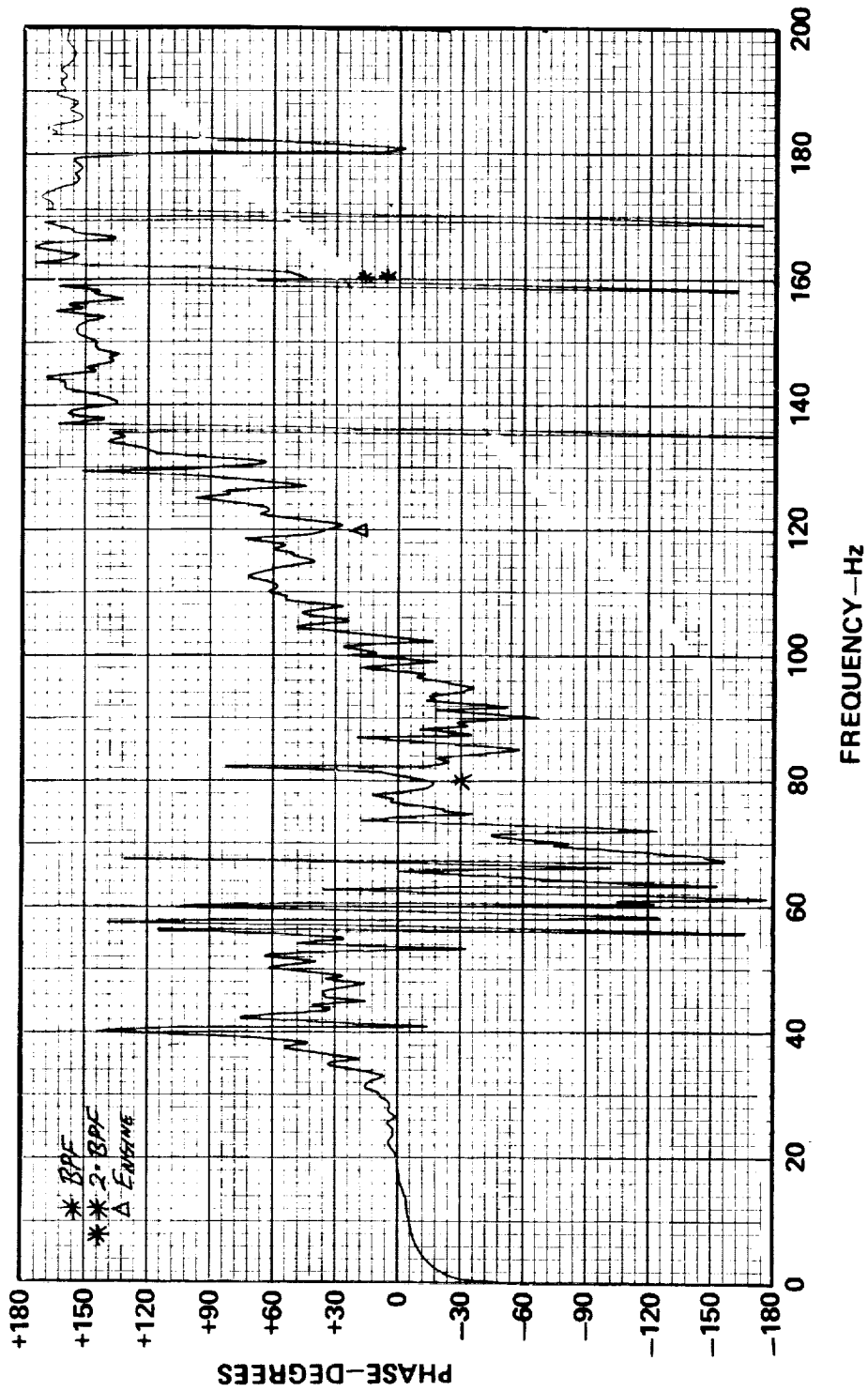
FIG. A.48. PHASE OF CROSS SPECTRUM BETWEEN MICROPHONES 2 and 1: AIRCRAFT C;
TWO-BLADED PROP; 2400 RPM
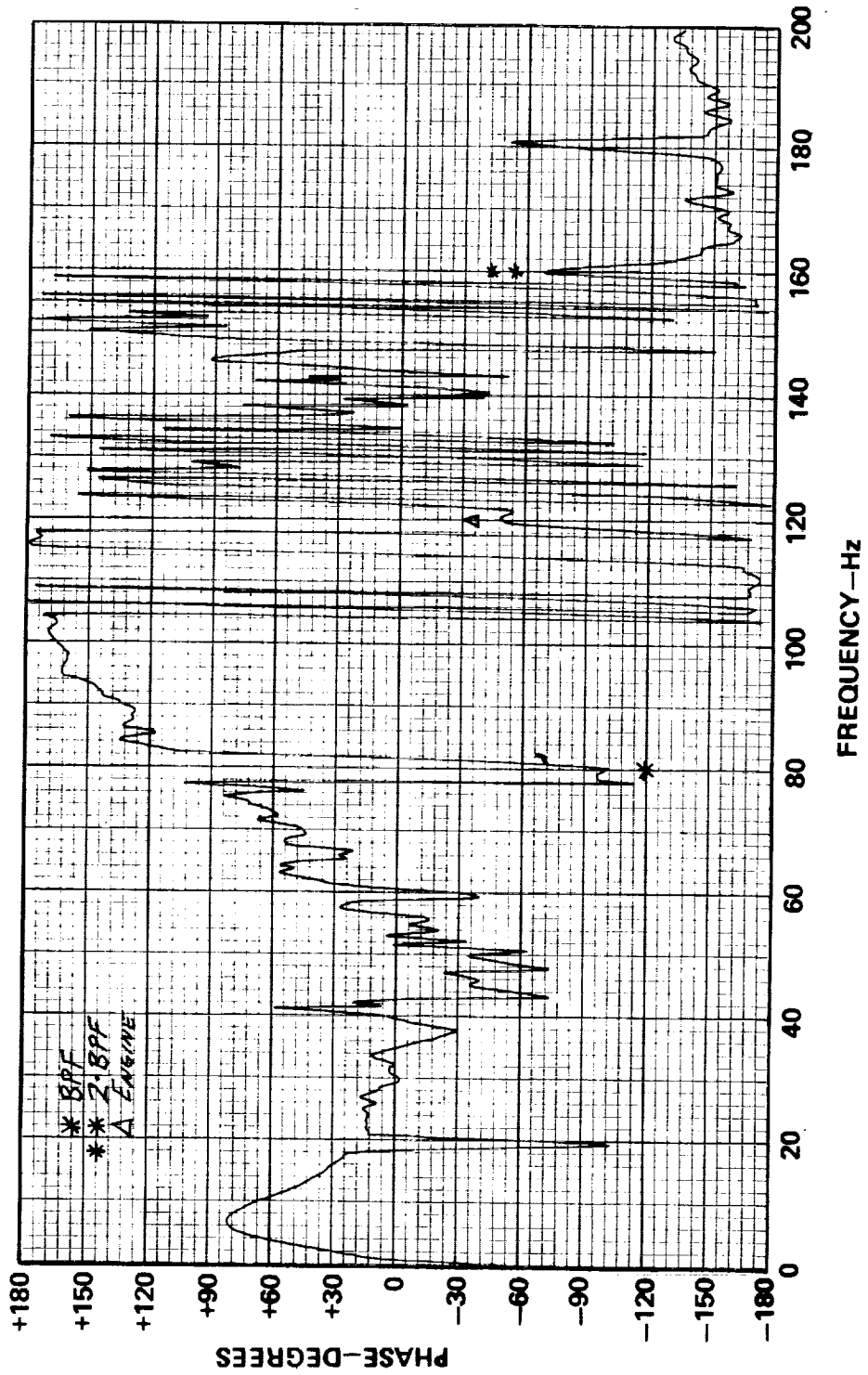
FIG. A.49. PHASE OF CROSS SEPCTRUM BETWEEN MICROPHONES 2 AND 3; AIRCRAFT C;
TWO-BLADED PROP; 2400 RPM

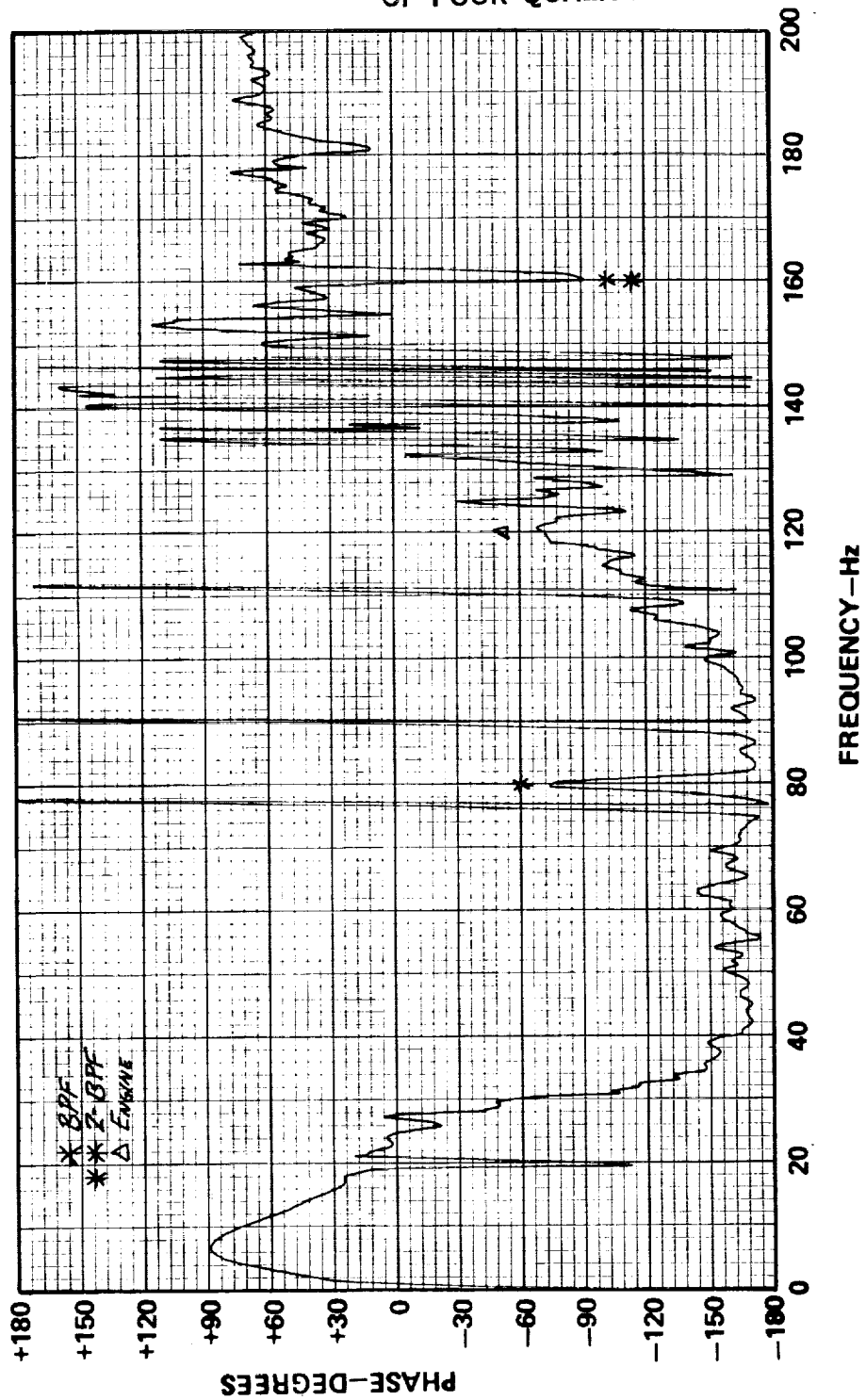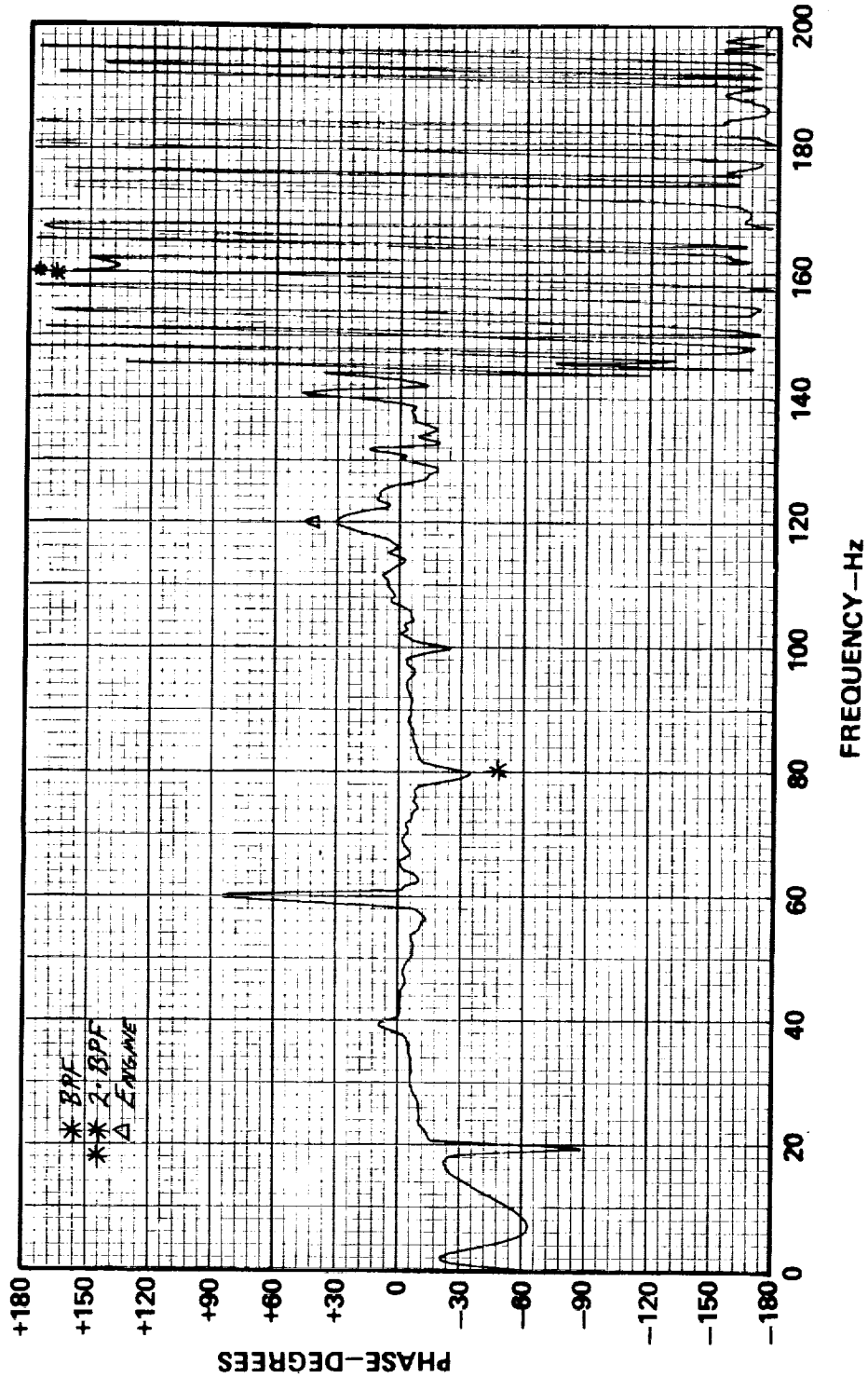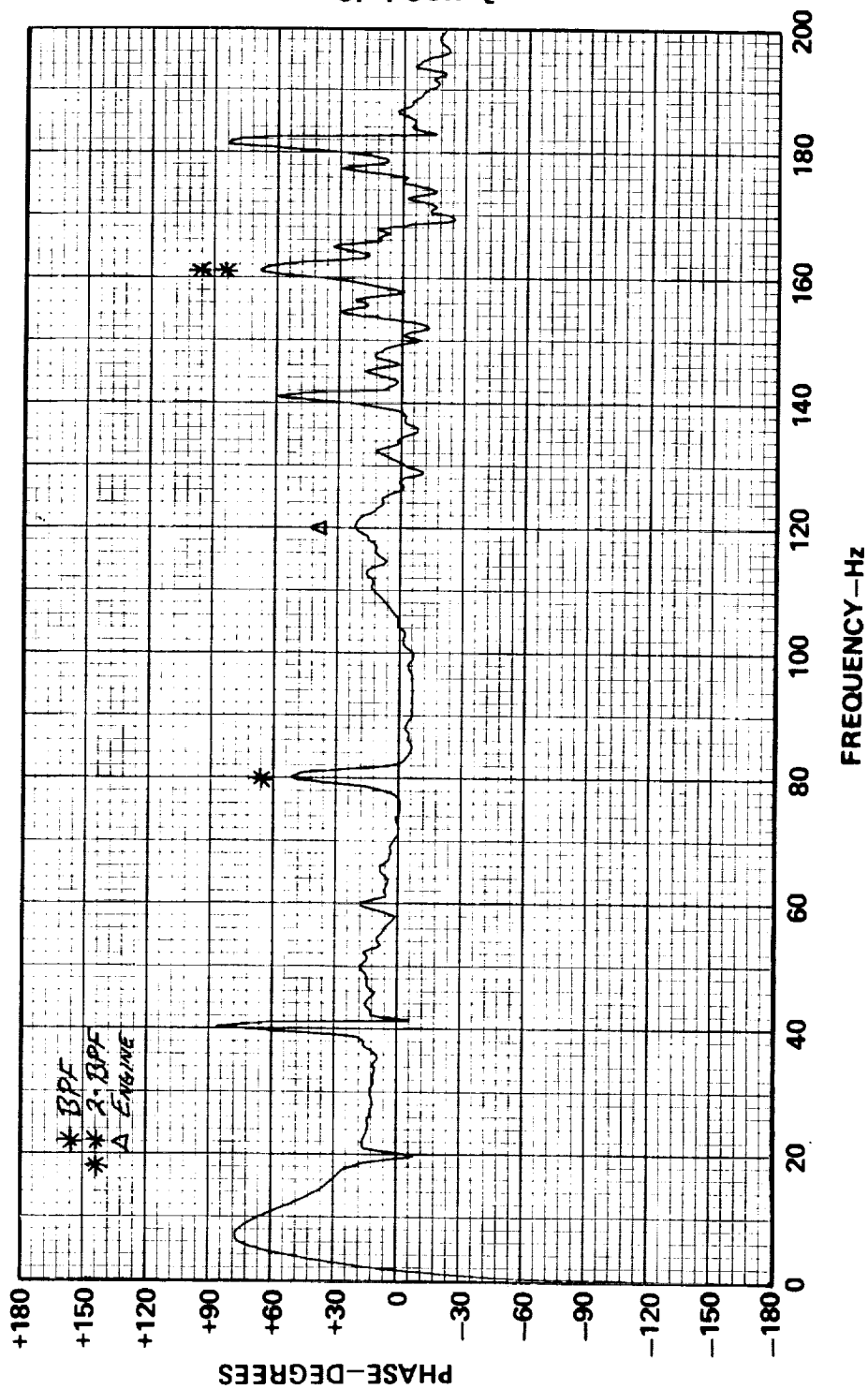FIG. A.50. PHASE OF CROSS SPECTRUM BETWEEN MICROPHONES 1 AND3; AIRCRAFT C;
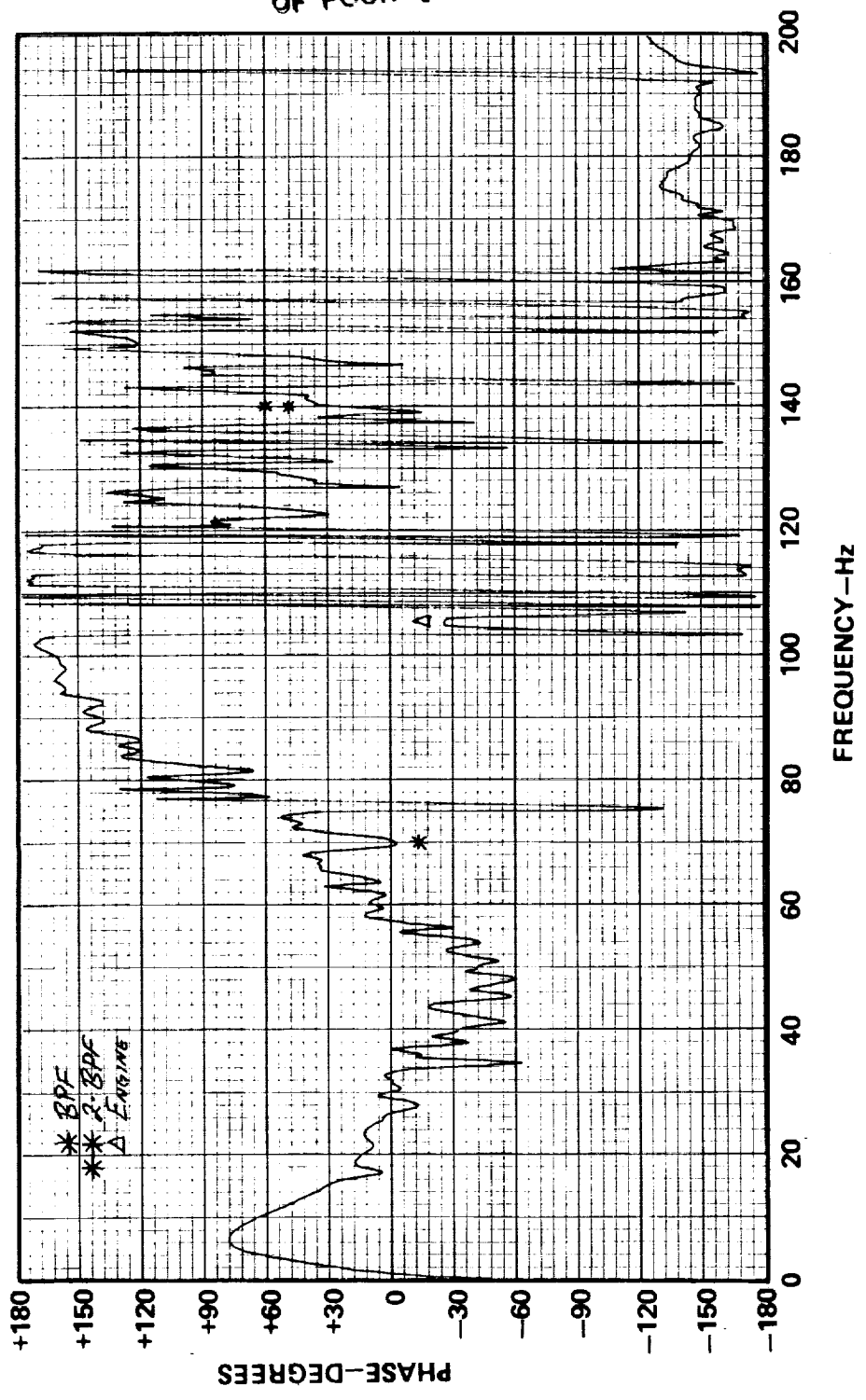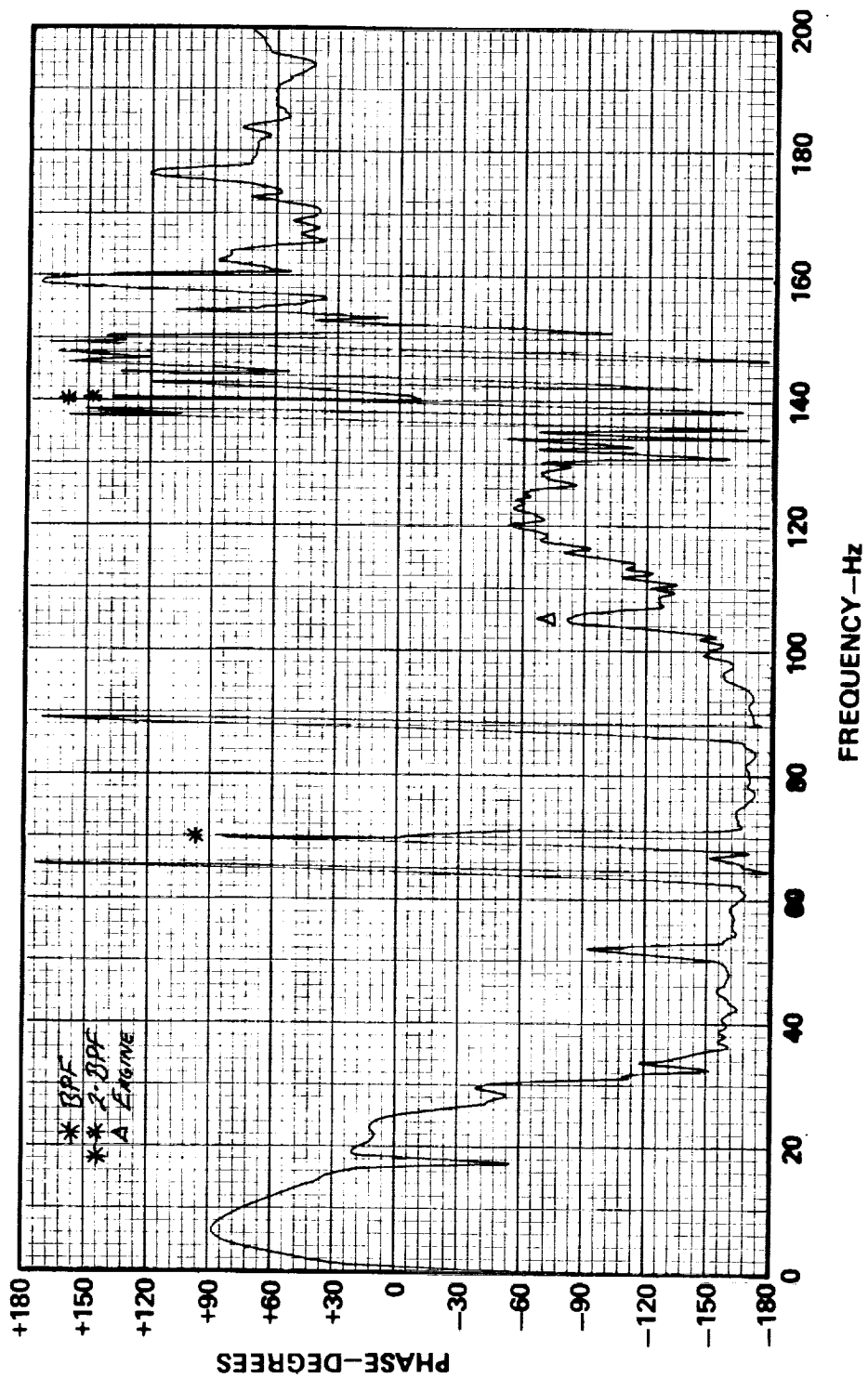TWO-BLADED PROP; 2400 RPM

FIG. A.51. PHASE OF CROSS SPECTRUM BETWEEN MICROPHONES 4 AND 5; AIRCRAFT C; TWO-BLADED PROP; 2400 RPM

FIG. A.52. PHASE OF CROSS SPECTRUM BETWEEN MICROPHONES 2 AND 6; AIRCRAFT C;
TWO-BLADED PROP; 2400 RPM
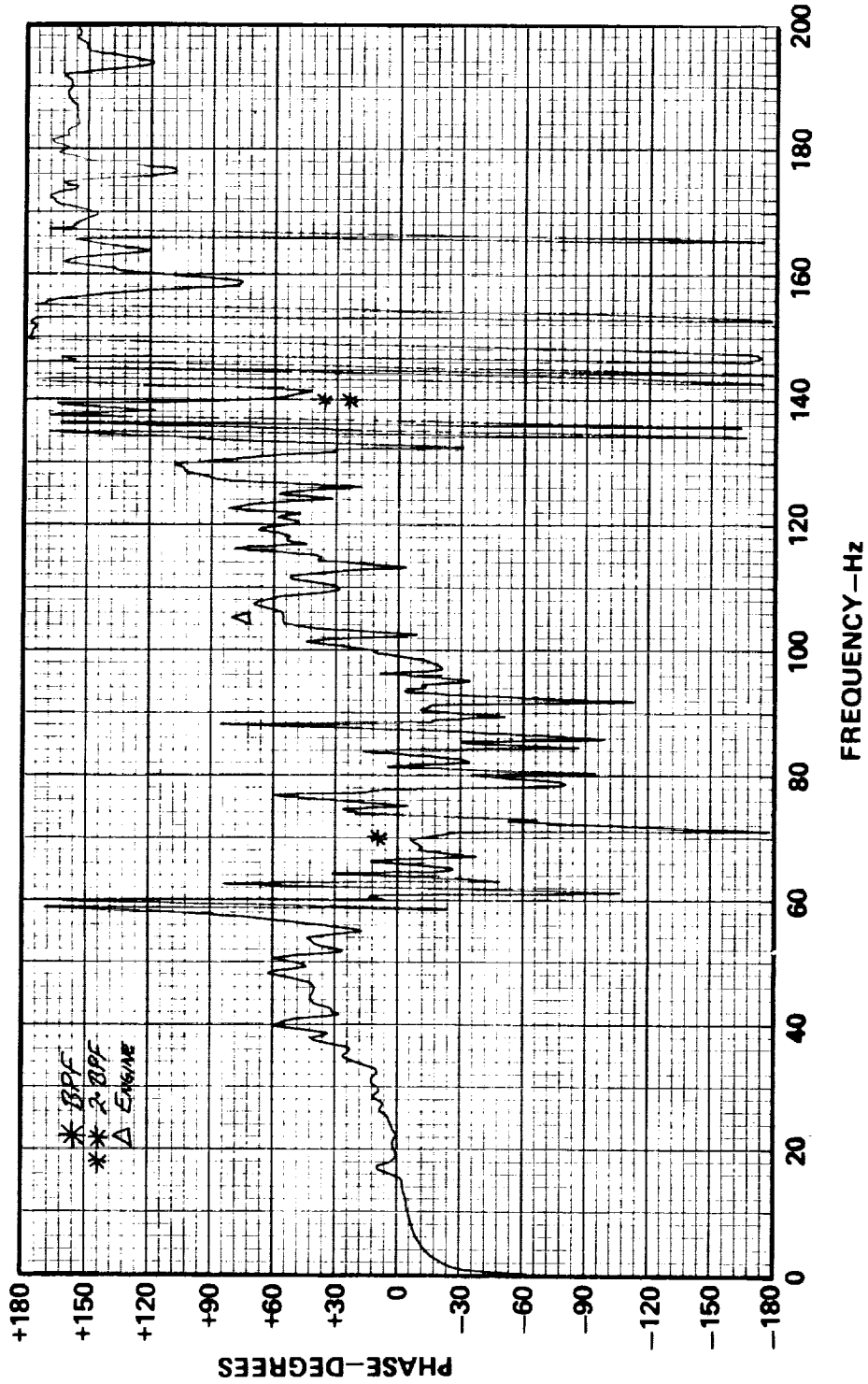
FIG. A.53.   PHASE OF CROSS SPECTRUM BETWEEN MICROPHONES 2 AND 1; AIRCRAFT C;
TWO-BLADED PROP; 2100 RPM

FIG. A.54. PHASE OF CROSS SPECTRUM BETWEEN MICROPHONES 2 AND 3: AIRCRAFT C; TWO-BLADED PROP; 2100 RPM

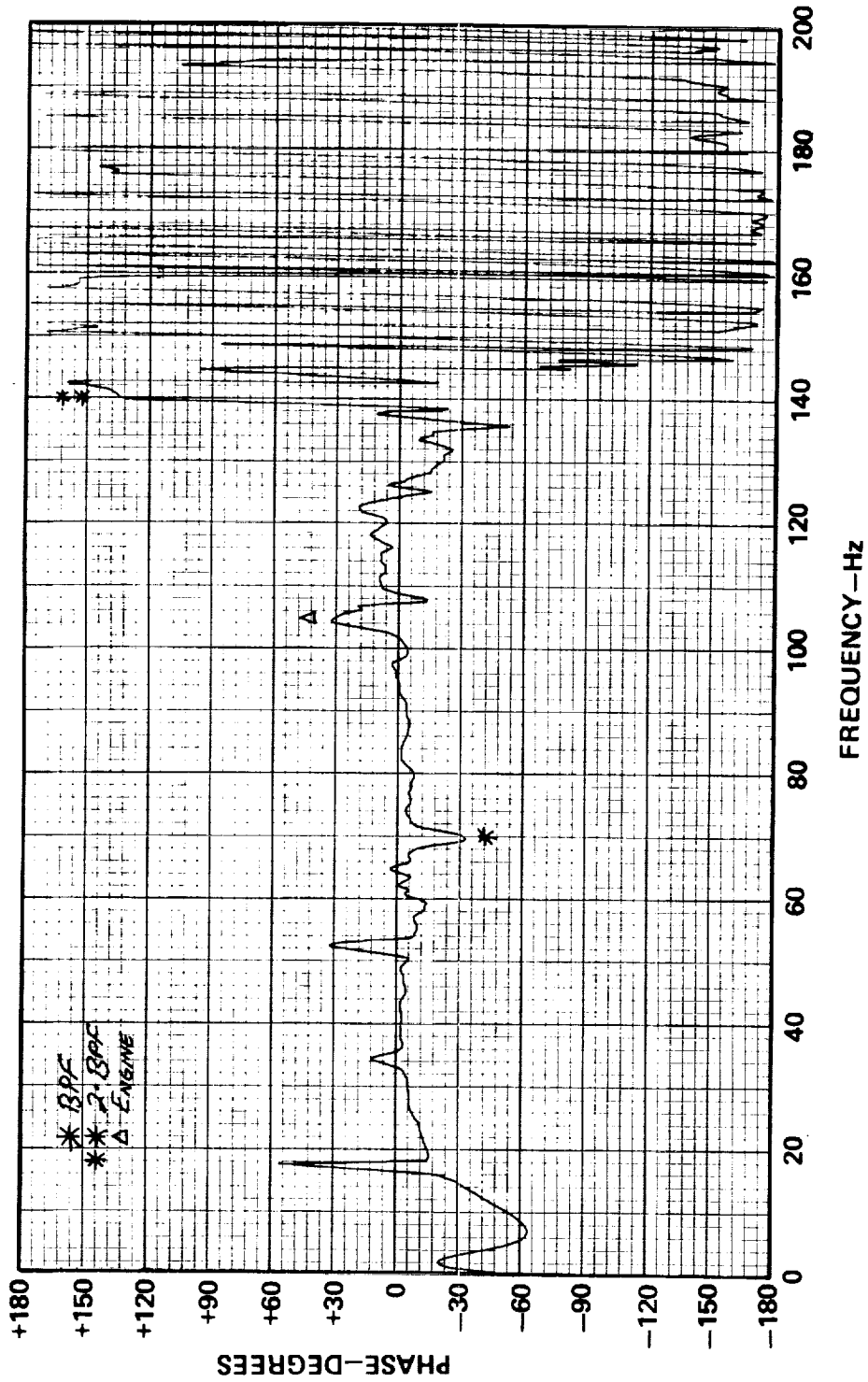FIG. A.55. PHASE OF CROSS SPECTRUM BETWEEN MICROPHONES 1 AND 3; AIRCRAFT C; TWO-BLADED PROP1 2100 RPM

FIG. A.56. PHASE OF CROSS SPECTRUM BETWEEN MICROPHONES 2 AND 3: AIRCRAFT C;
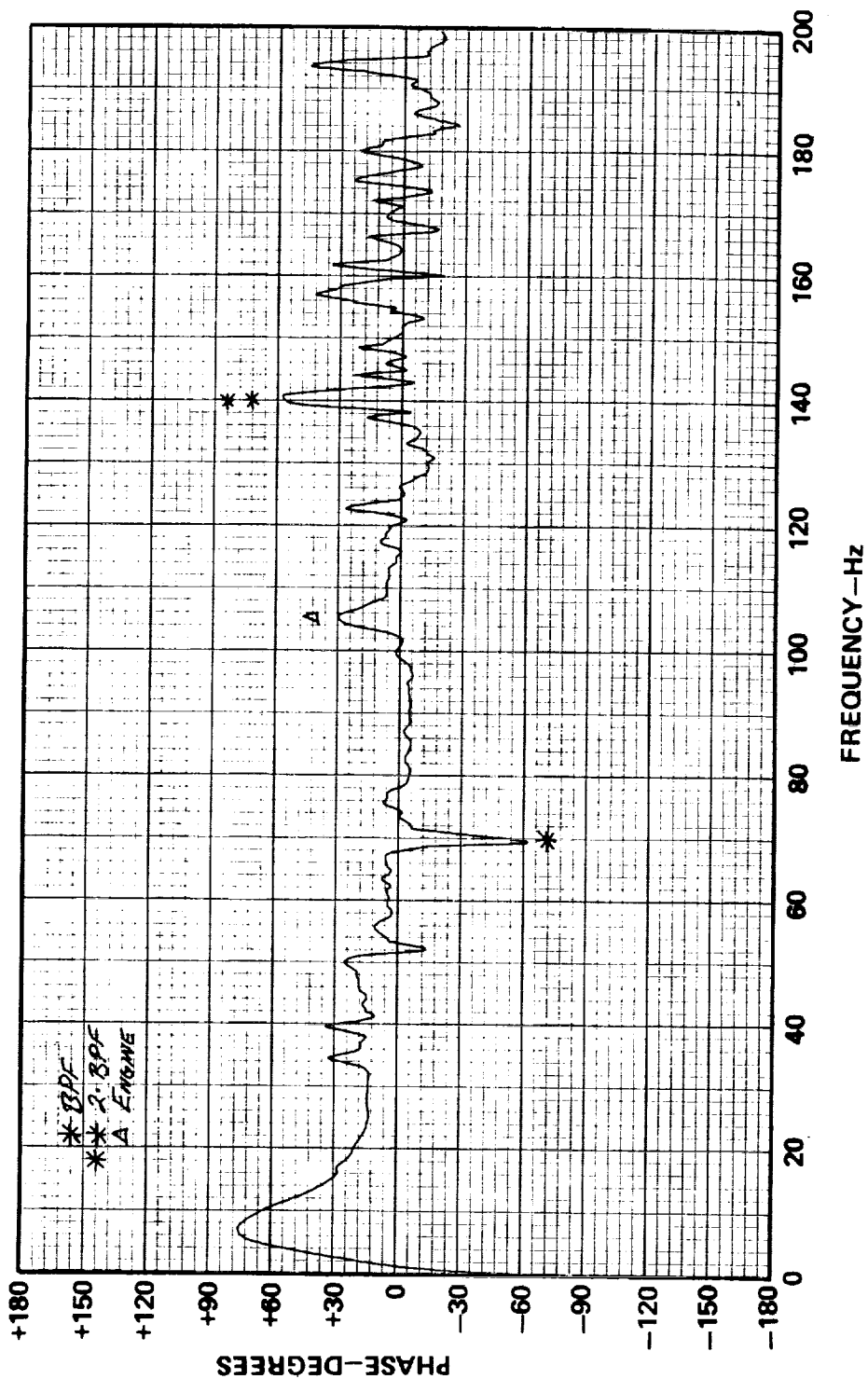TWO-BLADED PROP; 2100 RPM

FIG. A.57. PHASE OF CROSS SPECTRUM BETWEEN MICROPHONES 2 AND 6; AIRCRAFT C; TWO-BLADED PROP; 2100 RPM

The microphone array in Aircraft F is sketched in Figure A.58. The array is arranged to detect longitudinal modes only. A brief examination of Figures A.59 through A.69 will show that the sound at microphone 1 has very little to do with the sound at microphones 4 or 6. That is, sound appears to enter the stripped interior along its length. This condition is pointed out in Figure A.62 where the coherence between microphones 1 and 4 is plotted. The only frequencies of high coherence are at the engine rotation rate, blade harmonics, engine firing rate, and at 180 Hz. The tone at 180 Hz has not been identified. Traveling waves are evident in some plots, particularly in the frequency regime between 80 and 140 Hz. The first longitudinal mode in the cabin is expected to appear at about 45 Hz. Some activity is seen in Figures A.63 and A.68 between microphones 1 and 5, which should be on opposite sides of the node line. The difficulty of interpreting the phase information again suggests that more signal processing, specifically coherence calculations for all microphone pairs, will be needed to adequately address the matter of the importance of cabin modes.
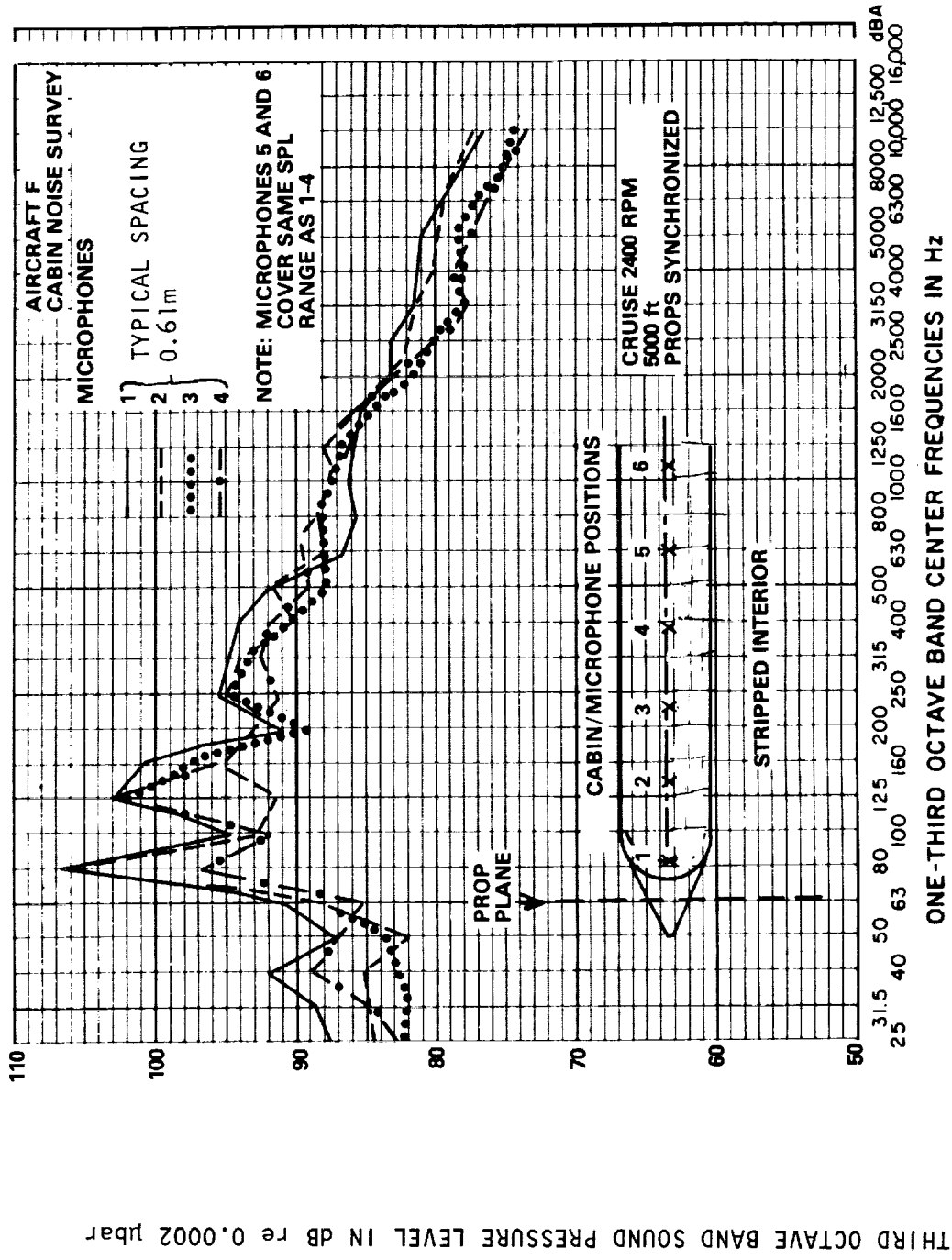
FIG. A.58. MICROPHONE ARRANGEMENT AND DISTRIBUTION OF LEVELS INSIDE TWIN WITH STRIPPED INTERIOR.
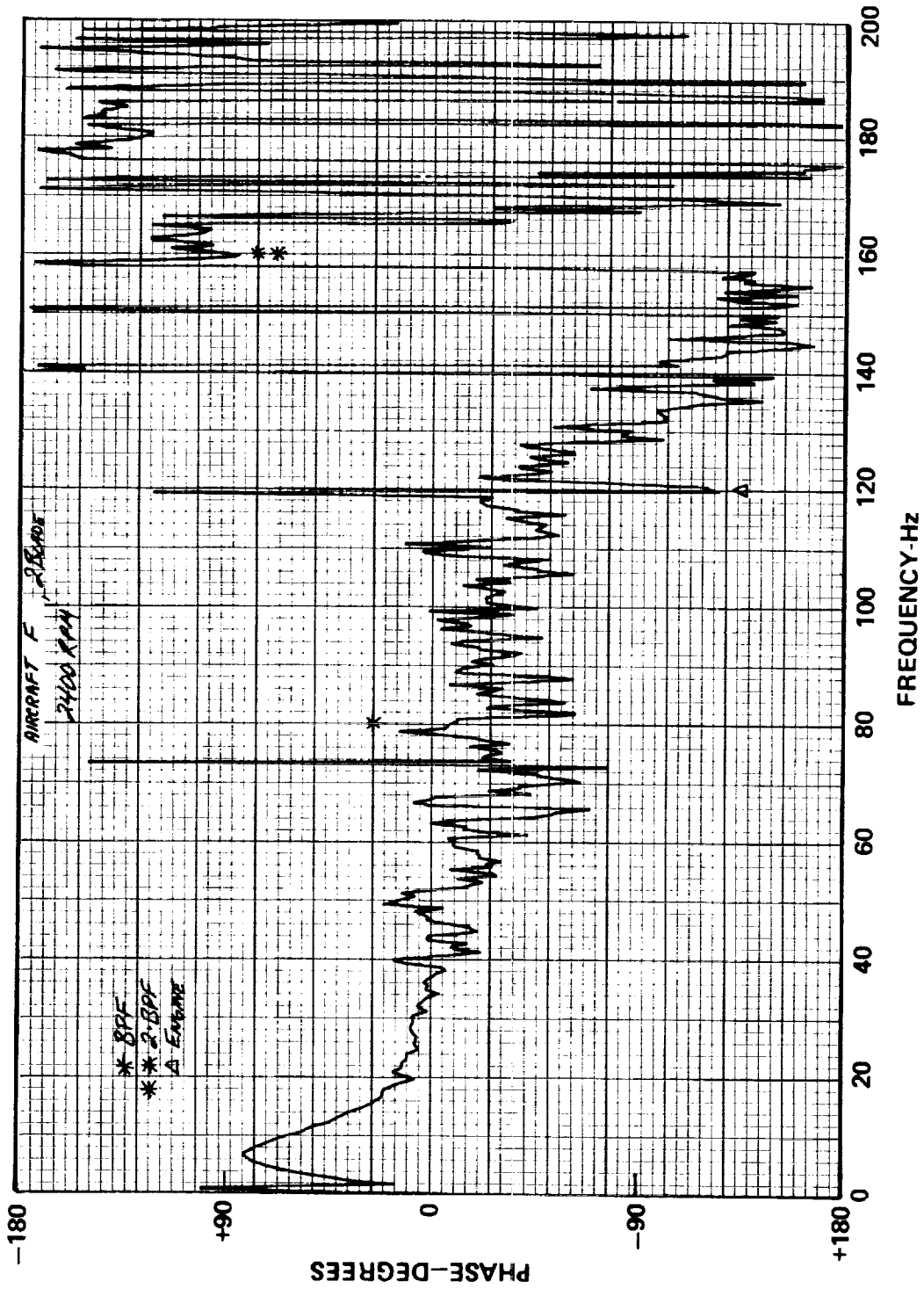
FIG. A.59.   PHASE OF CROSS SPECTRUM BETWEEN MICROPHONES 1 AND 2; AIRCRAFT F;
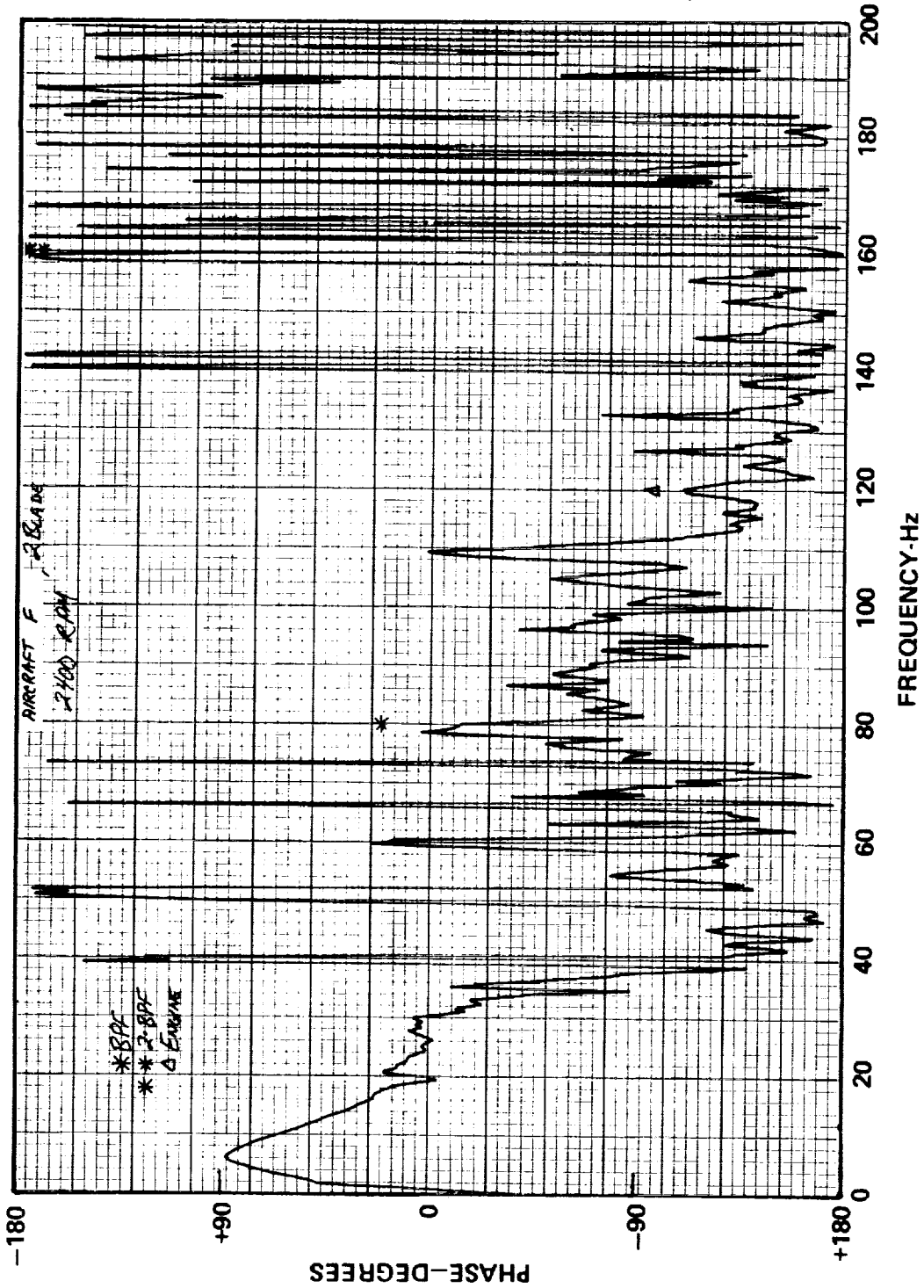TWO-BLADED PROPS; 2400 RPM

FIG. A.60.   PHASE OF CROSS SPECTRUM BETWEEN MICROPHONES 1 AND 3; AIRCRAFT F;
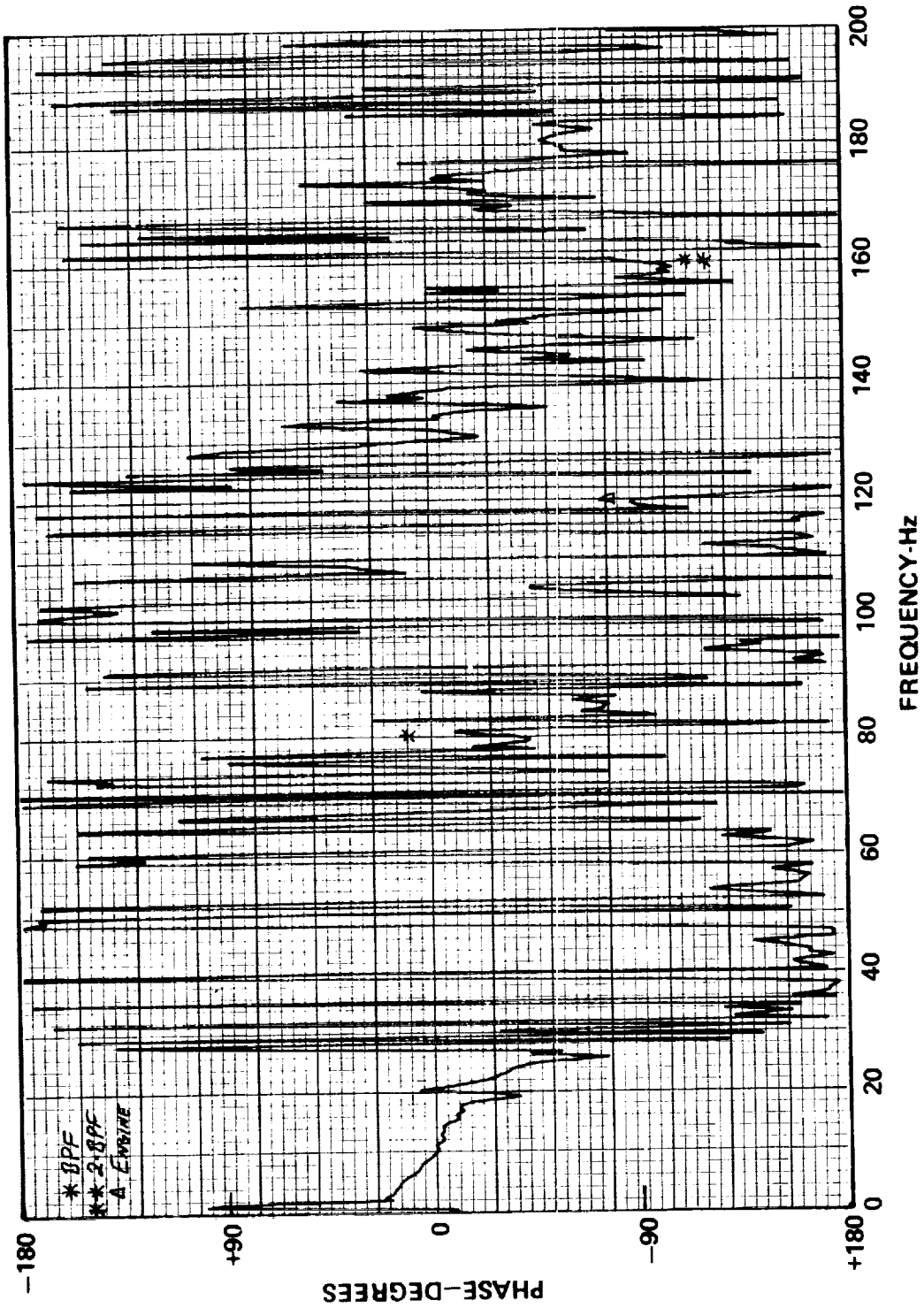TWO-BLADED PROPS; 2400 RPM

FREQUENCY-Hz

PHASE-DEGREES

* BPF
** 2 BPF
△ Engine

FIG. A.61.   PHASE OF CROSS SPECTRUM BETWEEN MICROPHONES 1 AND 4; AIRCRAFT F;
TWO-BLADED PROP - 2400 RPM

A-80
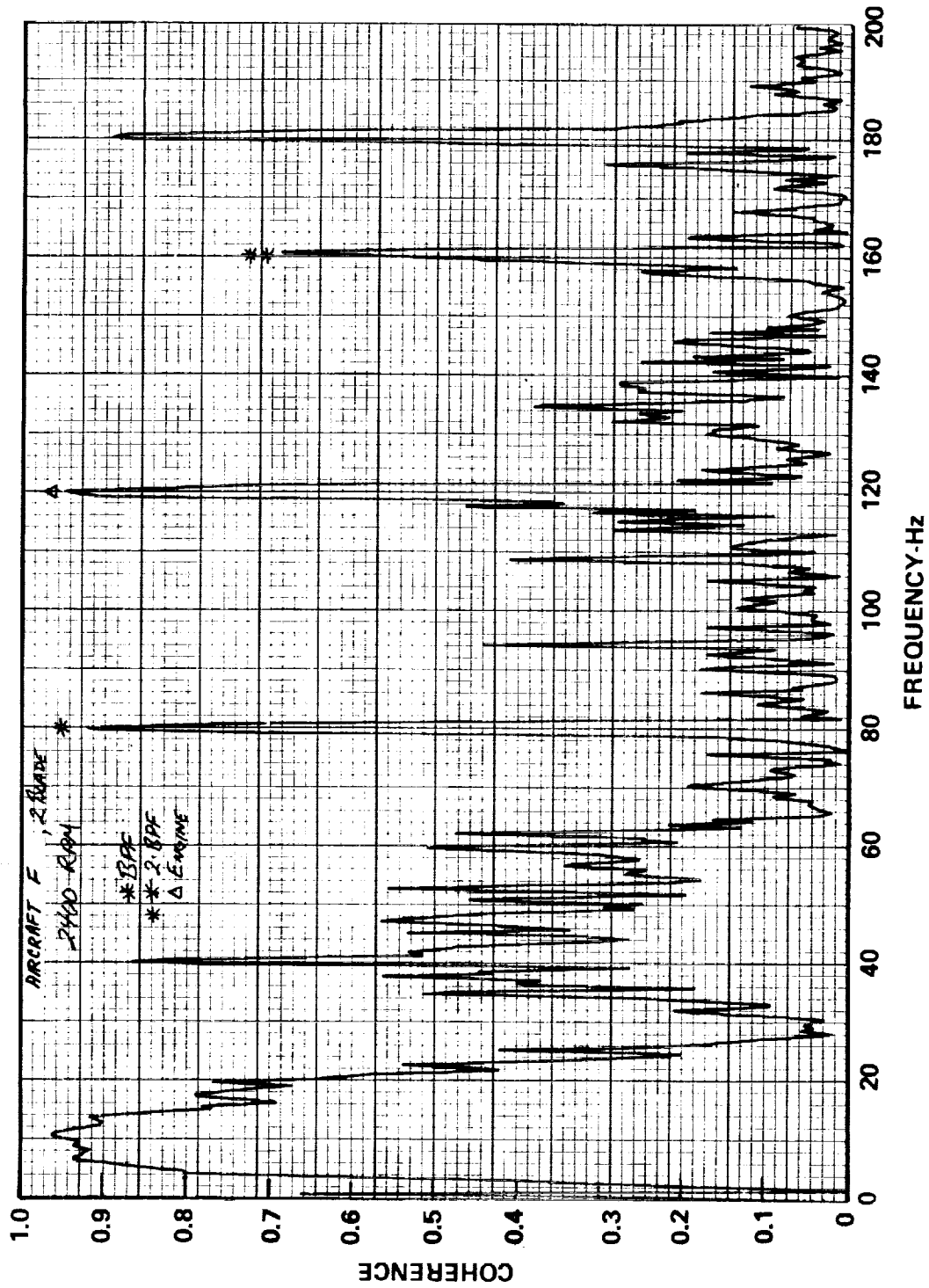
FIG. A.62. COHERENCE BETWEEN MICROPHONES 1 AND 4; AIRCRAFT F; TWO-BLADED PROPS; 2400 RPM; STRIPPED INTERIOR

A-81

FIG. A.63. PHASE OF CROSS SPECTRUM BETWEEN MICROPHONES 1 and 5: AIRCRAFT F; TWO-BLADED PROPS – 2400 RPM

FIG. A.64. PHASE OF CROSS SPECTRUM BETWEEN MICROPHONES 1 AND 6; AIRCRAFT F;
TWO-BLADED PROPS1 2400 RPM

A-83

FIG. A.65. PHASE OF CROSS SPECTRUM BETWEEN MICROPHONES 1 AND 2; AIRCRAFT F; TWO-BLADED PROPS; 2100 RPM

FIG. A.66. PHASE OF CROSS SPECTRUM BETWEEN MICROPHONES 1 AND 3: AIRCRAFT F;
TWO-BLADED PROPS; 2100 RPM

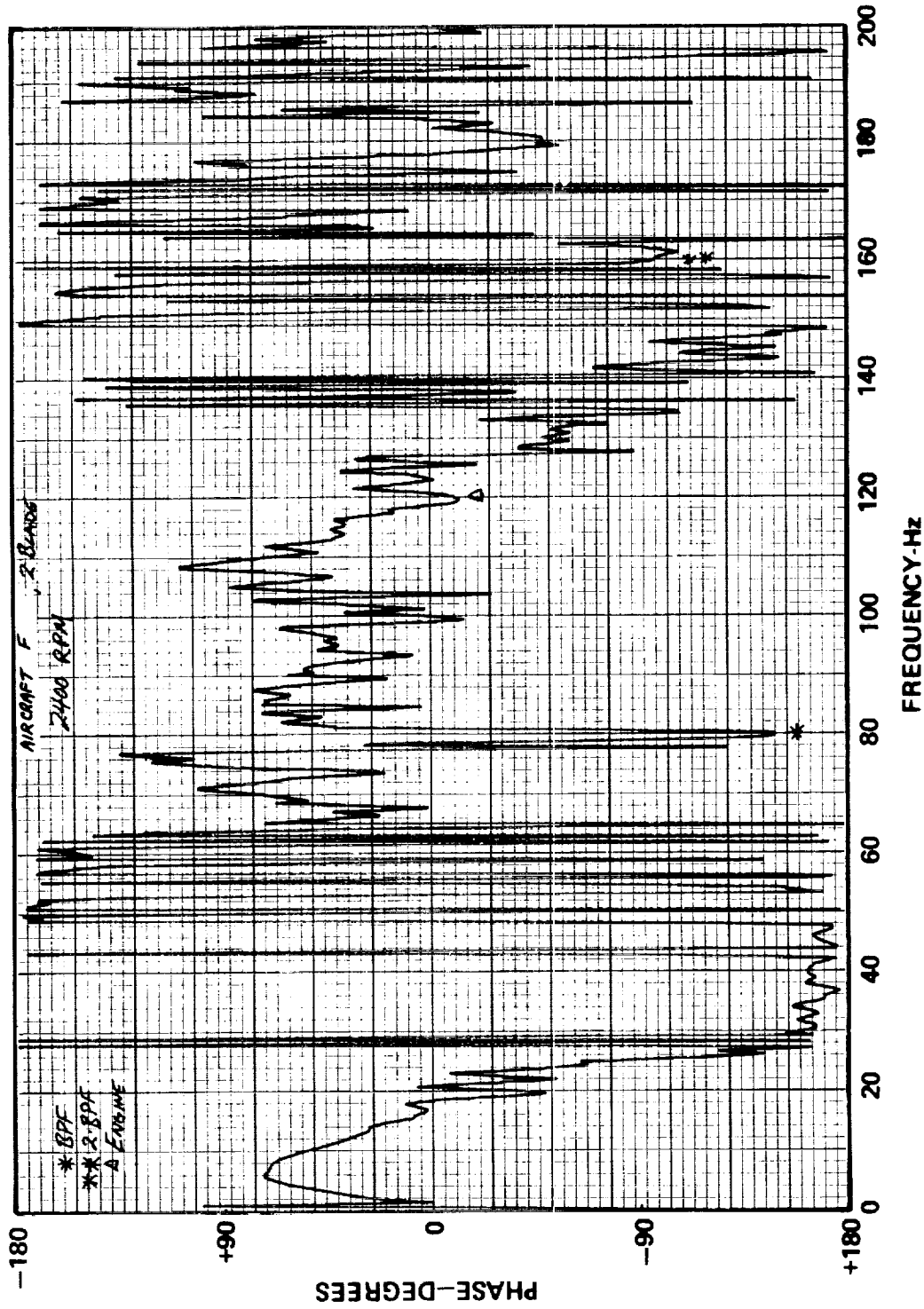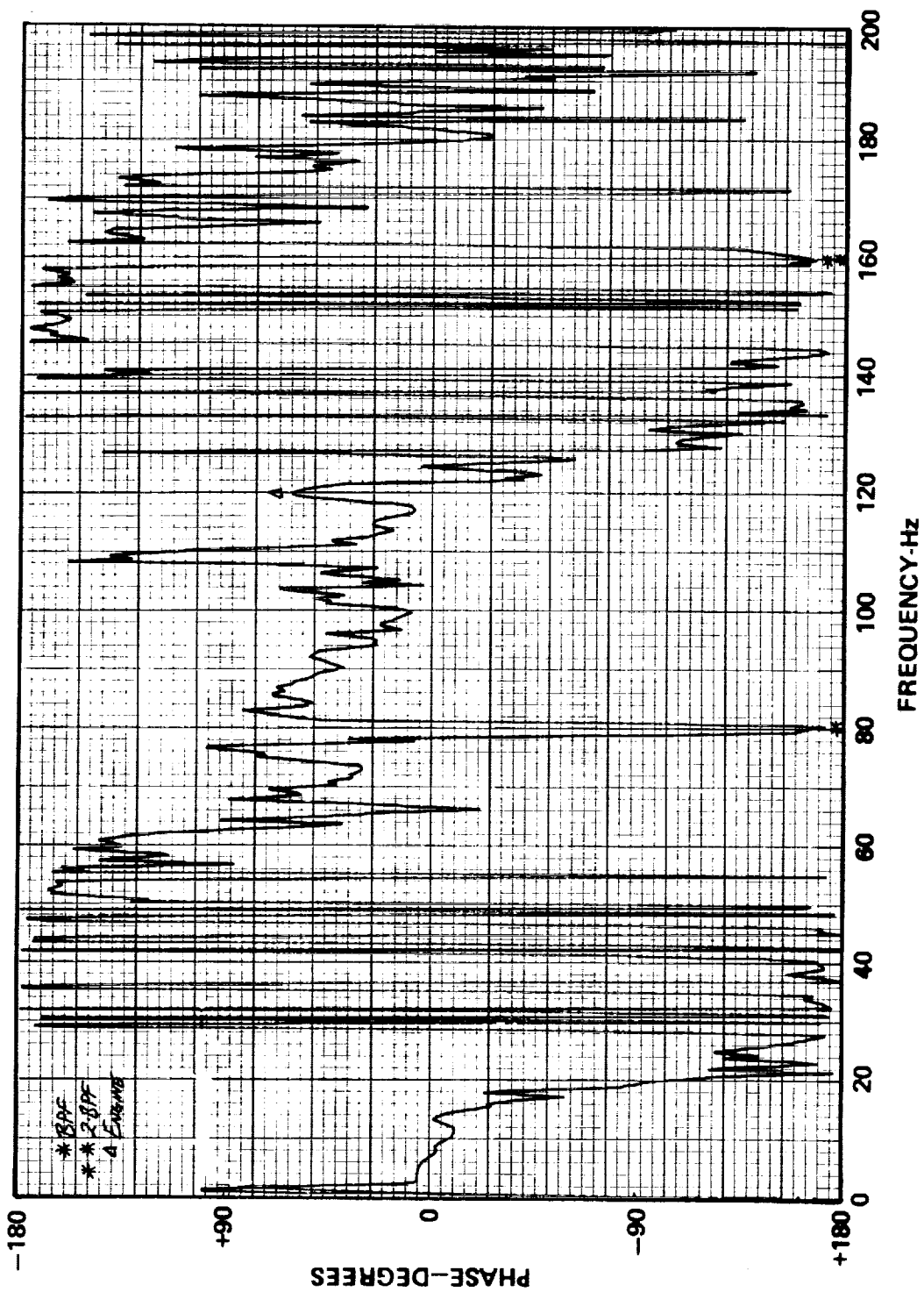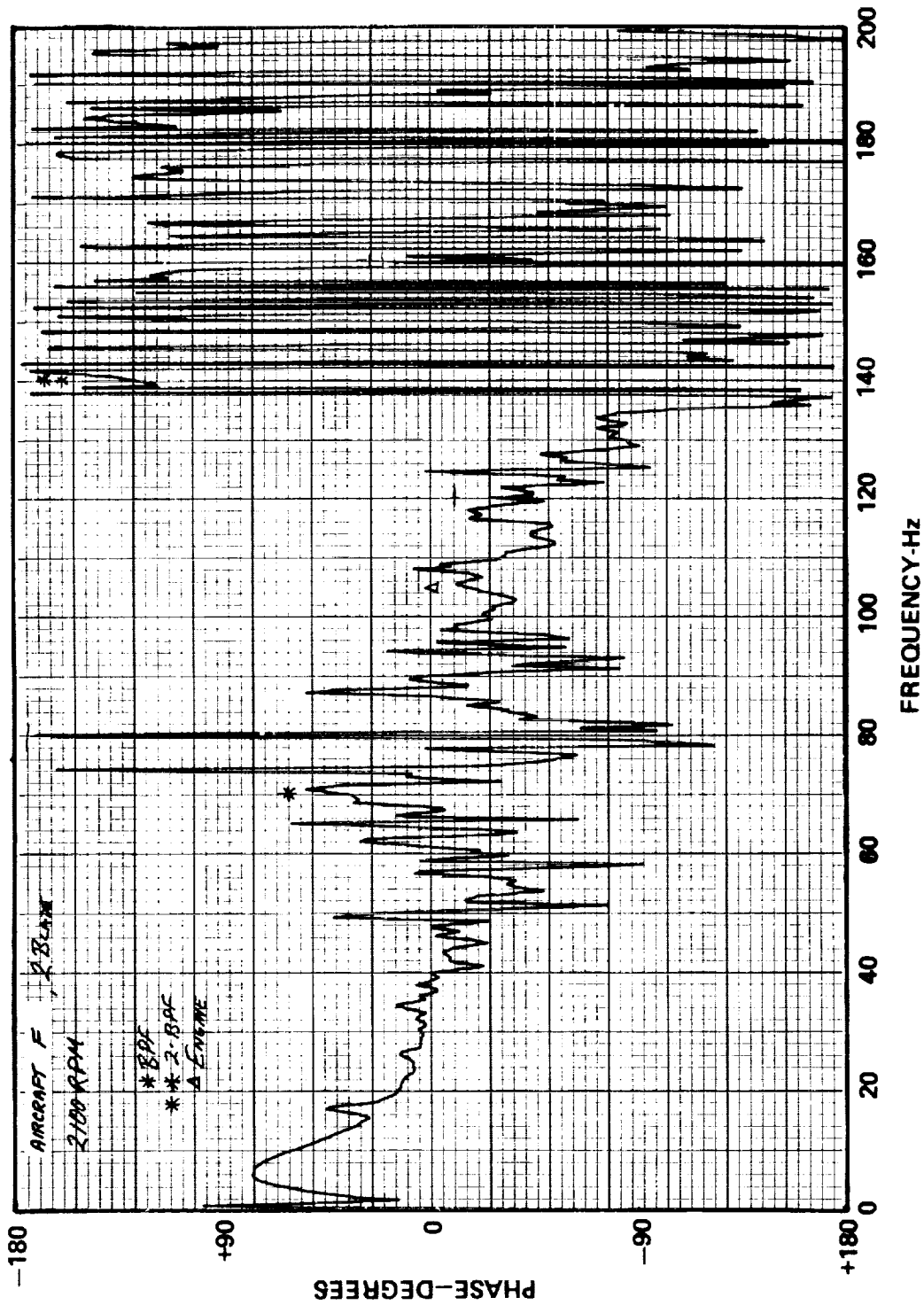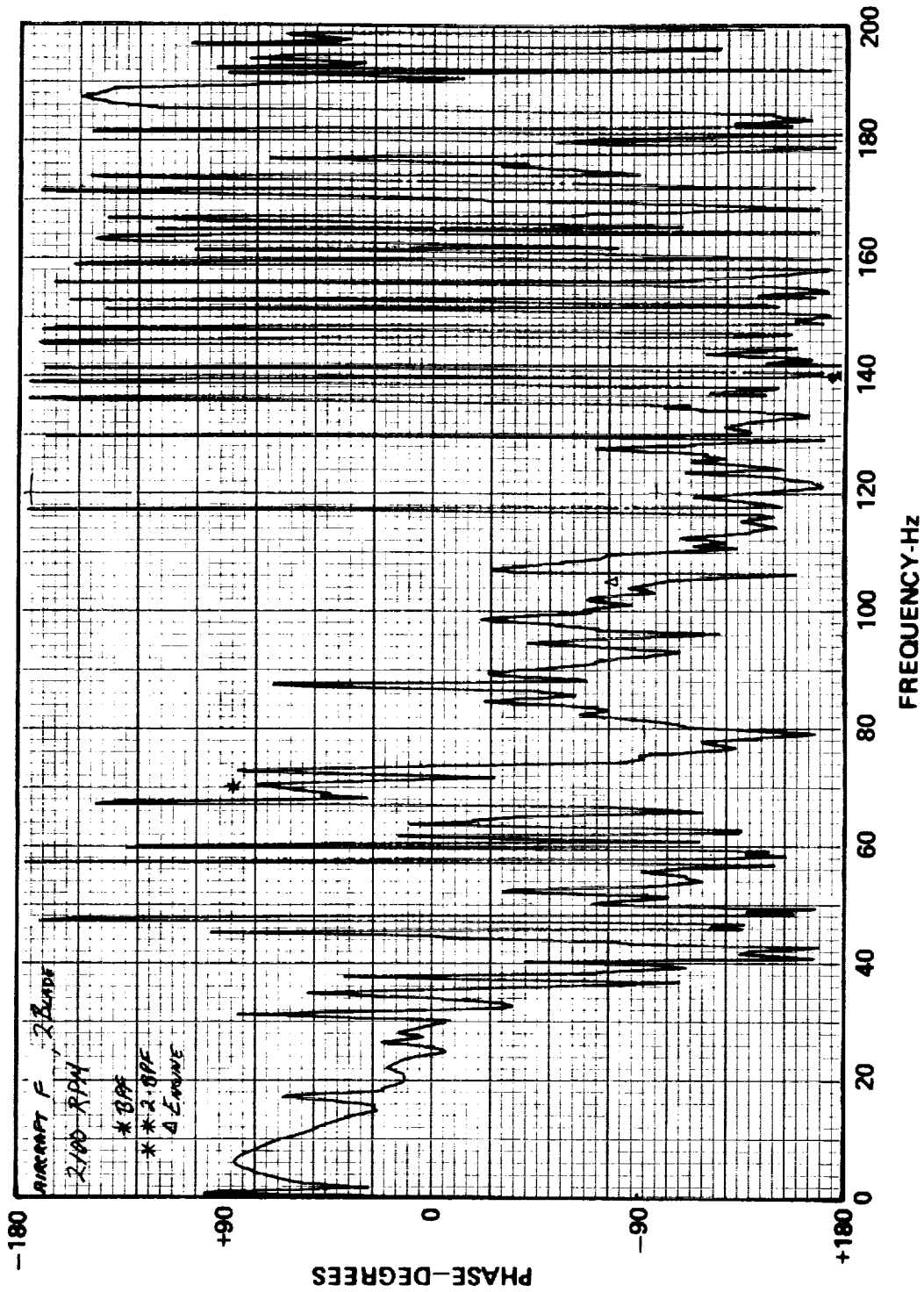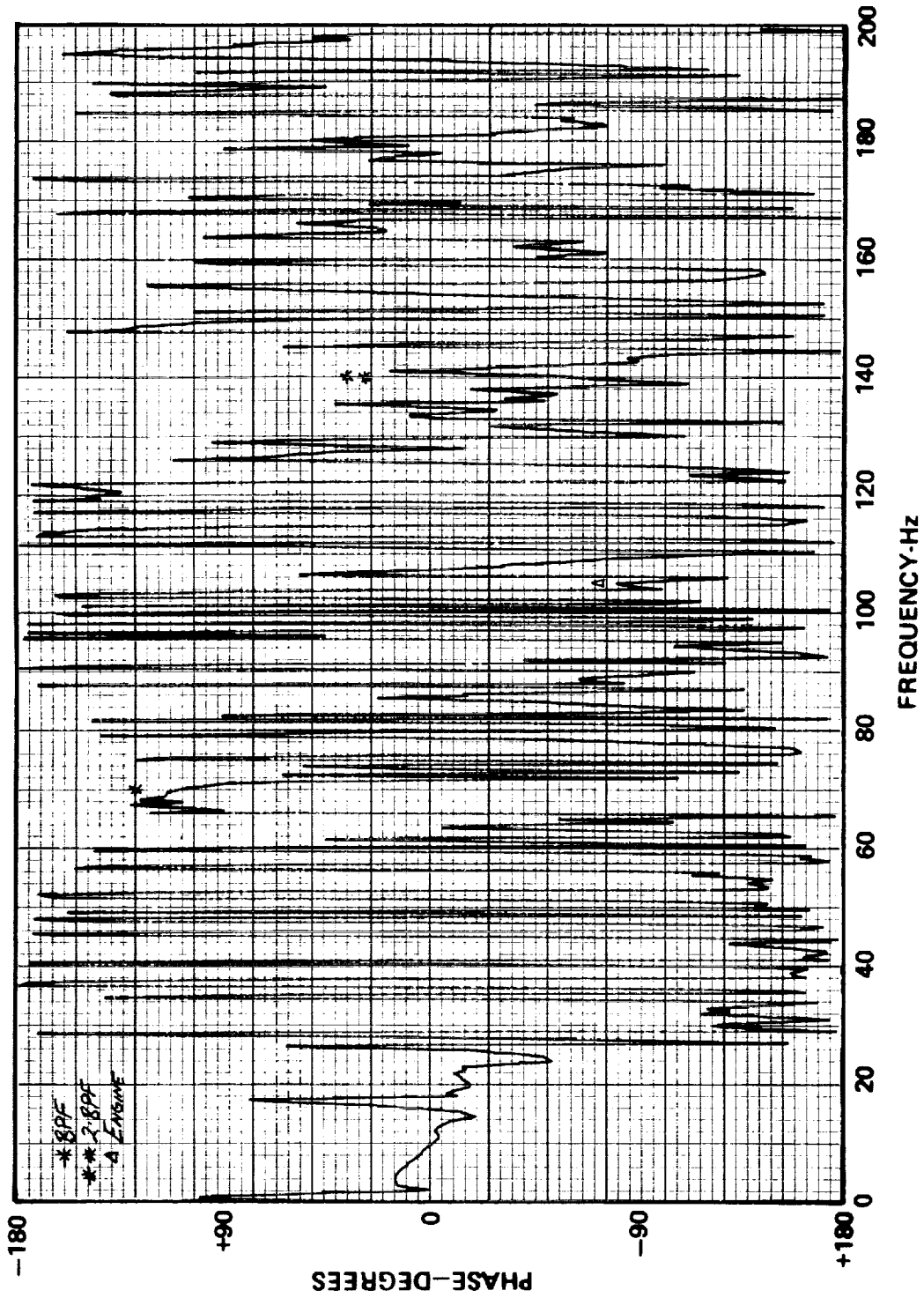FIG. A.67. PHASE OF CROSS SPECTRUM BETWEEN MICROPHONES 1 AND 4; AIRCRAFT F; TWO-BLADED PROPS; 2100 RPM

FIG. A.68. PHASE OF CROSS SPECTRUM BETWEEN MICROPHONES 1 AND 5; AIRCRAFT F; TWO-BLADED PROPS: 2100 RPM
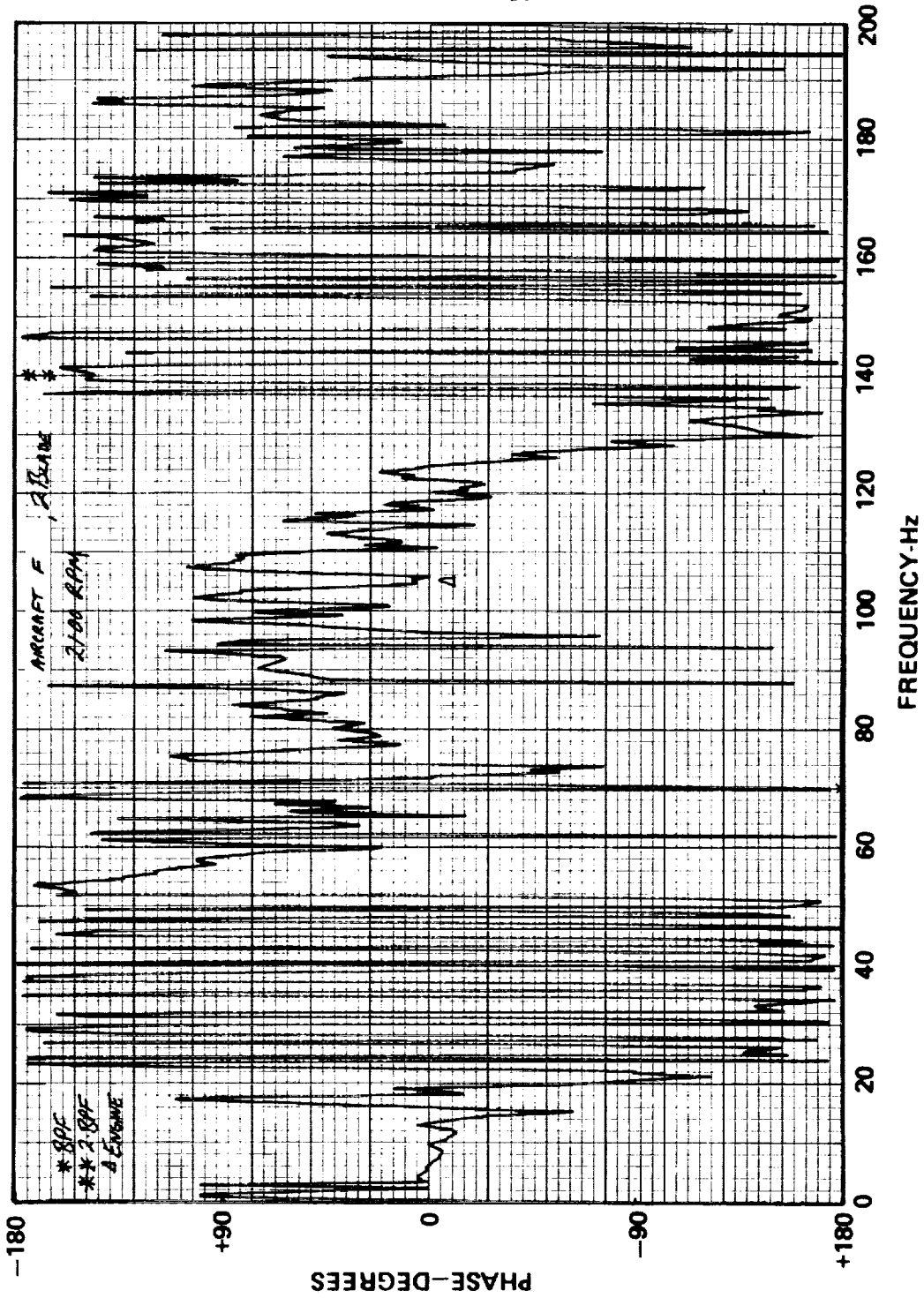
FIG. A.69. PHASE OF CROSS SPECTRUM BETWEEN MICROPHONES 1 AND 6; AIRCRAFT F; TWO-BLADED PROPS; 2100 RPM
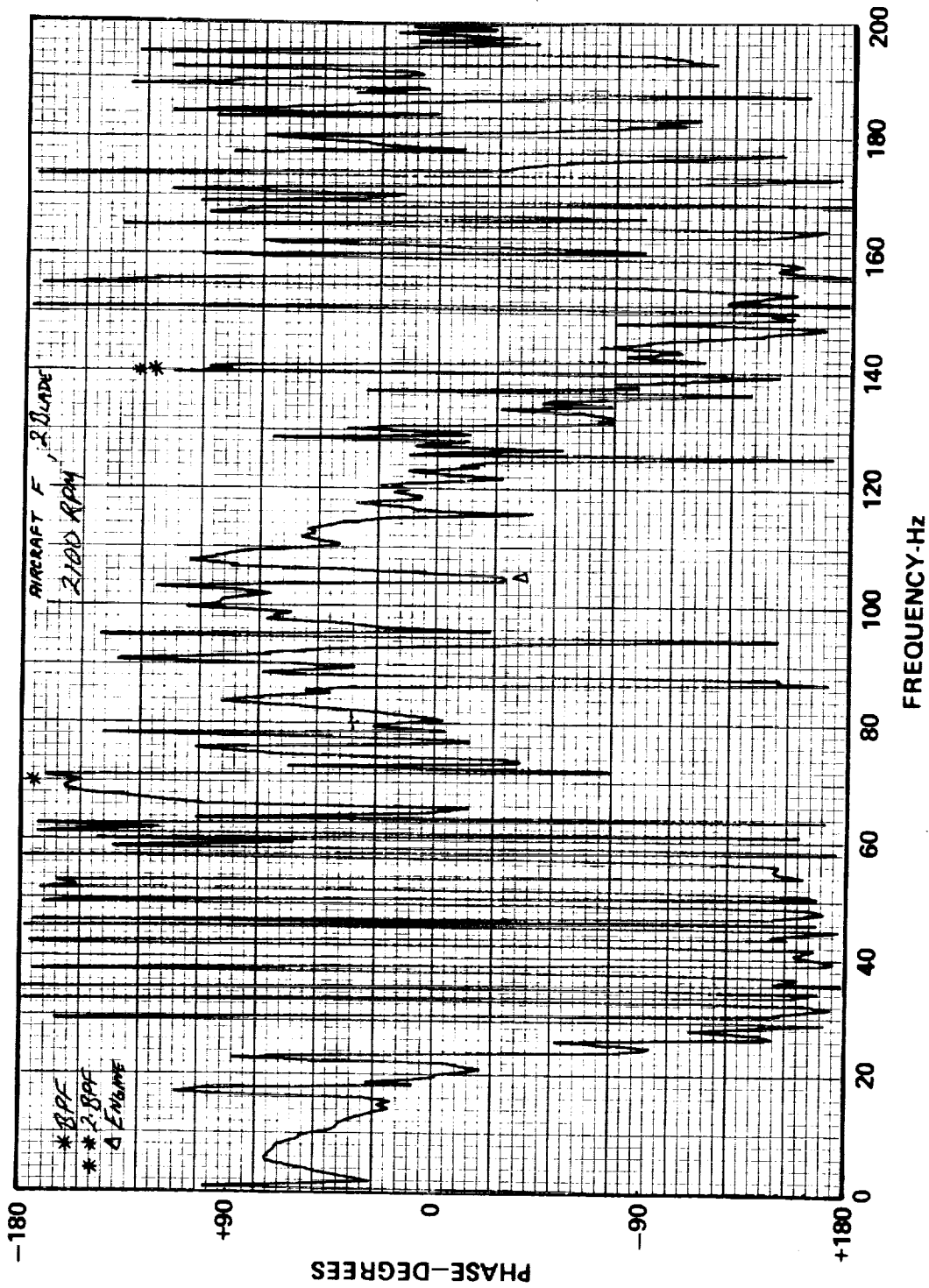
c. Noise Reduction of Cabin Walls

The measured noise reduction for Aircraft C and D (same airframe except for turbocharging) is shown in Figure A.70 for two levels of interior treatments. Also given in the figure are data for another single engine aircraft published by Jha and Catherines (Ref. 14). Inasmuch as this test is central to the preliminary diagnosis developed in Sec. 3.6 (Figs. 31 and 32), details are presented there.

d) Structural Vibration Transfer Functions

The results of measuring the cabin noise in Aircraft C and D while shaking an engine mount are shown in Figure A.71. One-third octave spectra were measured at both the engine mounts and in the cabin center. The acceleration used in the calculation is the energy average of 3 axes on a particular mount. This test was not repeated for all mounts, so there may be some differences among mounts. There is little difference between the transfer functions for stripped and treated interiors. A complete discussion of these tests and implications for interior noise control is presented in Secs. 3.6 and 3.7 of the main body of the text.

FIG. A.70. NOISE REDUCTION OF CABIN WALL (AIRCRAFT C AND D) DERIVED FROM STATIC TEST IN HANGAR.

FIG. A.71.   MEASURED TRANSFER FUNCTION: ENGINE MOUNT STRUT VIBRATION TO
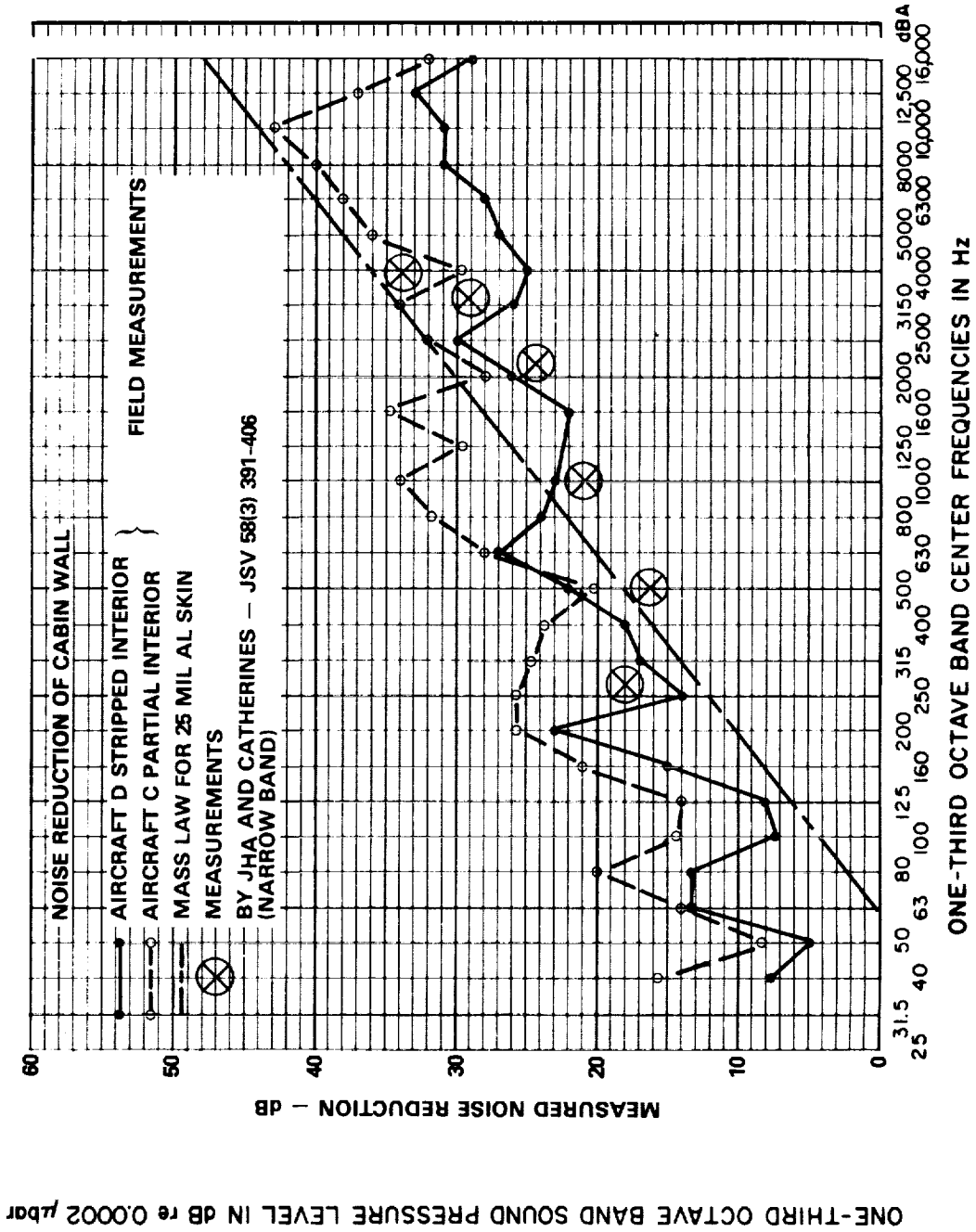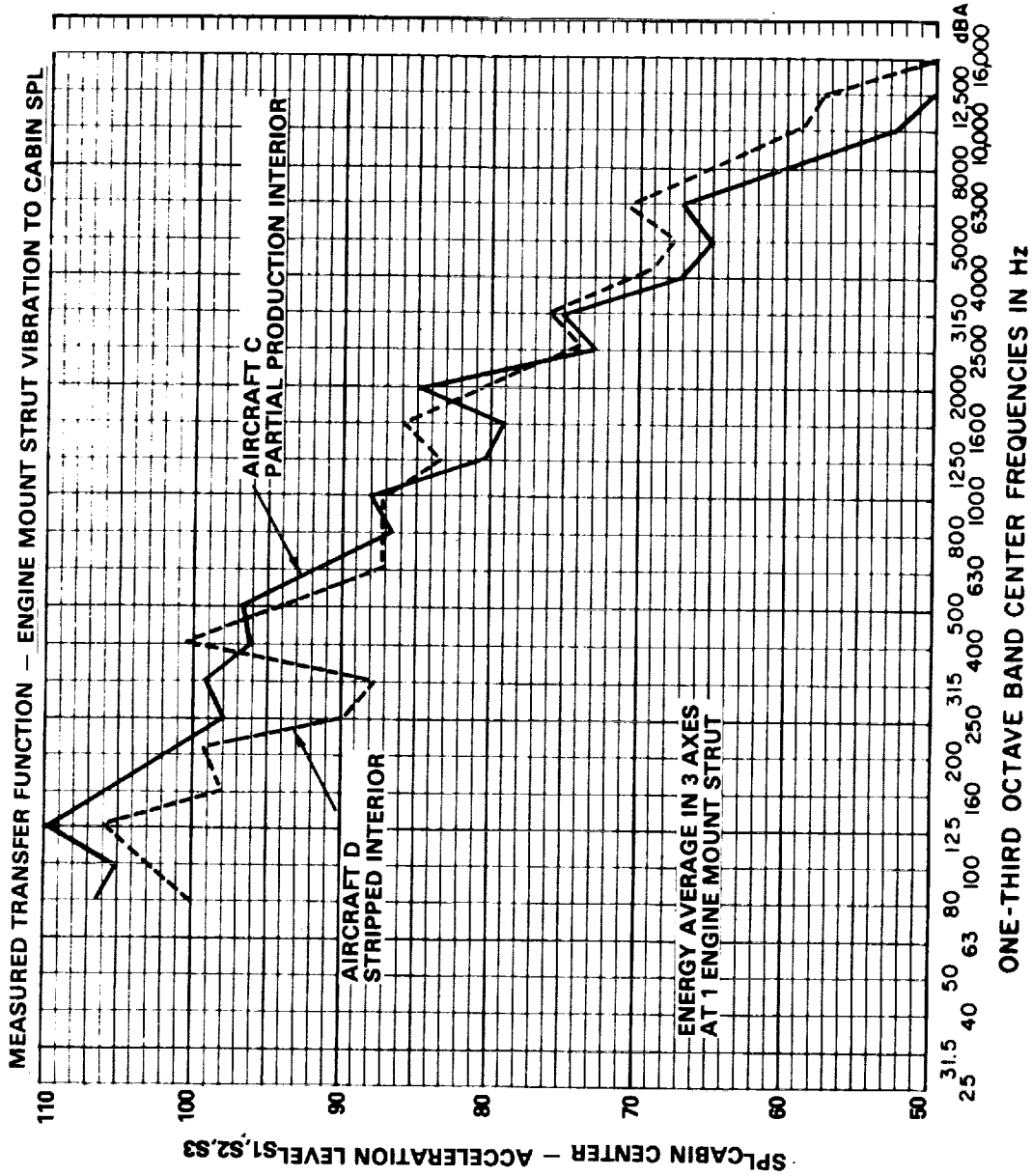CABIN SOUND PRESSURE LEVEL.   (GROUND TEST)

REFERENCES

1. Barton, C.K., "Structural Stiffening as an Interior Noise Control Technique for Light Twin-Engine Aircraft," Ph.D. Thesis, North Carolina State University (1979).

2. Barton, C.K., Mixson, J.S., "Characteristics of Propeller Noise on an Aircraft Fuselage," Journal of Aircraft, 18, 3, 200-205 (1981).

3. Barton, C.K., Mixson, J.S., "Noise Transmission and Control for a Light, Twin-Engine Aircraft," Journal of Aircraft, 18, 7, 570-575 (1981).

4. Bray, D.E., "Noise Environments in Public Transportation," Sound and Vibration, 8, 4, 16-20 (1974).

5. Catherines, J.J., Mayes, W.H., "Interior Noise Levels of Two Propeller-Driven Light Aircraft," NASA TMX-72716 (1975).

6. Catherines, J.J., Jha, S.K., "Sources and Characteristics of Interior Noise in General Aviation Aircraft," NASA TM-X72839, April 1976.

7. Galleithner, H., "Schallpegelmessungen in Cockpit and Kabine von Flugzeugen der DFVLR-Flugbereitschaft Oberpfaffenhofen (Ergebnisse einer ersten Messreihe) DFVLR Report IB555-74/11, December 1974.

8. Gasaway, D.C., "A-Weighted Sound Levels in Cockpits of Fixed- and Rotary-Wing Aircraft," USAF School of Aerospace Medicine, Brooks AFB, TX, Report SAM-TR-75-22 (1974).

9. Gasaway, D.C., "Noise Levels Measured within Aircraft During Takeoff, Climb, and Cruise (Low, Normal, and High)," USAF School of Aerospace Medicine, Brooks AFB, TX, Report SAM-TR-76-9 (October 1975).

10. Geisler, D.L., "Experimental Modal Analysis of an Aero Commander Aircraft," NASA CR-165750 (1981).

11. Howlett, J.T., Williams, L.H., Catherines, J.J., Jha, S.K., "Measurement, Analysis and Prediction of Aircraft Interior Noise," AIAA Paper 76-551 (1976).

12. Howlett, J.T., Schoenster, J.A., "An Experimental Study of Propeller-Induced Structural Vibration and Interior Noise," SAE Paper 790625 (1979).

13. Jha, S.K., Catherines, J.J., "Interior Noise Studies for General Aviation Types of Aircraft, Part I: Field Studies," Journal of Sound and Vibration, 58, 3, 375-390 (1978).

14. Jha, S.K., Catherines, J.J., "Interior Noise Studies for General Aviation Types of Aircraft, Part II: Laboratory Studies," Journal of Sound and Vibration, 58, 3, 391-406 (1978).

15. McGary, M.C., "Interior Noise Source/Path Identification on Propeller-Driven Aircraft Using Acoustic Intensity Methods," Proceedings of Noise-Con 81, 261-264 (1981).

16. Miller, L.N., "Noise Evaluation and Control Recommendations for Cessna Model 310 Aircraft," BBN Report 445 (January 1957).

17. Mixson, J.S., Barton, C.K., Vaicaitis, R., "Investigation of Interior Noise in a Twin-Engine Light Aircraft," Journal of Aircraft, 15, 4, 227-233 (1978).

18. Mixson, J.S., Barton, C.K., Piersol, A.G., Wilby, J.F., "Characteristics of Propeller Noise on an Aircraft Fuselage Related to Interior Noise Transmission, "AIAA Paper 79-0646 (1979).

19. Mixson, J.S., Roussos, L.A., Barton, C.K., Vaicaitis, R., Slazak, M., "Laboratory Study of Efficient Add-On Treatments for Interior Noise Control of Light Aircraft," AIAA Paper 81-1969 (1981).

20. Mixson, J.S., Barton, C.K., Vaicaitis, R., "Interior Noise Analysis and Control for Light Aircrft," SAE Paper 770445 (1977).

21. Pearsons, K.S., Bennett, R.L., "Effects of Interior Aircraft Noise on Speech Intelligibility and Annoyance," NASA CR-145203 (1977).

22. Piersol, A.G., Wilby, E.G., Wilby, J.F., "Evaluation of Aero Commander Sidewall Vibration and Interior Acoustic Data: Static Operations," NASA CR-159290 (1980).

23. Roussos, L.A., Mixson, J.S., "Acceleration Response of Fuse-lage Sidewall Panels on a Twin-Engine, Light Aircraft," Proceedings of Noise-Con 81, pp 291-294 (1981).

24. Rufp, J.A., "Noise Effects on Passenger Communication in Light Aircraft," SAE Paper 770446 (1977).

25. Succi, G.P., "Design of Quiet Efficient Propellers"; SAE Paper 790585; SAE Transactions, Soc. of Automotive Engineers, Warrendale, PA, April 1979.

26. Succi, G.P., "On the Design and Test of a Low Noise Propeller" , NASA CR-165938, November 1981.

27. Tobias, J.V., "Cockpit Noise Intensity: Fifteen Single-Engine Light Aircraft," Aerospace Medicine, **40**, 9, 963-966 (1969).

28. Tobias, J.V., "Noise in Light Twin Engine Aircraft," Sound and Vibration, 3, 9, 16-19 (1969).

29. Unruh, J.F., Scheidt, D.C., Pomerening, D.J., "Engine Induced Structural Borne Noise in a General Aviation Aircraft," NASA CR-159099, 1979.

30. Unruh, J.F., Scheidt, D.C., "Engine Induced Structural-Borne Noise in a General Aviation Aircraft," SAE Paper 790626 (1979).

31. Unruh, J.F., Scheidt, D.C., "Engine Isolation for Structural-Borne Interior Noise Reduction in a General Aviation Aircraft," NASA CR-3427 (1981).

32. Waterman, E.H., "New Means of Reducing Propeller Induced Cabin Noise," Proceedings of the Institute of Acoustics (1981).

33. Wilby, J.F. and J.I. Smullin, "Interior Noise of STOL Aircraft and Helicopters," Noise Control Engineering, 12 (3), May-June, 1979. (Also similar paper at NOISE-CON 77: NASA Langley Research Center, Hampton, VA.)

34. Wilby, J.F., "Interior Cabin Noise Levels of Commander 112A," NASA CR-137712, June 1975.

35. Wilby, J.F., "An Investigation of the Low Frequency Noise Levels in the Cessna Model 441 Airplane," BBN Report 3561, August 1977.

36. Wilby, J.F., Piersol, A.G., Wilby, E.G., "Evaluation of Aero Commander Propeller Acoustic Data: Static Operations," NASA CR-158919, May 1978.

37. Wilby, J.F., Piersol, A.G., Wilby, E.G., "Evaluation of Aero Commander Acoustic Data - Taxi Operations," NASA CR-159124, July 1979.

38. Wilby, J.F., Piersol, A.G., Wilby, E.G., "Evaluation of Aero Commander Sidewall Vibration and Interior Acoustic Data: Static Operations," NASA CR-159240, October 1980.

LIST OF SYMBOLS

Symbol	Definition	Units
a	acceleration	g (1g = acceleration of gravity)
AL	acceleration level (= 20 log a)	dB re 1g
BHP	Brake horsepower	hp, or kw
BDF	Blade passing frequency	Hz
c_o	Sound speed	m/s
d	Distance between microphones; or diameter	m
EFR	Engine firing rate	Hz
f	Frequency	Hz
f_c	Critical or coincidence frequency	Hz
K	Transfer function - mount acceleration to cabin sound pressure	$N/m^2/g$
KTAS	"Knots true airspeed;" airspeed relative to undisturbed air at sea level	Knots
p	Acoustic pressure	N/m^2
P	Static pressure	N/m^2 or bars
r	Correlation coefficient	—
RPM	Engine rotation rate	revolution/minute
SPL	Sound pressure level	dB re 2×10^{-5} N/m^2
T	Temperature	°C
U	Flow velocity	m/s

S-1

U_c	Convection velocity	m/s
ρ	density	Kg/m^2
θ	phase angle	degrees

1. Report No.	2. Government Accession No.	3. Recipient's Catalog No.
NASA CR-172152		

4. Title and Subtitle	5. Report Date
A STUDY OF INTERIOR NOISE LEVELS, NOISE SOURCES AND TRANSMISSION PATHS IN LIGHT AIRCRAFT	July 1983
	6. Performing Organization Code

7. Author(s)	8. Performing Organization Report No.
R.E. Hayden, B.S. Murray, M.A. Theobald	BBN Report No. 4704
	10. Work Unit No.

9. Performing Organization Name and Address	08108
Bolt Beranek and Newman Inc. 10 Moulton Street Cambridge, Massachusetts 02238	11. Contract or Grant No.
	NAS1-16138
	13. Type of Report and Period Covered

12. Sponsoring Agency Name and Address	Contractor Report
National Aeronautics and Space Administration Washington, D.C. 20546	14. Sponsoring Agency Code

15. Supplementary Notes

Langley Technical Monitor: Dr. John S. Mixson
Final Report

16. Abstract

This study consisted of a systematic survey of the interior noise levels and spectral characteristics of 18 single-and twin-engine propeller-driven light aircraft, as well as an in-depth source-path diagnosis of a single-engine aircraft which was considered representative of a large part of the fleet.

The purpose of the flight surveys was to measure internal noise levels and identify principal noise sources and paths under a carefully-controlled and standardized set of flight procedures. Once the survey had been completed and the results analyzed, one aircraft model was chosen for more detailed application of advanced noise source and path diagnosis. This aircraft was subjected to a second round of flight tests in which more detailed measurements of sources and paths were made and additional diagnostic ground tests were performed.

The detailed diagnostic tests consisted of flights and ground tests in which various parts of the aircraft, such as engine mounts, the engine compartment, exhaust pipe, individual panels, and the wing strut were instrumented to determine source levels and transmission path strengths using the transfer function technique. The tests were limited to those which could be conducted on flightworthy aircraft in an operational environment (i.e., at an airfield, in a hangar, or in-flight), but the results were suitably conclusive to provide identification of predominant source and path combinations.

The report describes experimental techniques, analysis of data, transfer function calculations to derive source-path contributions to the cabin acoustic environment, and implications of the findings for noise control design.

17. Key Words (Suggested by Author(s))	18. Distribution Statement
Aircraft interior noise Propeller aircraft noise and vibration Transfer function methods Noise control	

19. Security Classif. (of this report)	20. Security Classif. (of this page)	21. No. of Pages	22. Price
UNCLASSIFIED	UNCLASSIFIED	190	